

Novel oxygenases acting on phenolic compounds

Promotoren:

Prof. dr. ir. I.M.C.M. Rietjens
hoogleraar Toxicologie
Wageningen Universiteit

Prof. dr. S.C. de Vries
hoogleraar Biochemie
Wageningen Universiteit

Copromotor:

Dr. W.J.H. van Berkel
universitair hoofddocent
Laboratorium voor Biochemie
Wageningen Universiteit

Promotiecommissie:

Prof. dr. M. Schlömann, TU Bergakademie Freiberg
Prof. dr. D.B. Janssen, Rijksuniversiteit Groningen
Prof. dr. J. van der Oost, Wageningen Universiteit
Dr. M.C.R. Franssen, Wageningen Universiteit

Dit onderzoek is uitgevoerd binnen de voormalige onderzoekschool M&T en
gecontinueerd in onderzoekschool VLAG

Novel oxygenases acting on phenolic compounds

Maria J.H. Moonen

Proefschrift
ter verkrijging van de graad van doctor
op gezag van de rector magnificus
van Wageningen Universiteit,
Prof. dr. ir. L. Speelman,
in het openbaar te verdedigen
op maandag 30 mei 2005
des namiddags te half twee in de Aula.

ISBN: 90-8504-185-6

Für Peter Mies

Vor 22 Jahre nanntest du mich schon Frau Dokter. Schade daß du heute nicht mehr unter uns bist, aber du bist in meinen Gedanken.

Contents

Abbreviations		8
Chapter 1	Introduction: Oxygenating enzymes involved in the catabolism of 4-hydroxyacetophenone by <i>Pseudomonas fluorescens</i> ACB	9
Chapter 2	Flavoenzyme-catalyzed oxygenations and oxidations of phenolic compounds	19
Chapter 3	4-Hydroxyacetophenone monooxygenase from <i>Pseudomonas fluorescens</i> ACB. A novel flavoprotein catalyzing Baeyer-Villiger oxidation of aromatic compounds	35
Chapter 4	¹⁹ F NMR study on the biological Baeyer-Villiger oxidation of acetophenones	53
Chapter 5	Enzymatic Baeyer-Villiger oxidation of benzaldehydes	67
Chapter 6	Biochemical and genetic characterization of the 4-hydroxyacetophenone degradation pathway in <i>Pseudomonas fluorescens</i> ACB	79
Chapter 7	Hydroquinone dioxygenase from <i>Pseudomonas fluorescens</i> ACB. A novel member of the family of non-heme iron(II)-dependent dioxygenases	99
References		123
Summary		141
Samenvatting		149
Nawoord		159
Curriculum vitae		163
List of publications		165
Training and Supervision M&T and VLAG		167

Abbreviations

ADP	adenosine diphosphate
APCI	atmospheric pressure chemical ionization
ATCC	American type culture collection
BSA	bovine serum albumin
BVMO	Baeyer-Villiger monooxygenase
DMF	dimethyl formamide
DTT	dithiothreitol
DIG	digoxigenin
EDTA	ethylenediaminetetraacetic acid
ES-complex	enzyme-substrate complex
ESI-MS	electrospray ionization mass spectrometry
E(LUMO)	energy of the lowest unoccupied molecular orbital
FAD	flavin adenine dinucleotide
FMN	flavin mononucleotide
FPLC	fast performance liquid chromatography
GC-MS	gas chromatography mass spectrometry
HAO	3-hydroxyanthranilate 3,4-dioxygenase
HAPMO	4-hydroxyacetophenone monooxygenase
HbpA	2-hydroxybiphenyl 3-monooxygenase
HF	heat of formation
HHQ	hydroxyhydroquinone; 1,2,4-trihydroxybenzene
HHQDO	hydroxyhydroquinone 1,2-dioxygenase
4-HMSA	4-hydroxymuconic semialdehyde
HPAH	3-hydroxyphenylacetate 6-hydroxylase
HPLC	high performance liquid chromatography
HQDO	hydroquinone dioxygenase
LB	Luria-Bertani
LC-MS	liquid chromatography mass spectrometry
Maldi-Tof	matrix assisted laser desorption/ionization time of flight
NADH	nicotinamide adenine dinucleotide
NADPH	nicotinamide adenine dinucleotide phosphate
NMR	nuclear magnetic resonance
ORF	open reading frame
PCR	polymerase chain reaction
PET	positron emission tomography
PHBH	<i>p</i> -hydroxybenzoate hydroxylase
PMSF	phenylmethylsulfonyl fluoride
ppm	parts per million
SDS	sodium dodecyl sulfate
SDS-PAGE	sodium dodecyl sulfate polyacrylamide gel electrophoresis
SEC-MS	size-exclusion chromatography mass spectrometry
VAO	vanillyl-alcohol oxidase

Chapter 1

General introduction:

**OXYGENATING ENZYMES INVOLVED IN THE
CATABOLISM OF 4-HYDROXYACETOPHENONE BY
PSEUDOMONAS FLUORESCENS ACB**

Background and aim of the thesis

This thesis deals with the characterization of the oxidative enzymes involved in the catabolism of 4-hydroxyacetophenone by the Gram-negative bacterium *Pseudomonas fluorescens* ACB. Although many studies have been devoted to the biodegradation of aromatic compounds, relatively little is known about the oxygenases involved in the catabolism of acetophenones. More insight into the biocatalytic features of these enzymes is of importance for the development of more environmentally benign and clean synthetic methodologies.

The aim of the thesis is twofold. The first aim is to obtain a detailed insight in the mode of action of 4-hydroxyacetophenone monooxygenase (HAPMO). This enzyme is known to catalyze the first step in the degradation of 4-hydroxyacetophenone in *P. fluorescens* ACB, but has never been purified. The second aim is to elucidate the biodegradation pathway of 4-hydroxyacetophenone along the ring-cleavage step. Literature data suggest that 4-hydroxyacetophenone is metabolized through the formation of hydroquinone.^[75] However, the enzyme(s) involved in the further degradation of hydroquinone are unknown.

In this introductory chapter, first an outline is given about the microbial degradation of acetophenones and hydroquinones. Then, some information is presented about the usefulness of organofluorine compounds in biotransformation studies. Next, attention is given to the different types of oxygenases discussed in this thesis. Finally, it is explained why the newly described enzymes might be useful for biocatalytic applications.

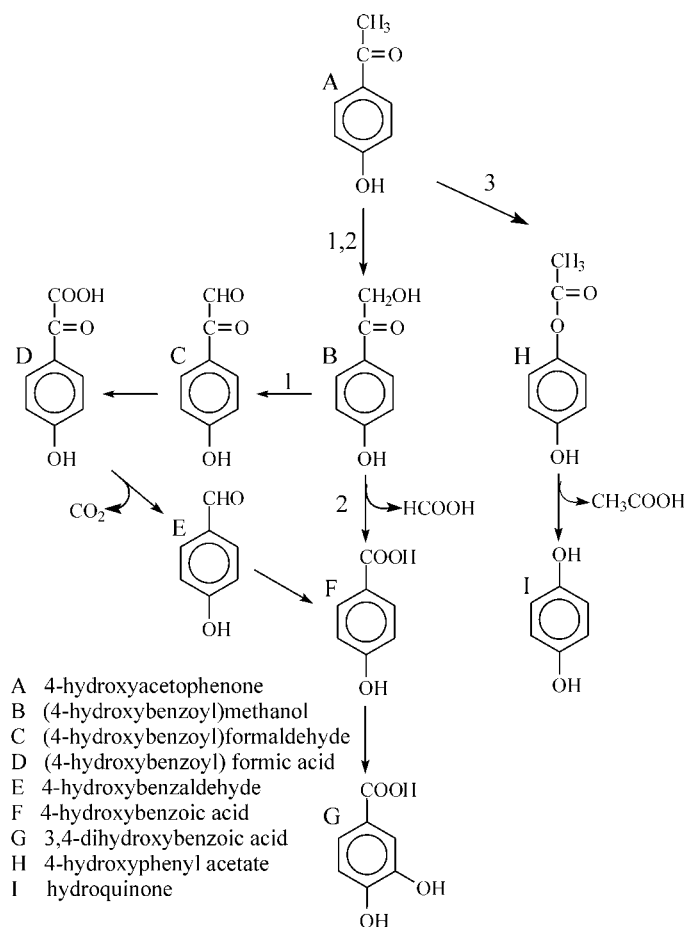
Microbial degradation of 4-hydroxyacetophenone

Acetophenones are aromatic compounds widely found in the environment as degradation products of industrial chemical compounds. Ring-chlorinated acetophenones originate from the microbial degradation of insecticides,^[19-21] PCBs^[12,14,15] and chloroxanthenes.^[301] Non-chlorinated acetophenones have been identified as intermediates in the microbial degradation of ethylbenzene,^[50,305] 1-phenylethanol,^[53] 4-ethylphenol^[154] and the flame-retardant tetrabromobisphenol A.^[185,250]

Several aerobic microorganisms are capable of utilizing acetophenones for their growth.^[52,53,55,127,133,135] 4-Hydroxyacetophenone was shown to be metabolized through different pathways (Scheme 1). 4-Hydroxyacetophenone can be converted in two different ways to 4-hydroxybenzoate (pathway 1 and 2 in Scheme 1).^[115,135,164] 4-Hydroxybenzoate then enters the β -keto adipate pathway via the formation of protocatechuate (3,4-dihydroxybenzoate) as ring fission substrate.^[153] 4-Hydroxyacetophenone may also be converted to hydroquinone (pathway 3 in Scheme 1).^[55]

The β -keto adipate pathway, leading from an aromatic compound to β -keto adipate, is widely distributed among taxonomically diverse eubacteria and fungi. It is almost always chromosomally encoded and plays a central role in the processing and degradation of naturally-occurring aromatic compounds derived from lignin and other plant components, as well as in the degradation of some environmental pollutants. Enzyme studies and amino acid sequence data indicate that the pathway is highly conserved in diverse bacteria.^[126] Two additional steps accomplish the conversion of

β -ketoacid to tricarboxylic acid cycle intermediates (acetyl-CoA and succinyl-CoA).^[126]

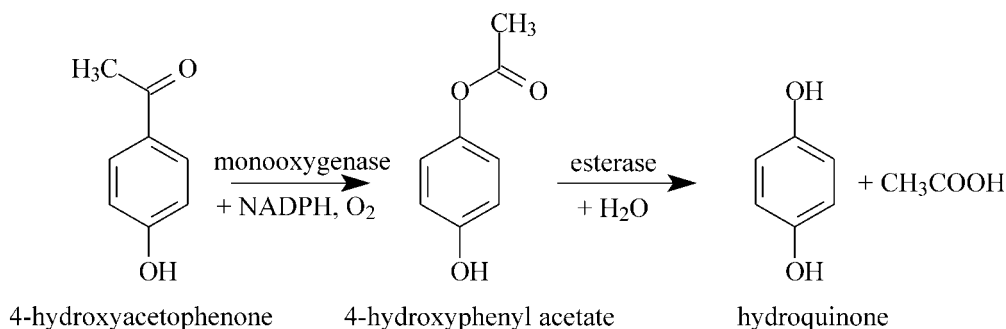


Scheme 1. Pathways for the microbial degradation of 4-hydroxyacetophenone.
1 *Alcaligenes* sp.;^[135] **2** *Pseudomonas fluorescens* A.3.12;^[115] *Bacterium* NCIB 8250;^[164]
3 *Pseudomonas putida* JD1;^[55] *Aspergillus fumigatus* ATCC 28282,^[154] *Pseudomonas fluorescens* ACB.^[133]

Degradation of 4-hydroxyacetophenone by *Pseudomonas fluorescens* ACB

Pseudomonas fluorescens ACB originally was isolated from activated sewage sludge by enrichment and serial transfer with 4-hydroxyacetophenone.^[133] The strain was able to grow on 4-hydroxyacetophenone, 4-hydroxypropiophenone, (4-hydroxy)benzoate, 4-hydroxybenzaldehyde, hydroquinone and phenyl acetate. *P. fluorescens* ACB was used to investigate the microbial metabolism of halogenated acetophenones. The bacterium was capable of converting 2-halo- and 4-haloacetophenones as well as 3-fluoroacetophenone.^[133]

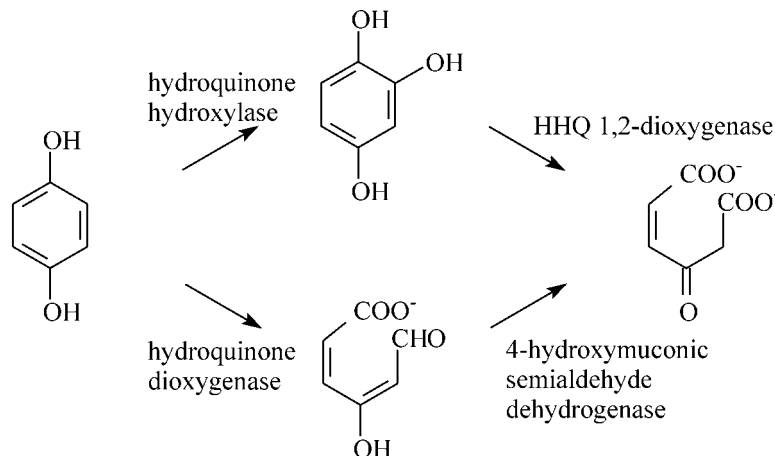
The initial steps of 4-hydroxyacetophenone mineralization were shown to comprise a Baeyer-Villiger oxidation to 4-hydroxyphenyl acetate and subsequent ester hydrolysis to hydroquinone (Scheme 2).^[133] However, the further degradation of hydroquinone by *P. fluorescens* ACB remained elusive.



Scheme 2. Degradation of 4-hydroxyacetophenone to hydroquinone by *P. fluorescens* ACB by a monoxygenase and an esterase

Microbial degradation of hydroquinone

Hydroquinone can be degraded by aerobic microorganisms through two different pathways (Scheme 3). The first pathway involves the initial hydroxylation of hydroquinone to hydroxyhydroquinone (HHQ; 1,2,4-trihydroxybenzene).^[88,313] For the ascomycetous yeast *Candida parapsilosis* it was shown that this reaction is catalyzed by a flavin-dependent phenol hydroxylase.^[88,313] The HHQ product is then ring-split and converted to maleylacetate by the action of an intradiol HHQ 1,2-dioxygenase (HHQDO).^[149,178,245,313] The second pathway of hydroquinone degradation is more uncommon. In this pathway, hydroquinone serves as ring fission substrate and 4-hydroxymuconic semialdehyde (4-HMSA) is produced. The enzyme responsible for this ring-cleavage reaction is hydroquinone dioxygenase (HQDO).^[33,55,207,274]



Scheme 3. Proposed routes for the microbial degradation of hydroquinone. Hydroquinone hydroxylase [EC 1.14.13.7] is present in *Candida parapsilosis*,^[88] *Trichosporon cutaneum*,^[156] *Brevibacterium fuscum*,^[219] *Pseudomonas* sp. CF600,^[222] *Acinetobacter calcoaceticus*,^[348] and *Pseudomonas pickettii*,^[175] HHQ 1,2-dioxygenase [EC 1.13.11.37] is present in *Arthrobacter* sp.,^[149] *Azotobacter* sp.,^[178] *Sphingomonas* sp. RW1,^[8] *Arxula adenivorans*,^[201] *Nocardioides simplex* 3E,^[17] *Pseudomonas putida*,^[39] *Burkholderia cepacia* AC1100,^[57] *Streptomyces rochei* 303,^[112] *Rhodococcus chlorophenolicus* PCP-1,^[304] *Phanerochaete chrysosporium*,^[245] *Trichosporon cutaneum*,^[289] *Bacillus spaericus* JS905,^[155] and *Candida parapsilosis*,^[313] hydroquinone dioxygenase is present in *Pseudomonas putida* JD1,^[55] *Moraxella* sp.,^[274] *Arthrobacter protophormiae* RKJ100,^[239] *Burkholderia cepacia* RKJ200,^[40] *Sphingomonas chlorophenolica* ATCC 39723,^[346] and *Sphingomonas paucimobilis* UT26,^[207] 4-Hydroxymuconic semialdehyde dehydrogenase is present in *Moraxella* sp.^[274]

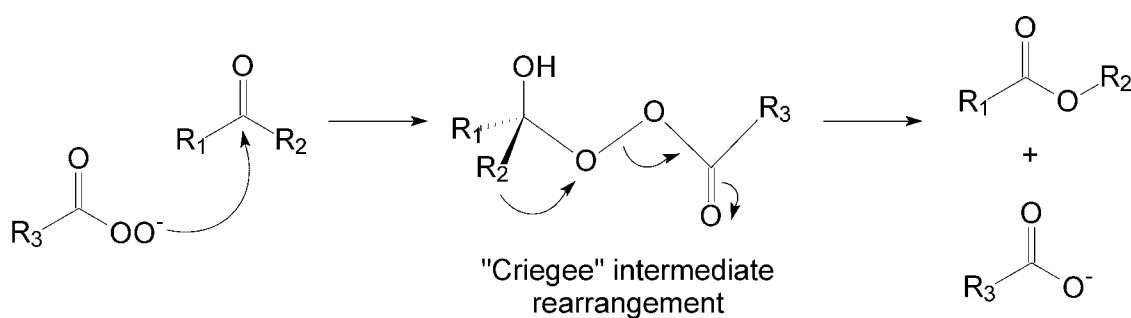
Biodegradation of organofluorine compounds

Fluorine is the thirteenth most abundant element in the earth's crust and the most abundant halogen,^[227] However, fluoride concentrations in surface water are low and fluorinated metabolites are extremely rare.^[65,226,347] How organofluorine compounds are biosynthesized remains a mystery.^[227] There is only one fluorinating enzyme identified, namely 5'-fluoro-5'-deoxyadenosine synthase.^[65,227] Nevertheless, fluorinated chemicals are growing in industrial importance, with applications in pharmaceuticals, agrochemicals and material products.^[65,142,192,255] ¹⁸F-containing compounds, for instance, are used in positron emission tomography (PET) studies.^[45]

In this thesis, fluorinated compounds have been used for biotransformation studies with whole cells, cell extracts and purified enzymes. Fluorinated compounds are very useful in such studies because they can be identified and quantified by ¹⁹F nuclear magnetic resonance (NMR) spectroscopy without the need of purification steps.^[22,25,246,334] The natural abundance of the ¹⁹F isotope is 100% and biological systems do not contain fluorinated endogenous compounds. The ¹⁹F nucleus has also a broad chemical shift range of about 500 ppm and the chemical shift of a ¹⁹F nucleus is highly sensitive to its molecular surroundings. Also the intrinsic sensitivity of the ¹⁹F nucleus is high, which is of particular importance in the detection of unstable intermediates.

Baeyer-Villiger monooxygenases

The Baeyer-Villiger reaction is a valuable tool for the chemical synthesis of esters and lactones. In this reaction, as first described by Adolf Baeyer and Victor Villiger in 1899,^[10] a (cyclic) ketone is attacked by a nucleophilic peroxy acid to form a so-called 'Criegee intermediate'^[51] (Scheme 4). This species undergoes a rearrangement *via* expulsion of a carboxylate ion and migration of a carbon-carbon bond, yielding the ester (or lactone) and the acid. One century after its discovery, the Baeyer-Villiger reaction still receives much attention in oxidation chemistry.^[16,243] This is due to the fact that the rate of rearrangement and migration preference can be directed by the type of reactants and the reaction conditions.^[243]



Scheme 4. Baeyer-Villiger oxidation reaction mechanism

The first enzymatic Baeyer-Villiger reaction was reported about 55 years ago and involved the biotransformation of steroids by fungi.^[303] Then, several Baeyer-Villiger monooxygenase (BVMO) enzymes (E.C. 1.14.13.x) were discovered.^[158] All of these BVMOs are flavoenzymes that stabilize a peroxyflavin intermediate^[268] which acts as the oxygenating nucleophile in substrate attack.^[193,267]

Willems has classified two types of BVMO, based on biochemical data. Type I BVMOs such as cyclohexanone monooxygenase,^[224] cyclopentanone monooxygenase,^[113] 2-tridecanone monooxygenase,^[31] 2-oxo- Δ^3 -4,5,5-trimethylcyclopentenyl-acetyl-coA monooxygenase,^[232] and progesterone/steroid monooxygenase^[145] all contain FAD, consist of one type of subunit and use NADPH as external electron donor.^[343] The best studied type I BVMO is cyclohexanone monooxygenase.^[42,66] This enzyme has a very broad substrate specificity^[331] and is widely used for synthetic applications.^[4,202,281,282] Sequence comparisons have shown that type I BVMOs can be identified using a specific protein sequence motif.^[103]

Type II BVMOs consist of only a few members, including 2,5-diketocamphane 1,2-monooxygenase and 3,6-diketocamphane 1,6-monooxygenase.^[152,295] These enzymes contain FMN as flavin cofactor, are composed of two types of subunits, and use NADH as source of electrons. Also several luciferases were classified as type II BVMOs,^[343] catalyzing a reaction similar to the Baeyer-Villiger oxidation.^[72]

4-Hydroxyacetophenone monooxygenase

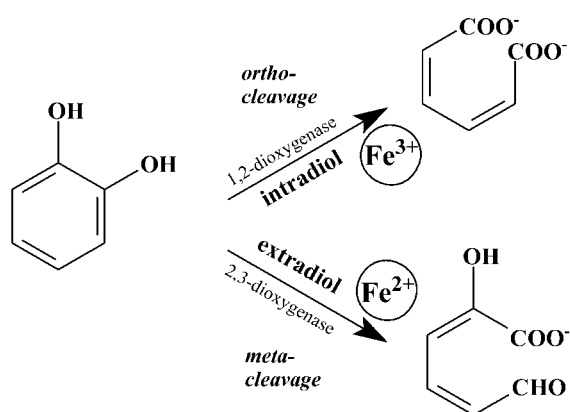
In 1990, Higson and Focht described that a BVMO is involved in the degradation of 4-hydroxyacetophenone in *P. fluorescens* ACB.^[133] A similar 4-hydroxyacetophenone monooxygenase (HAPMO) then was found in *Aspergillus fumigatus* ATCC 28282^[154] and *P. putida* JD1.^[55,294] Acetophenone monooxygenases were reported to be present in *Arthrobacter* sp.,^[52] *Nocardia* T5,^[53] and *Alcaligenes* sp. ACA,^[133] whereas a chloroacetophenone monooxygenase was detected in *Arthrobacter* sp.^[127] Although it was noticed that HAPMO is specific for NADPH,^[133,154] at the start of this thesis work, no BVMO acting on aromatic compounds was ever purified and characterized in detail.

The chemical Baeyer-Villiger oxidation makes use of environmentally unfriendly peroxides. Therefore, much interest exists in the development of BVMO biocatalysts, which use molecular oxygen as cheap and clean oxidant. BVMOs are extremely useful for enantioselective and regioselective oxidations but have also some drawbacks. A main disadvantage of type I BVMOs is their need of expensive NADPH. This can be overcome by engineering the coenzyme specificity^[160] or using whole cells.^[282] In *P. fluorescens* ACB an esterase is present, that converts the produced esters to phenolic compounds. Performing genetic manipulation to knock out the esterase could produce a whole cell system that regenerates NADPH and produces interesting acylcatechols.

Ring fission dioxygenases

Ring fission dioxygenases incorporate two atoms of molecular oxygen into the aromatic substrate, which results in opening of the benzene ring. Most of these enzymes harbor a non-heme iron in the active site. The non-heme iron-dependent dioxygenases can be divided in two groups (Scheme 5):

- A Intradiol/*ortho*/ferric (Fe^{3+}) dioxygenases like catechol 1,2-dioxygenase,^[30] protocatechuate 3,4-dioxygenase^[153] and hydroxyhydroquinone (1,2,4-trihydroxybenzene) 1,2-dioxygenase.^[245]
- B Extradiol/*meta*/ferrous (Fe^{2+}) dioxygenases like catechol 2,3-dioxygenase,^[166] biphenyl dioxygenase,^[119] homoprotocatechuate 2,3-dioxygenase,^[204] and protocatechuate 4,5-dioxygenase.^[285]



Scheme 5. Intra- and extradiol ring splitting by catechol dioxygenases

Hydroquinone dioxygenase

Hydroquinone dioxygenases have been indicated to be involved in the degradation of 4-ethylphenol,^[55] *p*-nitrophenol,^[40,239] 4-nitrocatechol^[40,41] and of the insecticide fenitrothion.^[128] However, none of these enzymes have been characterized in much detail.

Chlorohydroquinone dioxygenases were discovered recently. Chlorohydroquinones are formed in several microbial degradation pathways of pentachlorophenol,^[33] hexachlorocyclohexane^[207] and 2,4,6-trichlorophenol.^[187] *Sphingobium chlorophenolicum* ATCC 39723 contains a 2,6-dichlorohydroquinone 1,2-dioxygenase (PcpA) that converts 2,6-dichloro-, 2-chloro- and hydroquinone to the corresponding 4-hydroxymuconic semialdehyde.^[229,349] *Sphingomonas paucimobilis* UT26 contains a chlorohydroquinone 1,2-dioxygenase (LinE) that converts 2-chlorohydroquinone via the unstable 6-chloro-4-hydroxymuconic semialdehyde to maleylacetate.^[207] LinE can also catalyze the oxidation of non-chlorinated hydroquinone.

Muconic semialdehydes, the main products of hydroquinone dioxygenases, and corresponding acids might serve as building blocks for other interesting compounds. For instance, *cis,cis*-muconic acids may serve as raw materials in the production of novel pharmaceuticals, agricultural chemicals and functional resins.^[184] 2-Hydroxymuconic semialdehyde and α -amino- β -carboxymuconic acid- ϵ -semialdehyde are readily converted to picolinic acid^[197] and quinolinic acid.^[35] Picolinic acids are used as feedstocks for the synthesis of a variety of pharmaceuticals, agricultural chemicals, and dyes.^[275] Quinolinic acid is a building block for the synthesis of NAD.^[2]

Outline of the thesis

In this PhD research project we studied two oxygenases involved in the degradation of 4-hydroxyacetophenone by *Pseudomonas fluorescens* ACB: the Baeyer-Villiger enzyme 4-hydroxyacetophenone monooxygenase (HAPMO) and the ring-cleavage enzyme hydroquinone dioxygenase (HQDO). Furthermore, the gene cluster of the degradation pathway is described.

In **Chapter 2** an overview is given of the oxygenation and oxidation of phenolic compounds by different types of flavoproteins including BVMOs.

An extensive study of HAPMO is presented in **Chapter 3**. The gene cloning, sequence analysis, purification and biochemical characterization of HAPMO are reported.

Chapter 4 describes a ^{19}F NMR study on the biological Baeyer-Villiger oxidation of acetophenones. It is shown that phenyl acetates can be obtained in high yield when using purified HAPMO and relatively low pH.

Chapter 5 describes the HAPMO-mediated conversion of fluorinated benzaldehydes. These compounds can be transformed to the corresponding phenols, which can serve as synthons in the production of pharmaceutical and agrochemical specialities.

In **Chapter 6** the biodegradation pathway of 4-hydroxyacetophenone in *P. fluorescens* ACB is described. Also the *hap* gene cluster, coding for the enzymes of this degradation pathway, is presented. The involvement in this pathway of an unusual hydroquinone dioxygenase is established.

Chapter 7 describes the purification, sequence analysis and characterization of the novel hydroquinone dioxygenase (HQDO). The iron(II)-dependent enzyme is a heterotetramer and is active with a wide range of hydroquinones. This is the first described sequence of a dioxygenase that uses hydroquinone as the physiological substrate.

Chapter 2

FLAVOENZYME-CATALYZED OXYGENATIONS AND OXIDATIONS OF PHENOLIC COMPOUNDS

Mariëlle J.H. Moonen, Marco W. Fraaije, Ivonne M.C.M. Rietjens, Colja Laane and Willem J.H. van Berkel

Advanced Synthesis & Catalysis. 2002. Vol. 344, No. 10, pp.1023-1035

Flavin-dependent monooxygenases and oxidases play an important role in the mineralization of phenolic compounds. Because of their exquisite regioselectivity and stereoselectivity, these enzymes are of interest for the biocatalytic production of fine chemicals and food ingredients. In our group, we have characterized several flavoenzymes that act on phenolic compounds, including 4-hydroxybenzoate 3-hydroxylase, 3-hydroxyphenyl-acetate 6-hydroxylase, 4-hydroxybenzoate 1-hydroxylase (decarboxylating), hydroquinone hydroxylase, 2-hydroxybiphenyl 3-monooxygenase, phenol hydroxylase, 4-hydroxyacetophenone monooxygenase and vanillyl-alcohol oxidase. The catalytic properties of these enzymes are reviewed here, together with insights obtained from site-directed and random mutagenesis.

1 Introduction

Phenolic compounds constitute one of the largest groups of natural products. Being synthesized by plants, their microbial degradation forms a substantial part of the biogeochemical cycle. Besides natural phenols, many anthropogenic (halo)phenolic derivatives are found in soil. These compounds have been used as building blocks in chemical and pharmaceutical syntheses and as herbicides and pesticides, sometimes causing serious local contamination of the environment.

The mineralization of (halo)phenolic compounds by aerobic microorganisms is initiated by the action of inducible flavoenzymes. These include flavoprotein monooxygenases, which use electrons from NAD(P)H to activate and cleave a molecule of oxygen, enabling incorporation of an oxygen atom into the substrate, as well as flavoprotein oxidases which react with their substrates without the need of external cofactors using only molecular oxygen.

Flavoprotein monooxygenases that are active with phenolic compounds usually contain FAD as prosthetic group. They activate molecular oxygen through the formation of a reactive flavin (hydro)peroxide which can attack the substrate by an electrophilic or nucleophilic process depending on the protonation state of the flavin (hydro)peroxide and the nature and protonation state of the substrate. In aromatic hydroxylation reactions, the flavin hydroperoxide acts as an electrophile. However, in Baeyer-Villiger monooxygenation reactions, the flavin peroxide is active as a nucleophile.^[193]

Flavoprotein monooxygenases are of interest for biocatalytic applications, since they are able to perform regioselective and stereoselective oxidations under mild and environmentally friendly conditions.^[90] Aspects relevant for biotechnological application of flavoprotein monooxygenases are the substrate and cofactor specificity, the regioselectivity and stereoselectivity of the conversions and the efficiency of the reactions including chances of unwanted side reactions and products. Clearly, these important characteristics are highly dependent on the structure-activity characteristics dictated by the active site of the enzymes. So far, relatively little is known about the structure-function relationship of flavoprotein monooxygenases. Except for *p*-hydroxybenzoate hydroxylase (PHBH) from *Pseudomonas fluorescens*^[262] and phenol hydroxylase from *Trichosporon cutaneum*,^[76] no structural information is available at the atomic level. Furthermore, with the aromatic hydroxylases of known structure it is unclear how the protein interacts with the pyridine nucleotide coenzyme.^[84,333]

Based on sequence homology, FAD-dependent monooxygenases belong to the following subclasses.^[157,193]

- i) Aromatic hydroxylases. These enzymes share a typical dinucleotide binding domain for FAD binding, but lack a common NAD(P) binding fold.^[83] PHBH is the prototype of this subclass.
- ii) Baeyer-Villiger monooxygenases and *N*-hydroxylating enzymes. Many of these flavoproteins, like cyclohexanone monooxygenase and dimethylaniline monooxygenase, contain two dinucleotide binding motifs ($\beta\alpha\beta$ -folds), one for FAD binding and one for NAD(P) binding.^[103]

There are also aromatic hydroxylases that use FAD or FMN only as a coenzyme. With these enzymes, the reduced flavin is supplied by a flavin reductase at the expense of NAD(P)H. The protein partners of these aromatic hydroxylases do not tightly interact and contain no common dinucleotide binding motifs. Representatives of these two-component aromatic hydroxylases are pyrrole-2-carboxylate monooxygenase^[13] and 4-hydroxyphenylacetate 3-hydroxylase.^[108]

In addition to flavoprotein monooxygenases, also flavoprotein oxidases form an important group of flavin-dependent biocatalysts. Flavoprotein oxidases are attractive for synthetic applications because they constitute a group of enzymes that use molecular oxygen as a clean and cheap oxidant and do not require expensive cofactors. The best characterized flavoprotein oxidase which acts on phenolic compounds is vanillyl-alcohol oxidase (VAO).^[100] Unlike other flavoprotein oxidases such as glucose oxidase and *D*-amino acid oxidase,^[101,196] VAO is structurally not related to the flavoprotein aromatic hydroxylases.^[99]

In this review we discuss the different classes of flavin-dependent monooxygenases and oxidases that are active with phenolic compounds. For each class, a model enzyme is discussed to illustrate the catalytic potential as well as the limits and opportunities defined by their active site characteristics and mechanism of catalysis. For the flavoprotein aromatic hydroxylases, which form the largest subclass of flavin-dependent monooxygenases, a few other family members are discussed as well.

2 Flavoprotein Aromatic Hydroxylases

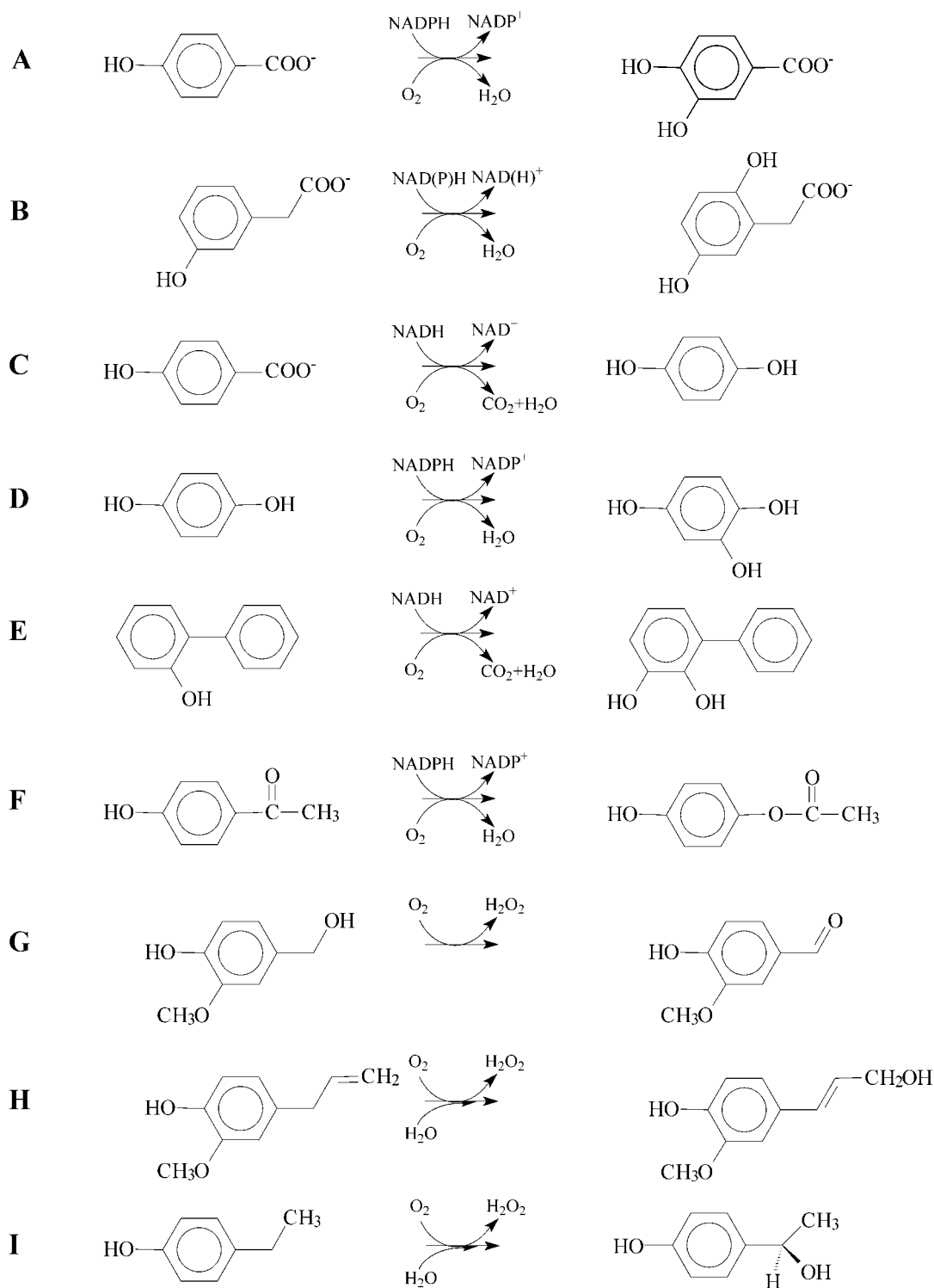
Flavoprotein aromatic hydroxylases have many catalytic properties in common and their substrate specificity is consistent with an electrophilic aromatic substitution mechanism.^[214] To illustrate the mechanism of action of flavoprotein aromatic hydroxylases and their catalytic potential and limitations, we start this review with a detailed overview of the properties of PHBH from *P. fluorescens*. This enzyme is the most well-studied member of this class of flavoenzymes and its catalytic mechanism is representative for the whole family.

4-Hydroxybenzoate 3-hydroxylase

PHBH from *P. fluorescens* is a homodimer of about 88 kDa with each subunit containing a non-covalently bound FAD.^[214] PHBH catalyses the conversion of 4-hydroxybenzoate into 3,4-dihydroxybenzoate (Scheme 1), a common intermediate step in the biodegradation of aromatic compounds in soil. The enzyme from *P. fluorescens* is strictly NADPH dependent.^[136] However, some PHBH enzymes from other strains prefer NADH as electron donor.^[147,266]

PHBH is one of the first flavoenzymes with known three-dimensional structure.^[340] Figure 1 presents a ribbon structure of the enzyme-substrate complex as refined at 1.9 Å resolution.^[262] The folding topology of PHBH is shared by several other oxidative flavoenzymes, including cholesterol oxidase,^[330] glucose oxidase,^[130] *D*-amino acid oxidase,^[194] and phenol hydroxylase.^[76] Crystal structures have also been obtained of PHBH in complex with substrate analogs and of a number of mutant enzymes.^[81,84-86,109,176,263,314,333] The PHBH structure can be divided in three domains.^[262] the FAD binding domain (residues 1-175), the substrate binding domain (residues 176-290) and the interface domain (residues 291-394). However, in recent structural classifications, the FAD binding domain and interface domain are regarded as a single domain, leaving PHBH as a two-domain protein.^[196]

The substrate binding site of PHBH is deeply buried in the protein.^[262] Crystallographic studies with substrate and flavin analogs have indicated that the flavin



Scheme 1. Reactions catalyzed by flavoprotein monooxygenases and oxidases described in this review. (A) *ortho*-hydroxylation of 4-hydroxybenzoate, (B) *para*-hydroxylation of 3-hydroxyphenylacetate, (C) oxidative decarboxylation of 4-hydroxybenzoate, (D) *ortho*-hydroxylation of hydroquinone, (E) *ortho*-hydroxylation of 2-hydroxybiphenyl, (F) Baeyer-Villiger oxidation of 4-hydroxyacetophenone, (G) oxidation of vanillyl-alcohol, (H) VAO-mediated hydroxylation of eugenol and (I) VAO-mediated hydroxylation of 4-ethylphenol.

ring moves out of the active site to allow substrate binding and product release.^[109,263,314]

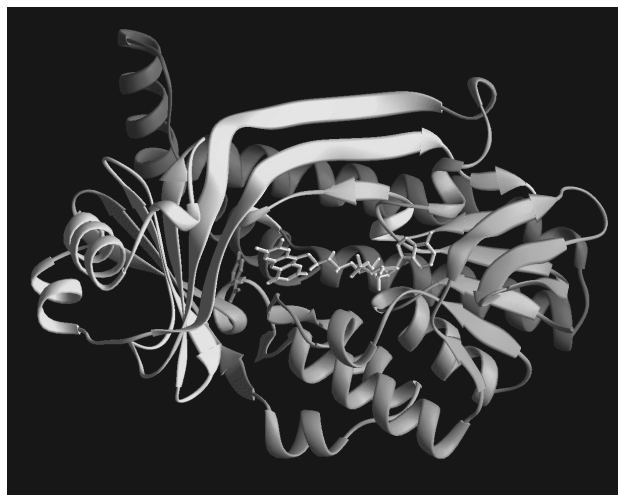


Fig. 1. Ribbon diagram of the crystal structure of the enzyme-substrate complex of *p*-hydroxybenzoate hydroxylase from *Pseudomonas fluorescens*.^[262] The isoalloxazine ring of the FAD is located close to the aromatic substrate in the interior position in the active site.

Figure 2 presents a close up of the substrate binding site. Arg214 forms a indispensable ionic interaction with the carboxyl group of the substrate.^[312] Ser212 and Tyr222 are also involved in binding the carboxylic moiety of 4-hydroxybenzoate. Substrate hydroxylation is facilitated by deprotonation of the phenol.^[244,270,309,325] The hydroxyl group of the substrate is at hydrogen bonding distance of Tyr201 that contacts Tyr385. Selective Phe replacements of these tyrosine residues strongly hamper substrate deprotonation and flavin reduction.^[79,89]

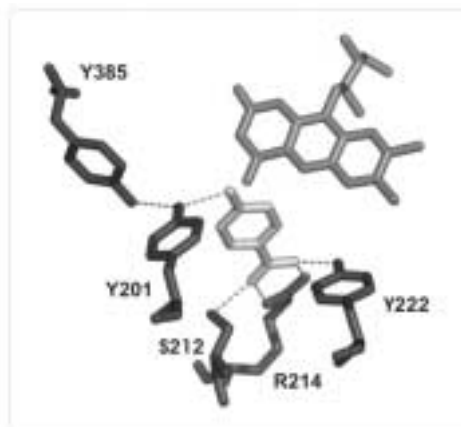
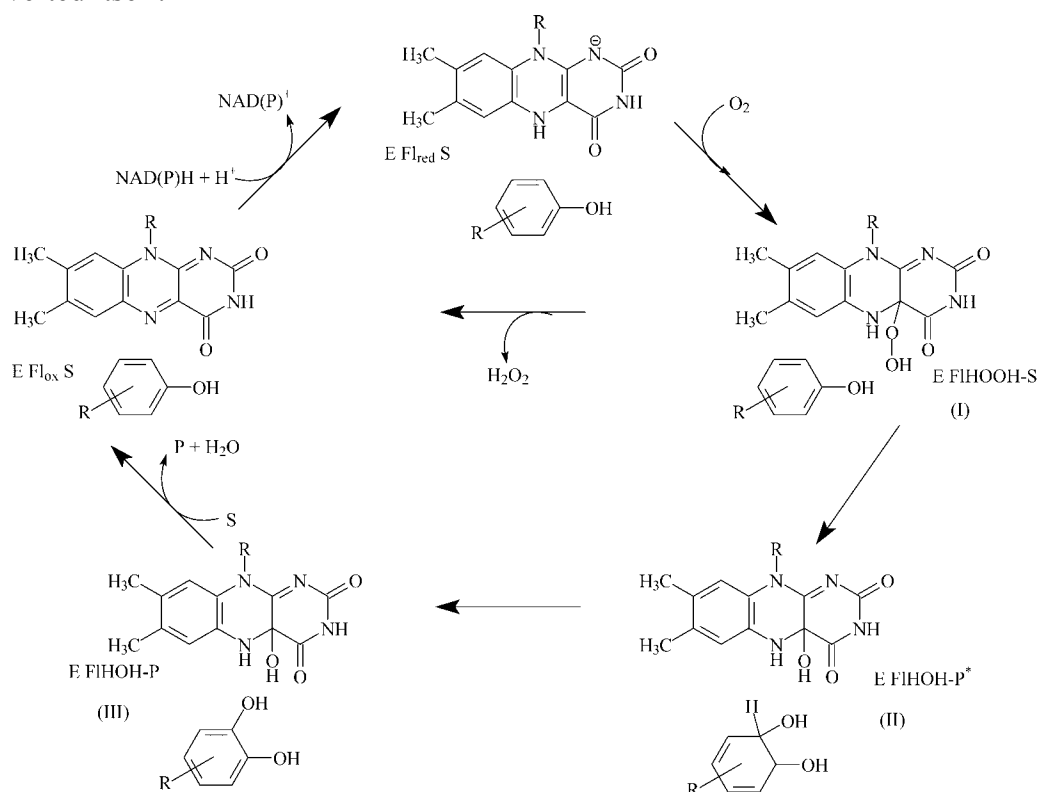


Fig. 2. The active site of the enzyme-substrate complex of *p*-hydroxybenzoate hydroxylase from *Pseudomonas fluorescens*.^[262] The FAD is gray, the aromatic substrate is white, and the protein residues are black. The *si* face of the flavin is the back of the page in this view; the *re* side is the front, as seen with the substrate phenol pointing out of the page.

Pro293 is another important active site residue and is located in a highly conserved loop. The peptide carbonyl oxygen of Pro293 is within hydrogen bonding distance of the phenolic oxygen of bound substrate. It has been inferred from site-directed mutagenesis that the backbone rigidity at residue 293 is important for controlling the

conformation of the flavin that is central to coordinating the complexities of catalysis.^[235]

The catalytic mechanism of PHBH has been studied by stopped-flow absorbance spectroscopy.^[77,78,140] The overall reaction can be divided into two half reactions, the reductive half reaction and the oxidative half reaction, each consisting of several reaction steps (Scheme 2). The reductive half reaction, which can be studied under anaerobic conditions, involves ternary complex formation. Only in the presence of substrate fast reduction of the FAD cofactor by NADPH is observed.^[136,221] In the absence of substrate, a binary complex between NADPH and the enzyme results in a reduction rate that is 10^5 times slower. Thus, the substrate is an essential component in the reduction reaction because it stimulates the rate of flavin reduction, without being converted itself.



Scheme 2. Catalytic cycle of flavoprotein aromatic hydroxylases.^[77,78,140] $EFl_{ox}S$, oxidized enzyme-substrate complex; $EFl_{red}S$, reduced enzyme-substrate complex; $EFl_{HOOH}S$, flavin C(4a)-hydroperoxide enzyme-substrate complex (intermediate I); $EFl_{OH}P^*$, flavin C(4a)-hydroxide enzyme-hydroxycyclohexanedione product complex (intermediate II); $EFl_{OH}P$, flavin C(4a)-hydroxide enzyme-product complex (intermediate III); S, substrate; P, product.

Only a few substrate analogs can stimulate the rate of flavin reduction.^[89,276] Some benzoate derivatives bind to the enzyme and elicit its reduction but are not converted, and are therefore called effectors. The potential substrate 4-aminobenzoate binds to the enzyme in a similar way as 4-hydroxybenzoate,^[263] but the reduction reaction in the presence of 4-aminobenzoate is very slow,^[77] indicating a fine-tuning of the mechanism by which the substrate exerts its effector action. The rate of reduction does not correlate with the orientation of the flavin ring observed in the crystal structures, and all evidence presently available suggests that the effector specificity is linked to the ionic state of the

substrate and the hydrogen bond network connecting the 4-hydroxyl group with the protein surface.^[234,263]

The fast release of NADP⁺ from the reduced ternary complex is well established.^[77,81,140] Furthermore, it has been demonstrated that the rate of dissociation of the substrate from the reduced enzyme-substrate complex is 5000 times slower than from the binary complex with the flavin in its oxidized state.^[77] In addition to the increased reduction rate induced by substrate binding, the slow rate of substrate dissociation from the reduced enzyme is a second mechanism by which the enzyme controls the optimal use of valuable reducing equivalents.

The oxidative half reaction includes the reaction steps that lead to the hydroxylation of the substrate.^[77,78] Upon reaction of the reduced enzyme-substrate complex with molecular oxygen the flavin C(4a)-hydroperoxide intermediate is formed. Several authors have discussed the actual way in which this reaction occurs, since in principle the reaction between singlet reduced flavin and triplet molecular oxygen is spin forbidden.^[215] The flavin C(4a)-hydroperoxide species is generally referred to as intermediate I and has a typical absorption spectrum.^[77,78] Protonation of the distal oxygen of the peroxide moiety increases the electrophilic reactivity of the flavin peroxide and facilitates its subsequent attack on the nucleophilic carbon centre of the substrate. In the hydroxylation step, the product 3,4-dihydroxybenzoate is formed together with the flavin C(4a)-hydroxide (Intermediate III). The aromatic product initially is formed in its keto isomeric form (Intermediate II)^[190,261] which isomerizes to give the energetically favoured dihydroxy isomer. Evidence for the initial formation of the quinoid form of the aromatic product comes from experiments with 2,4-dihydroxybenzoate as the substrate.^[77,78,336]

In PHBH, the electron density on the C3 reaction centre of the substrate is increased by deprotonation of the phenol. This is supported by spectroscopic binding studies,^[270,309,310] by molecular orbital calculations on the reactivity of the substrate,^[325] and by reaction pathway calculations.^[244] Moreover, the role of Tyr201 and Tyr385 in substrate activation is well established.^[80]

In the presence of non-substrate effectors, the flavin C(4a)-hydroperoxide decays to oxidized enzyme with release of hydrogen peroxide.^[276] Uncoupling can also occur with true substrates. The extent to which this uncoupling occurs is not only dependent on the nature and possibilities for activation of the substrate but is also influenced by the microenvironment of the active site. Other flavin dependent monooxygenases as well as mutant PHBH enzymes may vary in the efficiency of substrate hydroxylation.^[80]

The final steps in the catalytic cycle are the elimination of water from the flavin C(4a)-hydroxide and product release. Studies with 2-fluoro-4-hydroxybenzoate^[141] and with the related phenol hydroxylase^[190,296] have indicated that in this step a dead-end complex can be formed between the flavin C(4a)-hydroxide form of the enzyme and the substrate leading to substrate inhibition.

Studies from active-site variants have revealed that the scope of reactions, catalyzed by PHBH cannot easily be changed by site-directed mutagenesis. Nevertheless, replacement of Tyr385 by Phe affects the regiospecificity of hydroxylation^[79] and turns the enzyme into a more efficient dehalogenase.^[322] Studies with tetrafluoro-4-hydroxybenzoate revealed that the hydroxylation of this fluorinated substrate is not restricted to the C3 center of the aromatic ring but rather involves sequential oxygenation steps. ¹⁹F NMR analysis showed that the initial aromatic product 2,5,6-trifluoro-3,4-dihydroxybenzoate is further converted to 5,6-difluoro-

2,3,4-trihydroxybenzoate and that this reaction is most efficient with mutant Y385F. The initial dihydroxy product is not bound in a unique regiospecific orientation as also 2,6-difluoro-3,4,5-trihydroxybenzoate is formed. Due to elimination of the halogen substituent as a fluoride anion and the electron balance of the reaction, hydroxylation of tetrafluoro-4-hydroxybenzoate involves the formation of quinone intermediates as primary products of oxygenolytic dehalogenation.^[141] Ascorbate competes favorably with NADPH for the nonenzymatic reduction of these reactive intermediates and prevents the accumulation of nonspecific oxidation products.^[322]

PHBH does not contain a common dinucleotide fold for NADPH binding.^[83] Studies from site-directed PHBH mutants have gained some insight in the mode of coenzyme recognition. Based on the properties of His162 and Arg269 variants, an interdomain binding mode for NADPH was proposed, where His162 and Arg269 interact with the pyrophosphate moiety of NADPH.^[84] Furthermore, by changing several amino acid residues in the solvent exposed helix H2 region, it was possible to switch the PHBH coenzyme specificity.^[87] This is the first coenzyme reversion of a member of a superfamily of flavoenzymes where the exact binding mode of the cofactor is unknown. The coenzyme switch suggests that in PHBH, an arginine is important in the recognition of the 2'-phosphate moiety of NADPH and that an acidic group (Asp/Glu) is required for the recognition of the 2'-OH group of NADH. This strengthens the idea that in NAD(P)H-dependent enzymes the main determinants for coenzyme recognition are conserved^[36] and is in keeping with the hypothesis that biological specificity is caused to some extent by hydrogen bonding but is best mediated by charged residues.^[93]

Recently, the first crystal structure of PHBH with NADPH was obtained.^[333] In this structure of the R220Q mutant, the NADPH binds in an extended conformation at the enzyme surface in a groove that crosses the binding site of FAD. The pyrophosphate moiety is indeed situated in between the FAD binding domain and substrate binding domain but especially the nicotinamide moiety is located in a region, not expected to be relevant for catalysis. Therefore, a role was proposed for protein and ligand dynamics with multiple movements involving the protein, the two cofactors and the substrate.^[333] However, the R220Q mutation changes the interdomain interaction, possibly influencing the mode of NADPH binding.

In conclusion, PHBH is an enzyme with a rather narrow substrate specificity. Besides the natural substrate (Scheme 1), the enzyme can convert 2,4-dihydroxybenzoate and a series of fluorinated 4-hydroxybenzoates. Most substrates are regioselectively hydroxylated at the C3-position of the aromatic ring. With some substrate analogs and certain mutant enzymes, hydroxylation at C2 and C5 is feasible as well.

3-Hydroxyphenylacetate 6-hydroxylase

3-Hydroxyphenylacetate 6-hydroxylase (HPAH) is an NAD(P)H-dependent FAD-containing monooxygenase involved in the catabolism of phenylacetate in *Flavobacterium* sp. JS-7.^[311] The enzyme has a subunit mass of 63 kDa and exists mainly as a homodimer in solution. HPAH from *Flavobacterium* is optimally active around pH 8.3 but is most stable around pH 7.0. Above pH 7.5, the enzyme easily loses FAD and during purification, the presence of FAD and dithiothreitol are needed for high recovery of enzyme activity. Like many other flavoprotein monooxygenases, HPAH is severely inhibited by chloride ions, competitive to the aromatic substrate.

HPAH has a narrow substrate specificity. Besides 3-hydroxyphenylacetate which is stoichiometrically converted to 2,5-dihydroxyphenylacetate (Scheme 1), the only alternative substrate is 3,4-dihydroxyphenylacetate. This compound is exclusively converted to the (red) quinoid form of 2,4,5-trihydroxyphenylacetate. Due to severe uncoupling of hydroxylation (formation of hydrogen peroxide), more than two equivalents of NAD(P)H are needed for the conversion of one equivalent of 3,4-dihydroxyphenylacetate. Therefore, a catalase and glucose-6-phosphate containing NADPH generating system^[238] is recommended to generate this product at a large scale.

4-Hydroxybenzoate 1-hydroxylase

4-Hydroxybenzoate 1-hydroxylase from *Candida parapsilosis* CBS604 is a monomeric FAD-dependent monooxygenase of about 50 kDa.^[313] This enzyme is induced when the yeast is grown on either 4-hydroxybenzoate, 2,4-dihydroxybenzoate, or 3,4-dihydroxybenzoate as the sole carbon source.^[201] 4-Hydroxybenzoate 1-hydroxylase is optimally active at pH 8.0 and catalyzes the oxidative decarboxylation of a wide range of 4-hydroxybenzoate derivatives to the corresponding hydroquinones with the stoichiometric consumption of NAD(P)H and oxygen (Scheme 1).^[82] Interestingly, nearly no hydroxylation activity is observed with 4-aminobenzoates. 4-Hydroxybenzoate 1-hydroxylase prefers NADH as the electron donor and is inhibited by chloride ions and by 3,5-dichloro-4-hydroxybenzoate, 4-hydroxy-3,5-dinitrobenzoate and 4-hydroxyisophthalate which are competitors of the aromatic substrate. From the high activity of 4-hydroxybenzoate 1-hydroxylase with tetrafluoro-4-hydroxybenzoate and 4-hydroxy-3-nitrobenzoate and the molecular orbital characteristics of 4-hydroxybenzoate derivatives it was inferred that the phenolate form of the substrates is important for catalysis and that substrate hydroxylation involves the electrophilic attack of the putative flavinhydroperoxide at the C1-atom of the aromatic ring.^[82] The resulting benzoquinone species is subsequently converted to the hydroquinone by spontaneous release of the carboxyl side chain.^[82]

Hydroquinone hydroxylase

Hydroquinone hydroxylase is a homodimeric FAD-dependent monooxygenase of about 150 kDa, which is also involved in the degradation of 4-hydroxybenzoate in *Candida parapsilosis* CBS604.^[88] This enzyme is abundantly expressed when the yeast is grown either on 4-hydroxybenzoate, 2,4-dihydroxybenzoate, 1,3-dihydroxybenzene or 1,4-dihydroxybenzene as sole carbon source. Hydroquinone hydroxylase catalyzes the *ortho*-hydroxylation of a wide range of monocyclic phenols with the stoichiometric consumption of NADPH and oxygen (Scheme 1). The hydroxylation of monofluorinated phenols is highly regiospecific with a preference for C6 hydroxylation. This regiospecificity of hydroxylation resembles that of phenol hydroxylase from *T. cutaneum*,^[236] but differs from the regiochemistry experienced with whole cells of the gram-positive bacterium *Rhodococcus opacus* 1G, where it was found that oxidative dehalogenation of 2-halogenated phenols is preferred to hydroxylation of the aromatic ring at a non-halogenated position.^[26] It also differs from the transformation of monofluorophenols in whole cells of *R. opacus* 1cp, where it was found that the initially formed catechols are further converted to the corresponding fluoropyrogallols.^[94]

During purification it was noted that hydroquinone hydroxylase is sensitive to limited proteolysis.^[88] Proteolytic cleavage does not influence the enzyme dimeric nature but results in relatively stable protein fragments of 55, 43, 35 and 22 kDa.

N-terminal peptide sequence analysis revealed the presence of two nick sites and showed that hydroquinone hydroxylase from *C. parapsilosis* is structurally related to phenol hydroxylase from *T. cutaneum*. The latter enzyme has been overexpressed in *E. coli*^[156] and its three-dimensional structure was recently solved.^[76] From the crystallographic data it was argued that the severe uncoupling of hydroxylation in phenol hydroxylase is related to a movement of the flavin ring in concert with a large conformational change of a flexible protein segment which acts as an active site lid. The C-terminal part of this flexible segment is closest to the flavin and its amino acid sequence is not conserved in hydroquinone hydroxylase from *C. parapsilosis*.^[88] This suggests that the efficient hydroxylation of phenolic substrates in hydroquinone hydroxylase from *C. parapsilosis* is related to the performance of the active site lid and that an effective closure of this lid sequesters the hydroxylation site from solvent, thereby preventing the unproductive formation of hydrogen peroxide.

2-Hydroxybiphenyl 3-monooxygenase

2-Hydroxybiphenyl 3-monooxygenase (HbpA) is an inducible FAD-dependent aromatic hydroxylase involved in the degradation of the fungicide 2-hydroxybiphenyl by the soil bacterium *Pseudomonas azelaica* HBP1.^[287] This strain employs a *meta*-cleavage pathway with a broad substrate spectrum for breaking down 2-hydroxybiphenyls.^[169] HbpA is a homotetramer of about 250 kDa, is optimally active around pH 7.5 and prefers NADH as the electron donor. 2,3-Dihydroxybiphenyl, the product of the reaction with 2-hydroxybiphenyl (Scheme 1) is a non-substrate effector, strongly facilitating NADH oxidation and hydrogen peroxide formation without being hydroxylated.

HbpA catalyzes the *ortho*-hydroxylation of a wide range of 2-substituted phenols. Besides phenyl rings and aliphatic side chains, halogens are accepted as phenol substituents.^[131] The *hbpA* gene has been cloned in *E. coli*.^[287] and the recombinant strain was used as a whole cell biocatalyst for the large-scale production of 2-substituted catechols.^[132] The whole cell approach has the advantage of coenzyme recycling but can be problematic when the substrate and/or product are toxic to the cells. In case of HbpA, the toxic effects of 2-hydroxybiphenyl are minimized by feeding the substrate to the reactor at a rate slightly below the maximum biooxidation rate. Furthermore, the 3-phenylcatechol product can be removed by continuous adsorption on a solid resin.^[132] In another biocatalytic process, partially purified recombinant HbpA was used in combination with a formate/formate dehydrogenase cofactor recycling system for the preparative regioselective hydroxylation of 2-hydroxybiphenyl.^[258] By using organic/aqueous emulsions, coupled with *in situ* product recovery, volumetric productivities of up to 0.45 g l⁻¹ h⁻¹ were obtained.

The catalytic mechanism of HbpA has been investigated at 7°C by stopped-flow absorption spectroscopy.^[288] The reaction essentially follows the catalytic cycle depicted in Scheme 2. Binding of 2-hydroxybiphenyl highly stimulates the rate of enzyme reduction by NADH. During this reaction a transient charge-transfer complex is formed between the reduced flavin and NAD⁺. Free reduced HbpA reacts rapidly with oxygen to form oxidized enzyme with no appearance of intermediates. In the presence of 2-hydroxybiphenyl (but not in the presence of 3-phenylcatechol), two consecutive spectral intermediates are observed, representing the flavin C(4a)-hydroperoxide and the flavin C(4a)-hydroxide, respectively. These data are consistent with a ternary complex mechanism in which the aromatic substrate has strict control in both the reductive and

oxidative half-reaction in a way that reactions leading to substrate hydroxylation are favoured over those leading to the futile formation of hydrogen peroxide.

The catalytic scope and performance of HbpA have been improved by directed evolution using error-prone PCR.^[199] *In situ* screening of mutant libraries resulted in the identification of the I244V variant, which has an increased activity towards 2-*tert*-butylphenol, 2-methoxyphenol and the natural substrate 2-hydroxybiphenyl. The double replacement V368A/L417F was found to improve the efficiency of substrate hydroxylation by reducing the uncoupled oxidation of NADH. Sequence alignments revealed that the primary structure of HbpA shares 20% identity with phenol hydroxylase from *T. cutaneum*. Based on structure homology modeling it was inferred that Ile244 of HbpA is located in the substrate binding pocket and is involved in accommodating the phenyl substituent of the phenol. In contrast, Val368 and Leu417 are not close to the active site and would not have been obvious candidates for modification by rational design. In another study, laboratory evolution of HbpA resulted in an enzyme variant which hydroxylates indole and indole derivatives, such as hydroxyindoles or 5-bromoindole.^[200] This indigo-producing HbpA variant contains the amino acid substitutions Asp222Val and Val368Ala. Interestingly, Asp222 is located in the active site and corresponds to Tyr201 of PHBH and Tyr289 of phenol hydroxylase from *T. cutaneum*. Recent results from site-directed mutagenesis have indicated that Tyr289 in phenol hydroxylase is mainly involved in flavin reduction^[345] whereas Tyr201 in PHBH is also involved in substrate activation.^[79,89] In conclusion, these studies show that directed evolution is a powerful approach for changing the biocatalytic performance of a flavoenzyme.

Two-component aromatic hydroxylases

Besides from the single-component flavoprotein aromatic hydroxylases, there is also a group of flavin-dependent aromatic hydroxylases that consist of two protein components of different size. For 4-hydroxyphenylacetate 3-hydroxylase from *Pseudomonas putida* it was shown that the FAD-containing protein component acts as an NADH oxidase and that the presence of the other non-redox protein component is required for efficient substrate hydroxylation.^[9] So far, this is the only example of a flavoprotein hydroxylase where binding of another protein component is needed for the stabilization of the flavin hydroperoxide.

Another family of two-component flavin-dependent aromatic hydroxylases consists of a relatively small flavin reductase which generates reduced flavin at the expense of NAD(P)H and a large protein component which is essential for substrate hydroxylation.^[13,108] Besides from hydroxylases, also epoxide forming enzymes such as styrene monooxygenase^[231] and tryptophan 7-halogenase^[163] belong to this family. The exact mechanism by which the reduced flavin in these enzymes is transferred to the oxygenation site is as yet far from clear but it has been shown that the small reductase from the wild type strain can be replaced by a flavin reductase from another bacterium.^[108,163] In our group, we have characterized a two-component phenol hydroxylase from the thermophilic bacterium *Bacillus thermoglucosidasius* which is active with a range of simple phenols, including chlorophenols, fluorophenols and cresols.^[165] The large dimeric protein component of the recombinant phenol hydroxylase as expressed in *E. coli* is highly unstable in purified form, limiting structure-function relationship studies. The small dimeric flavin reductase on the other hand, is very stable in its recombinant form. Interestingly, each subunit of the reductase

contains a tightly bound FAD molecule which is involved in the NADH-dependent reduction of free flavins, including FAD, FMN and riboflavin.^[338] However, like tryptophan 7-halogenase,^[163] the large oxygenase component of phenol hydroxylase from *B. thermoglucosidasius* is specific for FAD.

3 Baeyer-Villiger monooxygenases

Baeyer-Villiger monooxygenases (BVMOs) are NAD(P)H-dependent flavoenzymes that catalyze Baeyer-Villiger reactions, i.e. the oxidation of ketones to esters or lactones.^[10,331] In the enzymatic Baeyer-Villiger reaction, the protein-bound flavin peroxide is active in its deprotonated form thereby performing a nucleophilic attack on the carbon atom of the substrate ketone.^[252,265] From rapid reaction studies on *Acinetobacter* cyclohexanone monooxygenase, evidence was obtained that the relatively stable flavin peroxide can undergo acid/base equilibrium.^[268] This might explain why BVMOs are also active with certain electron rich compounds^[331] and underlines the ambivalent character of the flavin (hydro)peroxide oxygenation species.

BVMOs are versatile biocatalysts that have been widely used for the regio- and stereoselective transformation of aliphatic ketones.^[248,331,343] In view of the need of NAD(P)H-recycling, most of these reactions have been performed with whole microbial cells.^[282] Relatively little is known about BVMOs that are active with aromatic compounds. However, several aerobic microorganisms are capable of utilizing aryl ketones for their growth^[294] and recently, we succeeded in the purification of a Baeyer-Villiger type flavoenzyme that catalyzes the first step in the degradation of 4-hydroxyacetophenone in *Pseudomonas fluorescens* ACB.^[157,209] Characterization revealed that this 4-hydroxyacetophenone monooxygenase (HAPMO) is a homodimer of about 140 kDa with each subunit containing a tightly non-covalently bound FAD. In contrast, HAPMO involved in the degradation of 4-ethylphenol in *P. putida* JD1 purifies as a monomer of 70 kDa.^[294]

HAPMO from *P. fluorescens* catalyzes the strictly NADPH-dependent and stoichiometric oxidation of 4-hydroxyacetophenone to 4-hydroxyphenyl acetate (Scheme 1). Besides the natural substrate, HAPMO is active with a wide range of other aryl ketones.^[157] The highest catalytic efficiency is observed with compounds bearing an electron donating substituent at the *para*-position of the aromatic ring. HAPMO is also active with 4-hydroxybenzaldehyde and 4-hydroxypropiophenone.

Ring-substituted phenyl acetates are valuable synthons for the production of fine chemicals and neuroactive pharmaceuticals.^[125] However, the large-scale production of phenyl acetates by whole cells of *P. fluorescens* ACB is limited by the presence of a highly active esterase.^[133,209] ¹⁹F NMR studies with purified HAPMO at pH 6 and pH 8 showed that the Baeyer-Villiger oxidation of 4-fluoroacetophenones occurs faster at pH 8 but that the fluorophenyl acetates produced are better stabilized at pH 6.^[209] Thus, the large-scale biocatalytic production of ring-substituted phenyl acetates requires carefully selected conditions and should either be performed by i) using an engineered microbial strain that lacks esterase activity or ii) by using isolated enzyme coupled with an efficient cofactor recycling system.^[146]

With the above considerations in mind, the DNA of *P. fluorescens* ACB was isolated and the gene cluster involved in the degradation of 4-hydroxyacetophenone was characterized.^[157] The fourth gene of this cluster (*hapD*) codes for 4-hydroxyphenyl acetate hydrolase whereas the fifth gene (*hapE*) encodes HAPMO. Sequence analysis revealed that except for an N-terminal extension of about 135 residues, HAPMO shares

30% sequence identity with two other characterized BVMOs, cyclohexanone monooxygenase and steroid monooxygenase, classifying the enzyme as a type I BVMO. These BVMOs are FAD and NADPH dependent and have identical subunits. Type II BVMOs on the other hand are FMN and NADH dependent and are composed of $\alpha_2\beta$ trimers.^[343] The role of the N-terminal extension in HAPMO is not clear, but studies of truncated forms indicate that the N-terminal domain is important for the protein structural integrity.^[157]

Type I BVMOs contain two dinucleotide binding motifs ($\beta\alpha\beta$ -folds), one for FAD binding and one for NAD(P) binding. Because no crystal structures of these flavoenzymes are available yet, it was of interest to probe the functional role of these sequence motifs in further detail. Using newly reported BVMO sequences, a BVMO identifying-sequence motif: FxGxxxHxxxW(P/D) was uncovered that is critically involved in catalysis.^[103] The important role of the histidine in this fingerprint sequence was confirmed by the negligible activity of the H296A mutant. The functional role of another sequence motif was assessed by replacement of the conserved Gly490.^[157] Analysis of the G490A mutant revealed a dramatic effect on the interaction with NADPH, suggesting that the ATG motif comprising Gly490 is involved in NADPH binding.

4 Flavoprotein oxidases

Flavoprotein oxidases react with their substrates without the need of external cofactors. Catalysis involves two half-reactions in which first the flavin cofactor is reduced by the substrate, and subsequently the reduced flavin is reoxidized by molecular oxygen.^[193] Vanillyl-alcohol oxidase (VAO) from *Penicillium simplicissimum* is the prototype flavoprotein oxidase that is active with phenolic compounds. VAO is a homooctamer of 520 kDa with each subunit containing a covalently bound 8α -(N3-histidyl)-FAD.^[59] VAO catalyzes the conversion of vanillyl alcohol to vanillin in the presence of molecular oxygen (Scheme 1). Besides from vanillyl alcohol, the enzyme is active with a wide range of other phenolic compounds.^[97,316] As discussed elsewhere,^[320] some of the VAO-mediated reactions are of industrial relevance.

Stopped-flow kinetic studies^[98] have indicated that the reaction of VAO with phenolic substrates involves the initial transfer of a hydride from the C α -atom of the substrate to the N5-atom of the flavin, resulting in the formation of a complex between reduced enzyme and *p*-quinone methide product intermediate. Next, the reduced flavin is reoxidized by molecular oxygen, yielding hydrogen peroxide, and the *p*-quinone methide intermediate is further converted by water in the enzyme active site. With eugenol as a substrate, this leads to the stoichiometric formation of coniferyl alcohol (Scheme 1), whereas with 4-ethylphenol, the hydroxyl group becomes exclusively inserted at the C α -atom, resulting in the formation of 1-(4'-hydroxyphenyl)ethanol (Scheme 1). With short-chain 4-alkylphenols, the protein-bound quinone methide is attacked by water in a stereoselective manner yielding the (*R*)-enantiomer of the alcohol product in high enantiomeric excess.^[67] However, with long-chain 4-alkylphenols, the *p*-quinone methide is no longer attacked by water and rearranges to the alkene.^[316] A similar observation was made when the reaction with 4-propylphenol was performed in organic solvents,^[321] leading to the conclusion that the outcome of products formed from short-chain and medium-chain 4-alkylphenols is due to variations in the intrinsic reactivity of the enzyme-bound *p*-quinone methide, the water accessibility of the enzyme active site, and the orientation of the alkyl side-chain of the substrate. No

catalytic activity was observed with 4-alkylphenols when the aliphatic side-chain is longer than seven carbon atoms.^[316] This is in line with structural data which show that the VAO active site cavity is completely filled when the inhibitor 1-(4'-heptenyl)phenol is bound.^[195]

From the VAO structure,^[195] several amino acid residues have been implicated to play an important role in catalysis. Studies from His61 and His422 mutants established that the covalent linkage between the C8 α atom of the isoalloxazine ring of the flavin and the N3 atom of His422 raises the redox potential of the FAD cofactor, thereby increasing the oxidative power of the enzyme.^[100,102] Catalysis is also facilitated by ionization of the phenolic moiety of the substrate as induced by hydrogen bonding to Tyr108, Tyr503, and Arg504 (Figure 3). Another key residue is Asp170, which is located close to the N5-atom of the flavin and the reactive methylene group of the substrate. With vanillyl alcohol, eugenol, and 4-(methoxymethyl)phenol as substrates, the conserved mutant D170E is up to 100-fold less active than wild type VAO whereas with other Asp170 variants a more than 1,000-fold decrease in enzyme activity is observed.^[318] As no structural changes were found in the mutant enzymes, this indicates that Asp170 is crucial for efficient redox catalysis.

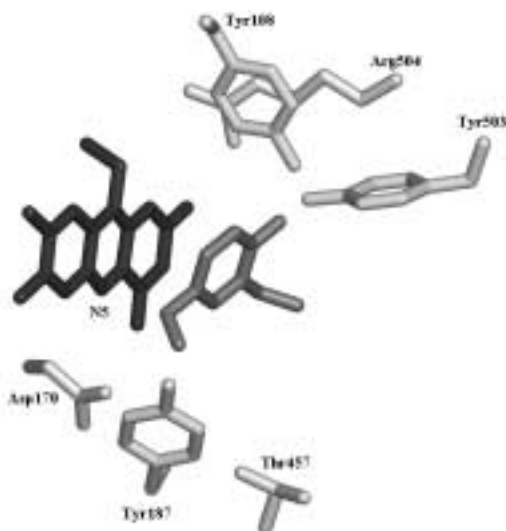


Fig. 3. Schematic representation of the active site of the enzyme-isoeugenol complex of vanillyl-alcohol oxidase from *Penicillium simplicissimum*.^[195] The isoalloxazine ring of FAD is black, the inhibitor is gray and the protein residues are white. Asp170 is positioned at 0.35 nm from flavin N5 and the C α -atom of isoeugenol.

Interestingly, substitution of Asp170 by Ser or Glu strongly influences the hydroxylation efficiency of VAO with 4-alkylphenols.^[319] Whereas the D170A and D170S mutants favor the hydration of the *p*-quinone methide intermediate, the D170E mutant favors the formation of alkenes. This suggests that the efficiency of hydroxylation of 4-alkylphenols is regulated by the bulkiness of the side-chain of residue 170 and not by its ionic character.

Studies from site-directed double mutants revealed that the stereochemistry of VAO with short-chain 4-alkylphenols is also related to the function of Asp170.^[317] D170A and D170S preferentially hydroxylate 4-ethylphenol to the (*R*)-enantiomer of 1-(4'-hydroxyphenyl)ethanol). However, when the acidic residue is relocated to the other face of the substrate binding pocket (D170A/T457E and D170S/T457E variants),

the enzyme exhibits an inverted stereoselectivity with 4-ethylphenol. This high preference for the (*S*)-enantiomer is likely explained by the Glu457 activated attack of a water molecule from the opposite face of the substrate.

5 Conclusion

Flavoprotein monooxygenases and oxidases are useful enzymes for the selective introduction of oxygen atoms in phenolic compounds. Flavoprotein monooxygenases work optimally around pH 8 whereas VAO is most active near pH 10. Flavoprotein aromatic hydroxylases have a unique regiochemistry, allowing the synthesis of a wide range of catechols and hydroquinones. Most flavoprotein aromatic hydroxylases have a narrow substrate specificity and can only be used for the synthesis of a selected range of products. The substrate specificity of PHBH can be broadened by site-directed mutagenesis, but only to a limited extent. Some flavoprotein aromatic hydroxylases like e.g. 4-hydroxybenzoate 1-hydroxylase and HbpA, have a relaxed substrate specificity, allowing the synthesis of a range of ring-substituted hydroquinones and catechols. Directed evolution has proven to be an attractive method for the improvement of the efficiency of substrate hydroxylation of HbpA and for the introduction of new activities.

Two-component flavin-dependent monooxygenases represent a newly recognized family of oxidative enzymes and their biocatalytic performance is unexplored. It is anticipated that studies from structural and functional genomics^[44] will allow a more thorough characterization of this class of monooxygenases and provide future possibilities for synthetic applications.

BVMOs are extremely useful for the synthesis of esters and lactones and for asymmetric oxidations. HAPMO is the first described BVMO that is active with phenolic compounds. The scope of reactions of HAPMO has not yet been fully explored but it is clear that this enzyme converts a wide range of acetophenones into the corresponding phenyl acetates.

Flavoprotein oxidases such as VAO are capable of introducing side chain modifications in *p*-substituted phenols. This is useful for the synthesis of flavors and fragrances and for the production of pure enantiomers. Studies from site-directed mutants have demonstrated that the stereoselectivity of VAO can be inverted by rational redesign.

Insight into the structure, mechanism and biochemical properties of oxidative flavoenzymes is of great help to select for biocatalysts with a high degree of chemo-, regio- and stereoselectivity. In view of the need of expensive cofactors, it is expected that NAD(P)H-dependent flavoprotein monooxygenases will be mainly used in whole cell systems.^[132,182,257,271,282,332] Structure-function relationship studies on PHBH and HAPMO have given some insight why these enzymes are strictly dependent on NADPH. Such studies are not only useful for the redesign of the coenzyme specificity but will also teach us more about the evolutionary relationship of flavoenzymes.

Acknowledgements

This work was supported by the Council for Chemical Sciences of the Netherlands Organization for Scientific Research (CW-NWO), division 'Procesvernieuwing voor een Schoner Milieu', by the Innovation Oriented Research Program (IOP) Catalysis of the Dutch Ministry of Economic Affairs (project IKA 96005) and by the European Community (Framework V, Copernicus project EC Grant ICA2-CT-2000-10006).

Chapter 3

4-HYDROXYACETOPHENONE MONOOXYGENASE FROM *PSEUDOMONAS FLUORESCENS* ACB

A NOVEL FLAVOPROTEIN CATALYZING BAEYER-VILLIGER OXIDATION OF
AROMATIC COMPOUNDS

Nanne M. Kamerbeek, Mariëlle J.H. Moonen, Jos G.M. van der Ven,
Willem J.H. van Berkel, Marco W. Fraaije and Dick B. Janssen

European Journal of Biochemistry. 2001. Vol. 268, No 9, pp. 2547-2557

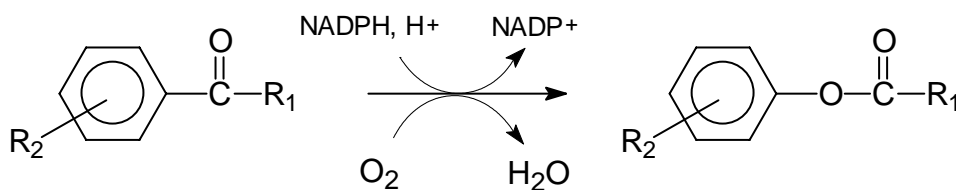
The novel nucleotide sequence data published here have been submitted to GenBank and are available under accession number AF355751

A novel flavoprotein, catalyzing the NADPH dependent oxidation of 4-hydroxyacetophenone to 4-hydroxyphenyl acetate, was purified to homogeneity from *Pseudomonas fluorescens* ACB. Characterization of the purified enzyme showed that 4-hydroxyacetophenone monooxygenase (HAPMO) is a homodimer of about 140 kDa with each subunit containing a non-covalently bound FAD molecule. HAPMO displays a tight coupling between NADPH oxidation and substrate oxygenation. Besides 4-hydroxyacetophenone a wide range of other acetophenones are readily converted via a Baeyer-Villiger rearrangement reaction into the corresponding phenyl acetates. The *P. fluorescens* HAPMO gene (*hapE*) was characterized. It encoded a 640-amino acid protein with a deduced mass of 71,884 Da. Except for an N-terminal extension of about 135 residues, the sequence of HAPMO shares significant similarity with two known types of Baeyer-Villiger monooxygenases: cyclohexanone monooxygenase (27-33% sequence identity) and steroid monooxygenase (33% sequence identity). The HAPMO sequence contains several sequence motifs indicative for the presence of two Rossmann fold domains involved in FAD and NADPH binding. The functional role of a recently identified flavoprotein sequence motif (ATG) was explored by site directed mutagenesis. Replacement of the strictly conserved glycine (G490) resulted in a dramatic effect on catalysis. From a kinetic analysis of the G490A mutant it is concluded that the observed sequence motif serves a structural function which is of importance for NADPH binding.

Introduction

The aerobic degradation of aromatic compounds by soil bacteria depends on the activity of oxygenases.^[122] So far two classes of flavoprotein hydroxylases have been shown to act as aromatic monooxygenases: the single component aromatic hydroxylases^[287] and two-component hydroxylases.^[9,13] The single component aromatic hydroxylases share a typical dinucleotide binding fold for complexation of the FAD cofactor while lacking an NAD(P) binding fold.^[83] An extensively studied member of this widespread class of flavoenzymes is *p*-hydroxybenzoate hydroxylase.^[80,87] Mechanistic studies have shown that the monooxygenation reactions catalyzed by single component aromatic hydroxylases are preceded by NAD(P)H mediated flavin reduction. The reduced flavin then reacts with dioxygen to form a reactive electrophilic hydroperoxyflavin intermediate which is able to introduce a hydroxyl group into an activated aromatic ring.^[77] The two-component hydroxylases typically consist of a relatively small flavin reductase which generates reduced flavin at the expense of NAD(P)H. After intermolecular transfer, the reduced flavin is used by the large oxygenating component to catalyze substrate hydroxylation.^[108,350] Although the genes of several of these two-component hydroxylases have been identified, mechanistic data on this type of monooxygenases are scarce.

Except for the above mentioned monooxygenation reactions another way of flavoenzyme mediated oxygenation of aromatic compounds has been suggested in the literature. For several bacteria it was found that their ability to degrade aromatic compounds depends on an enzyme-mediated Baeyer-Villiger reaction in which an oxygen atom is inserted between the aromatic ring and a ketone side-chain (Scheme 1). These Baeyer-Villiger reactions have been detected during studies on the microbial degradation of several ring-substituted acetophenones^[52,127,133] and 4-ethylphenol.^[55,154] Recently, a Baeyer-Villiger monooxygenase from *Pseudomonas putida* JD1, involved in 4-ethylphenol metabolism, was purified and partially characterized.^[294] However, enzymes involved in these atypical metabolic pathways have never been cloned.



Scheme 1. Baeyer-Villiger reaction observed during microbial degradation of aromatic compounds

All Baeyer-Villiger monooxygenases identified so far were shown to be flavoproteins.^[343] As for the single component hydroxylases, also for these enzymes a peroxygenated flavin has been proposed as the oxygenating species.^[252] However, in the Baeyer-Villiger reaction this reactive flavin intermediate is supposed to act as a nucleophile indicating that in these monooxygenases a peroxyflavin anion is involved in substrate attack.^[193,267]

Pseudomonas fluorescens ACB is able to use 4-hydroxyacetophenone as sole carbon and energy source.^[133] Since it was suggested that the microbial degradation of this phenolic compound is initiated by a Baeyer-Villiger reaction (Scheme 1), we started a study to identify this atypical aromatic monooxygenase. We here report on the

purification, gene cloning, sequence analysis and characterization of 4-hydroxyacetophenone monooxygenase (HAPMO). It is shown that the enzyme is a FAD-dependent Baeyer-Villiger monooxygenase that is active with a wide range of aromatic ketones. A preliminary report on the purification of HAPMO from *P. fluorescens* ACB has been presented elsewhere.^[208]

Material and Methods

Chemicals

Restriction enzymes, 7-deaza-dGTP, and isopropyl β -D-thiogalactopyranoside were obtained from Roche. NADH, NADPH, dithiothreitol (DTT), glucose oxidase (grade II) and catalase were from Boehringer. Tris, FAD, FMN and riboflavin were from Sigma. Q-Sepharose Fast Flow, phenyl-Sepharose Fast Flow, Superdex 200 Prep Grade, Superdex PG200 HR 10/30 and molecular weight markers were from Pharmacia. Bio-Gel P-6DG and Macro-Prep Ceramic Hydroxyapatite (Type I, particle size 20 μ m) were from Bio-Rad. Acrylamide, bisacrylamide and Coomassie brilliant blue G250 were from Serva. Aromatic ketones were purchased from Acros, Aldrich, Fluorochem and Lancaster. Stock ketone solutions were prepared in dimethyl formamide. $H_2^{18}O$ (97 atom % ^{18}O) was obtained from Campro (Elst, The Netherlands). All other chemicals were of commercially available analytical grade.

Bacterial strains and culture conditions

P. fluorescens ACB was kindly provided by Dr. D.D. Focht (Univ. of California, Riverside, USA). *P. fluorescens* ACB was isolated from activated sewage sludge by enrichment and serial transfer with 4-hydroxyacetophenone as growth substrate.^[133] *P. fluorescens* ACB was grown in 0.8% Nutrient Broth (Difco) at 30°C or in minimal medium based on Kröckel and Focht,^[172] containing per liter demineralized water: 3.5 g Na_2HPO_4 , 1.4 g KH_2PO_4 , 0.5 g $(NH_4)_2SO_4$, 0.2 g $MgSO_4 \cdot 7H_2O$, 10 mg yeast extract and 5 ml of a trace elements solution. The trace elements solution contained per liter: 780 mg $Ca(NO_3)_2 \cdot 4H_2O$, 200 mg $FeSO_4 \cdot 7H_2O$, 10 mg $ZnSO_4 \cdot 7H_2O$, 10 mg H_3BO_3 , 11.8 mg $CoSO_4 \cdot 7H_2O$, 4 mg $MnSO_4 \cdot 1H_2O$, 3 mg $Na_2MoO_4 \cdot 2H_2O$, 2 mg $NiCl_2 \cdot 6H_2O$, 10 mg $CuSO_4 \cdot 5H_2O$ and 2 mg $Na_2WO_4 \cdot 2H_2O$ (adjusted to pH 2 with H_2SO_4). The final pH of the medium was 7.0. Cells were grown on 10 mM 4-hydroxyacetophenone at 30°C in 2 l erlenmeyer flasks agitated at 270 rpm on an orbital shaker to provide suitable aeration. Large-scale growth, with 4-hydroxyacetophenone as the sole carbon and energy source, was performed batchwise in a 200-l fermentor (Bioengineering AG) at 30°C. During growth, the medium was stirred at 150 rpm and flushed with 30 liters of air/min and the pH was kept constant at pH 7.0 with NaOH. The fermentor was inoculated with 2 l of cell culture, and growth was induced by the addition of 5 mM 4-hydroxyacetophenone, followed by two portions of 10 mM 4-hydroxyacetophenone at 8-h intervals. The cells were harvested after 24 h and the cell paste (about 235 g (wet weight)) was frozen and stored at -80°C. Under these conditions, no significant loss of HAPMO activity occurred over a period of six months.

E. coli strains HB101, TOP10F' and BL21(DE3) pLysS were grown in Luria-Bertani medium supplemented with the appropriate antibiotic at 20°C, 30°C or 37°C.

Enzyme purification from *P. fluorescens* ACB

HAPMO was purified from *P. fluorescens* ACB to apparent homogeneity in two chromatographic steps. All purification steps were performed at 4°C. Cells (200 g wet weight) were suspended in 21 mM potassium phosphate, pH 7.1, and disrupted through a precooled Manton Gaulin press. The clarified cell extract was treated with 0.25%(w/v) protamine sulfate and the supernatant obtained after centrifugation was loaded onto a Q-Sepharose column (5 by 25 cm), equilibrated in 21 mM potassium phosphate, pH 7.1. After washing with two volumes of starting buffer, the HAPMO activity was eluted with a linear gradient of 0 – 0.7 M KCl in starting buffer. Active fractions were concentrated by ultrafiltration (Amicon YM-30 membrane) and diluted with three volumes of 10 mM potassium phosphate, pH 7.1. The enzyme solution was then adjusted to 1 M ammonium sulfate and loaded onto a phenyl Sepharose column (2.5 by 40 cm), equilibrated in 50 mM potassium phosphate, pH 7.1, containing 1 M ammonium sulfate. After washing with starting buffer, the HAPMO activity was eluted with a linear descending gradient of 1 – 0 M ammonium sulfate in 50 mM potassium phosphate, pH 7.1. Active fractions were concentrated by ultrafiltration, dialyzed in 50 mM potassium phosphate, pH 7.1, and stored at -80°C.

The 4-hydroxyphenyl acetate hydrolase was purified from *P. fluorescens* ACB in three chromatographic steps. Cell extract was loaded on a DEAE-Sepharose column (6 x 2.5 cm) equilibrated in 21 mM phosphate, pH 7.1. Esterase activity was eluted with a linear gradient of 0 – 0.7 M KCl in starting buffer. Active fractions were pooled, dialyzed against 1 mM phosphate, pH 7.1, and loaded on a hydroxyapatite column (7 x 3 cm) equilibrated in 1 mM phosphate, pH 7.1. Esterase activity was eluted with a linear gradient of 1 – 100 mM phosphate, pH 7.1. Active fractions were pooled, concentrated and loaded on a Sephacryl S-200 column (34 x 1 cm) running in 21 mM potassium phosphate, pH 7.1. The fractions with the highest esterase activity were pooled, resulting in an enzyme preparation which was more than 75% pure. For N-terminal sequencing, the esterase was isolated from a SDS-polyacrylamide gel.

Preparation of the genomic library

All DNA isolation and cloning procedures were carried out essentially as described by Sambrook et al.^[254] A genomic library of *P. fluorescens* ACB was constructed in the cosmid vector pLAFR3 according to the strategy described by Staskawicz et al.^[278] CsCl gradient centrifugation was used to purify pLAFR3 isolated from *E. coli* HB101. Constructed vector arms and inserts were ligated and subsequently packaged *in vitro* with a DNA-packaging kit (Boehringer). *E. coli* HB101 cells were infected with the packaging mix and transducts were selected on LB plates supplemented with tetracycline. From 10 transducts the plasmids were isolated and checked for insert by restriction analysis. All contained insert with an estimated average size of 17 kb. A total number of 2400 colonies were transferred to 96 well microtiter plates containing LB and tetracycline. After overnight growth, glycerol was added and the library was stored at -80°C until use.

“Touch down” PCR on total DNA

All PCR amplifications were performed as described by Innis and Gelfand.^[143] The 50- μ l reaction mixtures contained PCR buffer (Roche), 200 μ M of each dNTP, 20-30 pmol of primer, 1 to 5 units of *Taq* or *Pwo* polymerase and 10-100 ng template.

Cloning of 4-hydroxyacetophenone monooxygenase

The following degenerated primers were designed on the N-terminal amino acid sequences of the purified enzymes. For HAPMO: PAMOACB1 (forward) 5' GAAACCATGGCNGCNTTYAAYACNACNYTNCC 3' and PAMOACB2 (reverse) 5' GAAAACCATGGRTCTCTCTCTARTCNARNGWNGG 3', for the esterase (4-hydroxyphenyl acetate hydrolase): PESACB1 (forward) 5' GAAACCATGGCNCNTNGAYGTNGARWCNGCNCARCTNCTNGG 3'; and PESACB2 (reverse) 5' GAAAACCATGGYTCTGNCNAGYTGNCNAGNAGYTG 3'; (*Nco*I sites are underlined, the substituted nucleotide in PAMOACB1 is shown in bold). "Touch-down" PCR was performed on total DNA of strain *P. fluorescens* ACB.^[64] After initial denaturation for 5 min at 94°C, the cycling program was as follows: 1 min 94°C, 1 min 60°C (2°C decrease after each 2 cycles to 48°C) and elongation at 72°C for 2 min. In addition, 25 cycles were performed at a hybridization temperature of 48°C and elongation for 1 min at 72°C.

The fragment that was obtained by "touch-down" PCR, using the PESACB1 and PAPMO2 primers, was ligated into the pCR2.1-TOPO vector and then transformed to *E. coli* TOP10F' cells according to the recommendations of the manufacturer (Invitrogen). Plasmids containing insert were purified from overnight cultures with the High PureTM plasmid isolation kit (Roche).

Preparation of a DIG-labeled probe

To prepare the probe to screen the genomic library, the *hapD* gene in pCR2.1 was amplified with *Taq* polymerase (Roche) using the primers PESACBf (5' GAAACCATGGCTCTTGACGTCGAGACGGCACAGCTG 3') and PESACBr (5' GAAAGGATCCTAAAAAGGGTTTCAGCCAAGGCTTGAT 3') during 30 cycles of 1 min 94°C, 1 min 60°C and 1 min at 72°C. The amplified fragment was isolated from gel and DIG random-primed labeled according to the method described by the DIG system user's guide for filter hybridization (Boehringer) yielding the DIG-labeled probe HAP2.

Screening of the genomic library

For screening, the constructed library was plated from the frozen stock on LB plates supplemented with 12.5 µg/ml tetracycline and incubated overnight at 37°C. Colonies were transferred to cellulose nitrate membranes. The membranes were processed and subsequently hybridized with the DIG-labeled HAP2 probe at 68°C. Two primers, designed on the non-degenerated part of the *hapD* sequence were used to check *E. coli* clones which gave a positive signal after blotting: PESACB3 (5' GAAGCCGTTCCATTTCT 3') and PESACB4 (5' GCCAAGGCTTGATCTGATC 3'). Cycling parameters were as follows: 1 min at 94°C, 1 min at 57°C and 1 min at 72°C. As templates the pLAFR3 cosmids were isolated from the positive clones.

Cloning, expression and purification of recombinant HAPMO

The *hapE* gene was amplified with *Pwo* polymerase using the total DNA of *P. fluorescens* ACB as template. Therefore, two primers were designed: PAPMO1 (5' CACGGCATATGAGCGCCTTCAATACC 3', *Nde*I site is shown underlined) and PAPMO2 (5' CACGGGGATCCTCAACCTAGTTGGTAATCAGTCGG 3', *Bam*HI site is shown underlined). Cycling parameters were as follows: 30 cycles of 1 min at 94°C, 1 min at 56°C and 1 min at 72°C. After amplification, the gene was isolated from

gel, digested with *NdeI* and *BamHI* and ligated behind the T7 promoter of the *NdeI* / *BamHI* digested expression vector pET-5a (Promega) yielding pHAPE1.

E. coli BL21(DE3)pLysS was transformed with this construct and grown in LB-medium supplemented with 100 µg/ml ampicillin and 35 µg/ml chloramphenicol at a temperature of 30°C. When the OD₆₀₀ reached 0.8, 0.4 mM isopropyl β-D-thiogalactopyranoside was added and the cells were grown for another 12-14 hrs at 20°C. Cells (6 g) were harvested by centrifugation, resuspended in 50 mM potassium phosphate, pH 7.0, containing 0.1 mM EDTA and 0.1 mM DTT, and sonicated to prepare cell extract. After ultracentrifugation for 60 min at 110,000 g, the supernatant was applied onto a ceramic hydroxyapatite column (2.5 x 12 cm), equilibrated with 50 mM potassium phosphate, pH 7.0, and eluted with the same buffer. Fractions containing HAPMO activity were pooled and loaded onto a Q-Sepharose column (2.5 x 18 cm) equilibrated with 50 mM potassium phosphate, pH 7.0. After washing with starting buffer, the enzyme was eluted with a linear gradient of 0 - 1 M KCl in the same buffer. HAPMO eluted at a concentration of 0.6 M KCl. Active fractions were concentrated by ultrafiltration, dialyzed in 50 mM potassium phosphate, pH 7.0, and stored at -80°C.

PCR amplification to create truncated HAPMO variants

Two primers were designed to amplify truncated *hapE* genes. Primer PHAPMO3, 5' CACGGCATATGGCCAGCGGCCGCGACTTCAAGGTGGTG 3' annealed just upstream the part of the gene encoding the first Rossmann fold sequence motif. Val¹³⁶ was mutated to a methionine to create an *NdeI* site. Primer PHAPMO8, 5' CACGGCATATGGCCGAAGAAGCCGTGACCGCC 3' was used to create a mutant lacking the part encoding the first 114 amino acids. Due to the introduction of an *NdeI* site, Ile¹¹⁵ was replaced for a methionine (*NdeI* sites underlined, startcodon shown in bold, substituted codons shown in italic). PCR with *Pwo* polymerase, using either PHAPMO3 or PHAPMO8 in combination with PAPMO2 as the reverse primer, under the same conditions as described for *hapE* amplification, yielded fragments which were cloned *NdeI/BamHI* in the pET5-a vector yielding pHAPE2 and pHAPE3 respectively. Successful cloning was confirmed by plasmid sequencing.

Site-directed mutagenesis

The Quickchange site-directed mutagenesis kit from Stratagene was used to introduce a point mutation into HAPMO changing the glycine at position 490 into an alanine. Two primers were used, Primer 1 (5' GTGTATGGCACGGCGTTCCATGCC TCG 3') and primer 2 (5' CGAGGCATGGAACGCCGTGCCATACAC 3'). The mutagenic codon is shown in italic. The PCR reaction, with pHAPE1 as template, was performed under conditions as recommended by the manufacturer. Successful mutagenesis was confirmed by plasmid sequencing.

Steady-state kinetics

HAPMO activity was determined spectrophotometrically by monitoring the decrease of NADPH at 370 nm ($\epsilon_{370} = 2.7 \text{ mM}^{-1} \text{ cm}^{-1}$). Reaction mixtures (1 ml) typically contained 50 mM potassium phosphate pH 8.0, 0.25 mM NADPH and 50-100 nM enzyme. The reaction was started by the addition of 10 µl 0.1 M 4-hydroxyacetophenone in dimethylformamide. Specific activities were corrected for endogenous NADPH oxidase activity. One unit of HAPMO activity is defined as the

amount of protein that oxidized 1 μmol of NADPH per minute. All kinetic measurements were performed at 30°C using air-saturated buffers.

Steady-state kinetic parameters for acetophenone-derivatives were estimated using a concentration range from 2.0 μM – 5.0 mM and a fixed concentration of 0.25 mM NADPH. The K'_m and V'_{max} for NADPH were estimated using a fixed concentration of 200 μM 4-hydroxyacetophenone and an NADPH concentration range from 30 - 300 μM .

Formation of hydrogen peroxide was measured indirectly by adding a catalytic amount of catalase after completion of a HAPMO catalyzed conversion. Oxygen consumption and formation was monitored using an optical oxygen sensor “MOPS-1” (Prosense, Germany).

4-Hydroxyphenyl acetate hydrolase activity was determined spectrophotometrically by monitoring the production of *p*-nitrophenol at 405 nm ($\epsilon_{405} = 7745 \text{ M}^{-1} \text{ cm}^{-1}$, as determined experimentally at pH 7.0). Reaction mixtures contained 1-100 μg protein in 1 ml of a saturated solution of *p*-nitrophenyl acetate in phosphate buffer (pH 7.0).

Isotope labeling experiment

For ^{18}O incorporation experiments, 150 μl of H_2^{18}O was added to 327.5 μl of 1.0 mM aromatic substrate in 50 mM phosphate buffer, pH 7.0. After addition of HAPMO (2.5 μl , 200 μM) and NADPH (20 μl , 25 mM) the samples were incubated for 10 minutes and subsequently extracted with 1 ml of diethylether. GC-MS analysis of the ether extracts was performed on a Hewlett Packard HP 5890 series II gas chromatograph and a Hewlett Packard HP 5971 mass spectrometer equipped with a HP-5 column. Samples (1 μl) were injected without derivatization, and the temperature program was 1 min isothermal at 80°C followed by an increase to 150°C at 10°C min^{-1} and finally 4 min at this temperature.

Analytical methods

Protein content was determined with Coomassie Brilliant Blue using bovine serum albumin as the standard. SDS-polyacrylamide gel electrophoresis was carried out with 12.5% slab gels. The Amersham Pharmacia Biotech low molecular mass calibration kit containing phosphorylase *b* (94 kDa), bovine serum albumin (67 kDa), ovalbumin (43 kDa), carbonic anhydrase (30 kDa), soybean trypsin inhibitor (20.1 kDa), and α -lactalbumin (14.4 kDa) served as a reference. Proteins were stained with Coomassie Brilliant Blue G250. The relative molecular mass of native HAPMO was determined by FPLC gel filtration using a Superdex 200 HR 10/30 column (Pharmacia Biotech) running with 50 mM potassium phosphate buffer pH 7.0, containing 150 mM KCl. The column was calibrated with blue dextran 2000, thyroglobulin (669 kDa), ferritin (440 kDa), catalase (232 kDa), aldolase (158 kDa), lipoamide dehydrogenase (100 kDa), *p*-hydroxybenzoate hydroxylase (88 kDa), bovine serum albumin (67 kDa), ovalbumin (43 kDa), chymotrypsinogen A (25 kDa), myoglobin (17.8 kDa) and cytochrome *c* (12.3 kDa).

The flavin prosthetic group of HAPMO was isolated and identified by reverse-phase HPLC according to the procedure described for 4-hydroxybenzoate 1-hydroxylase.^[82]

Absorption spectra were recorded at 25°C on an Aminco DW-2000 spectrophotometer or a Perkin Elmer Lambda Bio 40 spectrophotometer. Flavin fluorescence emission spectra were recorded on an SPF-500 spectrofluorimeter essentially as described elsewhere.^[89]

DNA was cycle-sequenced with the Amersham Thermo Sequenase cycle-sequencing kit with 7-deaza-dGTP and Cy5 labeled fluorescent primers. Sequencing reaction mixtures were run on the Pharmacia ALF-Express DNA sequencer. The N-terminal amino acid sequences of purified HAPMO and 4-hydroxyphenyl acetate hydrolase were determined by automatic Edman degradation at Eurosequence BV (Groningen, The Netherlands). The BLAST program^[5] at the National Center for Biotechnology Information (www.ncbi.nlm.nih.gov/BLAST/) was used to search for proteins showing sequence similarity. Multiple sequence alignments were made with the Clustal W program at the European Bioinformatics Institute (www.ebi.ac.uk/clustalw).^[299]

Results

Purification of HAPMO from *P. fluorescens* ACB

Purification of HAPMO by anion exchange and hydrophobic chromatography resulted in a homogeneous enzyme preparation that is free of esterase activity. Table 1 summarizes a typical purification from 200 g of 4-hydroxyacetophenone grown *P. fluorescens* ACB cells. The enzyme was purified 25-fold with an overall yield of nearly 50%. SDS-PAGE revealed the presence of a single polypeptide chain, corresponding to an apparent molecular mass of about 70 kDa. The purified enzyme elutes from an analytical Superdex 200 gel filtration column in one symmetrical peak with an apparent molecular mass of 140 ± 5 kDa. This suggests that native HAPMO from *P. fluorescens* ACB occurs as a homodimer in solution.

Table 1. Purification of 4-hydroxyacetophenone monooxygenase from *P. fluorescens* ACB

Step	Volume	Protein	Activity	Specific activity	Yield
	ml	mg	U	U mg ⁻¹	%
Cell extract	800	30210	6552	0.22	100
Q-Sepharose	35	2610	4959	1.90	76
Phenyl Sepharose	25	569	3129	5.50	48

Spectral properties and identification of prosthetic group

The optical spectrum of HAPMO shows maxima at 382 and 440 nm, indicative of a flavoprotein (Fig. 1A). The ratio of the absorbance at 280 nm relative to that at 440 nm was 15.5.

Unfolding of the enzyme revealed that the flavin cofactor is non-covalently bound. Incubation for 10 min of native HAPMO in the presence of 0.1% SDS leads to a final spectrum, which corresponds to the absorbance of free FAD (Fig. 1A). The identity of the flavin prosthetic group was confirmed by HPLC and fluorescence analysis. From the absorbance difference between free and protein-bound FAD, a value of $12.4 \text{ mM}^{-1} \text{ cm}^{-1}$ is estimated for the molar absorption coefficient (ϵ_{440}) of HAPMO at pH 7.0. Moreover, from the absorbance at 440 nm and protein content, it is concluded that each HAPMO

subunit contains one molecule of FAD. The flavin fluorescence in HAPMO is strongly quenched. Comparison with flavin standards revealed that the relative fluorescence quantum yield of protein-bound FAD is less than 1% of free FAD (pH 7.0).

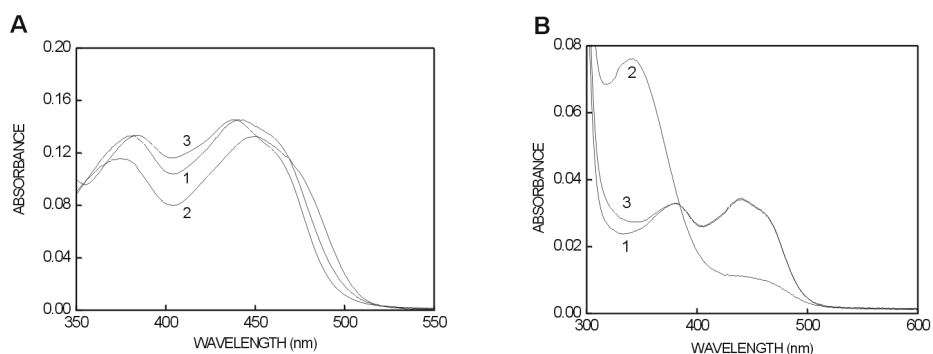


Fig. 1. Spectral properties of HAPMO from *P. fluorescens* ACB. The absorption spectra of HAPMO were recorded in 50 mM potassium phosphate buffer, pH 7.0. **A:** Absorption spectra of native (1) and unfolded HAPMO (2) and of the G490A mutant (3). HAPMO was unfolded by incubation of the enzyme in 0.1% SDS. **B:** Spectral properties of oxidized and reduced HAPMO (3.0 μM). Oxidized HAPMO (1) was fully reduced by addition of 15 μM NADPH (2). Upon restoring aerobic conditions, the flavin becomes fully reoxidized (3).

Catalytic properties

HAPMO from *P. fluorescens* ACB catalyzes the FAD-dependent conversion of 4-hydroxyacetophenone to 4-hydroxyphenyl acetate with consumption of stoichiometric amounts of NADPH and molecular oxygen. Nearly no activity was found with NADH. The pH and temperature optima for enzyme catalysis are 7.5 and 30°C, respectively. The specific activity of the purified enzyme is about 5.5 μmol of NADPH oxidized min⁻¹ mg⁻¹ under the conditions of the standard assay (pH 8.0). Addition of free FAD to the assay mixture did not stimulate HAPMO activity, indicating that the flavin cofactor is tightly bound. To assess whether the FAD cofactor is involved in catalysis the enzyme was titrated with NADPH under anaerobic conditions. It was found that the flavin is readily reduced by NADPH (Fig. 1B). The full two-electron reduction of the FAD cofactor, as evidenced by the absorption decrease in the region of 400-500 nm, indicates that all cofactor molecules participate in the reduction reaction. Upon restoring aerobic conditions by flushing the enzyme solution with air, the FAD cofactor is reoxidized within 5 min showing the ability of molecular oxygen to reoxidize the flavin cofactor. Oxygen consumption experiments performed in the absence or presence of catalase confirmed that in the absence of substrate the enzyme could act as an NADPH oxidase, forming hydrogen peroxide. Such an uncoupling reaction has also been observed for other flavin dependent monooxygenases.^[80,288] To determine the rate of the observed oxidase activity, consumption of NADPH was monitored in the absence of aromatic substrate revealing a low reactivity ($k'_{\text{cat}} = 0.11 \text{ s}^{-1}$, $K'_{\text{m(NADPH)}} = 5.0 \text{ μM}$). Furthermore, analysis of the amount of hydrogen peroxide produced during conversion of 4-hydroxyacetophenone or acetophenone showed that in the presence of these aromatic substrates the uncoupling reaction does not occur as no hydrogen peroxide could be detected.

Substrate specificity

HAPMO catalyzes the conversion of a wide range of acetophenone derivatives. The highest catalytic efficiency is observed with compounds bearing an electron donating substituent at the *para* position of the aromatic ring (Table 2). The apparent kinetic parameters listed in Table 2 indicate that the preference for these compounds is not only related to the rate of substrate conversion but also to substrate affinity. Table 2 also shows that the enzyme is rather active with the substrate analogs 4-hydroxybenzaldehyde and 4-hydroxypropiophenone. Cyclohexanone and cyclopentanone, which are substrates for some known Baeyer-Villiger monooxygenases,^[343] are not converted by HAPMO.

Table 2 Steady-state kinetic parameters of 4-hydroxyacetophenone monooxygenase. All experiments were performed at 30°C in air-saturated 50 mM potassium phosphate buffer pH 8.0. Apparent turnover rates (k'_{cat}) and apparent Michaelis constants (K'_m) were determined at fixed concentrations of either NADPH (250 μM) or 4-hydroxyacetophenone (200 μM).

Substrate	K'_m μM	k'_{cat} s^{-1}	k'_{cat}/K'_m $10^3 \text{ s}^{-1}\text{M}^{-1}$
NADPH	64 ± 14	9.3 ± 0.7	145
4-hydroxyacetophenone	39 ± 9.0	10.1 ± 1.1	259
4-aminoacetophenone	3.0 ± 1.0	12.3 ± 0.7	4100
4-methylacetophenone	161 ± 36	6.3 ± 0.5	39
4-methoxyacetophenone	541 ± 119	1.7 ± 0.2	3.1
4-fluoroacetophenone	1040 ± 301	0.6 ± 0.1	0.6
acetophenone	2270 ± 873	4.5 ± 1.2	2.0
4-hydroxy-3-methylacetophenone	380 ± 27	5.4 ± 0.1	14
4-hydroxypropiophenone	12 ± 0.5	10.6 ± 0.4	883
4-hydroxybenzaldehyde	101 ± 16	7.6 ± 0.3	75

Isotope labelling experiments

To confirm the Baeyer-Villiger monooxygenation reaction and the formation of ester product, the enzymatic conversion was carried out with acetophenone and 4-hydroxyacetophenone as substrates in the presence of 30% (v/v) H_2^{18}O . After extraction of the reaction mixture with diethylether, samples were analyzed by gas chromatography-mass spectrometry. As product from acetophenone conversion, phenyl acetate was identified giving a M^+ of m/z 136 and a base peak of m/z 94. The fragmentation pattern of the phenyl acetate spectrum was identical to that obtained after performing the enzymatic reaction with acetophenone in non-labeled H_2O . This excludes the possibility that the inserted oxygen atom is derived from water and confirms the nature of the enzymatic Baeyer-Villiger monooxygenation reaction. Incubation with 4-hydroxyacetophenone only showed the formation of non-labeled hydroquinone. This observation is attributed to the instability of the formed 4-hydroxyphenyl acetate.

Cloning strategy

During growth of *P. fluorescens* ACB on minimal medium with 4-hydroxyacetophenone as sole source of carbon and energy, it was observed that production of HAPMO coincided with an increase in esterase activity, causing hydrolysis of the formed 4-hydroxyphenyl acetate (data not shown). As both enzymes are metabolically coupled,^[133] it was expected that the corresponding genes might be located in one operon. Therefore, both enzymes were purified and the N-terminal amino acid sequences were determined. For HAPMO, 20 residues were identified (Ser-Ala-Phe-Asn-Thr-Thr-Leu-Pro-Ser-Leu-Asp-Tyr-Asp-Asp-Asp-Thr-Leu-Arg-Glu-His) while for the esterase 21 residues (Thr-Leu-Asp-Val-Glu-Ser-Ala-Gln-Leu-Leu-Gly-Gln-Leu-Ala-Glu-Arg-Gly-Ala-Lys-Pro-Phe) were identified.

Four degenerated primers based on the N-terminal amino acid sequences were designed; one forward primer and one reverse primer for each terminus. “Touch-down” PCR on total DNA of *P. fluorescens* ACB with the four logical primer combinations resulted in a fragment of 1035 bp, designated HAP1, when the primers PESACB1 and PAPMO2 were used. Taken the orientation of the primers into account it could be concluded that the esterase gene had been amplified. Analysis of the nucleotide sequence, after cloning HAP1 in the pCR2.1 TOPO vector, revealed an ORF of which the deduced amino acid sequence indeed showed high similarity with that of various lipases and esterases. Furthermore, the calculated molecular weight of about 33 kDa and the N-terminal amino acid residues confirmed that the ORF encoded the esterase. Downstream of the esterase gene, a partial ORF was identified that encodes a peptide fully consistent with the determined N-terminal peptide sequence of HAPMO. These findings prompted us to use the esterase gene, designated *hapD*, as a probe to screen a genomic library.

Genomic library screening and sequence of the *hapE* gene

A genomic library of *P. fluorescens* ACB was constructed using the cosmid vector pLAFR3 as described under “Materials and Methods”. The *hapD* gene was amplified from pCR2.1, DIG-labeled and used as a probe. Screening of 1440 clones yielded two positive clones. PCR analysis confirmed that the *hapD* sequence was present on both plasmids and therefore the flanking regions of the esterase gene were sequenced. Sequencing of a fragment of a total of 14 kb revealed that the gene encoding HAPMO is the fifth open reading frame of an operon encoding genes involved in the degradation of 4-hydroxyacetophenone (data not shown). We therefore designated it *hapE*. The sequence has been deposited in the GenBank. The *hapE* gene encodes a protein of 640 amino acids with a deduced molecular mass of 71,884 Da, which is in line with the subunit molecular mass determined for the native enzyme.

Protein sequence comparison

Alignment with the known Baeyer-Villiger monooxygenases showed that HAPMO possesses 33% and 27% sequence identity with steroid monooxygenase from *Rhodococcus rhodochrous* and cyclohexanone monooxygenase from *Acinetobacter* sp. NCIB 9871, respectively. Sequence identities with the two newly identified cyclohexanone monooxygenases from a *Brevibacterium* isolate were 31% for CHMO2 and 26% for CHMO3 (Fig. 2). Intriguingly, HAPMO has an extension of about 135 residues at the N-terminus that is not found in the other Baeyer-Villiger monooxygenase sequences. Furthermore, relatively high degrees of sequence identity

Chapter 3

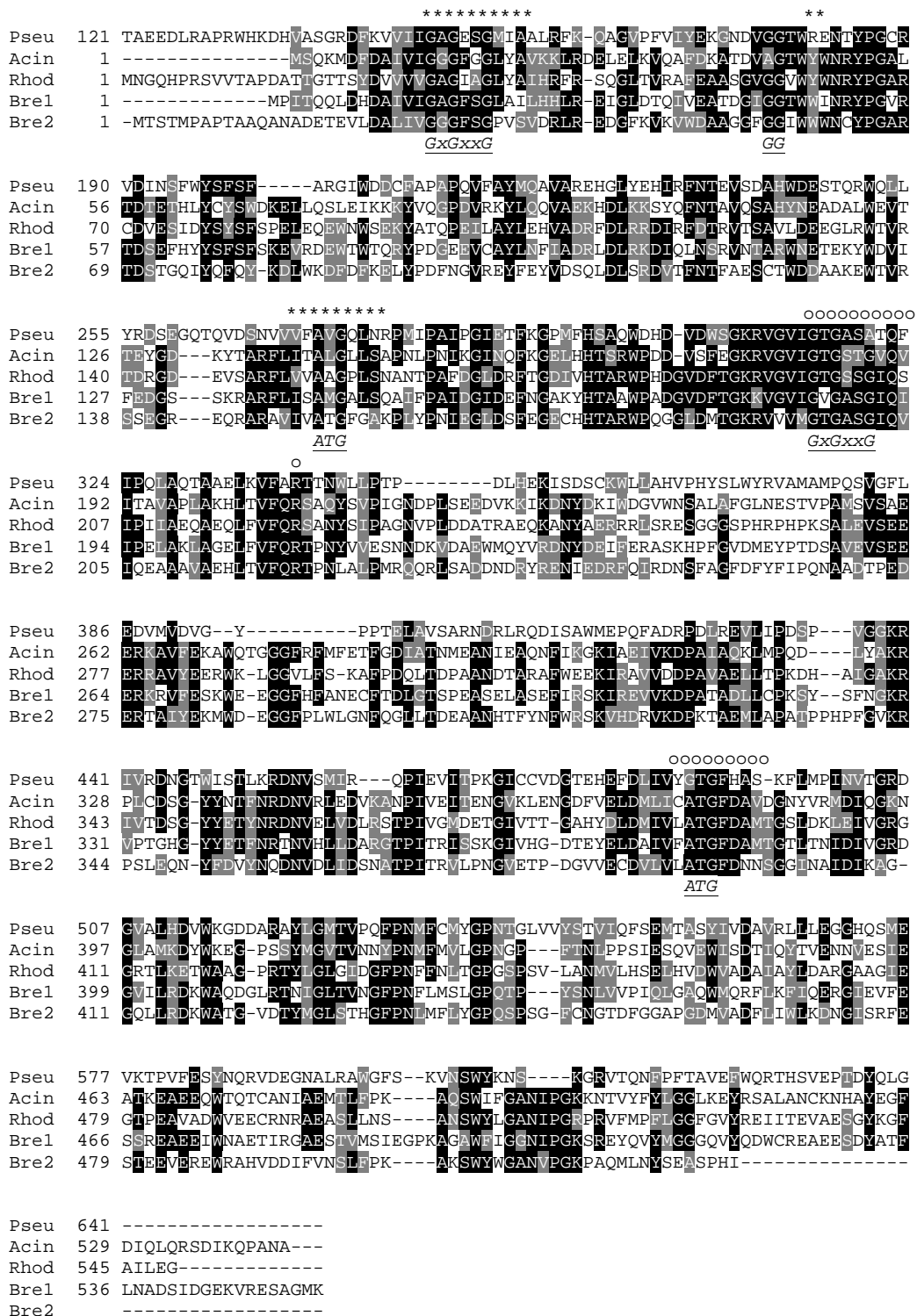


Fig. 2. Multiple sequence alignment of HAPMO from *P. fluorescens* ACB with other Baeyer-Villiger monooxygenases. The N-terminal truncated HAPMO sequence is aligned with cyclohexanone monooxygenase from *Acinetobacter* sp. NCIB 9871 (Acin, P12015),^[42] steroid monooxygenase from *Rhodococcus rhodochromus* (Rhod, BAA24454)^[212] and two cyclohexanone monooxygenases from a *Brevibacterium* isolate.^[32] The regions indicative for FAD and NADPH binding are marked with asterisks and circles, respectively.^[307]

were found for ORFs from *P. fluorescens* (38%), *Streptomyces coelicolor* (33%), *Mycobacterium tuberculosis* (33%), and a *Rhizobium* sp. (32%). This suggests that Baeyer-Villiger monooxygenases are widespread throughout the eubacterial kingdom. Lower degrees of sequence identity (20-25%) were found with the eukaryotic flavin containing monooxygenases (FMOs). The most conserved regions, located at the N-terminal half of the homologous sequences, contain two typical GXGXX(G/A) Rossmann fold fingerprints (Fig. 2). These two sequence motifs are indicative of the presence of two $\beta\alpha\beta$ dinucleotide binding folds^[342] binding the adenylate parts of the FAD and NAD(P)H cofactors.

Expression and purification of recombinant HAPMO

For expression in *E. coli*, the *hapE* gene was placed under control of a T7 promoter in the expression vector pET5-a. When expression of HAPMO was induced in cells grown at 30°C, part of the enzyme was produced as inclusion bodies as evidenced by SDS-PAGE analysis of whole cells. By lowering the temperature to 20°C, formation of inclusion bodies could be prevented while yielding reasonable expression of soluble and active enzyme. Recombinant HAPMO was purified from *E. coli* BL21(DE3)pLysS harboring pHAPE1 in a two-column procedure (Fig. 3). From a 1 liter culture, 30 mg enzyme could be purified with a yield of 70%. The A_{280}/A_{440} ratio of purified recombinant HAPMO was 15.6, which is similar to the value found for the enzyme isolated from *P. fluorescens* ACB. Moreover, the hydrodynamic properties and catalytic features of the recombinant enzyme are identical when compared with HAPMO purified from the wild-type strain.

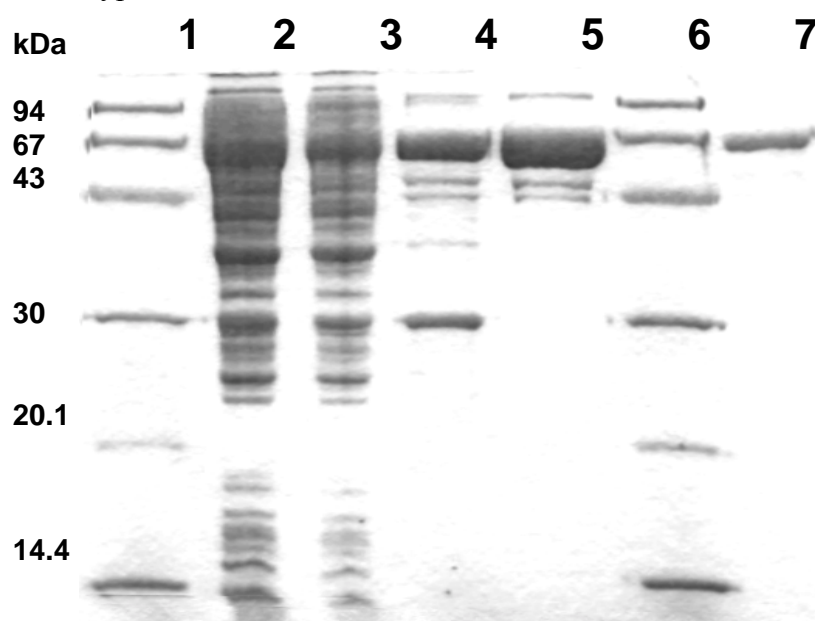


Fig. 3. SDS-PAGE of purification steps of recombinant 4-hydroxyacetophenone monooxygenase from *E. coli* BL21(DE3)pLysS. Lane 1 and 6, marker proteins; lane 2 and 3, cell extract at two concentrations; lane 4, hydroxyapatite fraction; lane 5 and 7, Q-Sepharose fraction at two concentrations.

Truncation of HAPMO

Since the N-terminal region of HAPMO does not show any similarity with known protein sequences it was anticipated that this part of the protein might not be essential for catalysis. To test this hypothesis, two mutant constructs were created pHAPE2 and pHAPE3, lacking the coding region for the first 135 and 114 N-terminal amino acid residues, respectively. However, SDS-PAGE analysis of cell extracts and whole cells, transformed with these constructs, showed that there was no visible expression of the truncated proteins at an induction temperature of 20°C. Upon raising the induction temperature to 30°C, formation of inclusion bodies was observed. At both induction temperatures no activity was detected in the cell extracts. Apparently, the N-terminal part of HAPMO is of importance for the structural integrity of the enzyme.

Properties of the G490A mutant

Recently, an ATG sequence motif was described to be common for FAD and NAD(P)H binding proteins.^[279,307] Since this sequence motif is also found in HAPMO (Fig. 2) and its function is still unclear, we decided to mutate the strictly conserved glycine⁴⁹⁰ into an alanine. The mutant was overexpressed and purified according to the protocol for wild-type HAPMO. Gel filtration showed that the mutant enzyme was purified as a dimer. The ratio of the absorbance at 280 nm relative to that at 440 nm was 17.5, indicating that the enzyme is saturated with FAD. However, the shape of the flavin spectrum of the Gly490Ala mutant significantly differs from that of the wild-type enzyme (Fig. 1A). The oxidase activity of this mutant is significantly higher than that of the wild-type enzyme ($k'_{\text{cat}} = 0.4 \text{ s}^{-1}$) but the Michaelis constant for NADPH is rather high ($K'_{\text{m(NADPH)}} = 700 \text{ }\mu\text{M}$). In contrast to the wild-type enzyme, addition of 4-hydroxyacetophenone did not stimulate the rate of NADPH oxidation. However, GC-MS analysis revealed that the Gly490Ala mutant is still able to catalyze the Baeyer-Villiger oxidation of the aromatic substrate.

Discussion

This paper describes the purification, characterization and cloning of HAPMO, a novel FAD-dependent Baeyer-Villiger monooxygenase which is induced when *P. fluorescens* ACB is grown on 4-hydroxyacetophenone. HAPMO catalyzes the first step in the degradation of 4-hydroxyacetophenone by inserting an oxygen atom in between the aromatic ring and the ketone side chain, yielding 4-hydroxyphenyl acetate. Except for the conversion of 4-hydroxyacetophenone, HAPMO catalyzes the oxygenation of a wide range of other aromatic ketones into the corresponding esters. By this, the enzyme is able to form a range of acylated phenols and catechols. As acylcatechols are valuable synthons for the fine chemical industry, HAPMO might develop as a useful biocatalytic tool. Furthermore, HAPMO resembles a recently isolated Baeyer-Villiger monooxygenase from *P. putida* JD1, displaying a similar substrate specificity and subunit molecular mass.^[294] From this enzyme, only the N-terminal amino acid sequence and two internal peptide sequences were determined which reveal a significant (80%) sequence identity with HAPMO. This indicates that Baeyer-Villiger monooxygenases acting on aromatic compounds frequently occur in nature.

Several Baeyer-Villiger monooxygenases acting on non-aromatic compounds have been identified in bacteria and fungi. All these enzymes were shown to contain a flavin cofactor.^[66,145,206,232,323] On the basis of the available biochemical data, Baeyer-Villiger

monooxygenases have been divided into two subclasses.^[343] Type I Baeyer-Villiger monooxygenases contain FAD as cofactor, are NADPH dependent and appear as monomers, homodimers or homotetramers. In contrast, type II Baeyer-Villiger monooxygenases contain FMN as cofactor, show NADH dependency and consist of two different subunits organized in a $\alpha_2\beta$ conformation. So far, only two type I Baeyer-Villiger monooxygenase have been cloned and characterized. These are steroid monooxygenase from *Rhodococcus rhodochrous*^[212] and cyclohexanone monooxygenases from *Acinetobacter* NCIB 9871^[42] and a *Brevibacterium* isolate.^[32] Within their N-termini, the Rossman fold fingerprint motif GxGxxG is found, which is thought to be involved in binding the ADP part of FAD.^[341]

HAPMO from *P. fluorescens* ACB is strictly dependent on NADPH and was found to be a homodimer with each 72-kDa subunit containing a non-covalently bound FAD. This and the significant sequence homology with cyclohexanone monooxygenase and steroid monooxygenase clearly classifies HAPMO as a type I Baeyer-Villiger monooxygenase. Besides the substrate specificity, there are some striking structural features which distinguishes HAPMO from the other type I Baeyer-Villiger monooxygenases. First, due to an N-terminal extension of about 135 amino acids, the HAPMO subunit is much larger than that of related enzymes. As a consequence, the Rossman fold sequence motif indicative for FAD binding is not localized within the first 30 N-terminal amino acid residues but situated 148 residues from the N-terminus (Fig. 2). In cyclohexanone monooxygenase, this fingerprint sequence starts at residue 12 and in steroid monooxygenase at residue 27. We constructed truncated forms of HAPMO to explore the functionality of the N-terminal extension. However, the truncated HAPMO variants could not be expressed in a soluble form, suggesting that the N-terminal domain of HAPMO is important for the protein structural integrity. Another unique feature of HAPMO concerns the absence of a conserved aspartate near the N-terminal GxGxxG motif proposed to be typical for type I Baeyer-Villiger monooxygenases.^[343] In the HAPMO sequence, a lysine (Lys143) is present at this position (Fig. 2). From the sequence analysis, we infer that this variance is probably not unique for type I Baeyer-Villiger monooxygenases as a similar feature is found in several of the HAPMO-related open reading frames.

Several sequence motifs have been described for proteins that bind both FAD and NADPH.^[73,83,307] Besides the classical Rossman fold sequence motif (GXGXXG/A), a recently described ATG motif was shown to be indicative for FAD and NAD(P) binding domains.^[307] Furthermore, two other short sequence motifs (GG and GD) have been identified to be indicative for a Rossman fold domain involved in FAD binding.^[73,307] Upon alignment of the type I Baeyer-Villiger monooxygenase sequences, most of these sequence motifs could be identified displaying the following arrangement: GXGXXG—GG—ATG—GXGXXG—ATG (Fig. 2). In the HAPMO sequence, the only variations within these sequence motifs involve the first ATG motif (T→V) and the second GXGXXG motif (last G→A). The variation in the first ATG motif has also been observed in other flavoproteins whereas the alanine substitution in the second GXGXXG motif suggests that it is part of the NADPH binding domain.^[27,211] This is in line with mutagenesis studies on a sequence related flavin containing monooxygenase from yeast where a conserved lysine near the second Rossman fold fingerprint was shown to be involved in binding of NADPH.^[286] At this position a strictly conserved arginine is found in the known type I Baeyer-Villiger monooxygenase sequences (Arg339 in HAPMO, see Fig. 2) which, in analogy, probably interacts with the

2'-phosphate moiety of NADPH. The second ATG motif was only recently recognized. While Stehr et al.^[279] have proposed a functional role of this hydrophobic sequence motif in substrate binding, analysis by Vallon^[307] suggested a primary role in NADPH binding. We have assessed the functional role of this sequence motif by replacing the strictly conserved glycine residue. Analysis of the Gly490Ala mutant revealed a dramatic effect on binding and oxidation of NADPH. The NADPH oxidase activity was increased to some extent while the Michaelis constant for NADPH increased by two orders of magnitude. The mutant was still able to convert 4-hydroxyacetophenone indicating that Gly490 is not crucial for substrate recognition. Furthermore, spectral analysis indicated a perturbation of the flavin microenvironment. These results suggest that in HAPMO, the second ATG motif serves a structural function which is of importance for NADPH binding as proposed by Vallon.^[307]

The arrangement of sequence motifs in type I Baeyer-Villiger monooxygenases resembles the sequence organization of the pyridine nucleotide dependent disulfide reductases^[307] (e.g. glutathione reductase and lipoamide dehydrogenase) and the β subunit of glutamate synthase.^[211] However, the Baeyer-Villiger monooxygenase sequences are lacking the GD motif involved in binding the FMN part of FAD.^[73] The absence of this sequence motif or any other significant sequence similarity in the C-terminal half might well reflect the unique catalytic properties of Baeyer-Villiger monooxygenases and mechanistically related *N*-hydroxylating enzymes.^[267,315]

Expression of HAPMO, under control of the T7 promotor,^[284] in *E. coli* BL21(DE3)pLysS resulted in relatively large amounts of soluble and active enzyme. This allows us to address in the near future the catalytic mechanism and structure-function relationship of this novel aromatic Baeyer-Villiger monooxygenase in further detail.

Acknowledgements

This work was supported by the Council for Chemical Sciences of the Netherlands Organization for Scientific Research (CW-NWO), division 'Procesvernieuwing voor een schoner milieu' and by the European Community (Framework IV, project BIO4-CT98-0267).

Chapter 4

¹⁹F NMR STUDY ON THE BIOLOGICAL BAEYER-VILLIGER OXIDATION OF ACETOPHENONES

Mariëlle J.H. Moonen, Ivonne M.C.M Rietjens, Willem J.H. van Berkel

Journal of Industrial Microbiology and Biotechnology. 2001. Vol. 26, No 1/2, pp. 35-42

The biological Baeyer-Villiger oxidation of acetophenones was studied by ¹⁹F nuclear magnetic resonance (NMR). The ¹⁹F NMR method was used to characterise the time-dependent conversion of various fluorinated acetophenones in either whole cells of *Pseudomonas fluorescens* ACB or in incubations with purified 4'-hydroxyacetophenone monooxygenase (HAPMO).

Whole cells of *P. fluorescens* ACB converted 4'-fluoroacetophenone to 4-fluorophenol and 4'-fluoro-2'-hydroxyacetophenone to 4-fluorocatechol without the accumulation of 4'-fluorophenyl acetates. In contrast to 4-fluorophenol, 4-fluorocatechol was further degraded as evidenced by the formation of stoichiometric amounts of fluoride anion.

Purified HAPMO catalysed the strictly NADPH-dependent conversion of fluorinated acetophenones to fluorophenyl acetates. Incubations with HAPMO at pH 6 and 8 showed that the enzymatic Baeyer-Villiger oxidation occurred faster at pH 8 but that the produced phenyl acetates were better stabilised at pH 6. Quantum mechanical characteristics explained why 4'-fluoro-2'-hydroxyphenyl acetate was more sensitive to base-catalysed hydrolysis than 4'-fluorophenyl acetate. All together, ¹⁹F NMR proved to be a valid method to evaluate the biological conversion of ring-substituted acetophenones to the corresponding phenyl acetates, which can serve as valuable synthons for further production of industrially relevant chemicals.

Introduction

Ring-substituted phenyl acetates are valuable synthons for the production of fine chemicals and neuroactive pharmaceuticals.^[125] These aromatic esters can be produced from treating the corresponding acetophenones with peroxy acids in a Baeyer-Villiger type of reaction.^[10,51,283] Because of the laborious clean-up methods required and the danger connected to the use of peroxy acids on a large scale, there is much interest for the development of more sophisticated procedures for the synthesis of substituted phenyl acetates. Production of these compounds by biotechnological processes would provide an attractive environmentally friendly alternative.

Several aerobic microorganisms are capable of utilising acetophenones for their growth.^[52,53,55,127,133,135] Among these species, *Alcaligenes* sp. strain ACA and *Pseudomonas fluorescens* ACB were found to be active with a wide range of substituted acetophenones.^[133] Furthermore, evidence was obtained that in these strains the mineralization of acetophenones involves the initial action of an NADPH-dependent monooxygenase that performs a biological Baeyer-Villiger type of reaction.^[52,133] Recently, we succeeded in the purification of this flavoprotein from 4'-hydroxyacetophenone grown cells of *Pseudomonas fluorescens* ACB and established that the enzyme is active with a wide range of fluorinated acetophenones.^[208] This prompted us to address in this paper the performance of the purified enzyme and whole-cell preparations for the production of phenyl acetates from acetophenones by ¹⁹F NMR.

Of all nuclear magnetic resonance (NMR)-observable isotopes, ¹⁹F is perhaps the one most convenient for biotransformation studies.^[246,334] First, the natural abundance of the ¹⁹F isotope is 100% and there are no background signals, because biological systems do not contain NMR-visible fluorinated endogenous compounds. Thus all resonances observed can be ascribed to the fluorinated substrate of interest and its biotransformation products. Second, the ¹⁹F nucleus has a broad chemical shift range of about 500 ppm. This is large compared to the chemical shift range of ¹H resonances of 15 ppm and of ¹³C of 250 ppm. Thus, the chemical shift of a ¹⁹F nucleus is highly sensitive to its molecular surroundings, resulting in relatively large changes in chemical shifts as a consequence of substrate conversion and reducing the chances of peak overlap. Third, the intrinsic sensitivity of the ¹⁹F nucleus is high and is almost comparable to that of ¹H. This is an important factor, because in whole-cell conversions, intermediate products are usually present in relatively low concentrations.

Materials and Methods

Chemicals

FAD was purchased from Sigma and NADPH (grade II) from Merck. 4'-Hydroxyacetophenone was from Aldrich. 2'-Fluoro-, 3'-fluoro-, and 4'-fluoroacetophenone, 2',4'-difluoroacetophenone, 3'-fluoro- and 4'-fluorophenyl acetate were obtained from Fluorochem and 4'-fluoro- and 5'-fluoro-2'-hydroxyacetophenone from Lancaster. Fluorinated substrates were more than 95% pure on the basis of ¹⁹F NMR analysis. All other chemicals were from Merck and the purest grade available.

Analytical methods

The activity of 4'-hydroxyacetophenone monooxygenase (HAPMO) was routinely determined spectrophotometrically by monitoring the 4'-hydroxyacetophenone stimulated oxidation of NADPH at 370 nm ($\epsilon_{370} = 2.7 \text{ mM}^{-1}\text{cm}^{-1}$). Activity was measured at 30°C in air-saturated 50 mM potassium phosphate, pH 8.0, containing 250 μM NADPH, and 1 mM 4'-hydroxyacetophenone.^[55] The reaction was started by the addition of cell extract or purified enzyme. Specific activities were calculated from initial rate determinations and were corrected for endogenous NADPH oxidase activity. One unit of HAPMO activity is defined as the amount of enzyme that catalyses the oxidation of 1 μmol NADPH per minute under the assay conditions at pH 8.

Conversion of fluorinated acetophenones by whole cells of *P. fluorescens* ACB

Cells of *P. fluorescens* ACB were grown in mineral medium with 4'-hydroxyacetophenone as sole carbon source at 30°C.^[133] Aliquots of 50 ml were centrifuged (10 min, 3000 g, 4°C) and the cells were washed three times with mineral medium.^[22,25] To test the biodegradation of 4'-fluoroacetophenone and 4'-fluoro-2'-hydroxyacetophenone, cells were resuspended in 50 ml mineral medium. The optical density at 450 nm of this cell suspension was 1.0. The acetophenone derivate to be tested was added to a final concentration of 1 mM and the cultures were incubated at 30°C on an orbital shaker. To prevent autooxidation of aromatic substrate and products, 1 mM sodium ascorbate (pH 7.0) was added at the start of the incubation. To monitor the time course of the reaction, 2 ml samples were taken at 0, 0.5, 1, 2, 3 and 4 hours. After the addition of another 2.5 mM ascorbate, each sample was immediately frozen in liquid nitrogen and stored at -20°C. Before ¹⁹F NMR analysis, samples were thawed and centrifuged (5 min, 15,000 g, 4°C) to remove any precipitate formed.

Conversion of fluorinated acetophenones by purified HAPMO from *P. fluorescens* ACB

4'-Hydroxyacetophenone monooxygenase (HAPMO) from *P. fluorescens* ACB was purified by Q-Sepharose and phenyl Sepharose chromatography as described elsewhere.^[208] The enzyme was free of esterase activity and more than 90% pure as evidenced by SDS-PAGE.^[208] The substrate specificity of HAPMO was studied by ¹⁹F NMR product analysis. Tested substrates included 2'-fluoroacetophenone, 3'-fluoroacetophenone, 4'-fluoroacetophenone, 2',4'-difluoroacetophenone, 4'-fluoro-2'-hydroxyacetophenone and 5'-fluoro-2'-hydroxyacetophenone. Enzymatic incubation mixtures (2 ml) consisted of 0.5 mM fluorinated aromatic substrate, 0.3 mM NADPH, 10 μM FAD, 1 mM ascorbate in air-saturated 50 mM potassium phosphate pH 8.0. Reactions were performed at 30°C and started by the addition of 0.05 U/ml HAPMO unless indicated otherwise. After 1 hour of incubation, the reaction samples were frozen in liquid nitrogen and stored at -20°C. Before ¹⁹F NMR analysis, samples were thawed and centrifuged (5 min 15,000 g, at 4°C). The pH optimum of the activity of HAPMO with 4'-fluoro-2'-hydroxyacetophenone was determined in 50 mM potassium phosphate pH 5.7 to 9.5. ¹⁹F NMR measurements at pH 6.0 and 7.0 were performed with an enzymatic incubation mixture consisting of 1 mM substrate, 1 mM NADPH, 2 mM ascorbate in air saturated 50 mM potassium phosphate. The reaction was started with 0.38 U/ml HAPMO.

¹⁹F NMR product analysis

¹⁹F NMR measurements were performed on a Bruker DPX 400 NMR spectrometer, essentially as described elsewhere.^[324] The temperature was 7°C. A dedicated 10 mm ¹⁹F NMR probehead was used. The spectral width for the ¹⁹F NMR measurements was 50,000 Hz. The number of data points used for data acquisition was 32768. Pulse angles of 30° were used. Between 1000 and 66,000 scans were recorded, depending on the concentrations of the fluorine-containing compounds and the signal to noise ratio required. The detection limit of an overnight run (60,000 scans) is 1 μM. The sample volume was 1.6 ml, containing 1.4 ml incubation mixture and 200 μl 0.8 M potassium phosphate pH 7.6 or alternatively, 1.6 ml incubation mixture for pH dependent studies. For calibration an insert containing D₂O and a calibrated amount of 4-fluorobenzoate was used which also served as deuterium lock for locking the magnetic field. Concentrations of the various fluorinated compounds were calculated by comparison of the integrals of their ¹⁹F NMR resonances to the integral of the 4-fluorobenzoate resonance. Chemical shifts are reported relative to CFCl₃. ¹⁹F NMR chemical shift values of the various fluorine containing compounds were identified using authentic fluorinated acetophenones and available fluorophenyl acetates. The resonances of fluorophenols and fluorocatechols have been reported previously.^[236] ¹H decoupling was achieved with a Waltz16 decoupling sequence.

Quantum mechanical calculations

Quantum mechanical molecular orbital calculations were carried out on a Silicon Graphics Indigo using Spartan (version 5.0)(Wavefunction), using the semiempirical AM1 method.^[61] The AM1 method has previously been shown to be suitable and accurate for studies on base-catalysed phenyl acetate hydrolysis.^[189] The input geometry was built using the AM1 optimised geometry characteristics reported previously for phenyl acetate and the most stable conformation of the tetrahedral hydroxyl adduct intermediate.^[189] For all calculations the geometry was fully optimised. The frontier orbital density for nucleophilic attack was calculated using the equation described by Fukui et al.^[107] The relative heat of formation (Δ HF) for the formation of the tetrahedral intermediate, formed in the rate limiting step in which a hydroxide anion attacks the carbonyl carbon of the phenyl acetate,^[189] is calculated as the heat of formation for the tetrahedral intermediate minus the heat of formation of the corresponding phenyl acetate, and presented relative to the lowest Δ HF value. Atomic charges were calculated on the basis of Mulliken analysis but also from electrostatic potential.

Results

Conversion of fluorinated acetophenones by whole cells of *P. fluorescens* ACB

Figures 1A and B present the ¹⁹F NMR spectra of a 1 h incubation of whole cells of *P. fluorescens* ACB with 4'-fluoroacetophenone and 4'-fluoro-2'-hydroxyacetophenone, respectively. Both spectra reveal the formation of a single major product with chemical shift at - 129.1 ppm (Figure 1A) and at - 126.7 ppm (Figure 1B).

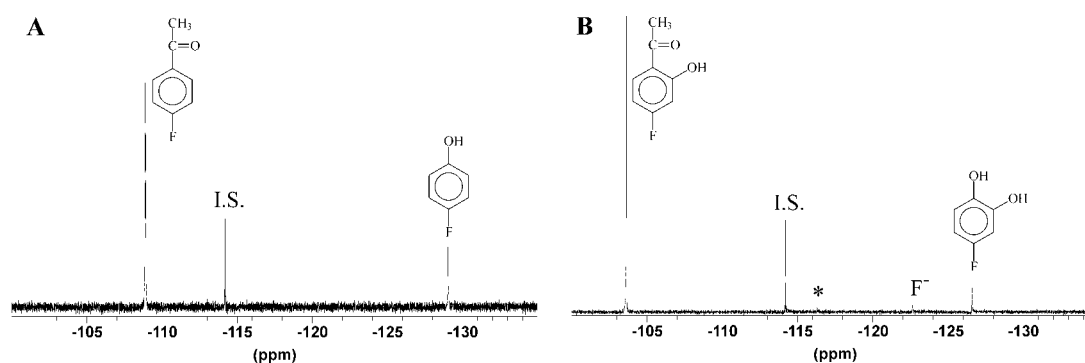


Fig. 1. ^{19}F NMR analysis of the conversion of 4'-fluoroacetophenones by whole cells of *P. fluorescens* ACB. (A) ^{19}F NMR spectrum after 1 h of incubation with 4'-fluoroacetophenone. (B) ^{19}F NMR spectrum after 1 h of incubation with 4'-fluoro-2'-hydroxyacetophenone. The resonance marked I.S. is from the internal standard 4-fluorobenzoate and * indicates a minor impurity in the substrate solution.

Based on the chemical shift values of reference compounds (Table 1) these metabolite peaks reflect the formation of 4-fluorophenol from 4'-fluoroacetophenone and of 4-fluorocatechol from 4'-fluoro-2'-hydroxyacetophenone. In the ^{19}F NMR spectrum of the incubation with 4'-fluoro-2'-hydroxyacetophenone an additional signal at -122.6 ppm, representing fluoride anion formation, is observed (Figure 1B). This fluoride anion formation is not observed in incubations with 4'-fluoroacetophenone (Figure 1A). The time dependent metabolite patterns of 4'-fluoro- and 4'-fluoro-2'-hydroxyacetophenone, presented in Figure 2A and B corroborate that *P. fluorescens* mediated conversion of 4'-fluoroacetophenone and 4'-fluoro-2'-hydroxyacetophenone shows a differential behaviour with respect to the accumulation of their phenol/catechol-type product and the fluoride anion formation. For 4'-fluoroacetophenone the amount of parent compound converted is fully recovered as 4-fluorophenol (Figure 2A). However, for 4'-fluoro-2'-hydroxyacetophenone formation of 4'-fluorocatechol appears to be a transient phenomenon (Figure 2B). The amount of parent substrate converted is, on the basis of fluoride signal intensity, fully recovered as fluoride anions pointing at further transformation of the 4-fluorocatechol formed. Because the frequent ascorbate addition to the samples has been shown to effectively block autooxidation of the fluorocatechol intermediates,^[22,25] the conversion of the 4-fluorocatechol is likely to be mediated by cells of *P. fluorescens* ACB.

The ^{19}F NMR results presented in Figure 1 and 2 indicate that during the time course of the reaction with both acetophenone substrates no other fluorinated products can be detected, pointing at the absence of accumulation of the corresponding 4'-fluorophenyl acetates. Based on literature,^[133] this phenomenon can best be ascribed to the swift hydrolysis of these 4'-fluorophenyl acetates by an esterase, resulting in formation of 4-fluorophenol and 4-fluorocatechol, the products actually observed. To eliminate this esterase activity and to provide better possibilities for the biosynthesis of the 4'-fluorophenyl acetates from the 4'-fluoroacetophenones, further studies were performed using purified HAPMO.

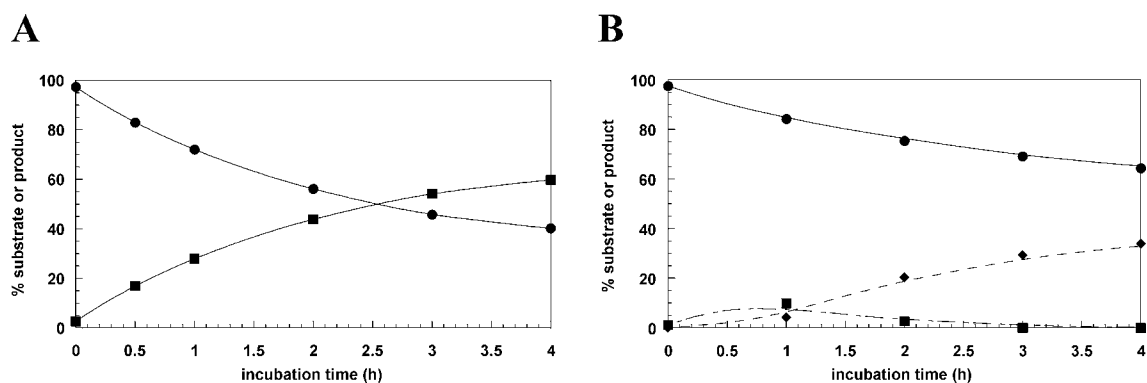


Fig. 2. Time dependent conversion of fluorinated acetophenones by whole cells of *P. fluorescens* ACB. (A) Degradation of 4'-fluoroacetophenone. (●) 4-fluoroacetophenone; (■) 4-fluorophenol. (B) Degradation of 4'-fluoro-2'-hydroxyacetophenone. (●) 4-fluoro-2'-hydroxyacetophenone; (■) 4-fluorocatechol; (◆) fluoride anion.

Conversion of fluorinated acetophenones by purified HAPMO from *P. fluorescens* ACB

Figure 3A and B present the ^{19}F NMR spectra of a 1 h incubation of 4'-fluoroacetophenone and 4'-fluoro-2'-hydroxyacetophenone with purified HAPMO at pH 8. Comparison of these ^{19}F NMR spectra to those obtained for incubations with whole cells show some marked differences.

In contrast to the results obtained with whole cells the incubation of 4'-fluoroacetophenone with purified HAPMO results in formation of a product with its ^{19}F NMR resonance at -120.9 ppm. This product can be identified as 4'-fluorophenyl acetate on the basis of comparison of its ^{19}F NMR chemical shift to that of an authentic standard (Table 1). In these incubations with 4'-fluoroacetophenone and purified HAPMO, formation of 4-fluorophenol is no longer detected (Figure 3A). This confirms

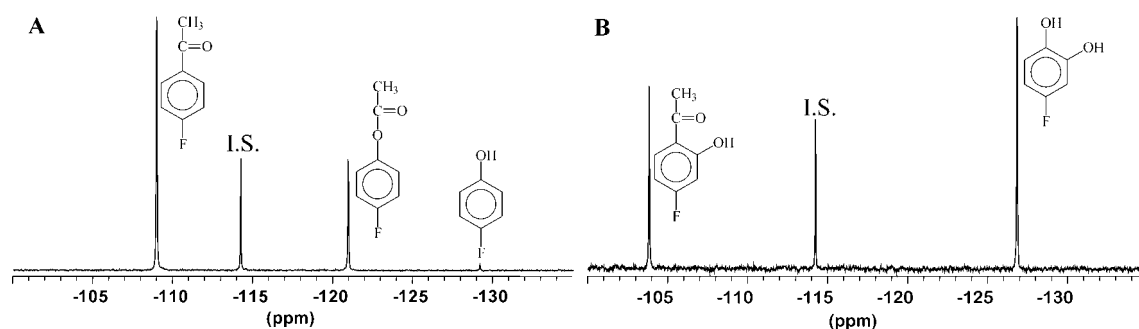


Fig. 3. ^{19}F NMR spectral analysis of the conversion of fluorinated acetophenones by 4'-hydroxyacetophenone monooxygenase from *P. fluorescens* ACB. (A) Conversion of 4'-fluoroacetophenone at pH 8.0. (B) Conversion of 4'-fluoro-2'-hydroxyacetophenone at pH 8.0. The resonance marked I.S. is from the internal standard 4-fluorobenzoate.

that in the absence of esterase activity, HAPMO catalysed formation of 4'-fluorophenyl acetate from 4'-fluoroacetophenone becomes feasible. In contrast, for 4'-fluoro-2'-hydroxyacetophenone the use of purified HAPMO still results in formation of 4-fluorocatechol as the major product and no accumulation of 4'-fluoro-2'-hydroxyphenyl acetate is observed (Figure 3B). Of interest to notice is, that in these

incubations of 4'-fluoro-2'-hydroxyacetophenone with purified HAPMO, 4-fluorocatechol formation is no longer accompanied by fluoride anion formation and further degradation of 4-fluorocatechol (Figure 3B). This corroborates that the transformation of 4-fluorocatechol observed in incubations with whole cells is enzyme dependent and not due to chemical degradation/instability of 4-fluorocatechol.

Table 1. ^{19}F NMR chemical shift values of fluorinated aromatic compounds at pH 7.6

Compound	Product of	^{19}F NMR chemical shift value [ppm]
4-fluorobenzoate ^a		-114.2
2'-fluoroacetophenone		-114.5
3'-fluoroacetophenone		-117.0
4'-fluoroacetophenone		-108.9
2',4'-difluoroacetophenone		-105.5 and -109.1
4'-fluoro-2'-hydroxyacetophenone		-103.8
5'-fluoro-2'-hydroxyacetophenone		-128.1
2'-fluorophenyl acetate ^b	2'-fluoroacetophenone	-134.0
3'-fluorophenyl acetate	3'-fluoroacetophenone	-115.6
4'-fluorophenyl acetate	4'-fluoroacetophenone	-120.9
2',4'-difluorophenyl acetate ^b	2',4'-difluoroacetophenone	-116.5 and -129.0
4'-fluoro-2'-hydroxyphenyl acetate ^b	4'-fluoro-2'-hydroxy-acetophenone	-118.6
5'-fluoro-2'-hydroxyphenyl acetate ^b	5'-fluoro-2'-hydroxy-acetophenone	-118.6
2-fluorophenol ^c	2'-fluorophenyl acetate	-141.9
3-fluorophenol ^c	3'-fluorophenyl acetate	-116.5
4-fluorophenol ^c	4'-fluorophenyl acetate	-129.1
2,4-difluorophenol	2',4'-difluorophenyl acetate	-126.1
4-fluorocatechol ^c	4'- or 5'-fluoro-2'-hydroxyphenyl acetate	-126.7
fluoride anion		-122.6

^a) internal standard

^b) not commercially available; estimated on the basis of other products and the known enzymatic reaction

^c) Peelen *et al.* ^[236]

The results obtained for the HAPMO-catalysed conversion of other fluorinated acetophenones were similar to those for 4'-fluoroacetophenone and 4'-fluoro-2'-hydroxyacetophenone (Table 2). Thus, 2'-fluoroacetophenone, 3'-fluoroacetophenone and 2',4'-difluoroacetophenone were converted to the corresponding phenyl acetate, whereas 5'-fluoro-2'-hydroxyacetophenone was mainly converted to 4-fluorocatechol. The ^{19}F NMR chemical shift values of the fluorinated substrates and their products are presented in Table 1.

Table 2 Rates and yields ^a of the conversion of fluorinated acetophenones by HAPMO

Substrate	pH	k_{cat} (s ⁻¹)	Phenyl acetate (%)	Phenol/catechol (%)
2'-fluoroacetophenone	6	n.d. ^b	100.0	0.0
	8	1.1±0.1	89.5	10.5
3'-fluoroacetophenone	6	n.d.	100.0	0.0
	8	1.1±0.0	90.0	10.0
4'-fluoroacetophenone	6	n.d.	100.0	0.0
	8	0.7±0.1	96.3	3.7
4'-fluoro-2'-hydroxy-acetophenone	6	n.d.	52.1	47.9
	8	2.9±0.3	0.0	100.0
5'-fluoro-2'-hydroxy-acetophenone	6	n.d.	26.3	73.7
	8	7.3±0.8	0.0	100.0
2',4'-difluoro-acetophenone	6	n.d.	88.4	11.6
	8	0.5±0.1	64.0	16.0

^a after 1 hour of incubation^b n.d. = not determined

pH dependent HAPMO-catalysed conversion of 4'-fluoro-2'-hydroxy-acetophenone

Figure 4 shows the pH dependent activity of HAPMO with 4'-fluoro-2'-hydroxyacetophenone, indicating the effect of pH on the activity of the enzyme. Optimal activity is observed around pH 7, whereas the enzyme is nearly inactive below pH 6 and above pH 9.5. Figure 5A and B present the ¹⁹F NMR spectra of incubations of 4'-fluoro-2'-hydroxyacetophenone with purified HAPMO at pH 7.0 and pH 6.0. These experiments were performed to investigate whether possible base-catalysed hydrolysis of the expected 4'-fluoro-2'-hydroxyphenyl acetate may be responsible for its swift hydrolysis to 4-fluorocatechol at pH 8.0, explaining the absence of its accumulation in these incubations. The results presented in Figure 5A and B indicate that lowering of the pH of the HAPMO incubation with 4'-fluoro-2'-hydroxyacetophenone to pH 6 results in a shift in the nature of the accumulated product, namely a decrease in the amount of 4-fluorocatechol accompanied by an increase in the amount of a fluorinated compound with its resonance at -118.6 ppm, identified as 4'-fluoro-2'-hydroxyphenyl acetate (Table 1). Comparison of the results for 4'-fluoro-2'-hydroxyphenyl acetate to those for 4'-fluorophenyl acetate indicate that the presence of the 2'-hydroxy moiety in 4'-fluoro-2'-hydroxyphenyl acetate makes the compound more sensitive to base-catalysed hydrolysis.

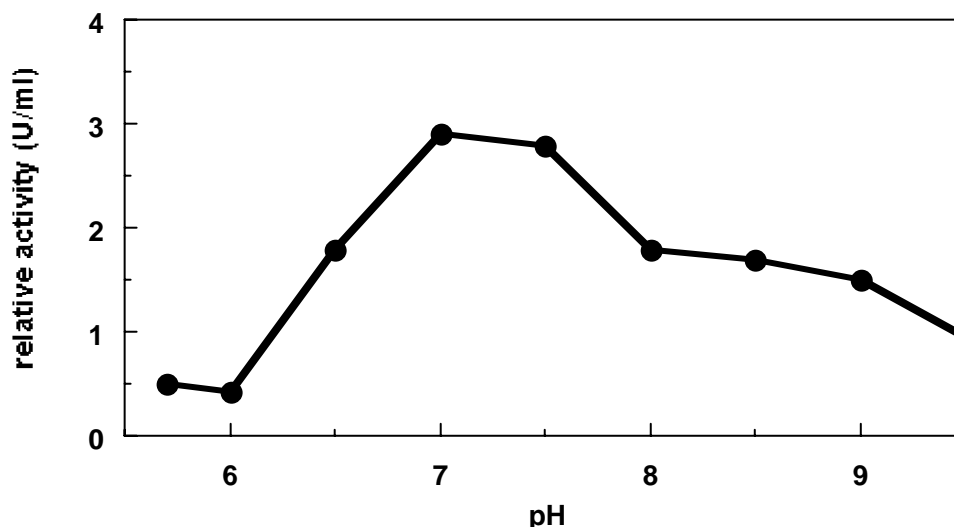


Fig. 4. pH-dependent activity of 4'-hydroxyacetophenone monooxygenase from *P. fluorescens* ACB with 4'-fluoro-2'-hydroxyacetophenone

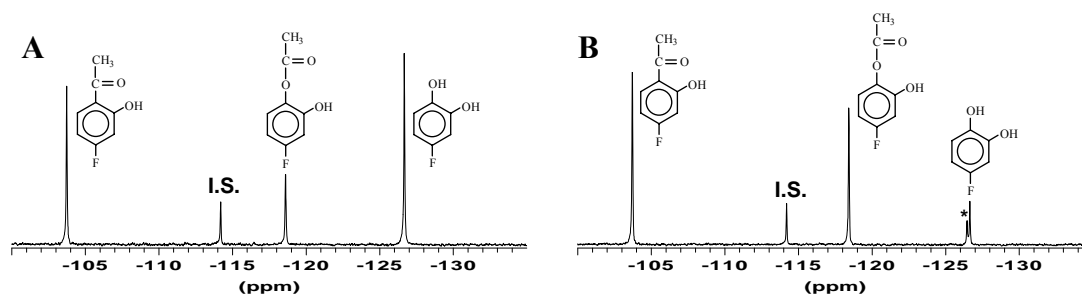


Fig. 5. ^{19}F NMR spectral analysis of the pH dependent conversion of 4'-fluoro-2'-hydroxyacetophenone by 4'-hydroxyacetophenone monooxygenase from *P. fluorescens* ACB at different pH values. (A) pH 7.0. (B) pH 6.0. * Marks an unidentified product.

Quantum mechanical characterisation of the sensitivity of 4'-fluorophenyl acetate and 4'-fluoro-2'-hydroxyphenyl acetate for base-catalysed hydrolysis

In order to obtain some insight in the factors underlying the differential sensitivity of 4'-fluorophenyl acetate and 4'-fluoro-2'-hydroxyphenyl acetate for base-catalysed hydrolysis, quantum mechanical calculations were performed. The hydrolysis appeared to be dependent on the pH (Figure 3B, 5A and B) and, thus, on the concentration of the hydroxyl anions. Therefore, especially the intrinsic reactivity of 4'-fluorophenyl acetate and 4'-fluoro-2'-hydroxyphenyl acetate for a nucleophilic attack by a hydroxyl anion on their carbonyl carbon atom was investigated in more detail. This step is known to be the rate-limiting step in base-catalysed hydrolysis of phenyl acetates.^[189] Table 3 shows the results obtained. The data indicate that the presence of the hydroxy moiety at C2 in 4'-fluoro-2'-hydroxyphenyl acetate, increases the electrophilic reactivity of the carbonyl carbon as compared to this carbonyl carbon in 4'-fluorophenyl acetate.

Table 3. AM1-calculated quantum mechanical parameters reflecting possible differences in intrinsic reactivity of 4'-fluorophenyl acetate and 4'-fluoro-2'-hydroxyphenyl acetate for an electrophilic attack by a hydroxyl anion at their carbonyl carbon centre

Parameter	4'-fluorophenyl acetate	4'-fluoro-2'-hydroxyphenylacetate
E(LUMO) in eV	- 0.08	- 0.23
Frontier density for electrophilic attack at C of C=O	0.043	0.024
Mulliken charge at C of C=O	+ 0.31	+ 0.30
Atomic charge from electrostatic potential at C of C=O	+ 0.80	+ 0.76
Relative Δ HF for formation of the OH-adduct at C of C=O in kcal/mol	23.9	0 ^{a)}

^{a)} Relative Δ HF set to zero

This increased reactivity for an attack by a hydroxyl anion is reflected especially by a lower energy of the lowest unoccupied molecular orbital (E(LUMO)). The relative low frontier orbital density for attack by a nucleophilic species at the carbon of the carbonyl group observed for both phenyl acetates indicates that the attack of the hydroxyl anion on the carbonyl carbon is not likely to be driven by Frontier orbital characteristics. This is in line with the fact that the hydroxyl anion is a hard not soft nucleophile, suggesting its reactivity to be dominated by the Coulomb term.

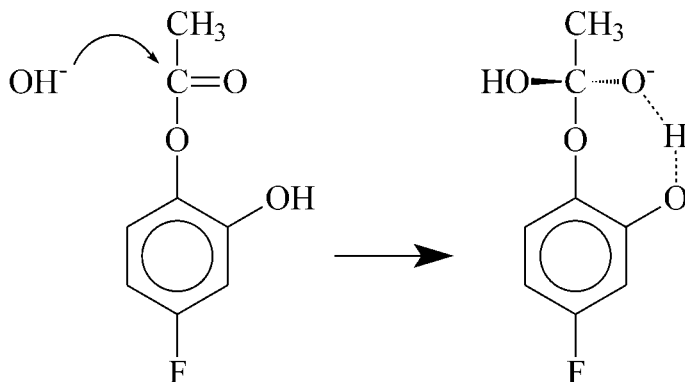


Fig. 6. Formation of the proposed tetrahedral intermediate upon base-catalyzed hydrolysis of 4'-fluoro-2'-hydroxyphenyl acetate, representing the rate-limiting step of this process^[189]

However, the calculated charges at the carbonyl carbon were only marginally different between the two 4'-fluorophenyl acetates suggesting that this Coulomb-type reactivity parameter cannot explain the observed differential sensitivity for base-catalyzed hydrolysis. The calculated parameter reflecting the differential reactivity of the two 4'-fluorophenyl acetates most clearly is the calculated relative difference in heat of formation for formation of the tetrahedral intermediate hydroxyl-adduct of the phenyl acetate (Figure 6), being relatively about 23.9 kcal/mol more favourable for 4'-fluoro-2'-hydroxyphenyl acetate than for 4'-fluorophenyl acetate.

Discussion

Baeyer-Villiger monooxygenases are versatile biocatalysts that have been widely used for the regio- and stereoselective transformation of aliphatic ketones.^[248,331,343] Relatively little is known about Baeyer-Villiger monooxygenases that are active with aromatic substrates. Early investigations on the bacterial metabolism of acetophenones revealed that in certain *Arthrobacter*, *Nocardia*, *Alcaligenes* and *Pseudomonas* species, the ketonic side chain is removed by the successive action of a monooxygenase and an esterase.^[52,53,55,127,133,135] Our results from ¹⁹F NMR analysis on the conversion of fluorinated acetophenones by whole cells of *P. fluorescens* ACB are in agreement with these findings and show that in this strain, 4'-fluoroacetophenone is rapidly converted to 4-fluorophenol without the accumulation of 4'-fluorophenyl acetate. Moreover, prolonged incubations with whole cells show that the 4-fluorophenol formed is not further degraded, suggesting that 4'-hydroxyacetophenone grown cells of *P. fluorescens* ACB lack phenol hydroxylase activity. When whole cells of *P. fluorescens* ACB were incubated with 4'-fluoro-2'-hydroxyacetophenone, again no formation of phenyl acetate was observed. However, the 4-fluorocatechol product observed initially was further degraded as evidenced by the formation of stoichiometric amounts of fluoride anion. This suggests that 4'-hydroxyacetophenone induced cells of *P. fluorescens* ACB contain a dioxygenase that is active with 4-fluorocatechol. Darby et al. showed that in 4'-hydroxyacetophenone induced cells of *Pseudomonas putida* JD1 hydroquinone served as a ring-fission substrate and was cleaved by an oxygen requiring system.^[55] Therefore, the question arises whether in *P. fluorescens* ACB, 4-fluorocatechol and hydroquinone are converted by a single enzyme. Hydroquinone dioxygenases acting on haloaromatic substrates have been characterised only recently.^[207,229,346] However, in all cases these enzymes appeared to be poorly active with halocatechols.

To obtain more insight in the possibilities for the production of fluorinated phenyl acetates from fluorinated acetophenones, studies were performed with purified HAPMO from *P. fluorescens* ACB. ¹⁹F NMR product analysis clearly established that conversion of 4'-fluoroacetophenone by purified HAPMO results in the accumulation of the expected product 4'-fluorophenyl acetate. This, and the fact that *P. fluorescens* esterase is optimally active around pH 8,^[351] confirmed that the HAPMO preparation is free of esterase activity. Enzymatic conversion of 4'-fluoro-2'-hydroxyacetophenone at pH 8.0 did not lead to the accumulation of the expected product 4'-fluoro-2'-hydroxyphenyl acetate, but instead resulted in the formation of 4-fluorocatechol. pH-dependent studies indicate that this was due to the base-catalysed non-enzymatic hydrolysis of 4'-fluoro-2'-hydroxyphenyl acetate. Optimal conditions for the accumulation of this compound over catechol formation were found at pH 6.0. However, at this pH value, the rate of ester formation was about 6 times slower than at pH 7, the pH optimum for the HAPMO-catalysed conversion of 4'-fluoro-2'-hydroxyacetophenone.

Quantum mechanical calculations provide some insight in the reason underlying this difference in sensitivity of 4'-fluoro- and 4'-fluoro-2'-hydroxyphenyl acetate for base-catalysed hydrolysis. This analysis was based on a mechanism for base-catalysed phenyl acetate hydrolysis as previously described.^[189] This mechanism includes a rate-determining step in which the hydroxyl anion performs a nucleophilic attack on the carbonyl carbon of the phenyl acetate resulting in formation of a tetrahedral reaction pathway intermediate (Figure 6). Especially calculation of the relative heat of formation for this reaction step for 4'-fluorophenyl acetate and 4'-fluoro-2'-hydroxyphenyl acetate

reveals that this rate limiting reaction step proceeds with a relative heat of formation that is about 23.9 kcal/mol more favourable for 4'-fluoro-2'-hydroxyphenyl acetate than for 4'-fluorophenyl acetate. It is important to note that this calculated heat of formation should be considered as a relative rather than an absolute value for the reaction enthalpy. Nevertheless this higher relative ΔH_f explains the increased sensitivity of 4'-fluoro-2'-hydroxyphenyl acetate for base catalysed hydrolysis, and, thus, its reduced stability at pH 8 as observed in the present study. Interestingly, the parameters characterising the intrinsic reactivity of the phenyl acetate itself do not reflect such marked differences in reactivity of the parent 4'-fluorophenyl acetates. Thus, the Frontier orbital type characteristics quantifying the relative electrophilicity of the phenyl acetate, the E(LUMO) and the frontier orbital density for electrophilic attack at the carbonyl carbon, vary only slightly. And the Coulomb parameter, i.e. the atomic charge at the carbonyl carbon, known to be of importance for reactions including hard nucleophiles such as the hydroxyl anion,^[95] does not vary between 4'-fluorophenyl acetate and 4'-fluoro-2'-hydroxyphenyl acetate. This suggests that the difference in heat of formation reflecting the higher reactivity of 4'-fluoro-2'-hydroxyphenyl acetate than of 4'-fluorophenyl acetate for base catalysed hydrolysis may especially originate from an extra stabilising factor in the tetrahedral intermediate as a result of the 2'-hydroxyl substituent. Clearly additional stabilisation of the tetrahedral reaction intermediate by an intramolecular hydrogen bond between the oxygen of the carbonyl moiety which becomes negatively charged in the tetrahedral reaction intermediate and the proton of the 2'-hydroxy moiety of the benzene ring may explain this stabilising effect of the hydroxyl substituent. The observation that in the optimised geometry of the tetrahedral intermediate the atomic distance between the carbonyl oxygen and the proton of the 2'-hydroxy group amounts to only 0.97 Å supports the formation of this hydrogen bond.

In conclusion, the studies presented here have yielded valuable information on the possibilities for the biocatalytic environmentally friendly production of substituted phenyl acetates from substituted acetophenones. Our studies show that the whole-cell approach for this type of biotransformations is only feasible with microbial preparations that lack esterase activity. This might be achieved by the inclusion of a suitable esterase inhibitor or in a more sophisticated way by metabolic engineering. Our studies also show that the use of purified enzyme preparations provide a good alternative. However, several bottlenecks remain to be solved to make such an approach economically attractive. These bottlenecks include amongst others the costs of the reduced pyridine nucleotide coenzyme and the stabilisation of the aromatic ester of interest.

In this study ¹⁹F NMR proved to be a valid method to evaluate the environmental-friendly biological conversion of ring-substituted acetophenones to the corresponding phenyl acetates, which can serve as valuable synthons for further biotechnological production of industrially relevant chemicals.

Acknowledgements

We thank Jacques Vervoort for the realisation of ¹⁹F NMR research at Wageningen University and Bep van Veldhuizen for assistance with technical NMR-problems. Furthermore we like to thank the Wageningen NMR Centre for the opportunity to write an article in this special issue.

This research has been financially supported by the Council for Chemical Sciences of the Netherlands Organisation for Scientific Research (CW-NWO), division Procesvernieuwing voor een Schoner Milieu (Project 700-26-711).

Chapter 5

ENZYMATIC BAEYER-VILLIGER OXIDATION OF BENZALDEHYDES

Mariëlle J.H. Moonen, Adrie H. Westphal, Ivonne M.C.M. Rietjens, Willem J.H. van Berkel

Advanced Synthesis & Catalysis. 2005. In press

The selectivity of the chemical Baeyer-Villiger oxidation of benzaldehydes depends on steric and electronic factors, the type of oxidizing agent and the reaction conditions. Here we report on the enzymatic Baeyer-Villiger oxidation of fluorobenzaldehydes as catalyzed by the flavoprotein 4-hydroxyacetophenone monooxygenase (HAPMO).

HAPMO was most active with 4-amino- and 4-hydroxybenzaldehydes. With these compounds significant substrate inhibition occurred. Monofluoro- and difluorobenzaldehydes were readily oxidized by HAPMO without substrate inhibition.

¹⁹F NMR analysis revealed that 4-fluoro-, 2,6-difluoro-, 3,4-difluoro-, 2-fluoro-4-hydroxy- and 3-fluoro-4-hydroxybenzaldehyde were quantitatively converted by HAPMO to the corresponding fluorophenyl formates. These products spontaneously hydrolyzed to fluorophenols. The HAPMO-mediated conversion of 2-fluoro-, 3-fluoro-, 2,3-difluoro- and 2,4-difluorobenzaldehyde yielded, besides fluorophenols, also minor amounts of fluorobenzoic acids.

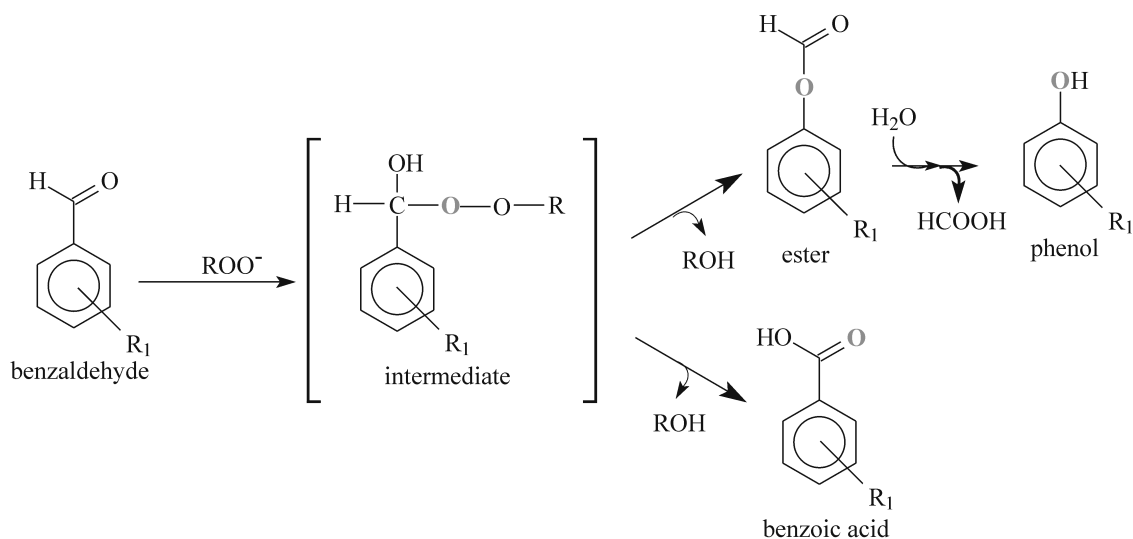
The high preference of HAPMO for the production of fluorophenols is in disagreement with the rule derived from chemical studies that electron-poor benzaldehydes form mainly benzoic acids. This suggests that interactions of the benzaldehyde substrates with amino acids and/or the flavin cofactor in the enzyme active site influence the selection of the migratory group in favor of the phenyl ring.

1. Introduction

Fluorinated chemicals are gaining in industrial importance, with applications in pharmaceuticals, agrochemicals and material products.^[65] Among these fluorinated chemicals, fluorophenols have attracted much attention due to their ability to modify the biological activity of molecules. Fluorophenols can serve as synthons for the production of drugs, including enzyme inhibitors^[249,293] and receptor antagonists.^[144] Catecholamines and amino acids with a radiolabelled [¹⁸F]-fluorophenol moiety have found applications for the *in vivo* imaging of amino acid metabolism^[171] and protein synthesis^[306] using positron emission tomography (PET).^[45]

Chemical methods to produce fluorophenols include diazotization/Sandmeyer decomposition with fluoroanilines, diazotization/thermal decomposition with aminophenols, alkaline hydrolysis with substituted fluorobenzene and F₂/N₂ gas/liquid phase conversion with phenol. All these methods display both economic or technological benefits and disadvantages, and none of them seem to be entirely satisfactory for the industrial production of fluorophenols.^[46]

Newer methods for the chemical synthesis of fluorophenols make use of the Baeyer-Villiger oxidation of aromatic ketones and benzaldehydes.^[46,49,74,188] In these reactions a nucleophilic peroxy moiety is incorporated into the starting compound yielding a tetrahedral "Criegee" intermediate.^[51,243] This unstable species undergoes a rearrangement involving migration of one of the substituents of the carbonyl carbon and subsequent heterolytic cleavage of the peroxidic bond, yielding either the ester or benzoic acid (Scheme 1). By using an aqueous base, the ester is hydrolyzed to give the desired phenol.



Scheme 1. Baeyer-Villiger oxidation of benzaldehydes.

In general, the migration preference of the Baeyer-Villiger rearrangement depends on the steric and electronic properties of the groups attached to the carbonyl carbon atom. The migration ability is also influenced by the type of oxidizing agent and the reaction conditions.^[46,48,49,188,225,243,298] Since all groups attached to the carbonyl carbon of acetophenones migrate in preference to the methyl group, substituted acetophenones show a strong preference for ester formation.^[105,174] For other aromatic alkyl ketones, migration of the alkyl group depends on its structure, while the migration of the aryl

group depends on the electron-donating or electron-withdrawing properties of the substituents.^[46,243] For benzophenones it was established that the product selectivity is strongly dependent on the type and position of the substituents in the phenyl rings.^[46,62,188] Benzaldehydes with electron donating substituent(s) in *ortho* and *para* position stimulated migration of the phenyl ring and formation of phenyl formates (upper pathway in Scheme 1). On the other hand, benzaldehydes lacking electron-donating substituents and/or possessing electron-withdrawing groups yielded benzoic acids (lower pathway in Scheme 1).^[74,188]

Ekaeva *et al.* reported the Baeyer-Villiger oxidation of [¹⁸F]-fluorobenzaldehydes.^[74] Using *m*-chloroperbenzoic acid in the presence of trifluoroacetic acid, it was shown that, in contrast to the above rules, fluorobenzaldehydes can be converted to fluorophenols to a significant extent.

The chemical Baeyer-Villiger reaction requires the use of potentially hazardous oxidants. Therefore, efforts have been made to replace the traditionally used peracids with safer oxidants. Most of these strategies rely on the use of transition metal catalysts or organocatalytic compounds in combination with hydrogen peroxide, peroxy acids or molecular oxygen.^[1,24,49,106,137,174,198,216,283,297,298] However, the most challenging “green chemistry” approach for the selective Baeyer-Villiger oxidation of ketones and aldehydes is offered by enzyme-mediated reactions.^[104,158,202]

Fluorobenzaldehydes are the most attractive starting compounds for the synthesis of fluorophenols because they are available via sustainable pathways. Several white-rot fungi have a great potential for the biocatalytic production of haloaromatic aldehydes.^[116] Bioconversion experiments with whole cells of *Bjerkandera adusta* showed that 2-fluoro-, 3-fluoro- and 4-fluorobenzoic acid and 2-fluoro- and 4-fluorocinnamic acid were reduced to the corresponding fluorobenzaldehydes.^[180] Fluorobenzaldehydes can also be obtained from the corresponding alcohols through the biooxidative activity of alcohol dehydrogenases^[173] and aryl-alcohol oxidases.^[92,114,320]

Recently, we described the purification, characterization and heterologous expression of 4-hydroxyacetophenone monooxygenase (HAPMO) from *Pseudomonas fluorescens* ACB.^[157,208] This homodimeric flavoenzyme is a type I Baeyer-Villiger monooxygenase^[158] that is active with a wide range of aromatic ketones.^[157,159] HAPMO also catalyzes the conversion of aliphatic ketones to lactones^[104,159,202] and the oxidation of aryl sulfides to chiral sulfoxides.^[159] Being highly active with aromatic compounds, HAPMO can be discriminated from the extensively studied cyclohexanone monooxygenase from *Acinetobacter* sp. NICMB 9871.^[4,202,241,242,331]

Relatively little is known about the reactivity of HAPMO with benzaldehydes. Preliminary experiments revealed that, in line with the chemical Baeyer-Villiger reaction, 4-hydroxybenzaldehyde is converted to 4-hydroxyphenyl formate, which after hydrolysis yields hydroquinone.^[159] To study in more detail the selectivity of the enzyme-mediated Baeyer-Villiger oxidation of aromatic compounds we addressed in this paper the reactivity and product specificity of HAPMO with fluorinated benzaldehydes. Unlike most chemical procedures, the enzymatic approach gives high yield and selectivity towards the sustainable production of fluorophenols.

2. Experimental section

2.1 Materials

4-Fluorobenzaldehyde, 3-fluorobenzoic acid and 4-hydroxyacetophenone were purchased from Aldrich. 2-Fluorophenol, 3-fluorophenol and 4-fluorophenol were from Across. 2-Fluoro-4-hydroxybenzaldehyde was synthesized as described earlier.^[313] All other fluorinated aromatic compounds were obtained from Fluorochem. Dimethylformamide (DMF) and potassium phosphate were from Merck. Glucose 6-phosphate, yeast glucose 6-phosphate dehydrogenase (grade I), NADPH and NADP⁺ were from Roche.

2.2 Enzyme purification

HAPMO was purified from *Pseudomonas fluorescens* ACB as described earlier.^[157]

2.3 Analytical methods

The activity of 4-hydroxyacetophenone monooxygenase (HAPMO) was routinely determined spectrophotometrically by monitoring the aromatic substrate-stimulated oxidation of NADPH at 370 nm ($\epsilon_{370} = 2.7 \text{ mM}^{-1}\text{cm}^{-1}$). The standard enzyme activity was measured at 25°C in 1.0 ml air-saturated 50 mM potassium phosphate, pH 8.0, containing 250 μM NADPH, and 200 μM 4-hydroxyacetophenone.^[157] The reaction was started by the addition of 10 μg HAPMO. Specific activities were calculated from initial rate determinations and were corrected for endogenous NADPH oxidase activity. One unit of HAPMO activity is defined as the amount of enzyme that catalyzes the oxidation of 1 μmol NADPH per minute under the standard assay conditions. Steady-state kinetics were performed under the above conditions with 250 μM NADPH as the fixed substrate and varying concentrations (1 μM – 20 mM) of aromatic substrate. With slow substrates, the enzyme concentration was increased ten-fold. The kinetic parameters K'_m and k'_{cat} were determined from non-linear regression analysis using the Michaelis Menten equation. In case of substrate inhibition, the kinetic data were treated according to:

$$k'_{obs} = \frac{k'_{cat} * [S]}{K'_m + [S] + ([S]^2 / K'_s)}$$

where k'_{obs} is the apparent initial rate observed, k'_{cat} is the apparent maximal rate at saturating substrate concentration, K'_m is the apparent Michaelis constant for the aromatic substrate at fixed values of the other substrates (NADPH and O₂) and K'_s is the apparent secondary-binding inhibition constant for the aromatic substrate.^[308]

2.4 Reactions with fluorinated benzaldehydes

Stock solutions of aromatic substrates (100 mM) were prepared in DMF. Enzymatic incubation mixtures (2.0 ml) contained 0.6 mM fluorinated benzaldehyde, 6 mM sodium ascorbate, and 0.4 - 1.0 mM NADPH in 50 mM potassium phosphate pH 8.0. Ascorbate was added to prevent autooxidation of aromatic substrates and products. Reactions were performed for 1 h at 30°C. At 10 min intervals, the reaction mixtures were saturated with air. Reactions were started by the addition of 10-100 μg HAPMO and stopped by freezing the samples in liquid nitrogen.

The enzymatic conversion of 2-fluorobenzaldehyde was studied at pH 6.0, 7.0 and 8.0 at 30°C. The incubation mixture (2.0 ml) contained 0.5 mM 2-fluorobenzaldehyde, 0.6 mM NADPH in 50 mM potassium phosphate. Reactions were started by the addition of 0.7 mg HAPMO. Incubation mixtures were exposed to air to have maximal conversion. Recording of ¹⁹F NMR spectra at 7°C was initiated after 10 min of incubation.

2-Fluorobenzaldehyde was also converted by HAPMO using an NADPH generating system. To that end, 5 mM 2-fluorobenzaldehyde was incubated for 2 h at 30°C in 50 mM potassium phosphate pH 8.0 with 0.9 mg HAPMO, 0.25 mM NADP⁺, 10 mM glucose 6-phosphate, and 7.5 mM ascorbate. The reaction (2.0 ml) was started by the addition of 0.5 mg glucose 6-phosphate dehydrogenase. At 10 min intervals, the reaction mixture was saturated with air.

2.5 ¹⁹F NMR product analysis

¹⁹F NMR experiments were performed on a Bruker DPX 400 NMR spectrometer, essentially as described elsewhere.^[324] The temperature was 7°C. A dedicated 10 mm ¹⁹F NMR probehead was used. The spectral width for the ¹⁹F NMR measurements was 50,000 Hz. The number of data points used for data acquisition was 32768. Pulse angles of 30° were used. Between 1000 and 66,000 scans were recorded, depending on the concentrations of the fluorine-containing compounds and the signal to noise ratio required. The detection limit for an overnight run (60,000 scans) is 1 μM. ¹H decoupling was achieved with a Waltz16 decoupling sequence.

The sample volume was 1.6 ml. For calibration, an insert containing D₂O and a calibrated amount of 4-fluorobenzoate was used which also served as deuterium lock for locking the magnetic field. For the enzymatic conversion of 4-fluorobenzaldehyde, a 1625 μl sample with addition of 100 μl D₂O was used without the insert. Concentrations of the various fluorinated compounds were calculated by comparison of the integrals of their ¹⁹F NMR resonances with the integral of the 4-fluorobenzoate resonance. Chemical shifts are reported relative to CFC₃. ¹⁹F NMR chemical shift values of the various fluorine containing compounds were identified using authentic fluorinated benzaldehydes, benzoic acids and phenols or previously reported resonances. The ¹⁹F NMR spectral data were corrected for impurities (< 5%) of fluorobenzoic acids and fluorophenols present in some substrate solutions.

3. Results

3.1 Substrate specificity

Kinetic studies revealed that HAPMO is active with a wide range of substituted benzaldehydes. 4-Aminobenzaldehyde appeared to be the best HAPMO aldehyde substrate (Table 1). However, with this compound significant substrate inhibition occurred (Fig. 1A). 4-Hydroxybenzaldehydes were also good HAPMO substrates. With these compounds, weak substrate inhibition was observed (Table 1). The kinetic parameters estimated with 4-hydroxybenzaldehyde slightly deviate from previous data where substrate inhibition was not taken into account.^[157]

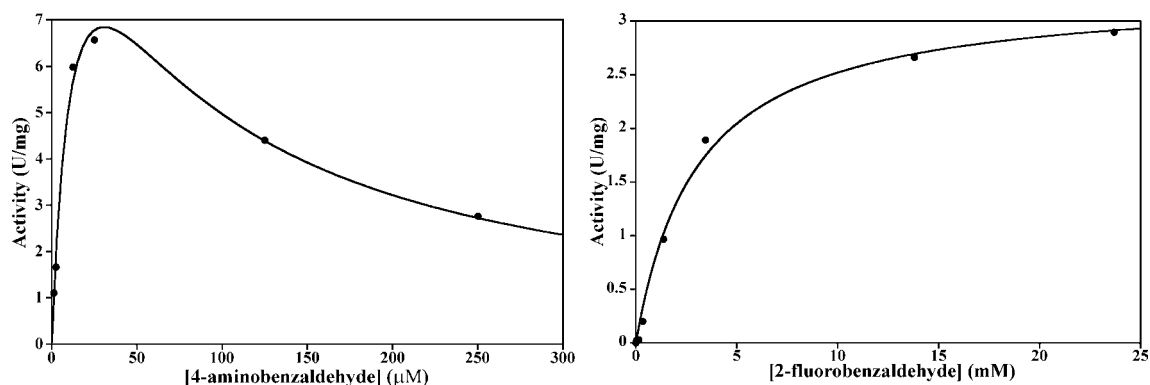


Fig. 1. Michaelis-Menten kinetics of the HAPMO-mediated conversion of substituted benzaldehydes. (A) 4-aminobenzaldehyde; (B) 2-fluorobenzaldehyde.

The HAPMO-mediated oxidation of fluorinated benzaldehydes was not sensitive to substrate inhibition (Table 1, Fig. 1B). As found for the corresponding acetophenones (Table 1), introduction of fluoro substituents in the benzaldehyde ring slightly decreased the reaction rate and increased the Michaelis constant to some extent. 3-Bromo-4-fluorobenzaldehyde was not a substrate for HAPMO.

Table 1. Kinetic parameters of the conversion of substituted benzaldehydes and acetophenones by 4-hydroxyacetophenone monooxygenase from *P. fluorescens* ACB

Substitution	Benzaldehyde			Acetophenone		
	K'_m mM	k'_{cat} s^{-1}	K'_s mM	K'_m mM	k'_{cat} s^{-1}	K'_s mM
Parent compound	3.4±0.5	5.2±0.3	-	2.0±0.8	4.6±1.2	-
2-fluoro-	3.0±0.4	3.9±0.1	-	1.6±0.2	1.0±0.1 ^a	-
3-fluoro-	4.8±0.4	4.0±0.1	-	0.7±0.1	1.0±0.1 ^a	-
4-fluoro-	4.0±0.1	2.6±0.0	-	1.0±0.3 ^b	0.7±0.1 ^a	-
2-fluoro-4-hydroxy-	0.8±0.6	3.2±1.6	1.5±1.2	2.0±0.2	12.4±0.8	3.7±0.4
3-fluoro-4-hydroxy-	3.4±0.3	7.0±0.3	-	1.8±2.0	14.2±10.2	4.8±5.6
2,3-difluoro-	14.7±1.4	0.7±0.0	-	ND	ND	ND
2,4-difluoro-	5.7±0.7	2.3±0.1	-	1.7±0.5	0.5±0.1 ^a	-
2,6-difluoro-	4.7±0.8	2.4±0.1	-	ND	ND	ND
3,4-difluoro-	7.9±1.0	0.7±0.0	-	ND	ND	ND
4-hydroxy-	0.27±0.02	12.5±0.4	4.8±0.4	0.006±0.001	8.3±0.3	0.9±0.1
4-amino-	0.014±0.004	15.9±2.4	0.07±0.02	0.006±0.003	20.4±3.4	0.3±0.2

^a From ref.^[209]; ^b From ref.^[157]; ND = not determined

3.2 Product analysis of the conversion of fluorinated benzaldehydes by HAPMO

The aromatic products formed in the reactions of HAPMO with fluorinated benzaldehydes were analyzed by ^{19}F NMR. Fig. 2A presents, as an example, the ^{19}F NMR spectrum recorded after incubation of 2-fluorobenzaldehyde (-124.7 ppm) with a limiting amount of NADPH. From this spectrum it is clear that two products are formed. On the basis of reference compounds, the main product (95%) was assigned to 2-fluorophenol (-142.0 ppm), whereas the minor product (5%) was assigned to 2-fluorobenzoic acid (-120.3 ppm). Under the conditions applied, no ester formation was observed.

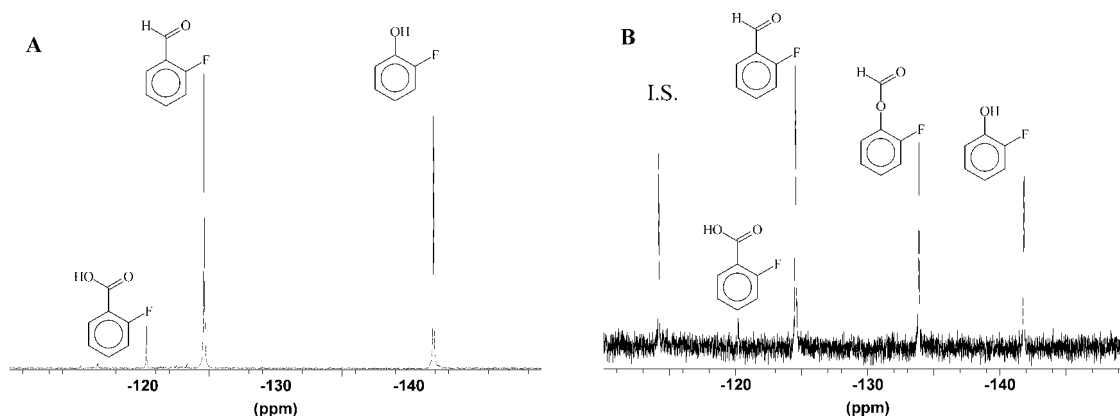


Fig. 2. ^{19}F NMR analysis of the enzymatic conversion of 2-fluorobenzaldehyde by 4-hydroxyacetophenone monooxygenase. **A)** Reaction at pH 8.0 with a limiting amount of NADPH to have about 50% substrate left at the end of the incubation (50,000 scans) **B)** Reaction at pH 6.0 with excess NADPH (5,000 scans). I.S. is the internal standard (4-fluorobenzoic acid, -114.2 ppm). See Experimental Section for further details.

Enzymatic incubations with other fluorinated benzaldehydes mainly resulted in the production of fluorinated phenols (Table 2). With 2-fluoro-, 3-fluoro-, 2,3-difluoro- and 2,4-difluorobenzaldehyde, some fluorinated benzoic acid was also formed. The enzymatic conversions of 2-fluoro-4-hydroxybenzaldehyde and 3-fluoro-4-hydroxybenzaldehyde both resulted in the exclusive formation of 2-fluorohydroquinone (Table 2). The chemical shift values of fluorinated benzaldehydes and their products obtained after conversion by HAPMO are listed in Table 3.

Table 2. Product ratio and yield of the conversion of fluorinated benzaldehydes by 4-hydroxyacetophenone monooxygenase from *P. fluorescens* ACB as determined by ^{19}F NMR. The mean standard error in the concentrations of fluorinated compounds was about 3%.

Substrate	Yield ^a	Product	
		phenol	benzoic acid
	%	%	%
2-fluorobenzaldehyde	88	95	5
3-fluorobenzaldehyde	83	82	18
4-fluorobenzaldehyde	75	100	0
2-fluoro-4-hydroxybenzaldehyde	86	100	0
3-fluoro-4-hydroxybenzaldehyde	91	100	0
2,3-difluorobenzaldehyde	25	73	27
2,4-difluorobenzaldehyde	64	95	5
2,6-difluorobenzaldehyde	70	100	0
3,4-difluorobenzaldehyde	31	100	0

^a total yield of phenol and benzoic acid in incubations with stoichiometric amounts of benzaldehyde and NADPH (see Experimental Section for further details).

Table 3. ^{19}F NMR chemical shifts of fluorinated benzaldehydes and their products after conversion by 4-hydroxyacetophenone monooxygenase from *P. fluorescens* ACB

Substitution	Benzaldehyde ppm	Benzoic acid ppm	Phenol ppm
2-fluoro-	-124.7	-120.3	-142.0 ^a
3-fluoro-	-116.7	-117.9	-116.6 ^a
4-fluoro-	-106.3	-114.2	-129.2 ^a
2-fluoro-4-hydroxy-	-121.8	-116.4	-138.8
3-fluoro-4-hydroxy-	-141.3	ND	-138.6
2,3-difluoro-	-142.2(F3) and -150.1(F2)	-142.8(F3) and -146.4(F2)	-143.1(F3) and -167.1(F2)
2,4-difluoro-	-101.8(F4) and -119.8(F2)	-111.5(F4) and -115.1(F2)	-126.3(F4) and -137.3(F2)
2,6-difluoro-	-119.6	-120.1	-139.3
3,4-difluoro-	-131.2(F4) and -140.7(F3)	-139.0(F4) and -142.6(F3)	-140.9(F3) and -154.3(F4) ^a

^a See ref.^[236]

3.3 Factors governing product yield

The product yield of the HAPMO-mediated conversion of fluorinated benzaldehydes was dependent on the type of substrate, the reaction conditions and the amount of enzyme used. With all substrates tested, no product inhibition was observed. Monofluorinated benzaldehydes were completely converted, providing that excess NADPH and oxygen was supplied. Using a NADPH generating system consisting of

NADP⁺, glucose 6-phosphate, glucose 6-phosphate dehydrogenase and air-saturating conditions, it was possible to convert mg amounts of 2-fluorobenzaldehyde into 2-fluorophenol (95%) and 2-fluorobenzoic acid (5%).

2,3-Difluorobenzaldehyde and 3,4-difluorobenzaldehyde were rather poor substrates for HAPMO (cf. Table 1). Substantial conversion of these compounds was only obtained at relatively high enzyme concentrations. Moreover, for high yields large excess of NADPH and oxygen were needed, because of the competing non-productive NADPH oxidase activity ($k'_{\text{cat}} = 0.11 \text{ s}^{-1}$).^[157]

Additional studies on factors governing product yield were performed using 2-fluorobenzaldehyde as the model substrate. Absorption spectral analysis of the enzymatic conversion of 2-fluorobenzaldehyde pointed at the initial formation of a compound with a low absorption in the 300-400 nm region (not shown). This absorption disappeared in time, indicative for the non-enzymatic hydrolysis of the intermediate ester product. Similar transient absorption changes were observed in the enzymatic conversion of other fluorobenzaldehydes. To get additional insight into ester formation, the HAPMO-mediated conversion of 2-fluorobenzaldehyde was studied as a function of pH and at relatively high enzyme concentration (Table 4).

Table 4. Product ratio and yield of the conversion of 2-fluorobenzaldehyde by 4-hydroxyacetophenone monooxygenase from *P. fluorescens* ACB at different pH values. ¹⁹F NMR spectra were recorded for 1 h at 7°C. The mean standard error in the concentrations of fluorinated compounds was about 3%.

pH	Product yield	Product ratio		
		2-fluorophenyl formate	2-fluorophenol	2-fluorobenzoate
	%	%	%	%
8.0	100	0	95	5
7.0	95	2	93	5
6.0	57	53	42	5

At pH 6.0, the enzymatic reaction was significantly slower than at pH 8.0, but ¹⁹F NMR product analysis clearly showed the initial formation of 2-fluorophenyl formate (-133.9 ppm, Fig. 2B). After 10 min incubation, 80% of the total amount of products was the ester which slowly decayed to yield 2-fluorophenol. After measuring for 1 h at 7°C, nearly half the amount of ester was hydrolyzed to the phenol (Table 4), whereas after 2 h less than 25% of the ester remained. At pH 7.0, 2-fluorobenzaldehyde was more readily converted, but almost no formate ester was detected by ¹⁹F NMR. Table 4 summarizes the product yields and product ratios of the reactions of HAPMO with 2-fluorobenzaldehyde at different pH values. At all pH values, formation of about 5% of 2-fluorobenzoate was observed.

4 Discussion

Fluorophenols are attractive building blocks for the synthesis of high-value fluorinated chemicals. Fluorophenols can be produced by the chemical Baeyer-Villiger

oxidation of fluorobenzophenones, fluoroacetophenones and fluorobenzaldehydes. With all these compounds, the amount of fluorophenol produced is dependent on the substituents in the aromatic ring(s), the type of oxidizing agent and the reaction conditions.^[46,74,188,225] The chemical Baeyer-Villiger oxidation of 3-bromo-4-fluorobenzaldehyde led to the corresponding fluorobenzoic acid as opposed to the desired phenol.^[1] With monofluorobenzaldehydes, the chemical conversion resulted in nearly equal amounts of fluorophenols and fluorobenzoic acids with a final yield of fluorophenols of about 25 %.^[74]

In a previous study we reported that 4-fluorophenols can be produced from 4-fluoroacetophenones using HAPMO as biocatalyst.^[209] Oxyfunctionalization by HAPMO at pH 6 resulted in the exclusive production of 4-fluorophenyl acetates. At pH 8.0, the reaction rate increased and the fluorinated phenyl acetate products readily hydrolyzed to the corresponding fluorophenols.^[209] Here we show that HAPMO is active with a wide range of fluorinated benzaldehydes. Under the conditions applied (pH 8.0), these reactions mainly resulted in the production of fluorophenols. At pH 6.0, transient formation of the initial ester product could be observed.

The enzymatic conversion of 4-amino-, 4-hydroxy- and 3-fluoro-4-hydroxy-benzaldehyde was sensitive to substrate inhibition. Interestingly, there was a clear correlation between the Michaelis constants of the aromatic substrates (K'_m) and the degree of substrate inhibition (K'_s). This suggests that the inhibition is directly related to catalysis and is not caused by binding of the substrate at a secondary site. For the related cyclohexanone monooxygenase, it was reported that NADP⁺ remains bound during the entire reaction cycle and that the interaction between the reduced enzyme and pyridine nucleotide is needed for the stabilization of the flavin C4a peroxide oxygenation species.^[268] Thus, it is unlikely that the inhibitory substrates are binding at the NADP(H) binding site. A more plausible explanation for the observed substrate inhibition is that the aromatic substrate competes with the aromatic product for binding to (one of) the enzyme intermediates which are formed after substrate oxygenation. A similar competition between substrate and product binding has been observed with flavoprotein aromatic hydroxylases.^[141,148,296] The HAPMO-mediated Baeyer-Villiger oxidation of other fluorobenzaldehydes was not sensitive to substrate inhibition. In line with the above notion, this might be related to a relatively weak binding of these compounds in the active site.

The HAPMO-mediated conversion of fluorobenzaldehydes mainly resulted in the production of fluorophenols. The high preference for the formation of phenols is in disagreement with the rule derived from chemical studies that aromatic substrates with electron-withdrawing substituents mainly form benzoic acids.^[46,188,298] Because the rearrangement of the tetrahedral Criegee intermediate (Scheme 1) of the enzymatic reaction is believed to be governed by the same stereoelectronic effects as in the non-enzymatic Baeyer-Villiger oxidation,^[202,264,265] this suggests that interactions of the benzaldehyde substrates with amino acids or the flavin cofactor in the active site influence the selection of the migratory group in favor of the phenyl ring. The first insight into the active site topology of Type I Baeyer-Villiger monooxygenases has recently come from the crystal structure determination of the uncomplexed form of phenylacetone monooxygenase.^[191] From this structure and sequence comparison it was deduced that an arginine residue (Arg440) plays a critical role in HAPMO catalysis. However, a deeper insight into the enzyme-substrate interaction must await the crystal structure determination of a protein complex.

In conclusion, we have shown in this paper that HAPMO catalyzes the conversion of a wide range of benzaldehydes to the corresponding esters. The latter compounds spontaneously hydrolyze to the corresponding phenols. The enzymatic reactions with fluorobenzaldehydes show high selectivity and product yield and are not sensitive to substrate inhibition. A main advantage of the enzymatic Baeyer-Villiger reaction is the use of a mild oxidant (i.e. the flavin C4a peroxide). Recent studies have shown that recombinant whole-cells expressing HAPMO can be used for the biooxidation of prochiral cyclobutanones.^[203] Such a whole-cell system is of particular interest from a preparative point of view because it avoids expensive cofactor recycling.^[3,282] Therefore, with proper upscaling and downstream processing,^[4,63,134,160,332] HAPMO may develop as an environmentally benign alternative for the synthesis of fluorophenols.

Acknowledgements

We thank Barend van Lagen for assistance in NMR experiments. This work was supported by the Council for Chemical Sciences of the Netherlands Organization for Scientific Research (CW-NWO), division “Procesvernieuwing voor een Schoner Milieu”.

Chapter 6

BIOCHEMICAL AND GENETIC CHARACTERIZATION OF THE 4-HYDROXYACETOPHENONE DEGRADATION PATHWAY IN *PSEUDOMONAS FLUORESCENS* ACB

Mariëlle J.H. Moonen, Nanne M. Kamerbeek, Adrie H. Westphal, Sjef A. Boeren, Marco W. Fraaije and Willem J.H. van Berkel

The catabolism of 4-hydroxyacetophenone in *Pseudomonas fluorescens* ACB proceeds through the initial formation of 4-hydroxyphenyl acetate and hydroquinone (1,4-dihydroxybenzene). Here we provide evidence that hydroquinone is further degraded through 4-hydroxymuconic semialdehyde and maleylacetate to β -keto adipate.

The *P. fluorescens* ACB genes involved in 4-hydroxyacetophenone utilization were cloned and characterized. Sequence analysis of an 14-kb DNA fragment showed the presence of 13 genes containing a gene cluster (*hapABCFGDE*) of which at least 4 encoded enzymes are involved in 4-hydroxyacetophenone degradation: 4-hydroxyacetophenone monooxygenase (*hapE*), 4-hydroxyphenyl acetate hydrolase (*hapD*), 4-hydroxymuconic semialdehyde dehydrogenase (*hapA*) and maleylacetate reductase (*hapB*). In between *hapB* and *hapD*, three genes were found which encode a putative intradiol dioxygenase (*hapC*), a protein of the *yci1* family (*hapF*) and a [2Fe-2S] ferredoxin (*hapG*). Downstream of the *hap* genes, 5 open reading frames are situated encoding three putative regulatory proteins (*orf2*, *orf4* and *orf5*) and two proteins possibly involved in a membrane efflux pump (*orf3* and *orf6*). Upstream of the *hap* genes, one gene (*orf1*) with unknown function was found.

Structure homology modeling showed that HapC has the typical domain architecture and iron(III)-binding active site of a homodimeric intradiol dioxygenase. This and the high sequence identity with hydroxyhydroquinone 1,2-dioxygenases lead us to propose that HapC is not responsible for the ring-cleavage of hydroquinone.

Introduction

Acetophenones are widely found in the environment as degradation products of industrial chemicals. Ring-chlorinated acetophenones originate from the microbial degradation of insecticides,^[19-21] PCBs^[12,14,15] and chloroxanthenes.^[301] Non-chlorinated acetophenones have been identified as intermediates in the microbial degradation of ethylbenzene,^[50,305] 1-phenylethanol,^[53] 4-ethylphenol^[153] and the flame-retardant tetrabromobisphenol A.^[185,250]

Several aerobic microorganisms are capable of utilizing acetophenones for their growth.^[52,53,55,127,133,135] 4-Hydroxyacetophenone can be converted in two different ways to 4-hydroxybenzoate.^[115,135,164] The latter compound then enters the β -ketoacid pathway via the formation of the ring cleavage substrate 3,4-dihydroxybenzoate.^[153] For *Pseudomonas fluorescens* ACB,^[133] *Pseudomonas putida* JD1^[55] and *Aspergillus fumigatus* ATCC28282^[154] it was shown that the initial steps of 4-hydroxyacetophenone mineralization comprise a Baeyer-Villiger oxidation to 4-hydroxyphenyl acetate and subsequent ester hydrolysis to hydroquinone (1,4-dihydroxybenzene) (Fig. 1).^[55,133,154,157] However, the subsequent degradation of hydroquinone, a potential human nephrocarcinogen,^[179] remained elusive.

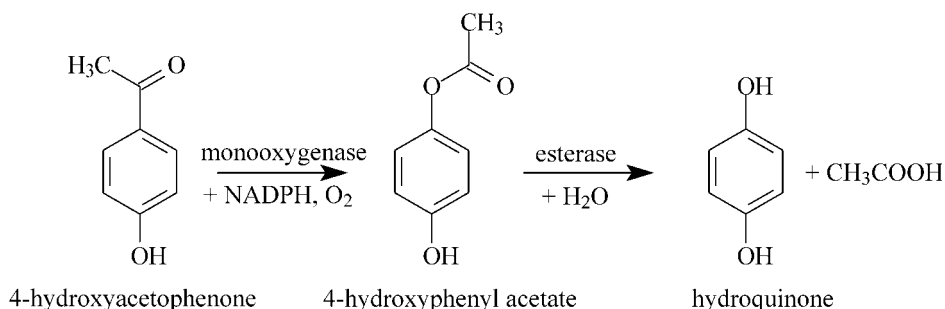


Fig. 1. Initial steps of the catabolism of 4-hydroxyacetophenone by *P. fluorescens* ACB. Enzymes: HAPMO, 4-hydroxyacetophenone monooxygenase; Esterase, 4-hydroxyphenyl acetate hydrolase.

The aerobic degradation of hydroquinones may proceed in two different ways (Fig. 2). Hydroquinone can be hydroxylated to hydroxyhydroquinone (HHQ, 1,2,4-trihydroxybenzene),^[88,313] followed by ring fission by an intradiol HHQ 1,2-dioxygenase.^[149,178,245] Alternatively, direct ring fission of hydroquinone to 4-hydroxymuconic semialdehyde by a hydroquinone 1,2-dioxygenase (HQDO) may occur,^[33,55,207,274] followed by 4-hydroxymuconic semialdehyde dehydrogenase. HQDOs have been indicated to be involved in the degradation of 4-ethylphenol,^[55] *p*-nitrophenol,^[40,133,239] 4-nitrocatechol^[40,41] and the insecticide fenitrothion.^[128] However, none of these enzymes have been characterized in much detail.

¹⁹F NMR studies have given some clues about the further degradation of hydroquinone in *P. fluorescens* ACB.^[208,209] Whole cells converted 4-fluoroacetophenone to 4-fluorophenol. Prolonged incubations showed that 4-fluorophenol is not further degraded, suggesting that 4-hydroxyacetophenone grown cells of *P. fluorescens* ACB lack phenol hydroxylase activity.^[208,209] Without such monooxygenase activity, hydroquinone can not be converted to HHQ.^[88]

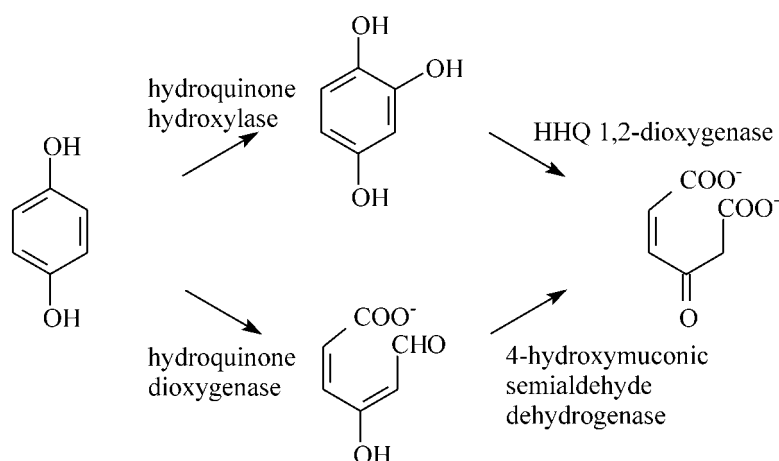


Fig 2. Proposed microbial degradation pathways of hydroquinone

In this paper we have addressed the further degradation of hydroquinone in the catabolism of 4-hydroxyacetophenone in *P. fluorescens* ACB. To that end, we studied the conversion of (fluorinated) hydroquinones by (dialyzed) cell extracts and cloned the *hap* gene cluster involved in 4-hydroxyacetophenone utilization. The biochemical and genetic characterization of the degradation pathway revealed that hydroquinone is metabolized through 4-hydroxymuconic semialdehyde and maleylacetate to β -keto adipate. However, no gene was found which function could be linked to the ring-cleavage of hydroquinone.

Material and Methods

Materials

NADH and NAD^+ were from Boehringer. Phenylmethylsulfonyl fluoride (PMSF) was from Merck. *N,N*-bis[2-hydroxyethyl]-2-aminoethanesulfonic acid (BES), was from Sigma. All other chemicals were of analytical grade.

2,3-Difluoro-4-hydroxybenzoic acid was synthesized from 2,3-difluorophenol according to Komiyama and Hirai^[170] and purified by straight phase HPLC (Kieselgel 60 μm , Merck) with a 1 to 40% linear gradient of ethanol in petroleum-ether 60-80. The identity of the product was demonstrated by ^1H NMR. Other fluorinated 4-hydroxybenzoic acids were synthesized and purified as described before.^[82,148]

Bacterial strains and culture conditions

P. fluorescens ACB^[133] was grown on 4-hydroxyacetophenone as reported before.^[157] Cell extract was prepared as described.^[157]

Enzymatic synthesis and transformation of difluorohydroquinones

2,3-Difluoro-, 2,5-difluoro- and 3,5-difluorohydroquinone were prepared from the corresponding difluorinated 4-hydroxybenzoates by incubation with 4-hydroxybenzoate 1-hydroxylase from *Candida parapsilosis* CBS604.^[82] The reaction mixtures contained 50 mM air-saturated potassium phosphate (pH 7.0), 10 μM FAD, 1 mM ascorbate, 0.3 mM difluoro-4-hydroxybenzoate, 0.25 mM NADH and 80 μl 4-hydroxybenzoate 1-hydroxylase in a total volume of 2.0 ml. The reactions were carried out at 25°C. After

2 hours of incubation, the reaction mixtures were frozen in liquid nitrogen. Completion of the reactions was checked with ^{19}F NMR. Next, the difluorohydroquinones (1800 μl) were incubated for two hours at an orbital shaker at 30°C in the presence of 20 μl *P. fluorescens* ACB cell extract. Formation of products was followed with ^{19}F NMR.

Analytical methods

Enzyme activity measurements were performed at 25°C using air-saturated buffer. Oxygen consumption was measured polarographically using a Clark electrode. The reaction vessel (3.0 ml) contained 20 mM air-saturated BES pH 7.0, 0.5 mM hydroquinone or HHQ (2.9 ml). Reactions were started with 0.1 ml cell extract.

Absorption spectra were recorded using a Hewlett-Packard 8453 diode array spectrophotometer.

HQDO activity was routinely determined by monitoring the formation of 4-hydroxymuconic semialdehyde at 320 nm ($\epsilon_{320} = 11.0 \text{ mM}^{-1} \text{ cm}^{-1}$).^[274] The assay mixture (1.0 ml) typically contained 50 μl cell extract, 10% (w/v) glycerol in 20 mM BES, pH 7.0. Reactions were started by the addition of 10 μl 50 mM hydroquinone in DMF. One unit of HQDO activity is defined as the amount of enzyme that forms 1 μmol of semialdehyde product per minute.

4-Hydroxymuconic semialdehyde dehydrogenase activity was measured by addition of 1 mM NAD^+ to the above produced semialdehyde and following the decrease of absorbance at 320 nm.^[274]

^{19}F NMR measurements were performed on a Bruker DPX 400 NMR spectrometer, essentially as described elsewhere.^[324] The sample temperature and sample volume were 7°C and 1.6 ml, respectively. For calibration an insert containing D_2O and a known amount of 4-fluorobenzoate was used which also served as deuterium lock for locking the magnetic field. Chemical shifts are reported relative to CFCl_3 . The resonance of the 4-fluorobenzoate internal standard was set at -114.2 ppm with respect to CFCl_3 . The detection limit of an overnight ^{19}F NMR measurement (60,000 scans) is 1 μM . The sample volume was 1.6 ml. ^{19}F NMR chemical shift values of the various fluorine-containing compounds were identified on the basis of authentic reference compounds,^[236] or as described in the present study.

High performance liquid chromatography (HPLC) analysis was performed on a WatersTM 600 controller system equipped with a reversed phase Alltima C18 column (150 x 4.6 mm) running in 10% (v/v) acetonitrile, containing either 1, 0.1 or 0% acetic acid. Products were detected with a WatersTM 996 photodiode array detector.

Liquid chromatographic-mass spectrometry (LC-MS) experiments were carried out on a LCQ "classic" (Thermo-Finnigan, San Jose, CA, USA). Reaction mixtures containing 20 μl 50 mM hydroquinone and 20 μl desalted cell extract in 940 μl sodium bicarbonate pH 7.8 were incubated for 7 min at 25°C . Separation was achieved on a 150 x 2 mm Alltima C18 (Alltech, Breda, The Netherlands) column running in 10% (v/v) acetonitrile. MS analysis was performed in the negative APCI mode using a vaporizer temperature of 450°C , a discharge voltage of 2 kV and a capillary temperature of 150°C with nitrogen as sheath gas (20%) and auxiliary gas (5%). MS-MS scans were recorded in the 'data dependent' mode when a MS base peak signal higher than 10^6 was obtained with a normalized collision energy of 35% and a 2 Da isolation width.

Cloning of the *hap* gene cluster

The *hap* gene cluster from *P. fluorescens* ACB was sequenced from a genomic cosmid library as described.^[157] In brief, using degenerated primers based on the N-terminal amino acid sequences of 4-hydroxyphenyl acetate esterase (HapD) and 4-hydroxyacetophenone monooxygenase (HAPMO; HapE) a PCR product was obtained which contained the esterase gene (*hapD*). This gene was used as a probe to screen the cosmid library, which yielded two positive clones.^[157] Sequencing of these cosmid clones resulted in a contiguous segment of 13,949 bp consisting of 13 complete open reading frames (*orfs*).

Sequence comparison

Protein sequence similarity searches were performed using the BLASTP option at www.ncbi.nlm.nih.gov. Multiple sequence alignments were made with the Clustal W program at the European Bioinformatics Institute (www.ebi.ac.uk/clustalw).^[299] BioEdit^[117] was used to calculate the pairwise identity and similarity scores (PAM250 matrix) from the aligned sequences and for the display of the alignment.

Structure homology modeling

Model building of HapC was performed with MODELLER^[253] using the CVFF force field.^[58] The three-dimensional structure of catechol 1,2-dioxygenase from *Acinetobacter* sp. ADP1 in complex with 4-methylcatechol (Protein Data Bank code 1DMH)^[324] was used as a template. HHQ was used as aromatic substrate in the HapC model. The model was verified after several rounds of energy minimization. The stereochemical quality of the homology model was verified by PROCHECK,^[177] and the protein folding was assessed with PROSAIL,^[272] which evaluates the compatibility of each residue with its environment independently.

Nucleotide sequence accession numbers

The nucleotide sequence data reported in this paper will appear in the DDBJ/EMBL/GenBank nucleotide sequence databases.

Results

Conversion of hydroquinone by desalted cell extract

To study the conversion of hydroquinone in the degradation pathway of 4-hydroxyacetophenone in *P. fluorescens* ACB, 0.5 mM hydroquinone was incubated with desalted cell extract in 20 mM BES pH 7.0 at 25°C. Oxygen consumption experiments pointed at oxygenase activity. A similar incubation with HHQ showed only 5% of the activity compared to hydroquinone. Absorption spectral analysis, performed in parallel, revealed that hydroquinone with a maximum absorption at 290 nm was converted into a product with a maximum absorption at 320 nm (Fig 3A).

HPLC analysis of the reaction mixture showed a spectrum (Fig. 3B), indicative for the formation of 4-hydroxymuconic semialdehyde.^[274] HPLC separation of substrate and product was achieved at neutral pH because acidic mobile phase conditions resulted in vanishing of the absorbance at 320 nm, a feature observed with maleyl-substituted ring fission products.^[39] The identity of the reaction product of the conversion of hydroquinone by *P. fluorescens* ACB was confirmed by LC-MS. The product eluted at 2.65 min and its mass spectrum gave a *m/z* of 141 in the negative mode (Fig 3C).

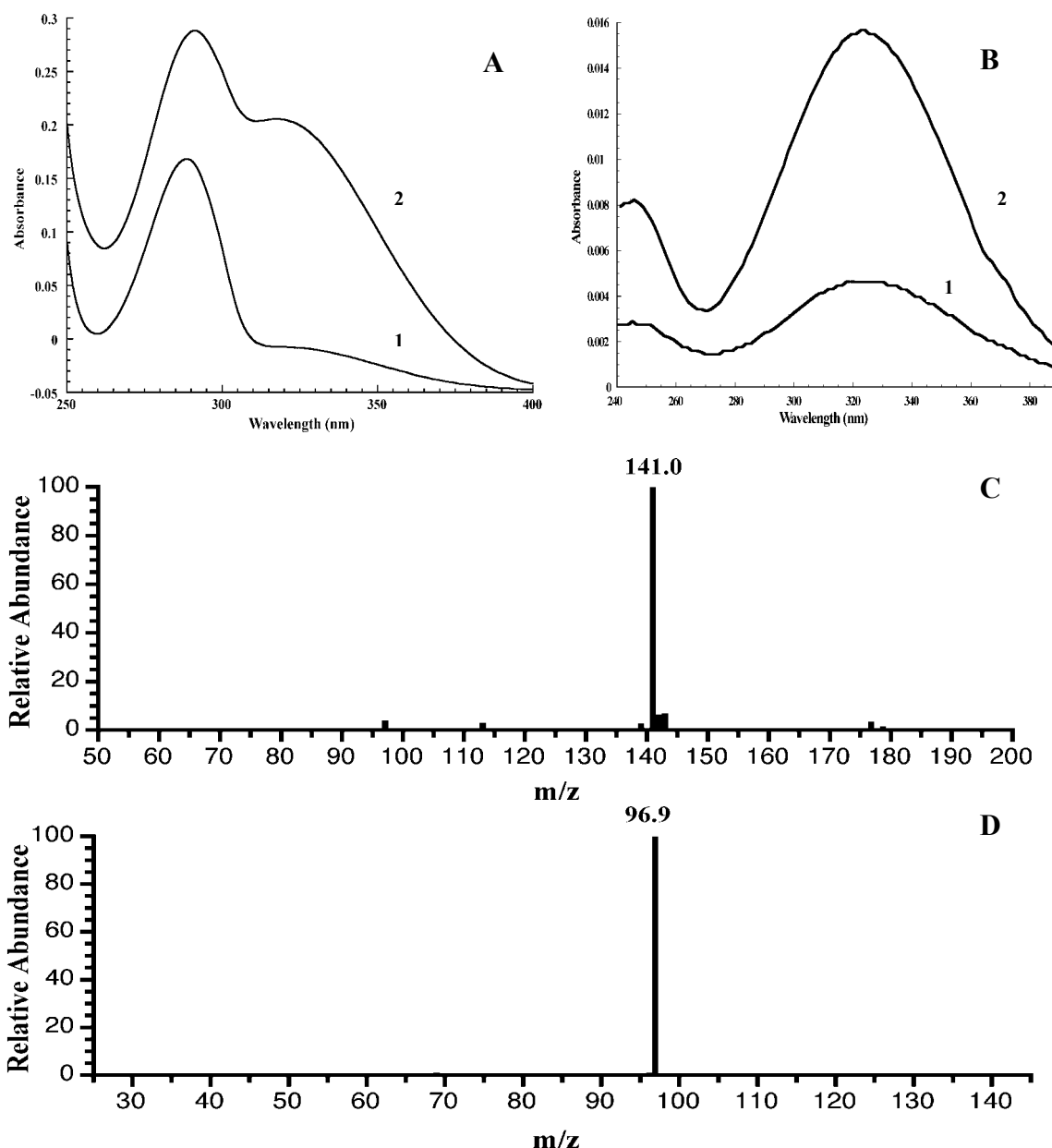


Fig. 3. Product analysis of the conversion of hydroquinone by cell extract of *P. fluorescens* ACB. (A) Absorbance spectrum of hydroquinone (1) and after conversion by HQDO (2) (B) HPLC diode array spectra of the 4-hydroxymuconic semialdehyde product with (1) and without (2) 0.1% acetic acid in the eluents (C) LC-MS and (D) LC-MS-MS spectra of 4-hydroxymuconic semialdehyde.

Collision-induced defragmentation showed a m/z of 97 (Fig. 3D) corresponding to the decarboxylation of 4-hydroxymuconic semialdehyde.^[274]

Addition of NAD^+ to the incubation mixture resulted in a decrease of absorbance at 320 nm, most likely due to conversion of 4-hydroxymuconic semialdehyde to maleylacetate (cf. Fig. 2, lower pathway). During this reaction, no increase at 340 nm was observed, suggesting that maleylacetate was rapidly further converted by an NADH-dependent maleylacetate reductase (see also below).

Degradation of difluorinated hydroquinones by *P. fluorescens* ACB.

To get more information about the degradation of hydroquinones by *P. fluorescens* ACB, several difluorinated hydroquinones were prepared from the corresponding difluorinated 4-hydroxybenzoates by the action of 4-hydroxybenzoate 1-hydroxylase from *Candida parapsilosis* CBS604. Table 1 gives an overview of the ¹⁹F NMR chemical shift values of the fluorinated 4-hydroxybenzoates and hydroquinones at pH 8.0. It should be mentioned here that difluorinated hydroquinones were selected for analysis because the oxidative ring opening of monofluorinated hydroquinones might result in nonfluorinated products that cannot be detected by ¹⁹F NMR.

Fig. 4 shows the ¹⁹F NMR spectra of the incubation of 2,3-difluorohydroquinone (**1**) with cell extract of *P. fluorescens* ACB. After 1 h, about 95% of the fluorinated aromatic substrate was converted (Fig. 4B), whereas all substrate was converted after 2 h of incubation (Fig. 4C). Formation of new signals at -129.0, -129.7, -130.3, -142.1, 154.0 and -154.4 ppm was observed to an extent that accounts for the decrease in the amount of 2,3-dihydroquinone. The resonance at -123.0 ppm originates from fluoride anions, indicating that defluorination has occurred. Based on their intensity, the other six signals could be attributed to the formation of three difluorinated products. The first product with chemical shift values at -129.7 and -154.4 ppm was assigned to 2,3-difluoro-4-hydroxymuconic semialdehyde (**2**).

Table 1. ¹⁹F NMR chemical shift values of fluorinated substrates and products

Compound	Product of	Chemical shift (ppm) pH 8.0
2,3-difluoro-4-hydroxybenzoate		-143.9(F2) and -167.4(F3)
2,3-difluorohydroquinone	2,3-difluoro-4-hydroxybenzoate	-163.8
2,3-difluoro-4-hydroxymuconic semialdehyde	2,3-difluorohydroquinone	-129.7(F2) and -154.4(F3)
<i>Enol</i> -2,3-difluoromaleylacetate	2,3-difluoro-4-hydroxymuconic semialdehyde	-130.3(F2) and -154.0(F3)
<i>Keto</i> -2,3-difluoromaleylacetate	2,3-difluoro-4-hydroxymuconic semialdehyde	-129.0(F2) and -142.1(F3)
2,5-difluoro-4-hydroxybenzoate		-121.4(F2) and -146.9(F5)
2,5-difluorohydroquinone	2,5-difluoro-4-hydroxybenzoate	-144.6
2,5-difluoro-4-hydroxymuconic semialdehyde or <i>enol</i> -2,5-difluoromaleylacetate	2,5-difluorohydroquinone	-110.7(F2) and -174.9(F5)
3,5-difluoro-4-hydroxybenzoate		-139.2
3,5-difluorohydroquinone	3,5-difluoro-4-hydroxybenzoate	-136.8

This assignment is based on the following considerations. The NMR spectra show no formation of monofluorinated products. Furthermore, possible hydroxylation by a HHQ 1,2-dioxygenase (cf. Fig. 2) can be excluded because the chemical shift values of the newly formed peaks are not consistent with the formation of 5,6-difluoro-1,2,4-trihydroxybenzene (-162.0 ± 1.2 and -174.8 ± 1.7 ppm).^[168] 2,3-Difluorohydroquinone can be splitted by HQDO between C1 and C2 or between C1 and C6. If ring fission would take place between C1 and C2, this would result in the formation of an acylhalide, as described for the conversion of 2-chlorohydroquinone by chlorohydroquinone dioxygenase.^[33,229,349] The acylfluoride will readily react with water yielding a monofluorinated maleylacetate.

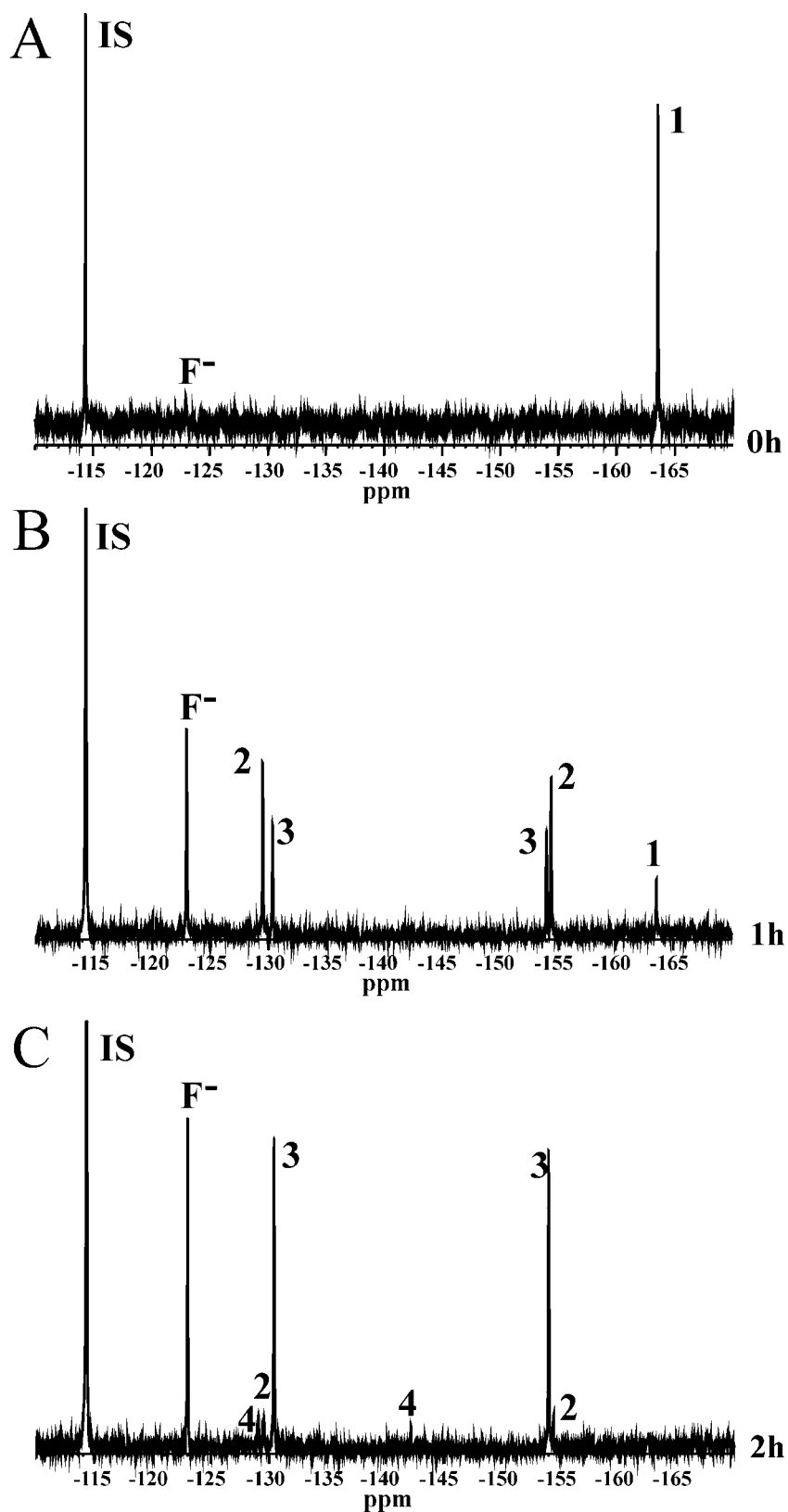


Fig. 4. ^{19}F NMR spectra of the conversion of 2,3-difluorohydroquinone by *P. fluorescens* ACB. A, before addition of cell extract; B after 1 h of incubation; C after 2 h of incubation.

From this we conclude that ring fission occurred between C1 and C6 yielding 2,3-difluoro-4-hydroxymuconic semialdehyde. Upon 2,3-difluoro-4-hydroxymuconic semialdehyde formation, the chemical surrounding of the C3 fluorine atom of 2,3-difluorohydroquinone changes more than that of the C2 fluorine atom.

Thus, the chemical shift of -129.7 ppm is assigned to the 2-fluoro substituent, whereas the chemical shift of -154.4 ppm is assigned to the 3-fluoro substituent of the semialdehyde (Table 1).

The second difluorinated product which is already formed after 1 h but most abundantly present after 2h incubation (Fig. 4C) is assigned to 2,3-difluoromaleylacetate. This assignment is based on the fact that 4-hydroxymuconic semialdehydes are readily converted by 4-hydroxymuconic semialdehyde dehydrogenases to the corresponding maleylacetates^[274,352] (cf. Fig. 2). Maleylacetates can exist in the keto and enol form.^[260] Conversion of the 2,3-difluoro-4-hydroxymuconic semialdehyde to *enol*-2,3-difluoromaleylacetate does not change the direct environment of the two fluorine atoms, and only small differences in chemical shift values will occur. Therefore the chemical shift values of -130.3 and -154.0 ppm are assigned to *enol*-2,3-difluoromaleylacetate (**3**). Fig. 4C also shows the formation of a minor compound with resonances at -129.0 and -142.1 ppm. This compound is assigned to *keto*-2,3-difluoromaleylacetate (**4**). The keto form of the maleylacetate drastically changes the chemical shift value of the 3-fluoro substituent, whereas the surrounding of the 2-fluoro substituent does not significantly change. Thus, the chemical shift value of -129.0 ppm is assigned to the 3-fluoro substituent, whereas the chemical shift value of -142.1 ppm is assigned to the 2-fluoro substituent of *keto*-2,3-difluoromaleylacetate.

Halogenated maleylacetates generally are further degraded by reductive dehalogenation to β -keto adipate.^[33,161,329] Therefore, the strong increase in fluoride anion observed in Fig. 4B and 4C most likely results from maleylacetate reductase activity present in *P. fluorescens* ACB.

An 2 h incubation of 2,5-difluorohydroquinone with cell extract of *P. fluorescens* ACB resulted in the conversion of about 80% of the aromatic substrate (results not shown). Formation of about 25% fluoride anions (-123.0 ppm) and one main difluorinated aromatic product with resonances at -110.7 and -174.9 ppm was observed, showing ring splitting between C1 and C6. This compound is tentatively assigned to 2,5-difluoro-4-hydroxymuconic semialdehyde or *enol*-2,5-difluoromaleylacetate (Table 1).

An 2 h incubation of 3,5-difluorohydroquinone with cell extract of *P. fluorescens* ACB did not show accumulation of fluorinated compounds (results not shown). Under the conditions applied, nearly 100% of the fluorinated aromatic substrate was converted into fluoride anions.

Cloning and sequencing of the *hap* gene cluster

As described before, we have sequenced 13,949 bp of the *P. fluorescens* ACB genome containing the 4-hydroxyphenyl acetate hydrolase (*hapD*) gene.^[157] Analysis revealed that the DNA sequence contains 13 complete *orfs* (Fig. 5 and Table 2). Except for ORF3, encoding a putative outer membrane channel protein, all *orfs* have the same direction. ORF1, coding for a putative protein for which no characterized homolog is known, is followed by a cluster of genes (7,041 bp) involved in the degradation of 4-hydroxyacetophenone (*hapABCFGDE*). Downstream of the *hap* genes, three genes

encoding putative regulatory proteins (ORF2, ORF4 and ORF5) and two genes coding for proteins possibly involved in a membrane efflux pump (ORF3 and ORF6) were found. The sequences of the *orfs* are presented in the appendix at the end of this chapter.

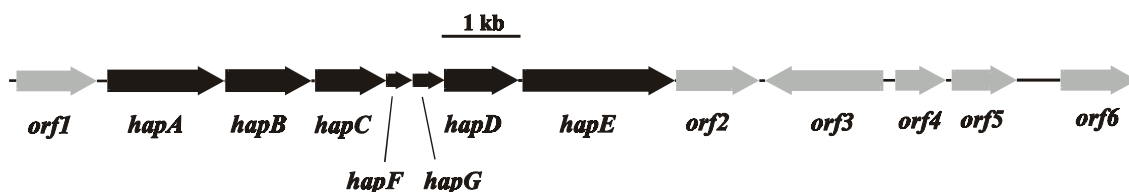


Fig. 5. The *hap* gene cluster and surrounding *orfs* of a 14-kb DNA fragment of *P. fluorescens* ACB

The *hapE* gene product, called HAPMO (E.C. 1.14.13.84), is the first enzyme in the degradation pathway. HapE converts 4-hydroxyacetophenone to 4-hydroxyphenyl acetate^[157,209] and is active with a wide range of aromatic and aliphatic ketones.^[157-159] HapE shows the highest sequence identity with the characterized steroid monooxygenase from *Rhodococcus rhodochrous*^[212] (Table 2) and belongs to the family of FAD-dependent Baeyer-Villiger monooxygenases.^[103,191]

HapD is the second enzyme of the 4-hydroxyacetophenone degradation pathway. This esterase (E.C. 3.1.1.2) was previously purified from *P. fluorescens* ACB grown on 4-hydroxyacetophenone.^[157] The enzyme efficiently converts 4-hydroxyphenyl acetate to hydroquinone. The determined N-terminal sequence of HapD^[157] exactly corresponds with the amino acid sequence derived from the *hapD* gene. The HapD sequence shows significant similarity with several lipases and esterases and contains a consensus motif GX SXG which includes the conserved active site serine.^[29] HapD shares the highest sequence identity (38%) with a characterized lipase from *Pseudomonas* sp. B11-1 (Table 2). This hydrolytic enzyme has been shown to be active with a range of *p*-nitrophenyl esters.^[43]

The *hapC* gene product shows 43% sequence identity with 6-chlorohydroxyhydroquinone 1,2-dioxygenase (6-chloro-HHQDO) of *Wautersia eutropha* JMP134, an intradiol dioxygenase that converts 6-chloroHHQ to chloromaleylacetate. Because hydroquinone is expected to be converted to 4-hydroxymuconic semialdehyde by an extradiol-type of dioxygenase,^[55,274] this raises the question whether *hapC* codes for HQDO (see below).

The deduced amino acid sequence of the fourth protein in the degradation pathway HapA, shows 45% sequence identity with CymC, a *p*-cumic aldehyde dehydrogenase, from *Pseudomonas putida*^[70] (Table 2). Based on the hydroquinone degradation experiments reported above, HapA is assigned to be an NAD⁺-dependent dehydrogenase (E.C. 1.2.1.61) that converts 4-hydroxymuconic semialdehyde to maleylacetate. Interestingly, HapA shows 37-43% sequence identity with 2-hydroxymuconic semialdehyde dehydrogenases, that are involved in the *meta*-cleavage pathways of catechol degradation.^[223,292] There is no other sequence of a 4-hydroxymuconic semialdehyde dehydrogenase known. However, genome projects show putative proteins that have up to 80% sequence identity with HapA from *P. fluorescens* ACB.

The gene coding for the fifth enzyme of the *hap* gene cluster (*hapB*), encodes a maleylacetate reductase (E.C. 1.3.1.32). HapB shows the highest sequence identity (56%) with the characterized maleylacetate reductase from *Pseudomonas cepacia*.^[56]

This enzyme converts maleylacetate to β -keto adipate, a well-known step in many degradation pathways, and it is present in the degradation of both hydroquinone and hydroxyhydroquinone.^[162]

In the *hap* gene cluster of *P. fluorescens* ACB, there are two genes that are not directly involved in the degradation of 4-hydroxyacetophenone. *HapF* codes for a conserved protein of the *yci1* family (pfam03795) but its function is unknown. *HapG* encodes a ferredoxin that might be involved in reduction of the iron-metal cofactor of extradiol dioxygenases.^[111,138,139,237,302]

Besides the *hap* gene cluster, there are six open reading frames present in the 14-kb DNA fragment of *P. fluorescens* ACB. *Orf1* codes for an unknown protein also found, next to a HapA-like dehydrogenase, in *Burkholderia cepacia* R18194 and *Photorhabdus luminescens* subsp. *laumondii* TT01.^[68] Sequence similarity searches suggest that *orf2*, *orf4* and *orf5* code for putative regulatory proteins while *orf3* encodes a putative outer membrane channel protein and *orf6* codes for a putative efflux pump.

Searching for comparison with other organisms we found that part of the *hap* gene cluster of *P. fluorescens* ACB has properties in common with the *pnp* gene cluster involved in the degradation of 4-nitrophenol by *P. fluorescens* ENV2030.^[352] The *pnp* gene cluster encodes a HapA (PnpD), HapB (PnpE) and HapC (PnpC)-like protein.

Alignment of HapC with ring fission dioxygenases

Sequence comparison revealed that HapC belongs to the family of iron(III)-dependent intradiol dioxygenases. The highest sequence identity (up to 40%) was found with a number of HHQDOs including the HHQDO from *Nocardioides simplex* 3E (Fig. 6). Significant sequence identity (up to 28%) was also observed with catechol 1,2-dioxygenases and in particular with CatA from *Acinetobacter calcoaceticus*, for which a crystal structure is available. From this structure and the data shown in Fig. 6, it could be inferred that the strictly conserved residues Tyr160, Tyr 194, His 218 and His220 of HapC (marked with * in Fig. 6) are involved in ligandation of the active site ferric ion.

HapC showed less than 10% sequence identity with PcpA (2,6-dichlorohydroquinone dioxygenase) from *Sphingomonas chlorophenolica* ATCC 39723^[33,229,346,349] and LinE (2-chlorohydroquinone dioxygenase) from *Sphingobium chlorophenolicum*,^[47] *Sphingomonas* sp. UG30 (GenBank accession number AAK28351) and *Sphingomonas paucimobilis*.^[207] Interestingly, these iron(II)-dependent chlorohydroquinone dioxygenases have been reported to also be active with non-chlorinated hydroquinone.

Table 2. Open reading frames of a 14-kb DNA fragment of *P. fluorescens* ACB

ORF	Frame	Position in sequence	Gene product nr. amino acids/weight (Da)	Function
<i>orf1</i>	+1	94-1119	341/38,345	Putative protein
<i>HapA</i>	+1	1210-2673	487/52,765	4-Hydroxymuconic semialdehyde dehydrogenase
<i>HapB</i>	+3	2682-3749	355/37,612	Maleylacetate reductase
<i>HapC</i>	+1	3793-4668	291/32,159	Hydroxyhydroquinone dioxygenase
<i>HapF</i>	+3	4665-4976	103/11,828	Putative protein yciI family
<i>HapG</i>	+3	4980-5369	129/13,866	Ferredoxin
<i>HapD</i>	+1	5359-6276	305/33,262	4-Hydroxyphenyl acetate esterase
<i>HapE</i>	+2	6329-8251	640/71,957	4-Hydroxyacetophenone monooxygenase
<i>orf2</i>	+3	8352-9284	310/35,222	Putative regulatory protein (LysR family)
<i>orf3</i>	-3	9356-10816	486/53,006	Putative outer membrane channel protein
<i>orf4</i>	+2	10964-11572	202/22,221	Putative regulatory protein (TetR family)
<i>orf5</i>	+3	11640-12431	263/28,189	Putative regulatory protein (Ic1R family)
<i>orf6</i>	+1	12991-13926	311/34,623	Putative efflux pump (EmrA family)

Characterization of the 4-hydroxyacetophenone degradation pathway

Closest characterized and uncharacterized homologs (GenBank accession number)	Organism	Identity (%)	Reference
^a putative protein (ZP_00217829)	<i>Burkholderia cepacia</i> R18194	78	
p-cumic aldehyde dehydrogenase (AAB62298)	<i>Pseudomonas putida</i> F1	45	[71]
NAD-dependent aldehyde dehydrogenase (ZP_00217828)	<i>Burkholderia cepacia</i> R18194	80	
maleylacetate reductase (Q45072)	<i>Burkholderia cepacia</i> AC1100	56	[56]
alcohol dehydrogenase, class IV (ZP_00274221)	<i>Ralstonia metallidurans</i> CH34	72	
6-chlorohydroxyquinol-1,2-dioxygenase (AAM55216)	<i>Wautersia eutropha</i> JMP134	43	[187]
protocatechuate 3,4-dioxygenase beta subunit (ZP_00274220)	<i>Ralstonia metallidurans</i> CH34	62	
^a putative protein (ZP_00217826)	<i>Burkholderia cepacia</i> R18194	53	
chloroplast-type ferredoxin XylT (P23103)^c	<i>Pseudomonas putida</i>	17	[121]
putative 4-nitrocatechol monooxygenase ferredoxin component protein (AAS87589)	<i>Ralstonia</i> sp. SJ98	40	
lipase (AAC38151)	<i>Pseudomonas</i> sp. B11-1	38	[43]
putative lipase (YP_075954)	<i>Symbiobacterium thermophilum</i> IAM 14863	39	
steroid monooxygenase (JC7158)	<i>Rhodococcus rhodochrous</i>	21	[212]
hypothetical protein (NP_960554)	<i>Mycobacterium avium</i> subsp. <i>paratuberculosis</i> k10	35	
HTH-type transcriptional regulator ptxR (P72131)	<i>Pseudomonas aeruginosa</i>	24	[118]
transcriptional regulator (ZP_00217831)	<i>Burkholderia cepacia</i> R18194	59	
outer membrane channel protein ttgF (CAB72260)	<i>Pseudomonas putida</i>	53	[213]
outer membrane protein OprM precursor (CAB72260)	<i>Pseudomonas aeruginosa</i> PA01	51	
regulatory protein TtgR (AAK15050)	<i>Pseudomonas putida</i>	23	[69]
efflux pump regulator SrpR (AAF16682)	<i>Pseudomonas putida</i> S12	25	
glycerol operon regulatory protein (P15360)	<i>Streptomyces coelicolor</i>	23	[273]
regulatory protein TtgV (AAK69562)	<i>Pseudomonas putida</i> DOT-T1E	56	
multidrug resistance protein A (P27303)^c	<i>Escherichia coli</i>	21	[186]
putative membrane fusion protein (AAN66777)	<i>Pseudomonas putida</i> KT2440	41	

^a no significant sequence similarity with a characterized protein

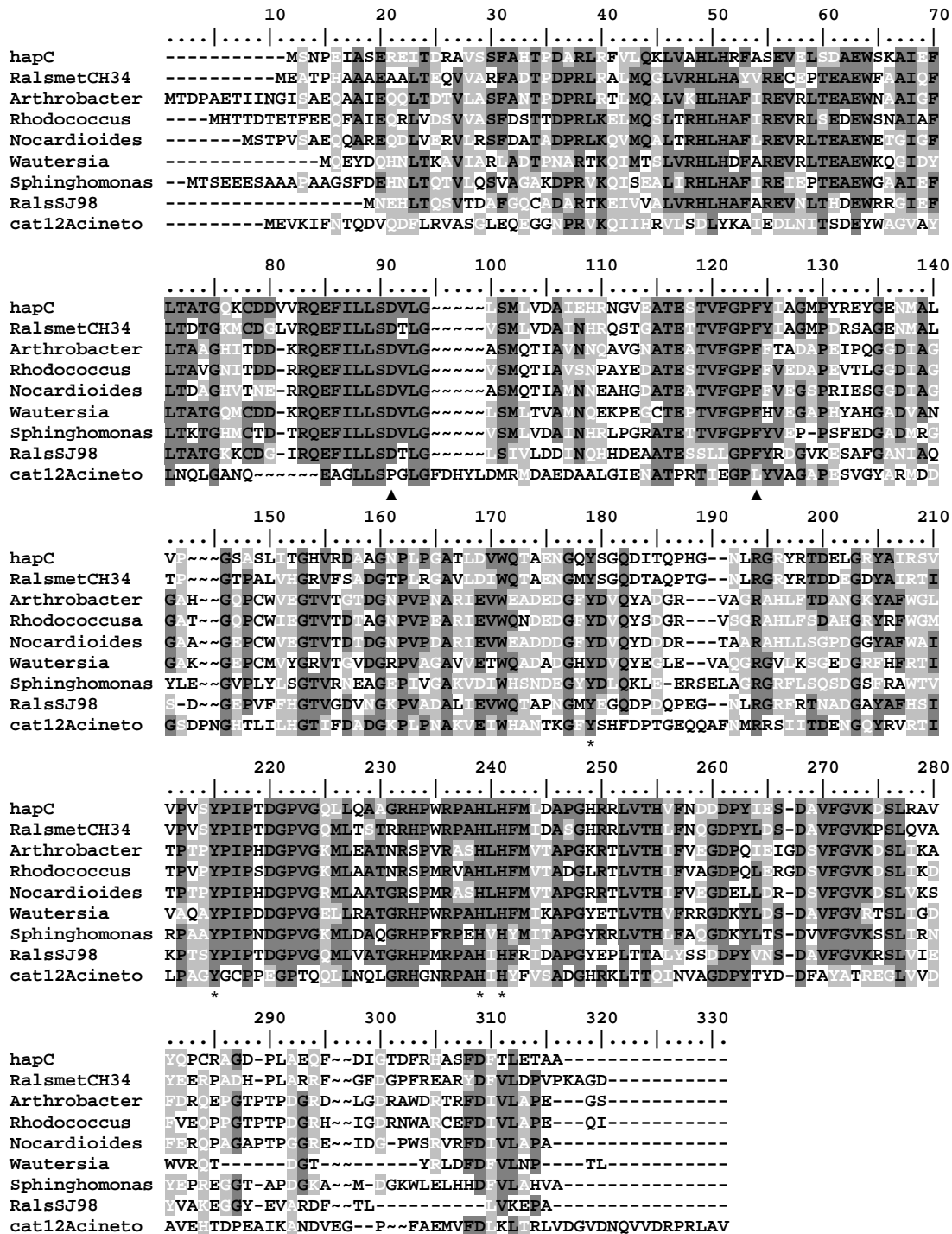


Fig. 6. Sequence alignment of HapC with HHQDOs and catechol 1,2-dioxygenase. HapC: putative intradiol dioxygenase from *P. fluorescens* ACB; putative HHQDO from *Ralstonia metallidurans* CH34 (ZP_00274220); HHQDO from *Arthrobacter* sp. BA-5-17 (BAA82713);^[217] HHQDO from *Rhodococcus opacus* SAO101 (BAD30043);^[167] HHQDO from *Nocardioides simplex* 3E (AAV71144);^[91] 6-Cl-HHQDO from *Wautersia eutropha* JMP134 (AAM55216);^[187] HHQDO from *Sphingomonas* sp. RW1(CAA51371);^[8] putative HHQDO from *Ralstonia* sp. SJ98 (AAS87586); catechol 1,2-dioxygenase from *Acinetobacter* sp. ADP1 (P07773). HapC is aligned with catechol 1,2-dioxygenase on basis of the secondary structure. The iron(III) ligands are marked with an asterisk (*). The amino acids expected to show interaction with HHQ are marked with a triangle (▲).

Structure homology model of HapC

The crystal structure of HHQDO from *N. simplex* 3E has recently been published but its coordinates are not yet available.^[91] Therefore, we used the three-dimensional structure of dimeric CatA from *Acinetobacter calcoaceticus*^[327] and the sequence alignment of Fig. 6 to build a model of HapC (Fig. 7). The iron(III) atom and aromatic substrate were fit in the model at the same position and orientation as CatA.

As found for CatA, each HapC subunit consists of two domains. The catalytic domain (residues 98-200 and 210-291) exists of 13 sheets and a small helix and harbors the active site. The interface domain (residues 1-97 and 201-209) exists of 6 helices and links the subunits to a dimer. As predicted from the sequence alignments, Tyr160, Tyr194, His218 and His220 are in perfect position for binding an iron(III) ion. When substrate and oxygen are absent, two water molecules form then the fifth and sixth ligand of the metal cofactor.



Fig. 7. Structural model of the ES-complex of HapC. The subunits of the homodimer are shown in light and dark gray. The iron atom is depicted as a sphere and the substrate and iron ligands are shown in ball-and-stick.

The three-dimensional models of free and HHQ-bound HapC suggest that Tyr194 has to bend away to let the aromatic substrate enter the active site as has been observed for other intradiol dioxygenases.^[228,326,327] The HapC model also suggests that Asp80 might be involved in binding the 4-hydroxy moiety of HHQ. This aspartate is conserved in the HHQDO family in the RQEFILLSDxLG motif, but is replaced by a proline or alanine in the catechol 1,2-dioxygenase family in the LxA/PGLGxxxxLDx motif. Phe108, conserved in HHQDOs in the ATE_xTVFGPF_x motif, seems to stack with HHQ and is replaced by a leucine in the xTPRTIEGPLY motif in catechol 1,2-dioxygenases. The HHQDO family shows another conserved region, xYPIPxDGPVG, that is replaced by GYGxxPxGxTQ in the catechol 1,2-dioxygenase family. This region forms the link between the catalytic and the interface domain. The tyrosine within this motif (Tyr194 in HapC) bends away when the substrate enters the active site. The proline rich region points at a structural function, probably involved in the in-out mechanism of this tyrosine residue.

Discussion

This paper describes the biochemical and genetic characterization of the 4-hydroxyacetophenone degradation pathway in *P. fluorescens* ACB. Earlier studies revealed that the degradation of 4-hydroxyacetophenone is initiated by a Baeyer-Villiger oxidation to 4-hydroxyphenyl acetate and then proceeds through the formation of hydroquinone.^[133,157] Here we showed that *P. fluorescens* ACB converts

hydroquinone to 4-hydroxymuconic semialdehyde and that difluorinated hydroquinones are converted via difluorinated 4-hydroxymuconic semialdehydes to the corresponding difluoromaleylacetates in both the *enol*- and *keto*-form as also described for a *Pseudomonas* sp. HH35 converting methylhydroquinones.^[260] Formation of significant amounts of fluoride anion pointed at the activity of maleylacetate reductase.^[161,162,329]

Cloning and sequence analysis of the genes involved in the catabolism of 4-hydroxyacetophenone revealed a gene cluster (*hapABCFGDE*) of which at least 4 encoded enzymes are directly involved in 4-hydroxyacetophenone degradation: 4-hydroxyacetophenone monooxygenase (*hapE*); 4-hydroxyphenyl acetate hydrolase (*hapD*); 4-hydroxymuconic semialdehyde dehydrogenase (*hapA*) and maleylacetate reductase (*hapB*). From this and the product analysis studies we propose that *P. fluorescens* ACB degrades 4-hydroxyacetophenone to β -keto adipate by the pathway depicted in Fig. 8.

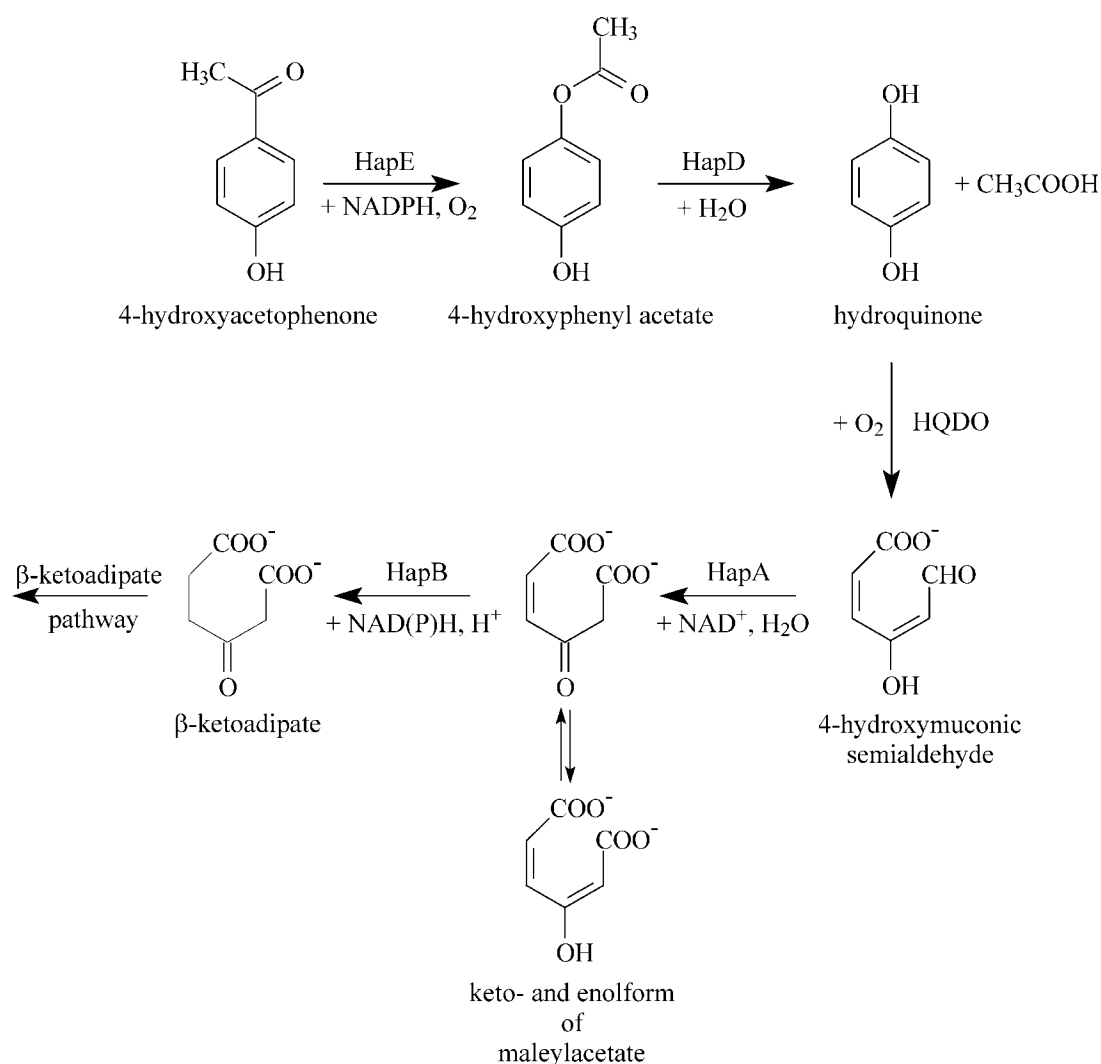


Fig. 8. Degradation pathway of 4-hydroxyacetophenone by *P. fluorescens* ACB

In the *hapABCFGDE* cluster no gene was found which function could be linked to the conversion of hydroquinone to 4-hydroxymuconic semialdehyde (Fig. 8). This reaction presumably is catalyzed by an iron(II)-dependent extradiol dioxygenase.^[346]

These enzymes generally contain a His₂-Glu triad involved in binding the iron atom.^[166,256,285,300,328] Interestingly, the *hapG* gene was found to encode a [2Fe-2S] ferredoxin. In several related microorganisms, this electron transfer protein is required for the reductive reactivation of catechol 2,3-dioxygenases.^[111,138,139,237,302] This leads us to suggest that in *P. fluorescens* ACB, HapG might be involved in the reactivation of the highly unstable HQDO (see Chapter 7).

Structure homology modeling indicated that HapC has many structural properties in common with the iron(III)-containing HHQDOs and catechol 1,2-dioxygenases. This strongly suggests that the *hapC* gene is not coding for HQDO and is not involved in the degradation pathway of 4-hydroxyacetophenone (Fig. 8). In line with this, HapC might be responsible for the observed activities of *P. fluorescens* ACB with 4-fluorocatechol^[209] and HHQ (this chapter). The reason why *hapC* is embedded in the *hap* gene cluster is not clear. However, it is interesting to note that there are more examples of HHQDO-containing organisms where a HQDO serves as a key enzyme in the degradation pathway of aromatic compounds (see also Chapter 7).^[274,352]

The *hap* gene cluster of *P. fluorescens* ACB shows similarities with the *pnp* gene cluster of *P. fluorescens* ENV2030 involved in 4-nitrophenol utilization.^[352] The *hapABC* genes have the same size and orientation as the *pnpDEC* genes. Bang and Zylstra reported that *pnpD* (corresponding to *hapA*) codes for a 4-hydroxymuconic semialdehyde dehydrogenase showing homology with both eu- and prokaryotic aldehyde dehydrogenases and that *pnpE* (corresponding to *hapB*) codes for a maleylacetate reductase.^[11] Furthermore, it was concluded that *pnpC* codes for the dioxygenase involved in the formation of 4-hydroxymuconic semialdehyde from hydroquinone.^[11] The *pnpC* gene corresponds to the *hapC* gene and the amino acid sequence of the PnpC protein has a high level of sequence similarity with HHQDOs.^[11,352] Thus, also for the 4-nitrophenol pathway of *P. fluorescens* ENV2030 it can be questioned whether PnpC is involved in this pathway. So far, no biochemical evidence has been provided that HapC and PnpC show HQDO activity. With this in mind, we aim to characterize the HQDO from *P. fluorescens* ACB by a reverse genetics approach (see Chapter 7).

ACKNOWLEDGEMENTS

We thank Ludwin van Aart and Bep van Veldhuizen for assistance in NMR experiments.

This work was supported by the Council for Chemical Sciences of the Netherlands Organization for Scientific Research (CW-NWO), division ‘Procesvernieuwing voor een Schoner Milieu’.

Appendix

Orf1

MAMLEAVETANALSFAADDLVTASAPHLVGTGYKAFELGSFNLSRDEYFARIEWPAKGEQRSHLIPADAFRLR
SVMRDVAWGFFYGWVNFHDHVFGRNHYGKVDVYAGTFNGVLKAAGVDYTEQFETPLIMATFKAILRDWVN
AGFDPPFAAPAETGTAFGRKNGENIEAIERFRVATRRMPGLADDSPLRNDLPVNRQFADVVQDEPEVHAAD
GFEGELHAFSLYKYLRSRSDVSWNPSVTSVCGASLFCPTTEEFILPIVHGNDRIEWFLLQLSDEI IWDIGDK
DDGDPRARITMRAGDICAMPADIRHQYSTKRSMLLVWENATPNLPQRYESGELKPYPVFE

HapA aldehyde dehydrogenase

MQNQLFIDGQFVPALEGGEDVNVNPASGELITRIAAAKAEDVDRAVAAAKRAFPAWAAMPGAERGRLLLLK
LADRIEACTDELARLES�DTGHPLRDSRILDVPRTAACFRYFGGIADKIEGKVI PVDAGFLNYVQRKPIG
VVGQIVPWNFPLMFTSWKMGPALAAGNTVVLPSELTPPLSTRIAELMKEVGF PNGVVNI VPGYGHGTAGQ

Chapter 6

RLAEHPDVGKIAFTGSTATGRRIVEASQGNLKRVLQLELGGKGANIVFEDANLEAAVNGAAWAI FHNQGQA
CIAGSRLLLQESI ADEFLEFVSLARSIRLGDPLDGTTEMGPLTSALHRDRVLSFVDIARQQGGRILTGG
KAPSDPSLASGFYVEPTIVEASPGDRVAQEEVFGPFVTVLRFKTEEEALAIANGTDYGLGSGLWTRDLQR
AHLRAAQISAGMCWINCYKRVSPGSPFGGLGQSGYGREMGFDAIHDYTEARSVWVNVDAKILPHYPR

HapB maleyl acetate reductase

MNSFIYQGTATRVIFGPGKLASLGDEIQRGAQRALILTTPQEELGEQVARLLGDRSAGVYPKAVMHVP
LETAQAAREEALRREADCCVAVGGGSTIGLGKAIAMDSGLPILAVPTTYAGSEMTPITYGLTENRLKKTGR
DPRVLPRTVIYDPQLTLTLPVGLSACSGMNAHAHAIEALYAEDANPVI SLMAEESIRALAQSLPKVVDDP
QNV DARGQALQGAWLAGICLGSVGMAIHHKLCHTLGGTFNLPHAQAHAI VLPHAAHYNRDAAAEP LRRVA
RALGGERADEVGP LLYALNRR LGIPLALAEVGFPEHGPKAARIACANPYYNPRPFEQDAIGDLLARALK
GQAPA

HapC intradiol dioxygenase

MSNPEIASEREITDRAVSSFAHTPDARLRFVQLKLV AHLRFASEVELSDAEWSKAI EFLTATGQKCDDV
VRQEFILLSDVGLSMLVDAIEHRNGVEATESTVFGPFYIAGMPYREYGENMALVPGSASLITGHVRDAA
GNPLPGATLDVWQTAENGQYSGQDITQPHGNLRGRYRDELGRYAIRSVVPVSYPIPTDGPVGLLQAAG
RHPWRPAHLHFMLDAPGHRRLVTHVFNDDDPYIESDAVFGVKDSLRAVYQPCRAGDPLAEQFDIGTDFRH
ASFDFTLETAA

HapF yci1

MNQFFAIFATDKPDLEILRKQIRPQHRQYLREPHPHRVVRLGGPTLNSCAQVMNGTLLVVEAGSLHETE
AFFADDPYVRAGL FERVEIRPWSWGLGK PQMEA

HapG ferredoxin

MVAIALCAFEQVPEGGALGVQAMLHGRSTALVAVRRGAQVWVYHNRCPHFSIPLDYQPGTFSTYQGQLLM
CAHHAAMFRFADGHCIDGPCAGAYLDSVAVCERDGLWLAEVQDGPAGGPSCQEKHHDA

HapD esterase

MTLDVESAQLLGQLAERGA KPFFHLLDPAQARELIAGLRPQAHGPAMQHVENMKLGLARLRILRPSASVRG
AILYLHGGGWVVGGLDDDFDFARQLAQR TQCTVVLVDYRLAPEFPFPAALDDVESAAQWLVEHRTELAGA
ADGALIVAGDSAGGNLAAVFSQRAALRGDRHWALQVLIYPATQADLDGPAYRDPQRQLLSREDMAFWFG
HYIADIDQRQQSDASPLAAKDLGGVPPAVVLTAEFDVLR EEGQAYADRLAQAGITVIERCFSGQM HG FVT
LPALRASGDALDWLSDQIKPWLKPF

HapE HAPMO

MSAFNTTLP SLDYDDDTLREHLQGADIPTLLLTVAHLTGDLQILKPNWKPSIAMGVARS GM DLETEAQVR
EFCLQR LIDFRDSGQPAPGRPTSDQLHILGTWLMGPVIEPYLPLIAEEAVTAEEDLRAPRWHKDHVASGR
DFKVVII GAGESGMIAALRFKQAGVPFVIYEKGNVDVGTWRENTYPGCRVDINSFWYSFSFARGI WDDCF
APAPQVFAYMQAVAREHGLYEHIRFNTEVSDAHWDESTQRWQLLYRDESEGQTQVDSNVVVFVAVGQLNRPM
IPAIPGIETFFKGP MFHSAQWDHDVDWSGKRVGVI GTGASATQFIPQLAQTAELKV FARTTNWLLPTPDL
HEKISDCKWLLAHVPHYSLWYRVAMAMPQSVGFLEDVMVDVGYPPTELA VSARNDRLRQDISAWMEPQF
ADRPDLREVLIPDSPVGGKRIVRDNGTWISTLKRDNVSMIRQPIEVITPKGICCV DGT EHEFDLIVYGTG
FHASKFLMPINVTGRDGVALHDVWKGDARAYLGMTVPQFPNMF CMYGPNTGLVVYSTVIQFSEMTASYI
VDAVRL LLEGGHQSMEVKTPVFESYNQRVDEGNALRAWGF SKVNSWYKNSKGRVTQNF PFTAVEFWQRT H
SVEPTDYQLG

Orf2

MDRLLITEAFVRVAQTGSFAKAAEQ LGVTRSVITHRVQQLETFINSPLFHRSTRHVRLSDIGEAYFQECA
DMVAGFHGLTEKMRHQRSNLTGQLRVQVLQGFV D HLG PMLAKFTALHPEIEFDVVVNDRVDP IEEGFD
IAFQMFPPLAERLVVRKLF SVHRVFCASPQYLEERGAP EHPQHLKDHMMALFGGYPSRNRWQFVRGEECI
DLTLHGQVRSSSIHLLRDYALSGAGITCLPTLVASNELITGR LVPILT DYRLSSFDFAAVYPETQRRALR
VRTLIDFLIDHIGEMPHWDQSLHDGGII IH

Orf3

MTFKTLAIAILLGAGLQGCTLMPAYHRPAAPVDQSWPQGQAYKASSVGAANS AKSIADLHWQQFFRDPAM
RQLIGVALANNRDLRQAALNVDAYRALYRIQRSELTP TVDVS GSGAKQHLAGDLAIPGKTGT YGDYELNV
GVASYELDVFGRIQSLNESALQTYLSTEEVQR SVQVGLIASVANAYLTWR TDQEL LKIAQSTSDTYTRGL
NVMQSARAAGTMSDL SVRQARTLVDTARTKILAYTRRVAHDQNALALLLGTDI PRYIPD TDDWTQRM IAS
IPAGLPADILRQRPDVRAAERNLIAANANIGAARAAFYPSISLTANAGVASEQLSHLFAGGQGWTFVFPQ
VNIPIFNGRRLKANLDYAEIQKDIRVVAYEKSIQTAFSEVADGLASAGLYDEQLQAHRLAQDNNAYL DL
ALNFRFRHGVGNFLPVLDAQRNLF AAREELVGNRLLQLQSQVQLYRALGGGW DNT ELA GLRDQP HVE

Characterization of the 4-hydroxyacetophenone degradation pathway

Orf4

MGRKTVEESEQTRLKLM EAGTRIFAKHGFAYSTLNDIAHFAGLSRGAVYWHFKGKWELLQSIMNAAVLPL
EEFFVASAPTKGLEHLLKALGDTLCVQHHRDLCTILLKDG EIGLLECPVVVRWRVAQENLRVQLKLLLR
RQPAGMRSQEQLDALAH LIALSITGLITESLHNAQSVEK SISPVLVQALRELLGCAGAGVGGH

Orf5

MSDPGEPSE GKQPSIQVIARAAA I LRALGSNGGLSLSA IANIVKLPRSTVHRI I VALEEEHLVESIGPSG
GFRLGHALGQLIHETQADI ISSVREYLDNLCAQVRESVCLATLAGDKVNVVDCII IERELRVVFSVGIEA
PAYATAGGKIMLAALREDALQNILPKKLP ELTENTLTRAQLIEQLKDIRACAVAVDDQEHLEGVCTFAVA
LETYLGNY SISISI IAPSIRAGRYGDSYKAALIDCKRTIEKKIGRMPEGAVAGRK

Orf6

MKRAANMAMTLV LIGAIVICLFYIWD RYMYTPWTRDGRVRADV VNIAPDVSGWVDQLHAENSREVKEGDV
LFTVDRSRYQVAVDLAQAQSDTAKVAWDRASN VYKRRQTQMSVEAVSREELDT SRLDMM EKKASFTQSTAV
LNSAKIDLARTVYTSPASGKI INLELEKGDYVNRGVNRLALVKDGSYYVTGYFEETKIP SIRIGDKVEIW
LMAGTVKLDGHVSSIDSGISNSNAEPGTQMLPNVEATFAWVRLAQRIPVNIKIDHVPDGIHLSSGMSATV
KVVVQKATRVISARLYTRWMKSQGDVVAPSI

Chapter 7

HYDROQUINONE DIOXYGENASE FROM *PSEUDOMONAS FLUORESCENS* ACB

A NOVEL MEMBER OF THE FAMILY OF NON-HEME IRON(II)-DEPENDENT
DIOXYGENASES

Mariëlle J.H. Moonen, Willy A.M. van den Berg, Silvia Synowsky,
Robert H.H. van den Heuvel and Willem J.H. van Berkel

Hydroquinone 1,2-dioxygenase (HQDO), an enzyme involved in the catabolism of 4-hydroxyacetophenone in *Pseudomonas fluorescens* ACB, was purified to apparent homogeneity. Ligandation with 4-hydroxybenzoate prevented the enzyme from irreversible inactivation. HQDO was activated by iron(II) ions and catalyzed the ring-fission of a wide range of hydroquinones to the corresponding 4-hydroxymuconic semialdehydes. HQDO was inactivated by 2,2'-dipyridyl, *o*-phenanthroline and hydrogen peroxide and strongly inhibited by phenolic compounds. The inhibition with 4-hydroxybenzoate ($K_i = 14 \mu\text{M}$) was competitive with hydroquinone.

SDS-PAGE of the purified enzyme showed main protein bands at 18 and 38 kDa. On-line size-exclusion chromatography-mass spectrometry clearly showed that HQDO is an $\alpha_2\beta_2$ heterotetramer of 112.4 kDa, which is composed of an α -subunit of 17.8 kDa and a β -subunit of 38.3 kDa. N-terminal sequencing and MALDI-ToF-ToF-based peptide mapping and sequencing revealed that the HQDO subunits are encoded by neighboring open reading frames (*orf0* and *orf1*) of a gene cluster, implicated to be involved in 4-hydroxyacetophenone degradation.

The data presented here suggest that HQDO is a novel member of the family of non-heme iron(II)-dependent dioxygenases. The enzyme shows insignificant sequence identity with known dioxygenases.

Introduction

The catabolism of 4-hydroxyacetophenone in *Pseudomonas fluorescens* ACB proceeds through the initial formation of 4-hydroxyphenyl acetate to hydroquinone.^[133,157,209] In the previous chapter we showed that hydroquinone is further degraded via 4-hydroxymuconic semialdehyde and maleylacetate to β -ketoadipate:

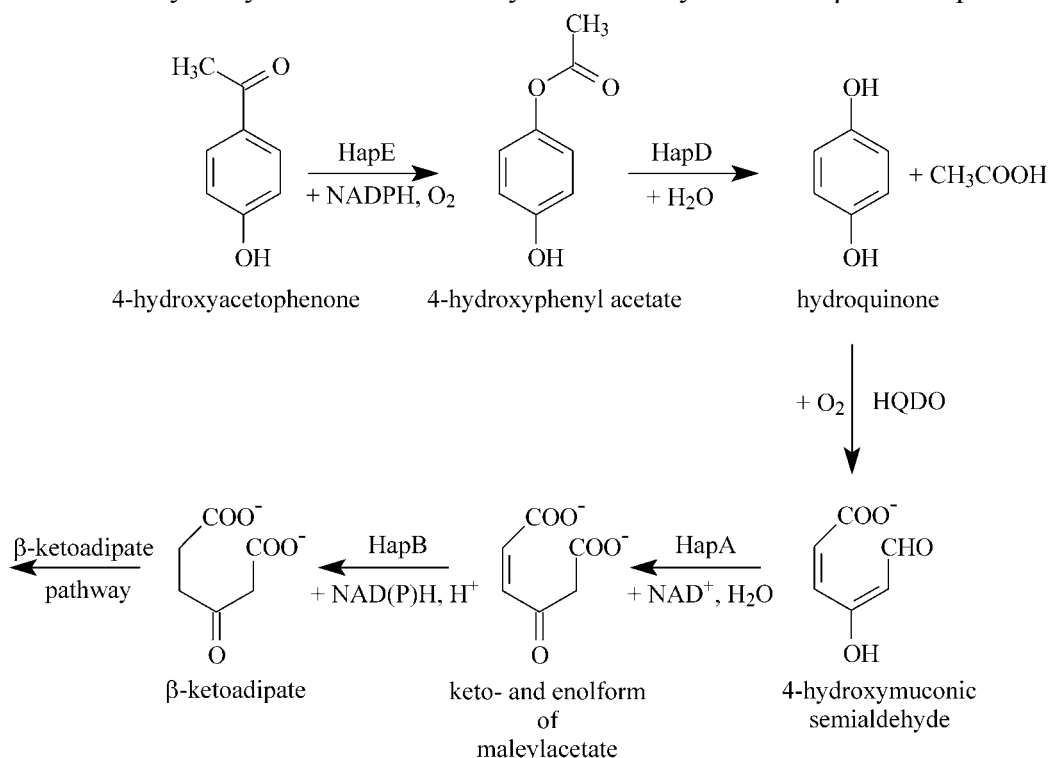


Fig 1. Degradation pathway of 4-hydroxyacetophenone in *Pseudomonas fluorescens* ACB

The genes of four enzymes involved in this pathway were found to belong to the *hapABCFGDE* gene cluster of *P. fluorescens* ACB (Chapter 6). However, no gene was found which function could be linked to the conversion of hydroquinone to 4-hydroxymuconic semialdehyde.

Several ring-cleavage enzymes acting on substituted hydroquinones have been described. These include intradiol dioxygenases acting on hydroxyhydroquinone (HHQ),^[149,245] and extradiol dioxygenases that are active with (homo-)gentsate^[7,123] or chlorohydroquinone.^[34,207,229] However, enzymes that use hydroquinone as the physiological ring-cleavage substrate have not been characterized. Here we report on the purification and properties of hydroquinone dioxygenase (HQDO) from *P. fluorescens* ACB. It is shown that the heterotetrameric enzyme is a novel member of the family of non-heme iron(II)-dependent dioxygenases and that the HQDO-encoding genes are located directly upstream of the *hapABCFGDE* cluster. The present results confirm our earlier proposal (Chapter 6) that the *hapC* gene is not involved in 4-hydroxyacetophenone degradation. This finding has important implications for the function of related genes involved in the catabolism of other aromatic compounds.

Materials and Methods

Materials

Phenolic compounds were purchased from Aldrich or Acros. NADPH, NADH, NAD⁺, dithiothreitol (DTT), DNase, and RNase were from Boehringer. Phenylmethylsulfonyl fluoride (PMSF) was from Merck. *N,N*-bis[2-hydroxyethyl]-2-aminoethanesulfonic acid (BES), bis(2-hydroxyethyl)imino-tris(hydroxymethyl)-methane (BisTris), 3-[cyclohexyl amino]-1-propanesulfonic acid (CAPS), bovine serum albumin (BSA), 2,2'-dipyridyl and protamine sulfate were from Sigma. Phenanthroline was from Fluka. All other chemicals were of analytical grade.

Bacterial strains and enzymes

P. fluorescens ACB^[133] was grown on 4-hydroxyacetophenone as described before.^[157] *p*-Hydroxybenzoate 1-hydroxylase from *Candida parapsilosis* CBS640,^[82] *p*-hydroxybenzoate 3-hydroxylase from *P. fluorescens*,^[312] lipoamide dehydrogenase from *A. vinelandii*,^[337] *D*-amino acid oxidase from pig kidney,^[54] and 4-hydroxyacetophenone monooxygenase (HAPMO) from *P. fluorescens* ACB^[157] were purified as described.

Purification of HQDO from *P. fluorescens* ACB

Purification steps were performed at 4°C, unless stated otherwise. *P. fluorescens* ACB cells (5 g wet weight) were suspended in 5 ml 20 mM BisTris-chloride pH 7.0 containing 1 mM 4-hydroxybenzoate, 10% (v/v) glycerol and 0.1 mM PMSF (buffer A). Immediately after the addition of 1 mM EDTA, 2 mM MgCl₂ and 1 mg DNase, cells were disrupted three times through a precooled French press at 10,000 psi. After centrifugation (27,000g, 30 min), the clarified cell extract was adjusted to 25% ammonium sulfate saturation. The precipitate thus formed was removed by centrifugation (27,000 g, 30 min) and the supernatant was loaded onto a Phenyl Sepharose column (1.6 x 11 cm), equilibrated in buffer A, containing 25% ammonium sulfate. After washing with 3 column volumes of starting buffer, the HQDO activity was eluted with a 100 ml linear gradient of 25–0% ammonium sulfate in buffer A. Active fractions were pooled and adjusted to 60% saturation with pulverized ammonium sulfate. The precipitate was collected by centrifugation (27,000 g, 30 min), dissolved in 1 ml buffer A and eluted over a Superdex 75 PG column (2.6 x 54 cm), equilibrated with buffer A, containing 50 mM NaCl. Active fractions were pooled and applied onto a Resource 30Q column (1.6 x 5 cm), equilibrated in buffer A, containing 50 mM NaCl. After washing with 3 volumes of starting buffer, the HQDO activity was eluted with a 180 ml linear gradient of 50 – 350 mM NaCl in buffer A. Under these conditions, HQDO eluted at 170 mM NaCl whereas the HAPMO activity eluted at 300 mM NaCl. Active HQDO fractions were pooled, concentrated by ultrafiltration (Amicon Ultra-4, 10 kDa membrane) and stored at a concentration of 4.6 mg/ml in 20 mM BisTris-Cl, 10% glycerol, 170 mM NaCl, pH 7 at -20°C. The HAPMO pool served as a reference in MALDI-ToF peptide mapping (see below).

Enzyme activity and stability studies

Enzyme activity measurements were performed at 25°C using air-saturated buffer. The activity of HAPMO was determined as described before.^[157]

For activity studies with HQDO, the stock enzyme solution (1 ml) was freshly incubated for at least 1 min with 100 μM FeSO_4 and desalted over a Biogel P-6DG column (1 x 10 cm), running in 20 mM BisTris pH 7.0, containing 10% glycerol.

HQDO activity was routinely determined spectrophotometrically by monitoring the formation of 4-hydroxymuconic semialdehyde at 320 nm ($\epsilon_{320} = 11.0 \text{ mM}^{-1} \text{ cm}^{-1}$).^[274] The assay mixture (1.0 ml) typically contained 50-200 nM enzyme, 10% (w/v) glycerol in 20 mM BES, pH 7.0. Reactions were started by the addition of 10 μl 50 mM hydroquinone in DMF. One unit of HQDO activity is defined as the amount of enzyme that forms 1 μmol of semialdehyde product per minute.

Potential aromatic substrates (freshly dissolved in DMF) were tested at concentrations ranging from 10 μM to 10 mM with the total amount DMF never exceeding 1%. Conversion of 2-fluorohydroquinone was studied by ^{19}F NMR. For this purpose, 0.3 mM 2-fluoro-4-hydroxybenzaldehyde was incubated with 0.5 mM NADPH and 0.74 nM HAPMO in 50 mM Tris-HCl pH 7.5 at 30°C. After NADPH consumption had ceased, the reaction mixture was divided in two parts. One part was incubated for 10 minutes with 1 μM HQDO, whereas the other part was used as a control. Immediately after the incubation, both samples were frozen in liquid nitrogen and stored at -20°C.

Potential phenolic inhibitors (freshly dissolved in DMF) were tested at a concentration of 200 μM with 50 μM hydroquinone. For estimation of steady-state kinetic parameters and inhibition constants, hydroquinone concentrations were varied and fixed amounts of inhibitor were used. Experiments with tetrafluorohydroquinone were performed in the presence of 1 mM ascorbate to suppress autooxidation.

The thermal stability of HQDO was studied by incubating 6 μM of purified enzyme at 30°C in 20 mM BisTris-Cl, 10% glycerol pH 7.0 in the absence or presence of 1 mM 4-hydroxybenzoate. At time intervals, aliquots were withdrawn from the incubation mixtures and assayed for standard HQDO activity.

The metal ion specificity of HQDO was determined by measuring the activity of non-liganded enzyme in the presence of either 0.1 mM FeSO_4 , 1 mM $(\text{NH}_4)_2\text{Fe}(\text{SO}_4)_2$, 1 mM FeCl_3 and 1 mM MnSO_4 .

Time-dependent inactivation of HQDO was studied by incubating 34 μM of enzyme at 0°C in 20 mM BisTris-Cl, 10% glycerol pH 7.0 in the absence or presence of respectively 0.1 and 1 mM 2,2'-dipyridyl, 0.1 mM *o*-phenanthroline and 0.1 and 1 mM hydrogen peroxide. At time intervals, aliquots were withdrawn from the incubation mixtures and assayed for standard HQDO activity.

Analytical methods

^{19}F NMR measurements were performed as described earlier.^[210] Absorption spectra were recorded using a Hewlett-Packard 8453 diode array spectrophotometer. Protein content was determined with the microbiuret method^[110] using bovine serum albumin as a standard. Desalting or buffer exchange of protein solutions was performed with Biogel P-6DG columns (Biorad).

SDS-polyacrylamide gel electrophoresis was carried out with 15% Tris-glycine gels.^[335] The Amersham Pharmacia Biotech low molecular mass calibration kit containing phosphorylase *b* (94 kDa), bovine serum albumin (67 kDa), ovalbumin (43 kDa), carbonic anhydrase (30 kDa), soybean trypsin inhibitor (20.1 kDa), and

α -lactalbumin (14.4 kDa) served as a reference. Proteins were stained with Coomassie Brilliant Blue G250.

The relative molecular mass of native HQDO was determined by FPLC gel filtration using a Superdex 200 HR 10/30 column (Amersham Biosciences) running with 20 mM BisTris-Cl pH 7.0, containing 10% glycerol and 50 mM NaCl. The column was calibrated with catalase (232 kDa), aldolase (158 kDa), lipoamide dehydrogenase (102 kDa), *p*-hydroxybenzoate 3-hydroxylase (88 kDa), *D*-amino acid oxidase (80 kDa), bovine serum albumin (67 kDa), ovalbumin (43 kDa), chymotrypsinogen A (25 kDa), RNase (13.7 kDa) and FMN (480 Da).

Mass spectrometry

For nanoflow electrospray ionization mass spectrometry of HQDO, samples were prepared in 50 mM ammonium acetate, pH 6.7. Protein samples were introduced into the nanoflow electrospray ionization source of a Micromass LCT mass spectrometer (Waters), modified for high mass operation and operating in positive ion mode. Mass determinations were performed under conditions of increased pressure in the source and intermediate pressure regions in the mass spectrometer (Pirani gauge readback 7 mbar and Penning gauge readback 1.2×10^{-6} mbar).^[259,290] HQDO was infused in the mass spectrometer by using in-house pulled and gold-coated borosilicate needles (Kwik-Fil, World Precision Instruments). Borosilicate capillaries were pulled on a P-97 puller (Sutter Instruments) to prepare needles with an orifice of about 5 μ m and coated with a thin gold layer (\sim 500 Å) using an Edwards Scancoat six Pirani 501 sputter coater (Edwards High Vacuum International). Electrospray voltages and source temperature were optimized for transmission of HQDO (capillary voltage 1500 V, sample cone voltage 50 V, extraction cone voltage 0 V and capillary temperature 80°C).

For on-line size-exclusion-electrospray mass spectrometry of HQDO, samples were prepared in 20 mM BisTris-Cl, containing 10% glycerol and 50 mM NaCl, pH 7.0. 15 μ l of a 20 μ M enzyme solution was loaded onto a 10 μ l sample loop in a 6-port valve. The enzyme was then injected onto a Superdex 200 H/R size-exclusion column (3.2 mm x 300 mm; Amersham Biosciences) using a mobile phase of 50 mM ammonium acetate, pH 6.7 at a rate of 50 μ l/min, in the presence or absence of 20 μ M FeSO₄ and 15 μ M 4-hydroxybenzoate. The post-column eluent was guided into the electrospray source using a fused silica emitter. In these experiments we did not use the nanoflow source, as the flow was two orders of magnitude too high to desolvate the droplets originating from the ionization process. The electrospray source was optimized for transmission of HQDO (capillary voltage 3,000 V, cone voltage 125 V, extraction cone voltage 5 V and capillary temperature 250°C). All other settings were similar with the experiments with the borosilicate capillaries. Apparent molecular masses were determined using a calibration curve made with standards from a molecular weight marker kit (BioRad) containing thyroglobulin (670 kDa), bovine γ -globulin (158 kDa), chicken ovalbumin (44 kDa), equine myoglobin (17 kDa) and vitamin B₁₂ (1.35 kDa).

MALDI-ToF peptide mapping and MALDI-ToF-ToF peptide mapping and sequencing

Purified HQDO was subjected to SDS-PAGE. Stained protein bands of interest were pierced from the gel with a pipette tip. After destaining with 50% acetonitrile in 10 mM NH₄HCO₃ pH 8.0, the protein-containing gel slices were incubated with 10 mM DTT in 10 mM NH₄HCO₃ for 1 h at 56°C, followed by a 1 h incubation with 55 mM

iodoacetamide at room temperature. The slices were washed three times with 10 mM NH_4HCO_3 and after drying in a vacuum centrifuge, treated with trypsin as described.^[251,269] The extracted peptides were co-precipitated with α -cyano-4-hydroxycinnamic acid using the “dried droplet” method on a Anchorchip plate and measured on an Ultraflex MALDI-ToF (Bruker Daltonics, Bremen, Germany). Analysis of mass data was done with Flex Analysis 2.0 (Bruker Daltonics). Peak Erazor 1.50 (Lighthouse Data, Denmark) was used to eliminate the peaks in the blank and peaks of the matrix, trypsin and keratin. GPMW 6.10 (Lighthouse Data) was used to compare the peaks with known sequences.

For peptide sequencing an identical approach was followed, but in these experiments the MS and MS/MS measurements were performed on a MALDI-ToF-ToF (AB 4700 Proteomics Analyzer, Applied Biosystems) in a reflectron positive ion mode using delayed extraction. The instrument is equipped with a 200Hz Nd:YAG laser operating at 355 nm. Typically 2,000 shots/spectrum were acquired in the MS-mode and 15,000 shots/spectrum in the MS/MS mode. During MS/MS analysis air was used as the collision gas. All spectra were calibrated externally using a peptide mixture that consists of 100 fmol des-Arg Bradykinin, Angiotensin I, GluFib, ACTH 1-17, ACTH 7-38 and ACTH 18-39. Mass accuracy is within 50 ppm. The data were analyzed using *de novo* sequencing by GPS software (Applied Biosystems) and was confirmed by manual examination.

N-terminal sequencing

The N-terminal sequence of HQDO was determined by Edman degradation. The contents of a 15% SDS-PAGE gel (140 x 120 x 1.5 mm) loaded with 9.2 and 18.4 μg purified enzyme were blotted onto a poly(vinylidene difluoride) Immobilon-P support (Millipore) in 10 mM CAPS pH 11.0, containing 10% ethanol. After staining with 0.1% Coomassie R-250 in 50% methanol, the main bands corresponding to relative molecular masses of 38, 32 and 18 kDa were excised. Gas-phase sequencing of the polypeptide on the Immobilon support was carried out at the sequencing facility of Leiden University, The Netherlands.

For sequence alignment studies, a PSI-BLAST^[5] search was performed at the National Centre for Biotechnology Information (NCBI). Multiple sequence alignments and an unrooted tree were made with the Clustal W program at the European Bioinformatics Institute (www.ebi.ac.uk/clustalw).^[299] BioEdit^[117] was used to calculate the pairwise identity and similarity scores (PAM250 matrix) from the aligned sequences and for the display of the alignment. Treeview was used for visualization of the dendrogram.^[233]

RESULTS

Purification of HQDO from *P. fluorescens* ACB

Purification of HQDO was not straightforward. Initial purification attempts, performed either in the absence or presence of 1 mM dithiothreitol, resulted in rapid loss of enzyme activity. In these procedures, part of the activity could be restored by incubation of the partially purified enzyme with iron(II) salts. Addition of ascorbate had almost no effect. A dramatic improvement in the yield of active enzyme was obtained after the finding that the enzyme could be stabilized by ligandation with the inhibitor 4-hydroxybenzoate. Table 1 summarizes a typical purification from 5 g of

4-hydroxyacetophenone-grown cells. Purification by four steps resulted in a yield of 38%, a purification factor of 22.5 and a specific activity of 5.9 U mg⁻¹.

Table 1. Purification scheme for hydroquinone dioxygenase from *P. fluorescens* ACB

Step	Volume (ml)	Activity (U)	Protein (mg)	Sp. Act. (U mg ⁻¹)	Yield (%)
Cell extract	7	141	545	0.26	100
Ammonium sulfate	8.5	130	507	0.26	92
Phenyl-Sepharose	91	89	146	0.61	63
Superdex 75 PG	27	74	36.7	2.02	52
Source 30Q	23.5	54	9.2	5.89	38

SDS/PAGE analysis of the purified enzyme revealed the presence of one main protein band, corresponding to a molecular mass of about 38 kDa, and several minor bands (Fig. 2). The purified HQDO eluted from an analytical Superdex 200 column in one symmetrical peak with an apparent molecular mass of 105 ± 5 kDa.

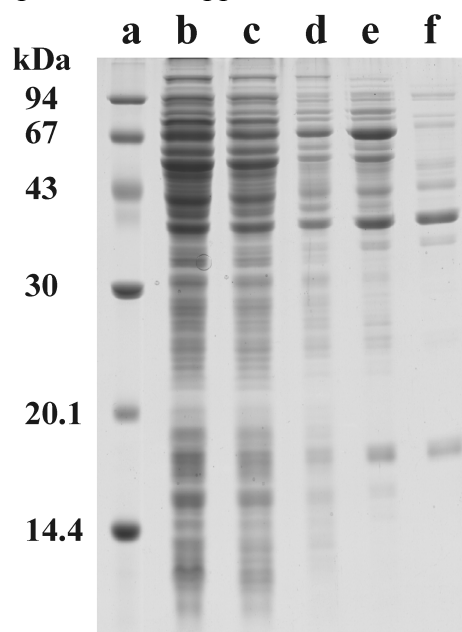


Fig. 2. SDS-PAGE of hydroquinone dioxygenase from *P. fluorescens* ACB. Lanes: a, marker proteins; b, cell extract; c, ammonium sulfate fractionation supernatant; d, phenyl-Sepharose pool; e, Superdex 200PG pool; f, Source 30Q pool.

Spectral properties.

HQDO from *P. fluorescens* ACB showed a maximum UV absorption at 279 nm (Fig. 3). In the visible region no clear absorbance band was observed. A similar feature was described for extradiol dioxygenases.^[291,346] For comparison, intradiol dioxygenases display a maximum in the visible region around 450 nm,^[183,220] due to tyrosine ligandation.^[240]

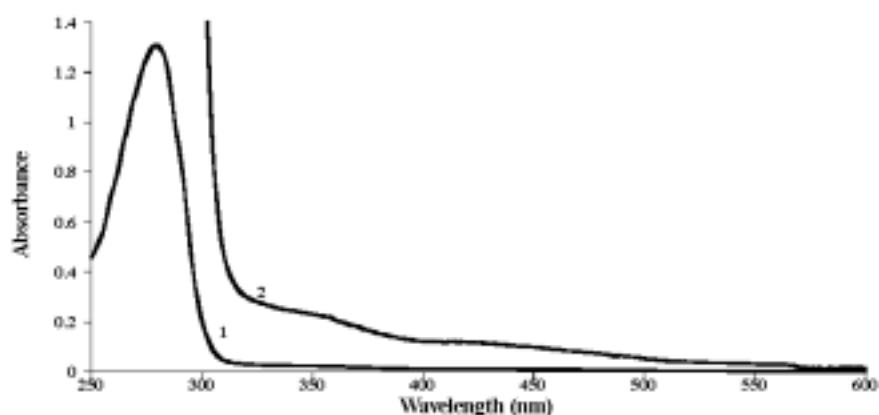


Fig. 3. Absorption spectrum of hydroquinone dioxygenase of *P. fluorescens* ACB. UV-VIS absorbance spectrum (1) and the scale is expanded 10 times (2).

Catalytic properties of HQDO

HQDO from *P. fluorescens* ACB catalyzed the ring-cleavage of hydroquinone to 4-hydroxymuconic semialdehyde with the consumption of stoichiometric amounts of molecular oxygen. The pH optimum for catalysis was between pH 7 and pH 8. At 25°C and pH 7.0, an apparent maximal turnover rate, $k'_{\text{cat}} = 2.1 \pm 0.1 \text{ s}^{-1}$ and an apparent K'_m of $37 \pm 3 \text{ }\mu\text{M}$, were estimated.

HQDO from *P. fluorescens* ACB catalyzed the conversion of a wide range of hydroquinones. Besides from the parent substrate and the difluorinated hydroquinones described in Chapter 6, activity was found with methyl-, methoxy- and chlorohydroquinone and, to a minor extent, with bromohydroquinone (data not shown). Strong substrate inhibition occurred with methoxyhydroquinone and to a lesser extent with chloro- and bromohydroquinone. Tetrafluorohydroquinone, hydroxyhydroquinone (1,2,4-trihydroxybenzene) gentisate (2,5-dihydroxybenzoate), catechol (1,2-dihydroxybenzene), resorcinol (1,3-dihydroxybenzene), pyrogallol (1,2,3-trihydroxybenzene) and phenol were not converted.

The activity of HQDO was strongly inhibited by the substrate analog 4-hydroxybenzoate. Kinetic studies revealed that the inhibition was competitive with hydroquinone with an inhibition constant, K'_i of $14 \pm 3 \text{ }\mu\text{M}$. Many other phenolic compounds served as HQDO inhibitors. The strongest inhibition was observed with 4-hydroxybenzylic compounds, 4-hydroxycinnamates, tetrafluorohydroquinone and hydroxyhydroquinone (Table 2).

Weak or no inhibition was found with 2-hydroxy-, 3-hydroxy-, 2,3-dihydroxy-, 2,5-dihydroxy-, 2,6-dihydroxy-, 3,4-dihydroxy-, 3,4,5-trihydroxy-, 3-chloro-4-hydroxy-, tetrafluoro-4-hydroxy-, 3-amino-4-hydroxy-, 4-hydroxy-3-methoxy-, 4-amino- and methyl 4-hydroxybenzoate, 6-hydroxynicotinate, 4-hydroxypropiophenone, 4-hydroxymandelate, 4-hydroxyphenylglycine, 4-hydroxybenzenesulfonic acid, 4-methyl-, 4-methoxy- and 4-aminophenol.

Table 2. Phenolic inhibitors of hydroquinone dioxygenase

Inhibitor (I)	Activity %	[I] μ M	Inhibitor (I)	Activity %	[I] μ M
none	100		ferulic acid	24	40
4-hydroxybenzoate	12	200	4-hydroxycinnamate	50	20
2,4-dihydroxybenzoate	13	200		0	200
	6	400		0	100
2,3,4-trihydroxybenzoate	81	200	caffeic acid	77	20
2,4,6-trihydroxybenzoate	40	200		59	80
2-fluoro-4-hydroxybenzoate	12	200		68	40
3-fluoro-4-hydroxybenzoate	19	200	tetrafluorohydroquinone	0	200
2-chloro-4-hydroxybenzoate	23	200		9	100
4-methoxybenzoate	76	200		35	40
4-hydroxybenzotrile	0	200		64	20
	0	40	hydroxyhydroquinone	9	200
	5	2	phenol	83	200
4-hydroxyphenylacetate	3	200	catechol	86	200
4-hydroxybenzylalcohol	8	200	4-nitrophenol	0	200
4-hydroxybenzaldehyde	12	200		9	100
4-hydroxybenzyleyanide	24	200		32	20
vanillin	33	200	isoeugenol	74	200
	61	100	chavicol	82	200
4-hydroxyphenethylalcohol	76	200	eugenol	85	200
vanillylalcohol	78	200			
4-hydroxyacetophenone	83	200			

Thermal inactivation studies showed that HQDO was rather unstable. At 30°C and pH 7.0, more than half of the enzyme activity was lost within two hours (Fig. 4). Binding of the competitive inhibitor 4-hydroxybenzoate strongly increased the stability of HQDO. Using the same incubation conditions as for the free enzyme, about 90% of the activity remained (Fig. 4).

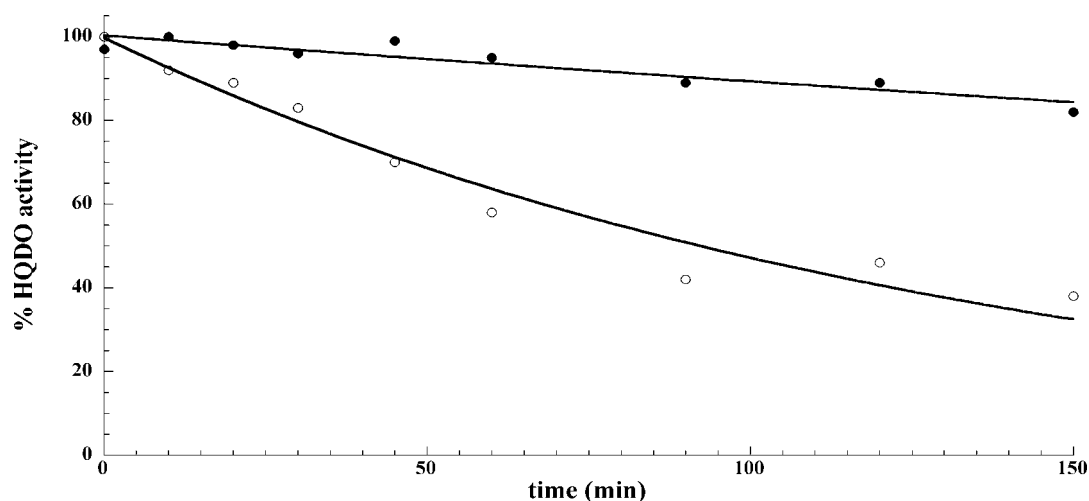


Fig. 4. Thermal stability of hydroquinone dioxygenase from *P. fluorescens* ACB. In absence(○) and presence(●) of 1 mM 4-hydroxybenzoate.

HQDO also lost activity when the enzyme was stored at -20°C in diluted or non-liganded form. Part of the activity could be restored by the addition of Fe^{2+} ions (added as FeSO_4 or $(\text{NH}_4)_2\text{Fe}(\text{SO}_4)_2$). Addition of Fe^{3+} (FeCl_3) or Mn^{2+} (MnSO_4) had no effect. HQDO was inactivated in a time-dependent manner by the iron(II) chelators 2,2'-dipyridyl and *o*-phenanthroline (Table 3). This suggests that the enzyme contains a non-heme iron(II) ion in the active site.^[38,40,120,274] In line with this, HQDO was inactivated by the oxidizing agent hydrogen peroxide (Table 3).

Table 3. Time-dependent inactivation of HQDO by iron(II) modifying agents

Inactivation agent	Concentration (mM)	Half time of inactivation at 30°C (min)
2,2'-dipyridyl	0.1	60
	1.0	20
<i>o</i> -phenanthroline	0.1	40
hydrogen peroxide	0.1	1.5
	1.0	3.5

Studies on other dioxygenases have shown that hydrogen peroxide acts on iron(II)-dependent extradiol dioxygenases and not on Mn(II)- and Mg(II)-dependent extradiol dioxygenases.^[6,23,339,344]

Regioselectivity of dioxygenation

Absorption spectral analysis indicated that the regioselectivity of dioxygenation of halogenated hydroquinones by HQDO differs with the type and position of the halogen substituents. Activity measurements with chloro- and bromohydroquinone resulted in an increase in absorption at 320 nm, pointing at the formation of a halogenated 4-hydroxy muconic semialdehyde product. In contrast, incubation of fluorohydroquinone with HQDO did not result in an absorption increase at 320 nm. ^{19}F NMR confirmed that in the latter reaction no semialdehyde was formed but that the fluorohydroquinone substrate was enzymatically defluorinated in a time-dependent manner compared to no fluoride anion production in the control experiment. This suggests that the ring cleavage of the fluorinated substrate takes place in between the hydroxyl and fluorine substituent. Such ring cleavage will result in an unstable acylhalide which readily reacts with water yielding nonfluorinated maleylacetate and halide anion, as described for the conversion of chlorohydroquinones by chlorohydroquinone dioxygenase.^[33,229,349] The regioselectivity of the HQDO-stimulated ring cleavage of fluorohydroquinone is different from that of the corresponding reaction with difluorinated hydroquinones (Chapter 6). For instance 2,3-difluorohydroquinone undergoes no ring-fission in between a fluoro substituent and hydroxyl substituent, but in between C1 and C6.

N-terminal sequence analysis

The N-terminus of the protein corresponding to the major band in SDS-PAGE (lane f in Fig. 2) was determined by Edman degradation (Table 4). The N-terminus of this 38 kDa protein was found to be: AMLEAVETEN. Except for the starting methionine

and the last glutamic acid (alanine in ORF1 see chapter 6), this sequence corresponds with the N-terminal part of *orf1* of the 14-kb DNA fragment containing the *hapABCFGDE* cluster (Chapter 6). The 32 and 18 kDa protein bands observed in lane f of Fig. 2 were also analyzed by Edman degradation. The 32 kDa band was selected because its mass corresponds to that of HapC. The 18 kDa band was selected because during purification it always co-elutes with the 38 kDa protein. The 32 kDa protein showed the following N-terminal sequence: AAITAALVKE. This sequence is specific for the translation elongation factor Ts present in many *Pseudomonas* organisms and suggests that the 32 kDa protein represents an impurity in the HQDO preparation. The N-terminus of the 18kDa protein was found to be STQPAFKTVF. This sequence aligns well with the N-terminal sequences of proteins in *Burkholderia cepacia* R18194 (Bcepa03000438) and *Photorhabdus luminescens* subsp. *laumondii* TT01^[68] (plu0141) that are positioned next to the proteins Bcepa03000437 and plu0141, respectively, which are neighboring ORF1 of *P. fluorescens* ACB (see also below).

Table 4. N-terminal sequences of the three most abundant protein bands observed in SDS-PAGE of purified HQDO (lane f in Fig. 2)

gel band	N-terminal sequence	Position in <i>hap</i> gene cluster	Aligns with (%SI) ^a	Function
38 kDa	AMLEAVETEN	<i>orf1</i>	<i>Burkholderia</i> ^b ZP_00217829 (78%) <i>Photorhabdus</i> ^c NP_927510 (54%)	β-subunit of HQDO (see below)
32 kDa	AAITAALVKE	not present	<i>Pseudomonas putida</i> KT2440 NP_743749 (100%) ^d	the translation elongation factor Ts
18 kDa	STQPAFKTVF	<i>orf0</i> ^e	<i>Burkholderia</i> ^b ZP_00217830 (73%) ^f <i>Photorhabdus</i> ^c NP_927509 (51%) ^f	α-subunit of HQDO (see below)

^a %SI: percentage of sequence identity; ^b *Burkholderia cepacia* R18194; ^c *Photorhabdus luminescens* subsp. *laumondii* TTO1; ^d on basis of the N-termini; ^e *orf0* is positioned upstream of *orf1* and only the C-terminal sequence is present in the DNA fragment; ^f sequence identity based on N- and C-termini of *P. fluorescens* ACB protein.

Structural characterization of HQDO

Initial analysis of HQDO by size-exclusion chromatography suggested a protein complex with a size corresponding to a molecular mass of about 105 kDa. This result either suggested that HQDO is a homotrimer with a molecular mass of 114.6 kDa (3 x 38.2 kDa) or that HQDO is a heterooligomer.

We initially carried out the electrospray mass spectrometry analysis of HQDO in the absence of FeSO₄ and 4-hydroxybenzoate using borosilicate capillaries (Fig. 5). This figure clearly shows 2 series of protein ions having a different number of charges and different molecular masses. Mass determination of both ion series revealed masses of 30,295 ± 5 Da and 112,529 ± 50 Da. The 30 kDa protein is likely to be the translation elongation factor Ts, which was identified already by Edman degradation. The 112 kDa protein is likely to be the protein that is identified by size-exclusion chromatography as a protein with a mass of about 105 kDa. However, these analyses did not allow us to determine the subunit composition of the protein assembly.

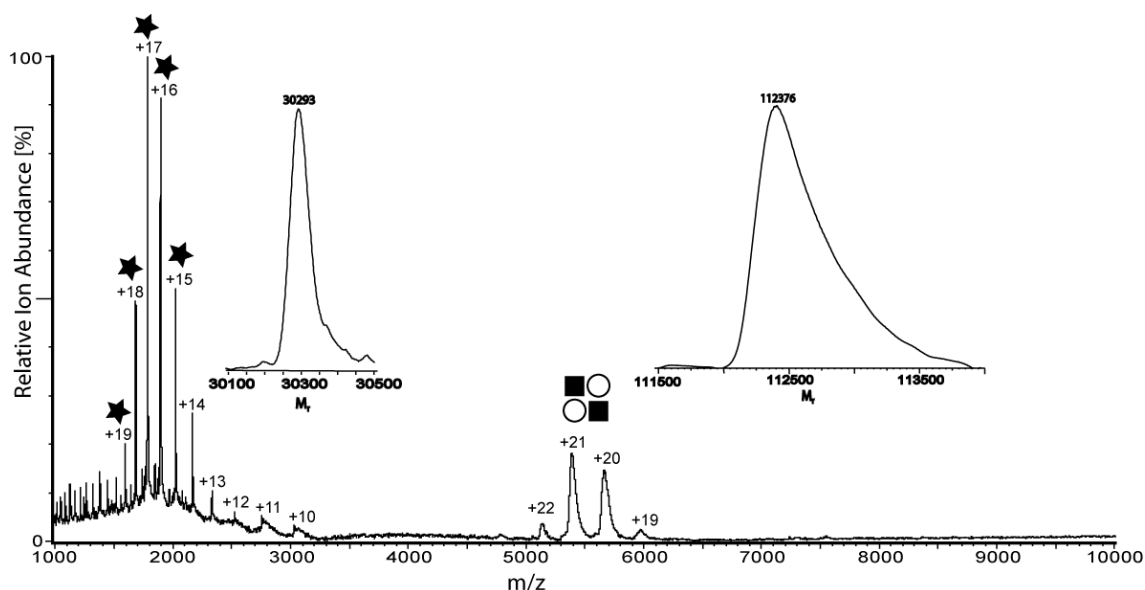


Fig. 5. ESI-MS analysis of HQDO using borosilicate capillaries. This spectrum shows 2 charge distributions. The first ion series at m/z 1,000-3,200 reveals after deconvolution a mass of 30.3 kDa (★) corresponding to the translation elongation factor, Ts, whereas the second charge envelope (■ $_2$ O $_2$) corresponds with the heterotetrameric HQDO.

These results encouraged us to determine the composition of the protein by coupling size-exclusion chromatography (SEC) to mass spectrometry (MS) using a Superdex 200 H/R column and a standard ionization source. We initially injected 10 μ l of a 20 μ M HQDO solution (without 4-hydroxybenzoate and FeSO $_4$) onto the column using 50 mM ammonium acetate, pH 6.7 as eluent and we analyzed the ion chromatogram and the different ion series (Fig 6A and 6B). The ion chromatography clearly shows 2 protein peaks eluting around 27 (peak 1) and 31 minutes (peak 2). The late-eluting compounds around 41 minutes (peak 3) are smaller molecules and the peak around 47 minutes (peak 4) corresponds with the total volume of the column. Peak 1 showed multiple ion series from 1,300 m/z up to 8,500 m/z . The determined molecular masses from these ion peaks were $17,769 \pm 1$ Da, $38,288 \pm 10$ Da, and $94,477 \pm 45$ Da. As the elution volume of this peak suggests a hydrodynamic volume corresponding to a mass of about 100 kDa the observed proteins in the mass spectrum were likely to be fragments of the larger protein assembly. Intriguingly, the mass of the smaller 18 kDa protein corresponds with the molecular mass calculated from the lower band in the SDS-polyacrylamide gel of the purified HQDO preparation, suggesting that this protein is part of the HQDO assembly. The second eluting peak contained the 30.3 kDa elongation factor (mass spectrum not shown).

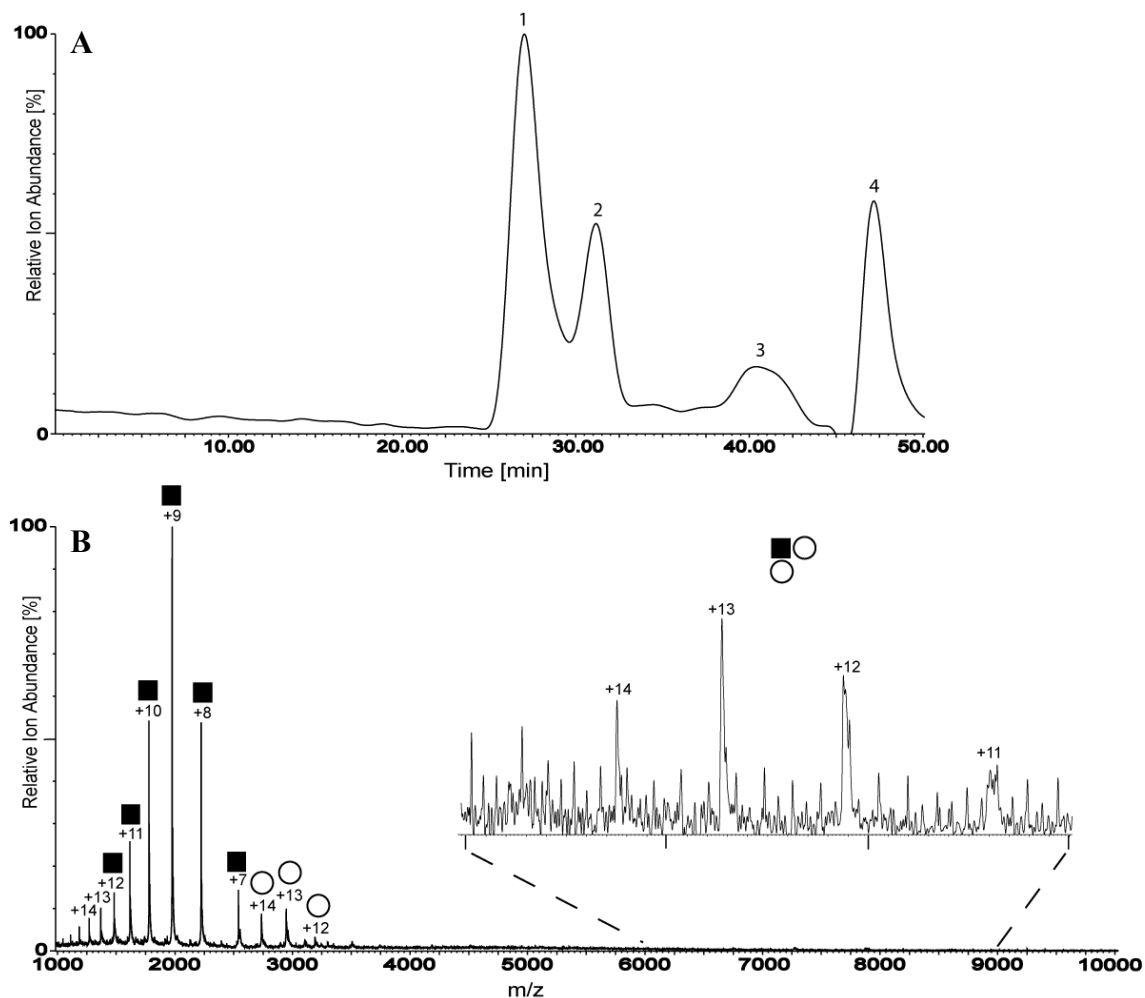


Fig. 6. On-line SEC-MS analysis of HQDO in the absence of FeSO_4 and 4-hydroxybenzoate. (A) Elution ion chromatogram of HQDO and subsequent analysis by ESI-MS. Peak 1 corresponds to HQDO, peak 2 to a 30 kDa protein, possibly the translation elongation factor Ts, and peak 3 to small molecules. Peak 4 is consistent with the void volume of the column. (B) ESI mass spectrum of peak 1 by combining scans from peak 2. This spectrum shows mainly 2 charge distributions between m/z 1,000 and 3,500. The first charge envelope (■) corresponds to the α -monomer of HQDO with a mass of 17.8 kDa, the second charge distribution (○), corresponds to the β -monomer with a mass of 38.3 kDa and the third charge state series corresponds with a molecular mass of 94.4 kDa (■ $_1$ O $_2$).

In the subsequent on-line size-exclusion-mass spectrometry experiment we added FeSO_4 and 4-hydroxybenzoate to the protein sample before injection onto the column (Fig. 7a). This protein sample yielded a similar elution chromatogram as the experiment without FeSO_4 and 4-hydroxybenzoate. However, the accumulated mass spectra of the peak around 27 minutes (peak 1) were clearly different (Fig. 7b). Mass determination of the ion series centered around 5,400 m/z revealed a mass of $112,387 \pm 50$ Da. This mass spectrum also showed ion series from which the determined protein mass is $17,769 \pm 5$ Da and $38,283 \pm 10$ Da and gas-phase dissociated sub-complexes with masses of $56,050 \pm 20$ Da for dimeric and $94,488 \pm 45$ Da for trimeric forms of both proteins.

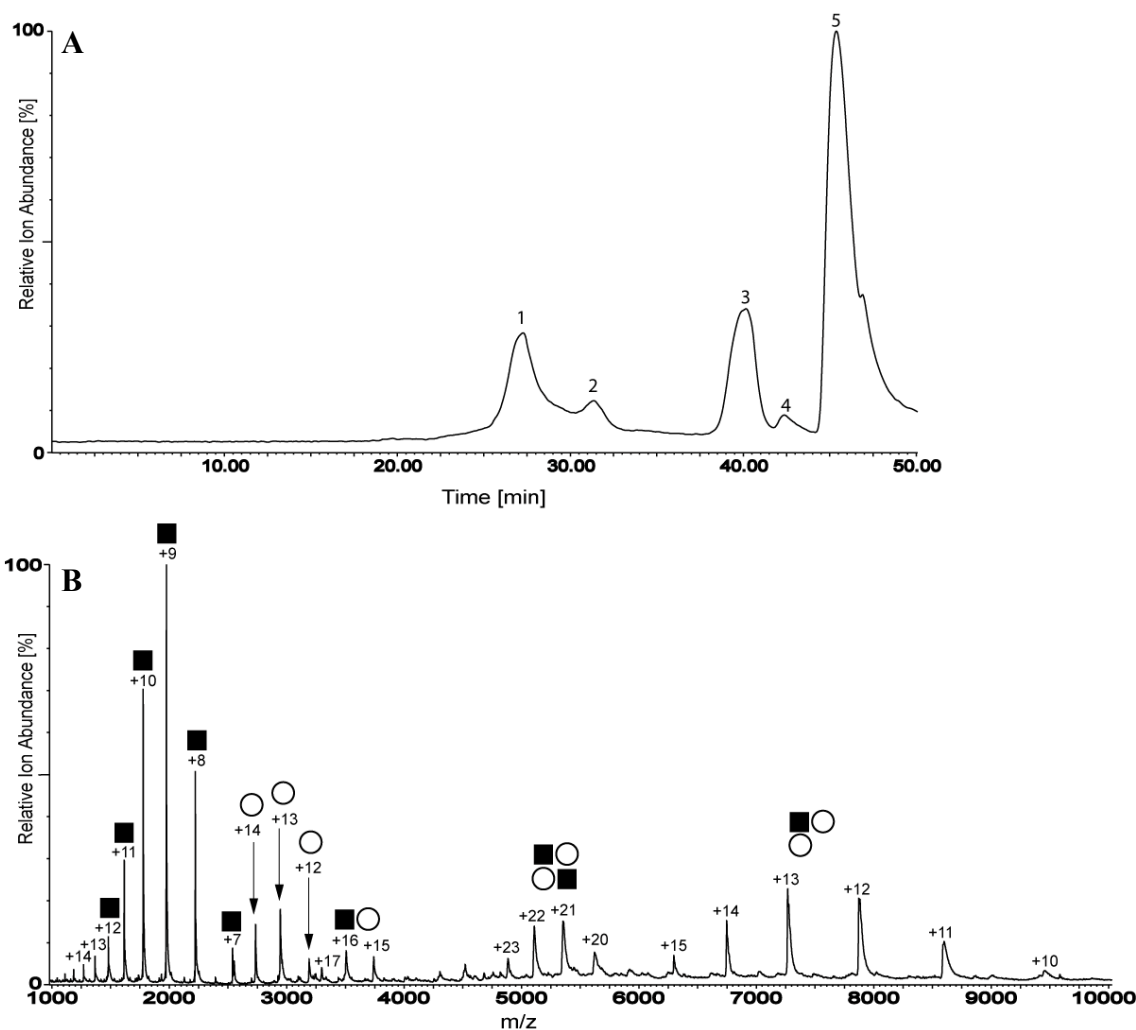


Fig. 7. On-line SEC-MS analysis of HQDO in the presence of FeSO_4 and 4-hydroxybenzoate. (A) Elution ion chromatogram of HQDO SEC and analyzed by ESI-MS. Peak 1 corresponds to HQDO, peak 2 to a 30 kDa protein, likely to be the translation elongation factor Ts, and peak 3 and 4 to small molecules. Peak 5 is the total volume of the column. (B) ESI mass spectrum of peak 1. This spectrum shows 5 major charge distributions. The first charge envelope (■) ranging from +7 to +14 at m/z 1,000-2,600, corresponds with the α -monomer of HQDO with a mass of 17.8 kDa. The second charge distribution (○) ranging from +12 to +14 at m/z 2,700-3,200, refers to the β -monomer with a mass of 38.3 kDa. The third charge series of +15 to +17 at m/z 3300-3800 is assigned to the dimer “■○” with a mass of 56.1 kDa. The fourth charge envelope from +20 to +23 at m/z 4800-5700, corresponds to the tetramer of HQDO ($\alpha_2\beta_2$) with a mass of 112.4 kDa. And the fifth charge distribution from +10 to +15 at m/z 6300 to 9500 refers to the trimer ($\alpha_1\beta_2$) with a mass of 94.4 kDa.

This strongly suggests that these 2 proteins form the heterotetrameric protein assembly of 112 kDa. Taking into account the additional peaks in the mass spectrum and the mass of the intact assembly these results unambiguously show that HQDO is composed of 2 α -subunits of 17,8 kDa and 2 β -subunits of 38.3 kDa. The addition of FeSO_4 clearly resulted in new ion peaks near the original ion peaks of the β -subunit. Mass determination revealed a mass difference of 55 Da, strongly indicating the interaction between the β -subunit and Fe^{2+} . This interaction is likely to be specific, as we did not

observe any interaction between the α -subunit and Fe^{2+} . The mass of the intact assembly is 313 Da higher as may be expected from the primary sequence, which may suggest that, under the experimental conditions applied, two 4-hydroxybenzoate molecules (molecular mass 138 Da) and one molecule of iron(II) are bound to the complex of HQDO.

Peptide mapping and sequencing

In-gel tryptic digestion of HAPMO (67 kDa band in lane e of Fig. 2) and subsequent MALDI-ToF analysis yielded 56 peptides. Comparison of these peptides with the known sequence of HAPMO^[157] gave 66% sequence overlap with 42 out of 56 peptides.

MALDI-ToF analysis of the tryptic digests of the 38kDa band of HQDO (lane f of Fig. 2) revealed 22 peptide fragments (m/z: 1239.6, 1557.7, 1868.7, 1884.8, 1979.8, 1985.8, 2007.2, 2021.8, 2033.9, 2135.9, 2231.9, 2247.9, 2296.9, 2326.9, 2424.9, 2476.9, 2750.6, 2756.3, 3209.0, 3248.1, 3368.1, and 3408.1). Database mass analysis of these peptides yielded no significant mapping with any protein in the Swissprot database. However, 14 peptides corresponded with the sequence of ORF1 and covered 55% of the protein sequence.

Analysis of the 18 kDa band showed that this band corresponds to the ORF0 protein. MALDI-ToF-ToF analysis of tryptic fragments confirmed not only the (partial) N-terminus of the protein but also revealed the partial primary sequence of the protein (Table 5). Peptide sequencing yielded 59% of the total sequence by mapping 7 of 16 expected peptides, which could be matched with the conserved stretches in 2 homologous proteins Bcepa03000438 from *B. cepacia* and plu0141 from *P. luminescens*. The number of expected peptides is based on the number of peptides after theoretical trypsin digestion of the two homologous proteins.

Table 5. MS/MS analysis of peptides of the α -subunit (17.8 kDa protein) of HQDO and alignment to homologous proteins

Precursor (m/z)	Amino acid sequence ^a	Position on basis of alignment with homologous proteins (Fig. 9)
1214.7	TVFGSLAKYTK	aa 8-18
1583.86	AHYAFSNIFEVAAK	aa 29-42
1711.97	FSNIFEVAA	aa 33-41
1645.06	ANLGYVIETLR	aa 53-58
2667.34	ACSHDEFIISVDGSVR	aa 72-87
1861.07	FIKLDETPLAGDGTR	aa 90-104
1413.78	GHQALLPA	aa 126-133

^a There is no mass difference observable between I and L and between K and Q (same mass). The choice between these two amino acid residues is based on the alignment with the two homologous proteins (see Fig. 9).

Location of hydroquinone dioxygenase genes

Combining the information about the proteins encoded by the 14-kb DNA fragment of *P. fluorescens* ACB described in Chapter 6 and the elucidated sequences of the two subunits of HQDO gives us the *hap* gene cluster shown in Fig. 7. ORF0 corresponds to the C-terminal sequence of the small α -subunit of HQDO. Furthermore, the N-terminal sequence of the HQDO α -subunit, as determined by Edman degradation, aligns with Bcepa03000438 from *B. cepacia* and plu0140 from *P. luminescens* and most probably

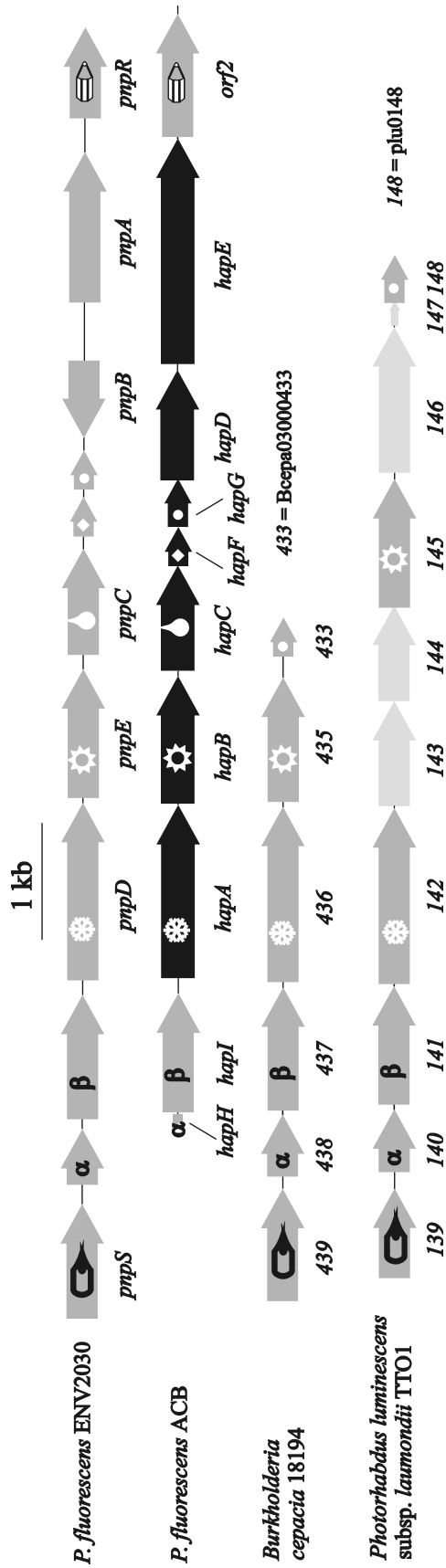


Fig. 7. The *hap* gene cluster of *P. fluorescens* ACB and corresponding gene clusters of other organisms

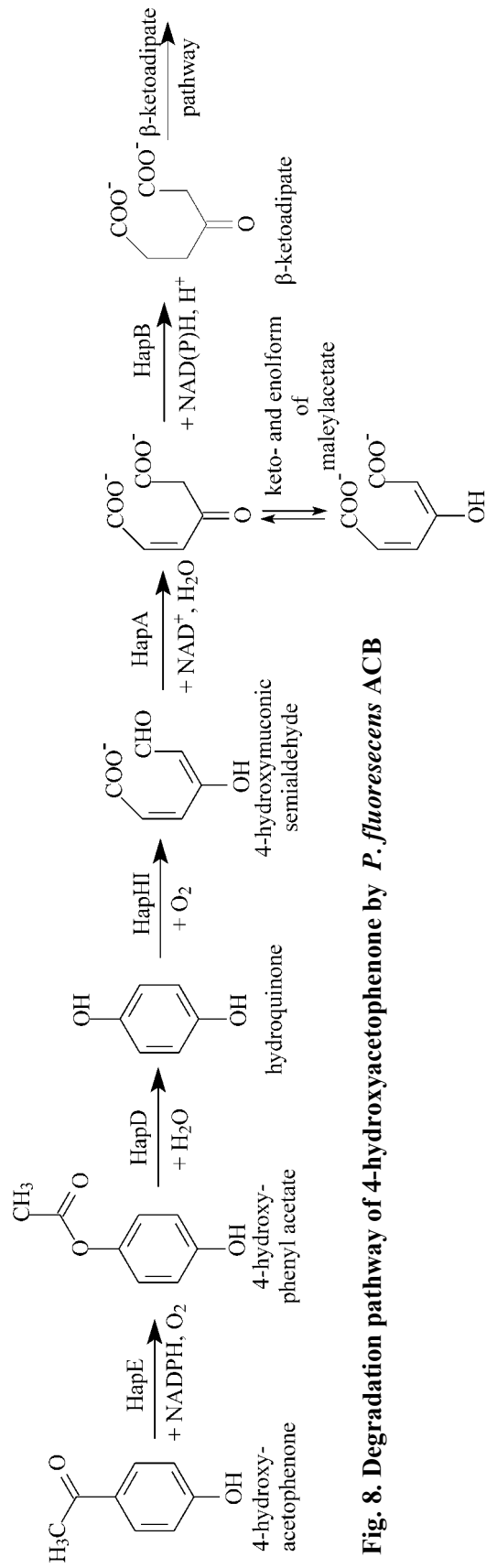


Fig. 8. Degradation pathway of 4-hydroxyacetophenone by *P. fluorescens* ACB

Hydroquinone dioxygenase from Pseudomonas fluorescens ACB

with the open reading frame found downstream of *pnpS* in *Pseudomonas fluorescens* ENV2030 (sequences of this last organism have not been published).^[11,352] ORF1 corresponds to the β -subunit of HQDO and aligns with Bcepa0300437 from *B. cepacia* and plu0140 from *P. luminescens* and most probably with the sequence of the protein encoded by the open reading frame located upstream of *pnpD* in *P. fluorescens* ENV2030. Because of the location of the two HQDO subunits in the *hap* gene cluster, *orf0* and *orf1* are renamed as *hapH* and *hapI* and HQDO is also referred to as HapHI as shown in Fig. 8. Sequence alignments of both subunits of HQDO are shown in Fig. 9.

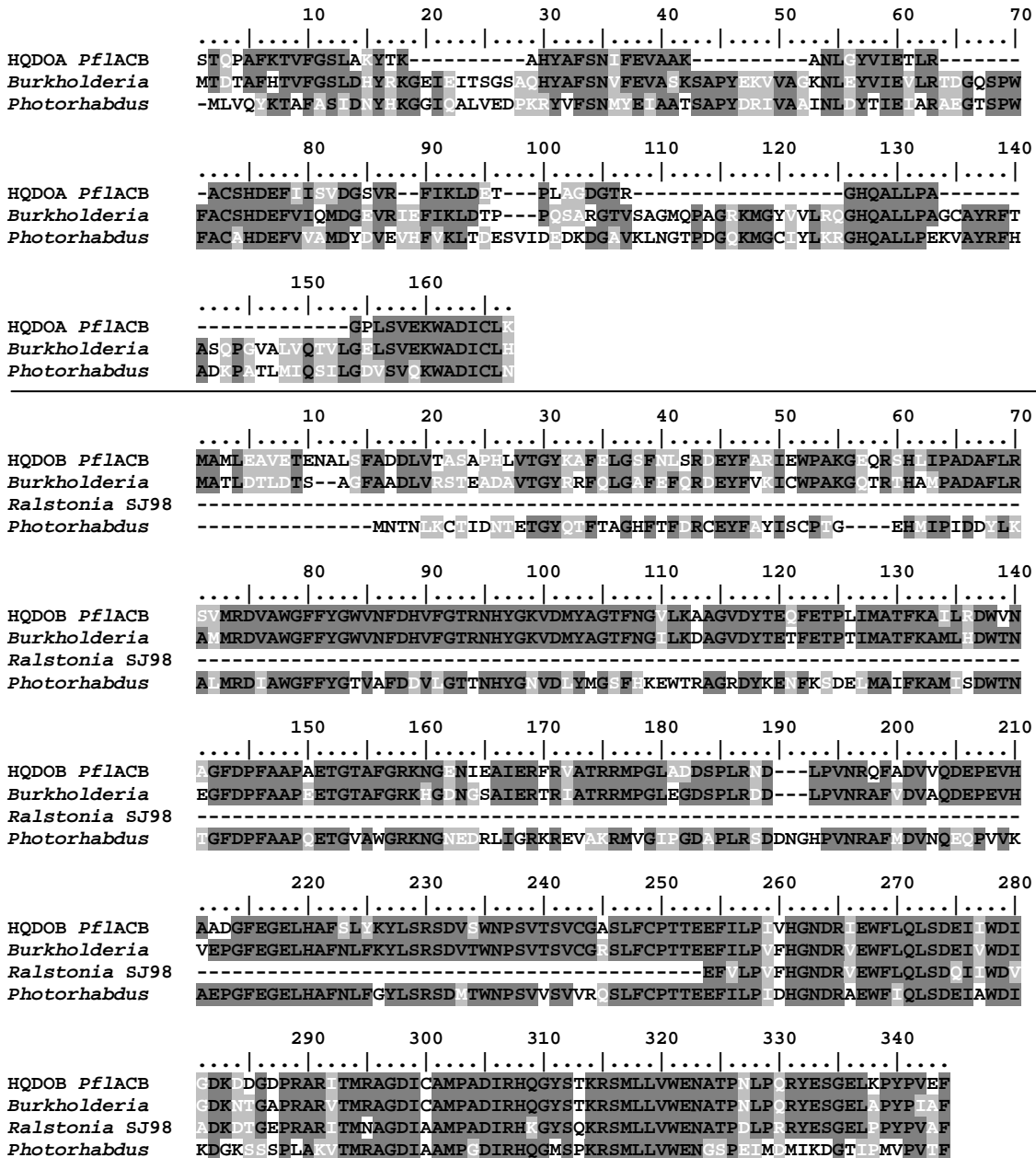


Fig. 9. Sequence alignments of both subunits of HQDO from *P. fluorescens* ACB. Alignment with orthologs of *B. cepacia* R18194, *P. luminescens* subsp. *laumondii* TT01 and *Ralstonia* sp. SJ98. The latter shows only a part of an *orf* encoded by nucleotide 1-276 (acc. nr. AY574278). For other accession numbers see Table 4.

For the α -subunit of HQDO (HapH), especially the C-terminus aligns very well with the *B. cepacia* and *P. luminescens* orthologs. Alignment of the β -subunit of HQDO (HapI) with the *B. cepacia* protein reveals a sequence similarity of 89%. The α - and β -subunits of the described HQDOs mutually have 9% sequence similarity in all three organisms. Probably the two subunits have a different ancestor. HapI shows no significant sequence identity (6-12%) with known non-heme iron(II)-dependent dioxygenases. Thus, HQDOs are new members of the family of the non-heme iron(II)-dependent extradiol dioxygenases as shown in the dendrogram of intra- and extradiol dioxygenases (Fig. 10).

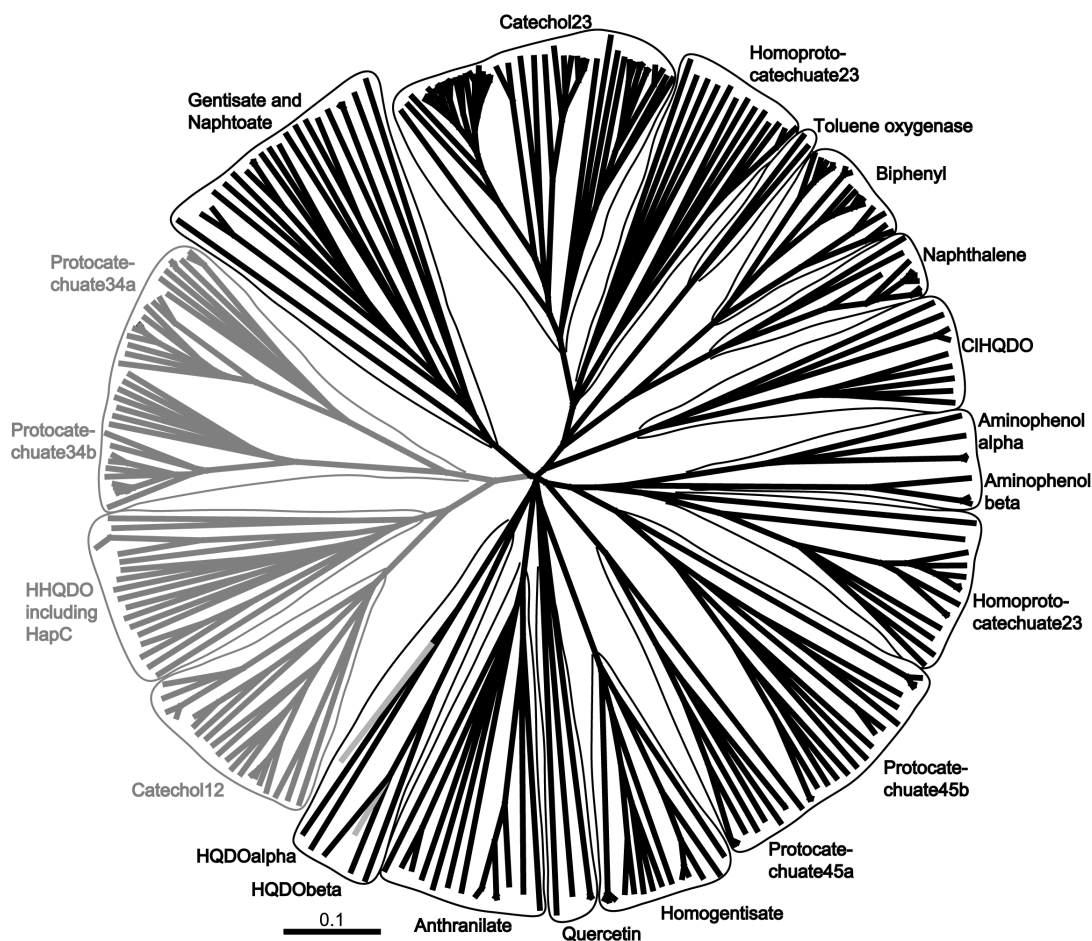


Fig. 10. Dendrogram of intra- and extradiol dioxygenases. Catechol12: catechol 1,2-dioxygenases; HHQDO: hydroxyhydroquinone 1,2-dioxygenases; Protocatechuate34a and 34b: α - and β -subunit of protocatechuate 3,4-dioxygenases; Gentisate: gentisate 1,2-dioxygenase;^[123] Naphthoate: 1-hydroxy-2-naphthoate dioxygenase; Catechol23: catechol 2,3-dioxygenases;^[277] Homoprotocatechuate23: homoprotocatechuate 2,3-dioxygenases;^[204] Toluene oxygenase: 2,4,5-trihydroxytoluene 5,6-dioxygenases;^[150] Biphenyl: 2,3-dihydroxybiphenyl 1,2-dioxygenases;^[119] Naphthalene: 1,2-dihydroxynaphthalene dioxygenase;^[60] ClHQDO: chlorohydroquinone dioxygenase;^[207,229] Aminophenolalpha and -beta: α - and β -subunit of 2-aminophenol 1,6-dioxygenases;^[129] Protocatechuate45a and 45b: α - and β -subunit of protocatechuate 4,5-dioxygenases;^[230] Homogentisate: homogentisate 1,2-dioxygenase;^[7] Quercetin: quercetin 2,3-dioxygenase; Anthranilate: 3-hydroxyanthranilate 3,4-dioxygenase; HQDOalpha and -beta: α - and β -subunit of hydroquinone dioxygenase. Intradiol dioxygenases in dark-gray, extradiol dioxygenases in black and HQDO subunits from *P. fluorescens* ACB in light-gray.

Interestingly, amino acids 258-319 of the β -subunit of HQDO show 35% sequence identity and 53% sequence similarity with amino acids 48-106 of 3-hydroxyanthranilate 3,4-dioxygenase (HAO) from *Xanthomonas campestris* (pv. *campestris*). This monomeric enzyme, which is involved in the kynurenine pathway,^[35] is also an iron(II)-dependent dioxygenase. HAOs contain two conserved histidines (His48 and His92 in *Xanthomonas*), which are thought to be involved in iron ligandation.^[218] Selective replacement of these residues by alanine resulted in no detectable activity.^[218] The conserved histidines of HAO correspond to His258 and His305 in HapI. Therefore, these histidines might serve as iron ligands in HapI.

DISCUSSION

This paper describes the purification and characterization of HQDO, an unusual ring-cleavage enzyme involved in the catabolism of 4-hydroxyacetophenone in *P. fluorescens* ACB. HQDOs have been described in degradation pathways of *Sphingobium chlorophenicum*,^[33] *Pseudomonas* sp. HH35,^[260] *Arthrobacter protophormiae*,^[40] *Burkholderia cepacia*,^[41] *Pseudomonas putida* JD1,^[55] and *Moraxella*.^[274] However, for none of these enzymes, purification procedures or amino acid sequence data were reported.

Binding of the competitive inhibitor 4-hydroxybenzoate increased the stability of HQDO and allowed, for the first time, to purify this enzyme in active form. Hydrogen peroxide and the iron chelators 2,2'-dipyridyl and *o*-phenanthroline inactivated HQDO. From this and its catalytic features, it is concluded that HQDO belongs to the family of non-heme iron(II)-dependent dioxygenases.

HQDO from *P. fluorescens* ACB catalyzed the ring-fission of a wide range of hydroquinones to the corresponding 4-hydroxymuconic semialdehydes. Substrate profiling showed that both *para*-hydroxyl groups of hydroquinone were crucial for enzyme activity. Hydroquinones with an electron donating methyl or methoxy group were readily converted. Hydroquinones containing electron withdrawing substituents were also converted, albeit at a lower rate. The number and position of fluorine substituents determined both the reaction rate and the regioselectivity of dioxygenation. With 2-fluorohydroquinone, ring splitting occurred in between C₁-OH and C₂-F. 2,3-Difluorohydroquinone was splitted in between C₁-OH and C₆-H (Chapter 6) and tetrafluorohydroquinone turned out to be a strong inhibitor. Introduction of a hydroxyl (HHQ) or carboxyl (gentisate) group at the *ortho*-position resulted in strong and weak enzyme inhibition, respectively. These results suggest that the activity of HQDO is determined by both electronic and steric constraints and that substrates may become differently oriented in the active site.

HQDO was reversibly inhibited by a large number of phenolic compounds. In general 4-hydroxybenzylic compounds and 4-hydroxycinnamates were strong inhibitors. From this and the fact that the inhibition by 4-hydroxybenzoate was found to be competitive with hydroquinone, it is concluded that the 4-hydroxyl group serves as the iron ligand and the *para*-substituent of the phenol is an important determinant for discriminating between weak and tight binding.

HQDO from *P. fluorescens* ACB appeared to be a heterotetramer built up by subunits of 18 and 38 kDa. This is the first example in which on-line size-exclusion chromatography-mass spectrometry (SEC-MS) is used to elucidate the components and stoichiometry of a protein assembly. Cavangah et al.^[37] used the coupling of size-exclusion chromatography to establish the oligomeric state of the transition state

regulator AbrB and the stoichiometry of its interaction with DNA. Here we showed the application of SEC-MS to heterogeneous protein complexes. The mass of the β -subunit agrees well with the theoretical mass based on the primary sequence of protein HapI encoded by the gene *hapI* (*orf1* in Chapter 6). The tenth amino acid of HapI is Ala according to the DNA sequence (Chapter 6). However, the N-terminal sequence determination of the large subunit of purified HQDO pointed at a Glu at this position. The actual presence of a Glu is supported by the determined molecular mass by on-line SEC-MS combined with simulations of the charge state distributions with either Ala or Glu at position 10.

Studies with 4-hydroxybenzoate showed that this competitive inhibitor interacts with the heterotetramer, but an adduct with only one of the two subunits was not found. Comparison of our dataset with the simulations suggests interaction of one iron molecule to the β -subunit. The calculated mass based on the primary sequence is 38268.98 without the Met at position 1 and excluding the iron. The observed mass by on-line SEC-MS is 38288 ± 10 Da in the absence of FeSO_4 and 4-hydroxybenzoate. The primary sequence of the α -subunit is still unknown. By MS/MS analysis stretches of the α -subunit were sequenced including amino acids of the N-terminus, determined by Edman degradation. These pieces of amino acid sequence show clearly that the α -subunit of HQDO has orthologs in *B. cepacia* and *P. luminescens*.

The small and large HQDO subunits are encoded by two open reading frames (*orf0* and *orf1*), located upstream of the *hapABCFGDE* cluster involved in 4-hydroxyacetophenone degradation. Therefore, this gene cluster now extends to *hapHIABCFGDE* with *hapH* and *hapI* coding for the α - and β -subunit of HQDO, respectively. Genome mining indicated that related HQDOs are present in *B. cepacia* R18194, *P. luminescens* subsp. *laumondii* TTO1 and *Ralstonia* sp. SJ98. Moreover, from gene cluster comparison, we propose that a similar two-subunit HQDO is involved in the degradation of *p*-nitrophenol in *P. fluorescens* ENV2030.^[11,352]

The fact that HQDO is encoded by *hapH* and *hapI* and not by *hapC* supports our proposal (Chapter 6) that HapC might be responsible for the intradiol dioxygenase activity of *P. fluorescens* ACB with HHQ and possibly other catechols. The reason why *hapC* is embedded in the *hap* operon is not clear. There are more examples of the presence of a HHQDO (HapC) in an organism where a HQDO serves as a key enzyme in the degradation pathway of aromatic compounds. For instance in the 4-nitrophenol pathways in *P. fluorescens* ENV2030,^[352] and in a *Moraxella* strain.^[274] Also in the degradation pathway of 2,4-dinitrotoluene in *Burkholderia cepacia* R34 a HHQDO is present but another extradiol dioxygenase carries out the ring-fission of 2,4,5-trihydroxytoluene.^[151] It seems that there is a progression in the organization of the pathway genes towards a compact region encoding the entire pathway. In that progression, remnants from assembly (like *hapC*) persist. The presence of *hapC* in the *hap* gene cluster might indicate an intermediate point in the evolution of an optimal system for 4-hydroxyacetophenone degradation.^[151] Embedded in the *hap* gene cluster, *hapC* might be available to assist in other degradation pathways for the intradiol splitting of HHQ or other catechols (*vide supra*).

With the elucidation of the HQDO genes and the observed instability of the HQDO protein, it is tempting to speculate on the function of *hapG*. As shown in Chapter 6, *hapG* codes for a ferredoxin. For catechol 2,3-dioxygenases it was described that in some degradation pathways, these proteins are needed for the reductive reactivation of

the iron cofactor.^[111,138,139,237,302] A similar *in vivo* protection of HQDO can be envisioned for HapG.

Except from the orthologs found in *B. cepacia* R18194, *P. luminescens* subsp. *laumondii* TTO1 and *Ralstonia* sp. SJ98, HQDO showed no significant sequence similarity with any other protein. The heterotetrameric character of HQDO clearly discriminates the enzyme from most other non-heme iron(II)-dependent dioxygenases. Except for protocatechuate 4,5-dioxygenase and 2-aminophenol 1,6-dioxygenase, they all consist of one type of subunit.^[18,291] From the sequence alignment it appears that HQDO is most related to 3-hydroxyanthranilate 3,4-dioxygenase, but that HQDO constitutes a new type of enzyme in the iron(II)-dependent dioxygenase family.

The size and subunit composition of HQDO suggest that the enzyme contains two active sites per heterotetramer. As for protocatechuate 4,5-dioxygenase^[285] and 2-aminophenol 1,6-dioxygenase^[181] these active sites are likely positioned in the larger subunits. On-line SEC-MS analysis indicated that there was one iron atom present in the heterotetrameric protein and that it was positioned in the β -subunit. This is reminiscent of other heteromeric extradiol dioxygenases that have one iron atom per $\alpha_2\beta_2$ tetramer,^[6,291] although protocatechuate 4,5-dioxygenase from *Pseudomonas pseudoalcaligenes* JS45 was shown to contain two iron atoms per $\alpha_2\beta_2$ tetramer.^[181] Probably, native HQDO contains two iron atoms per heterotetramer, but due to the unstability of the enzyme only one iron is detected in the SEC-MS analysis.

The active site of iron(II)-dependent dioxygenases generally harbors two histidines and a glutamate that are involved in binding the iron.^[256,300] Most of these enzymes use a catechol as substrate (Fig. 10). When a catecholic substrate binds, the two hydroxyl groups of the substrate replace two water molecules in iron ligation.^[256] The strong iron-chelating properties of a catecholic compound are nicely illustrated by the action of enterochelin, a catecholate siderophore that scavenges iron during bacterial infections.^[96] In case of HQDO, the question arises how the interaction between the phenolic substrate and the iron cofactor occurs. Here the situation has to be different because the hydroquinone substrate does not contain an *ortho*-hydroxyl group. The same is true for (homo-)gentisate dioxygenases. Based on the crystal structure of substrate-free human homogentisate dioxygenase^[300] and EPR studies,^[124] it was proposed that in this enzyme the carboxylate anion of homogentisate serves as an iron ligand just like the phenolate group of catechol in catechol dioxygenases. For HQDO, the active site residues involved in binding the iron could not be simply predicted from sequence alignments. Based on the partial similarity with HAOs, His258 and His305 could serve as iron ligands in HapI. In addition to the two histidines and an acidic residue, another residue might be involved in binding the metal cofactor.^[28,205,240,247,280]

Another possibility is that upon hydroquinone binding the iron atom remains bound to one or more water molecules. Without knowledge of the active site constituents, the catalytic mechanism of HQDO remains speculative. However, based on the assumption that a His₂Glu triad is present, and the properties of other dioxygenases,^[124,240,256,280,328] the following hypothesis can be made (Fig. 11). Upon binding to the iron, the hydroquinone substrate becomes activated via deprotonation of the C4OH group. Molecular oxygen, bound to the iron, will then attack the C1 atom of hydroquinone in a radical type of reaction. After lactone formation, the remaining iron-liganded oxygen atom will attack the C1 atom resulting in the semialdehyde product. In this reaction mechanism, both oxygen atoms from molecular oxygen are built in into the substrate. However, it cannot be excluded that the oxygen atom built in in the final step is derived

from the water molecule that remains bound to the iron during the entire reaction cycle. Reactions with $^{18}\text{O}_2$ might clarify this point.

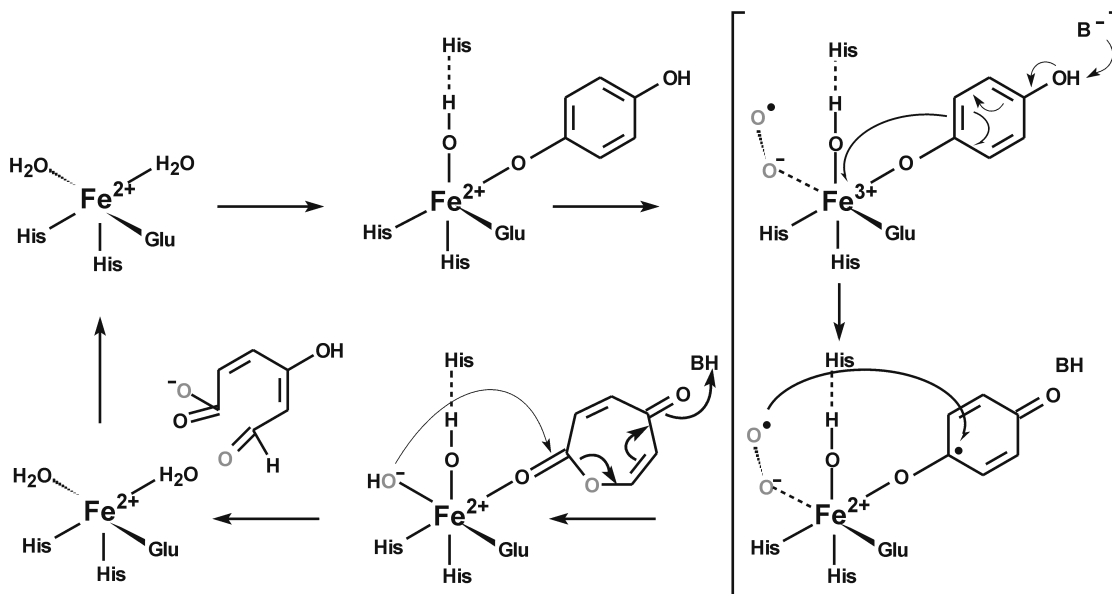


Fig. 11. Proposed mechanism of ring cleavage of hydroquinone by the iron(II) dependent hydroquinone 1,2-dioxygenase of *P. fluorescens* ACB.

In summary, this chapter describes the first purification and characterization of a HQDO. This enzyme is a heterotetramer composed of 18 and 38 kDa subunits and is the prototype of a novel subclass of the family of iron(II)-dependent dioxygenases.

ACKNOWLEDGEMENTS

We thank Sjef Boeren, Adrie Westphal and Olga Militsyna for help with some of the experiments. This work was supported by the Council for Chemical Sciences of the Netherlands Organization for Scientific Research (CW-NWO), division 'Procesvernieuwing voor een Schoner Milieu'.

References

1. Adejare, A., Shen, J. and Ogunbadeniya, A.M. 2000. Halogens halt aromatic group migration in Baeyer-Villiger oxidation. *J Fluorine Chem* **105**, 107-109.
2. Alberati-Giani, D., Ricciardi-Castagnoli, P., Kohler, C. and Cesura, A.M. 1996. Regulation of the kynurenine metabolic pathway by interferon- γ in murine cloned macrophages and microglial cells. *J Neurochem* **66**, 996-1004.
3. Alphand, V. and Furstoss, R. 1992. Microbiological transformations. 22. Microbiologically mediated Baeyer-Villiger reactions: a unique route to several bicyclic γ -lactones in high enantiomeric purity. *J Org Chem* **57**, 1306-1309.
4. Alphand, V., Carrea, G., Wohlgemuth, R., Furstoss, R. and Woodley, J.M. 2003. Towards large-scale synthetic applications of Baeyer-Villiger monooxygenases. *Trends Biotechnol* **21**, 318-323.
5. Altschul, S.F., Madden, T.L., Schaeffer, A.A., Zhang, J., Zhang, Z., Miller, W. and Lipman, D.J. 1997. Gapped BLAST and PSI-BLAST: a new generation of protein database search programs. *Nucleic Acids Res* **25**, 3389-3402.
6. Arciero, D.M., Lipscomb, J.D., Huynh, B.H., Kent, T.A. and Munck, E. 1983. EPR and Mossbauer studies of protocatechuate 4,5-dioxygenase. Characterization of a new Fe²⁺ environment. *J Biol Chem* **258**, 14981-14991.
7. Arias-Barrau, E., Olivera, E.R., Luengo, J.M., Fernandez, C., Galán, B., Garcia, J.L., Diaz, E. and Minambres, B. 2004. The homogentisate pathway: a central catabolic pathway involved in the degradation of L-phenylalanine, L-tyrosine, and 3-hydroxyphenylacetate in *Pseudomonas putida*. *J Bacteriol* **186**, 5062-5077.
8. Armengaud, J., Timmis, K.N. and Wittich, R.M. 1999. A functional 4-hydroxysalicylate/hydroxyquinol degradative pathway gene cluster is linked to the initial dibenzo-*p*-dioxin pathway genes in *Sphingomonas* sp. strain RW1. *J Bacteriol* **181**, 3452-3461.
9. Arunachalam, U., Massey, V. and Miller, S.M. 1994. Mechanism of *p*-hydroxyphenylacetate-3-hydroxylase. A two-protein enzyme. *J Biol Chem* **269**, 150-155.
10. Baeyer, A. and Villiger, V. 1899. Einwirkung des Caro'schen Reagens auf Ketone. *Ber Dtsch Chem Ges* **32**, 3625-3633.
11. Bang, S.-W. and Zylstra, G.J. 1997. Cloning and sequencing of the hydroquinone 1,2-dioxygenase, γ -hydroxymuconic semialdehyde dehydrogenase, maleylacetate reductase genes from *Pseudomonas fluorescens* ENV2030. In: *Abstracts of the 97th General Meeting of the American Society for Microbiology 1997*. American Society for Microbiology, Washington, D.C., abstr. Q-383, pp. 519.
12. Barton, M.R. and Crawford, R.L. 1988. Novel biotransformations of 4-chlorobiphenyl by a *Pseudomonas* sp. *Appl Environ Microbiol* **54**, 594-595.
13. Becker, D., Schröder, T. and Andreesen, J.R. 1997. Two-component flavin-dependent pyrrole-2-carboxylate monooxygenase from *Rhodococcus* sp. *Eur J Biochem* **249**, 739-747.
14. Bedard, D.L., Haberl, M.L., May, R.J. and Brennan, M.J. 1987. Evidence for novel mechanisms of polychlorinated biphenyl metabolism in *Alcaligenes eutrophus* H850. *Appl Environ Microbiol* **53**, 1103-1112.
15. Bedard, D.L. and Haberl, M.L. 1990. Influence of chlorine substitution pattern on the degradation of polychlorinated biphenyls by eight bacterial strains. *Microb Ecol* **20**, 87-102.
16. Beller, M. 2004. The current status and future trends in oxidation chemistry. *Adv Synth Catal* **346**, 107-108.
17. Benvenuti, M., Briganti, F., Scozzafava, A., Golovleva, L., Travkin, V.M. and Mangani, S. 1999. Crystallization and preliminary crystallographic analysis of the hydroxyquinol 1,2-dioxygenase from *Nocardioides simplex* 3E: a novel dioxygenase involved in the biodegradation of polychlorinated aromatic compounds. *Acta Crystallogr, Sec. D: Biol Crystallogr* **55**, 901-903.
18. Bertini, I., Briganti, F., Mangani, S., Nolting, H.F. and Scozzafava, A. 1995. Biophysical investigation of bacterial aromatic extradiol dioxygenases involved in biodegradation processes. *Coord Chem Rev* **144**, 321-345.
19. Beynon, K.I. and Wright, A.N. 1967. The breakdown of 14-C-chlorofenvinphos in soils and in crops grown in the soils. *J Sci Food Agric* **18**, 143-150.
20. Beynon, K.I. and Wright, A.N. 1969. Breakdown of the insecticide, Gardona, on plants and in soils. *J Sci Food Agric* **20**, 250-256.

21. Beynon, K.I., Hutson, D.H. and Wright, A.N. 1973. The metabolism and degradation of vinyl phosphate insecticides. *Residue Rev* **47**, 55-142.
22. Boersma, M.G., Dinarieva, T.Y., Middelhoven, W.J., van Berkel, W.J.H., Doran, J., Vervoort, J. and Rietjens, I.M.C.M. 1998. ¹⁹F nuclear magnetic resonance as a tool to investigate microbial degradation of fluorophenols to fluorocatechols and fluoromuconates. *Appl Environ Microbiol* **64**, 1256-1263.
23. Boldt, Y.R., Sadowsky, M.J., Ellis, L.B., Que, L., Jr. and Wackett, L.P. 1995. A manganese-dependent dioxygenase from *Arthrobacter globiformis* CM-2 belongs to the major extradiol dioxygenase family. *J Bacteriol* **177**, 1225-1232.
24. Bolm, C., Palazzi, C., Francio, G. and Leitner, W. 2002. Baeyer-Villiger oxidation in compressed CO₂. *Chem Commun*, 1588-1589.
25. Bondar, V.S., Boersma, M.G., Golovlev, E.L., Vervoort, J., van Berkel, W.J.H., Finkelstein, Z.I., Solyanikova, I.P., Golovleva, A. and Rietjens, I.M.C.M. 1998. ¹⁹F NMR study on the biodegradation of fluorophenols by various *Rhodococcus* species. *Biodegradation* **9**, 475-486.
26. Bondar, V.S., Boersma, M.G., van Berkel, W.J.H., Finkelstein, Z.I., Golovlev, E.L., Baskunov, B.P., Vervoort, J., Golovleva, L.A. and Rietjens, I.M.C.M. 1999. Preferential oxidative dehalogenation upon conversion of 2-halophenols by *Rhodococcus opacus* 1G. *FEMS Microbiol Lett* **181**, 73-82.
27. Bork, P. and Grunwald, C. 1990. Recognition of different nucleotide-binding sites in primary structures using a property-pattern approach. *Eur J Biochem* **191**, 347-358.
28. Boyington, J.C., Gaffney, B.J. and Amzel, L.M. 1993. The three-dimensional structure of an arachidonic acid 15-lipoxygenase. *Science* **260**, 1482-1486.
29. Brady, L., Brzozowski, A.M., Derewenda, Z.S., Dodson, E., Dodson, G., Tolley, S., Turkenburg, J.P., Christiansen, L., Huge-Jensen, B., Norskov, L., Thim, L. and Menge, U. 1990. A serine protease triad forms the catalytic centre of a triacylglycerol lipase. *Nature* **343**, 767-770.
30. Briganti, F., Pessione, E., Giunta, C. and Scozzafava, A. 1997. Purification, biochemical properties and substrate specificity of a catechol 1,2-dioxygenase from a phenol degrading *Acinetobacter radioresistens*. *FEBS Lett* **416**, 61-64.
31. Britton, L.N. and Markovetz, A.J. 1977. A novel ketone monooxygenase from *Pseudomonas cepacia*. Purification and properties. *J Biol Chem* **252**, 8561-8566.
32. Brzostowicz, P.C., Gibson, K.L., Thomas, S.M., Blasko, M.S. and Rouviere, P.E. 2000. Simultaneous identification of two cyclohexanone oxidation genes from an environmental *Brevibacterium* isolate using mRNA differential display. *J Bacteriol* **182**, 4241-4248.
33. Cai, M. and Xun, L. 2002. Organization and regulation of pentachlorophenol-degrading genes in *Sphingobium chlorophenolicum* ATCC 39723. *J Bacteriol* **184**, 4672-4680.
34. Cain, R.B., Fortnagel, P., Hebenbrock, S., Kirby, G.W., McLenaghan, H.J., Rao, G.V. and Schmidt, S. 1997. Biosynthesis of a cyclic tautomer of (3-methylmaleyl)acetone from 4-hydroxy-3,5-dimethylbenzoate by *Pseudomonas* sp. HH35 but not by *Rhodococcus rhodochrous* N75. *Biochem Biophys Res Commun* **238**, 197-201.
35. Calderone, V., Trabucco, M., Menin, V., Negro, A. and Zanotti, G. 2002. Cloning of human 3-hydroxyanthranilic acid dioxygenase in *Escherichia coli*: characterisation of the purified enzyme and its in vitro inhibition by Zn²⁺. *Biochim Biophys Acta* **1596**, 283-292.
36. Carugo, O. and Argos, P. 1997. NADP-dependent enzymes. I: Conserved stereochemistry of cofactor binding. *Proteins* **28**, 10-28.
37. Cavanagh, J., Thompson, R., Bobay, B., Benson, L.M. and Naylor, S. 2002. Stoichiometries of protein-protein/DNA binding and conformational changes for the transition-state regulator AbrB measured by pseudo cell-size exclusion chromatography-mass spectrometry. *Biochemistry* **41**, 7859-7865.
38. Chapman, P.J. and Hopper, D.J. 1968. The bacterial metabolism of 2,4-xyleneol. *Biochem J* **110**, 491-498.
39. Chapman, P.J. and Ribbons, D.W. 1976. Metabolism of resorcinylic compounds by bacteria: alternative pathways for resorcinol catabolism in *Pseudomonas putida*. *J Bacteriol* **125**, 985-998.
40. Chauhan, A., Chakraborti, A.K. and Jain, R.K. 2000. Plasmid-encoded degradation of *p*-nitrophenol and 4-nitrocatechol by *Arthrobacter protophormiae*. *Biochem Biophys Res Commun* **270**, 733-740.
41. Chauhan, A., Samanta, S.K. and Jain, R.K. 2000. Degradation of 4-nitrocatechol by *Burkholderia cepacia*: a plasmid-encoded novel pathway. *J Appl Microbiol* **88**, 764-772.

42. Chen, Y.-C.J., Peoples, O.P. and Walsh, C.T. 1988. *Acinetobacter* cyclohexanone monooxygenase: gene cloning and sequence determination. *J Bacteriol* **170**, 781-789.
43. Choo, D.-W., Kurihara, T., Suzuki, T., Soda, K. and Esaki, N. 1998. A cold-adapted lipase of an Alaskan psychrotroph, *Pseudomonas* sp. strain B11-1: gene cloning and enzyme purification and characterization. *Appl Environ Microbiol* **64**, 486-491.
44. Christendat, D., Yee, A., Dharamsi, A., Kluger, Y., Savchenko, A., Cort, J.R., Booth, V., Mackereth, C.D., Saridakis, V., Ekiel, I., Kozlov, G., Maxwell, K.L., Wu, N., McIntosh, L.P., Gehring, K., Kennedy, M.A., Davidson, A.R., Pai, E.F., Gerstein, M., Edwards, A.M. and Arrowsmith, C.H. 2000. Structural proteomics of an archaeon. *Nat Struct Biol* **7**, 903-909.
45. Coenen, H.H. 1993. Biochemistry and evaluation of fluoroamino acids. In: *PET studies on amino acid metabolism and protein synthesis* (Eds. B. Mazoyer, W.D. Weiss and D. Comar). Kluwer Academic Publisher, Netherlands, pp. 109-129.
46. Conte, L., Napoli, M., Gambaretto, G.P., Guerrato, A. and Carlini, F.M. 1994. Preparation of 4-fluorophenol and 4-fluorobenzoic acid by the Baeyer-Villiger reaction. *J Fluorine Chem* **67**, 41-45.
47. Copley, S.D. 2000. Evolution of a metabolic pathway for degradation of a toxic xenobiotic: the patchwork approach. *Trends Biochem Sci* **25**, 261-265.
48. Corma, A., Nemeth, L.T., Renz, M. and Valencia, S. 2001. Sn-zeolite beta as a heterogeneous chemoselective catalyst for Baeyer-Villiger oxidations. *Nature* **412**, 423-425.
49. Corma, A., Fornes, V., Iborra, S., Mifsud, M. and Renz, M. 2004. One-pot synthesis of phenols from aromatic aldehydes by Baeyer-Villiger oxidation with H₂O₂ using water-tolerant Lewis acids in molecular sieves. *J Catal* **221**, 67-76.
50. Cox, D.P. and Goldsmith, C.D. 1979. Microbial conversion of ethylbenzene to 1-phenethanol and acetophenone by *Nocardia tartaricans* ATCC 31190. *Appl Environ Microbiol* **38**, 514-520.
51. Criegee, R. 1948. Die Umlagerung der Dekalin-peroxydester als Folge von kationischem Sauerstoff. *Justus Liebigs Ann Chem* **560**, 127-135.
52. Cripps, R.E. 1975. The microbial metabolism of acetophenone. Metabolism of acetophenone and some chloroacetophenones by an *Arthrobacter* species. *Biochem J* **152**, 233-241.
53. Cripps, R.E., Trudgill, P.W. and Whateley, J.G. 1978. The metabolism of 1-phenylethanol and acetophenone by *Nocardia* T5 and an *Arthrobacter* species. *Eur J Biochem* **86**, 175-186.
54. Curti, B., Ronchi, S., Branzoli, U., Ferri, G. and Williams, C.H., Jr. 1973. Improved purification, amino acid analysis and molecular weight of homogenous D-amino acid oxidase from pig kidney. *Biochim Biophys Acta* **327**, 266-273.
55. Darby, J.M., Taylor, D.G. and Hopper, D.J. 1987. Hydroquinone as the ring-fission substrate in the catabolism of 4-ethylphenol and 4-hydroxyacetophenone by *Pseudomonas putida* JD1. *J Gen Microbiol* **133**, 2137-2146.
56. Daubaras, D.L., Hershberger, C.D., Kitano, K. and Chakrabarty, A.M. 1995. Sequence analysis of a gene cluster involved in metabolism of 2,4,5-trichlorophenoxyacetic acid by *Burkholderia cepacia* AC1100. *Appl Environ Microbiol* **61**, 1279-1289.
57. Daubaras, D.L., Saido, K. and Chakrabarty, A.M. 1996. Purification of hydroxyquinol 1,2-dioxygenase and maleylacetate reductase: the lower pathway of 2,4,5-trichlorophenoxyacetic acid metabolism by *Burkholderia cepacia* AC1100. *Appl Environ Microbiol* **62**, 4276-4279.
58. Dauber-Osguthorpe, P., Roberts, V.A., Osguthorpe, D.J., Wolff, J., Genest, M. and Hagler, A.T. 1988. Structure and energetics of ligand binding to proteins: *Escherichia coli* dihydrofolate reductase-trimethoprim, a drug-receptor system. *Proteins* **4**, 31-47.
59. de Jong, E., van Berkel, W.J.H., van der Zwan, R.P. and de Bont, J.A.M. 1992. Purification and characterization of vanillyl-alcohol oxidase from *Penicillium simplicissimum*. A novel aromatic alcohol oxidase containing covalently bound FAD. *Eur J Biochem* **208**, 651-657.
60. Denome, S.A., Stanley, D.C., Olson, E.S. and Young, K.D. 1993. Metabolism of dibenzothiophene and naphthalene in *Pseudomonas* strains: complete DNA sequence of an upper naphthalene catabolic pathway. *J Bacteriol* **175**, 6890-6901.
61. Dewar, M.J.S., Zoebisch, E.G., Healy, E.F. and Stewart, J.J.P. 1985. AM1: A new general purpose quantum mechanical molecular model. *J Am Chem Soc* **107**, 3902-3909.
62. Doering, W.v.E. and Speers, L. 1950. The peracetic acid cleavage of unsymmetrical ketones. *J Am Chem Soc* **72**, 5515-5518.
63. Doig, S.D., Avenell, P.J., Bird, P.A., Gallati, P., Lander, K.S., Lye, G.J., Wohlgemuth, R. and Woodley, J.M. 2002. Reactor operation and scale-up of whole cell Baeyer-Villiger catalyzed lactone synthesis. *Biotechnol Prog* **18**, 1039-1046.

64. Don, R.H., Cox, P.T., Wainwright, B.J., Baker, K. and Mattick, J.S. 1991. 'Touchdown' PCR to circumvent spurious priming during gene amplification. *Nucleic Acids Res* **19**, 4008.
65. Dong, C., Huang, F., Deng, H., Schaffrath, C., Spencer, J.B., O'Hagan, D. and Naismith, J.H. 2004. Crystal structure and mechanism of a bacterial fluorinating enzyme. *Nature* **427**, 561-565.
66. Donoghue, N.A., Norris, D.B. and Trudgill, P.W. 1976. The purification and properties of cyclohexanone oxygenase from *Nocardia globerula* CL1 and *Acinetobacter* NCIB 9871. *Eur J Biochem* **63**, 175-192.
67. Drijfhout, F.P., Fraaije, M.W., Jongejan, H., van Berkel, W.J.H. and Franssen, M.C. 1998. Enantioselective hydroxylation of 4-alkylphenols by vanillyl alcohol oxidase. *Biotechnol Bioeng* **59**, 171-177.
68. Duchaud, E., Rusniok, C., Frangeul, L., Buchrieser, C., Givaudan, A., Taourit, S., Bocs, S., Boursaux-Eude, C., Chandler, M., Charles, J.-F., Dassa, E., Deroose, R., Derzelle, S., Freyssinet, G., Gaudriault, S., Médigue, C., Lanois, A., Powell, K., Siguier, P., Vincent, R., Wingate, V., Zouine, M., Glaser, P., Boemare, N., Danchin, A. and Kunst, F. 2003. The genome sequence of the entomopathogenic bacterium *Photorhabdus luminescens*. *Nat Biotechnol* **21**, 1307-1313.
69. Duque, E., Segura, A., Mosqueda, G. and Ramos, J.L. 2001. Global and cognate regulators control the expression of the organic solvent efflux pumps TtgABC and TtgDEF of *Pseudomonas putida*. *Mol Microbiol* **39**, 1100-1106.
70. Eaton, R. 1997. *p*-Cymene catabolic pathway in *Pseudomonas putida* F1: cloning and characterization of DNA encoding conversion of *p*-cymene to *p*-cumate. *J Bacteriol* **179**, 3171-3180.
71. Eaton, R.W. 1996. *p*-Cumate catabolic pathway in *Pseudomonas putida* F1: cloning and characterization of DNA carrying the cmt operon. *J Bacteriol* **178**, 1351-1362.
72. Eckstein, J.W., Hastings, J.W. and Ghisla, S. 1993. Mechanism of bacterial bioluminescence: 4a,5-dihydroflavin analogs as models for luciferase hydroperoxide intermediates and the effect of substituents at the 8-position of flavin on luciferase kinetics. *Biochemistry* **32**, 404-411.
73. Eggink, G., Engel, H., Vriend, G., Terpstra, P. and Witholt, B. 1990. Rubredoxin reductase of *Pseudomonas oleovorans*. Structural relationship to other flavoprotein oxidoreductases based on one NAD and two FAD fingerprints. *J Mol Biol* **212**, 135-142.
74. Ekaeva, I., Barre, L., Lasne, M.-C. and Gourand, F. 1995. 2- and 4-[¹⁸F]Fluorophenols from Baeyer-Villiger oxidation of [¹⁸F]fluorophenylketones and [¹⁸F]fluorobenzaldehydes. *Appl Radiat Isot* **46**, 777-782.
75. Ellis, L.B.M., Hou, B.K., Kang, W. and Wackett, L.P. 2003. The University of Minnesota Biocatalysis/Biodegradation Database: post-genomic data mining. *Nucleic Acids Res* **31**, 262-265.
76. Enroth, C., Neujahr, H., Schneider, G. and Lindqvist, Y. 1998. The crystal structure of phenol hydroxylase in complex with FAD and phenol provides evidence for a concerted conformational change in the enzyme and its cofactor during catalysis. *Structure* **6**, 605-617.
77. Entsch, B., Ballou, D.P. and Massey, V. 1976. Flavin-oxygen derivatives involved in hydroxylation by *p*-hydroxybenzoate hydroxylase. *J Biol Chem* **251**, 2550-2563.
78. Entsch, B. and Ballou, D.P. 1989. Purification, properties, and oxygen reactivity of *p*-hydroxybenzoate hydroxylase from *Pseudomonas aeruginosa*. *Biochim Biophys Acta* **999**, 313-322.
79. Entsch, B., Palfey, B.A., Ballou, D.P. and Massey, V. 1991. Catalytic function of tyrosine residues in *para*-hydroxybenzoate hydroxylase as determined by the study of site-directed mutants. *J Biol Chem* **266**, 17341-17349.
80. Entsch, B. and van Berkel, W.J.H. 1995. Structure and mechanism of *para*-hydroxybenzoate hydroxylase. *FASEB J* **9**, 476-483.
81. Eppink, M.H.M., Schreuder, H.A. and van Berkel, W.J.H. 1995. Structure and function of mutant Arg44Lys of 4-hydroxybenzoate hydroxylase implications for NADPH binding. *Eur J Biochem* **231**, 157-165.
82. Eppink, M.H.M., Boeren, S.A., Vervoort, J. and van Berkel, W.J.H. 1997. Purification and properties of 4-hydroxybenzoate 1-hydroxylase (decarboxylating), a novel flavin adenine dinucleotide-dependent monooxygenase from *Candida parapsilosis* CBS604. *J Bacteriol* **179**, 6680-6687.
83. Eppink, M.H.M., Schreuder, H.A. and van Berkel, W.J.H. 1997. Identification of a novel conserved sequence motif in flavoprotein hydroxylases with a putative dual function in FAD/NAD(P)H binding. *Protein Sci* **6**, 2454-2458.

84. Eppink, M.H.M., Schreuder, H.A. and van Berkel, W.J.H. 1998. Interdomain binding of NADPH in *p*-hydroxybenzoate hydroxylase as suggested by kinetic, crystallographic and modeling studies of histidine 162 and arginine 269 variants. *J Biol Chem* **273**, 21031-21039.
85. Eppink, M.H.M., Schreuder, H.A. and van Berkel, W.J.H. 1998. Lys42 and Ser42 variants of *p*-hydroxybenzoate hydroxylase from *Pseudomonas fluorescens* reveal that Arg42 is essential for NADPH binding. *Eur J Biochem* **253**, 194-201.
86. Eppink, M.H.M., Bunthol, C., Schreuder, H.A. and van Berkel, W.J.H. 1999. Phe161 and Arg166 variants of *p*-hydroxybenzoate hydroxylase. Implications for NADPH recognition and structural stability. *FEBS Lett* **443**, 251-255.
87. Eppink, M.H.M., Overkamp, K.M., Schreuder, H.A. and van Berkel, W.J.H. 1999. Switch of coenzyme specificity of *p*-hydroxybenzoate hydroxylase. *J Mol Biol* **292**, 87-96.
88. Eppink, M.H.M., Cammaart, E., van Wassenaar, D., Middelhoven, W.J. and van Berkel, W.J.H. 2000. Purification and properties of hydroquinone hydroxylase, a FAD-dependent monooxygenase involved in the catabolism of 4-hydroxybenzoate in *Candida parapsilosis* CBS604. *Eur J Biochem* **267**, 6832-6840.
89. Eschrich, K., van der Bolt, F.J.T., de Kok, A. and van Berkel, W.J.H. 1993. Role of Tyr201 and Tyr385 in substrate activation by *p*-hydroxybenzoate hydroxylase from *Pseudomonas fluorescens*. *Eur J Biochem* **216**, 137-146.
90. Faber, K. 2000. *Biotransformations in organic chemistry*. Springer, Berlin, 453 p.
91. Ferraroni, M., Seifert, J., Travkin, V.M., Thiel, M., Kaschabek, S., Scozzafava, A., Golovleva, L., Schlömann, M. and Briganti, F. 2005. Crystal structure of the hydroxyquinol 1,2-dioxygenase from *Nocardioides simplex* 3E, a key enzyme involved in polychlorinated aromatics biodegradation. *J Biol Chem*, in press.
92. Ferreira, P., Medina, M., Guillén, F., Martínez, M.J., van Berkel, W.J.H. and Martínez, Á.T. 2005. Spectral and catalytic properties of aryl-alcohol oxidase, a fungal flavoenzyme acting on polyunsaturated alcohols. *Biochem J*, in press.
93. Fersht, A.R. and Winter, G.P. 1985. Redesigning enzymes by site-directed mutagenesis. *Ciba Found Symp* **111**, 204-218.
94. Finkelstein, Z.I., Baskunov, B.P., Boersma, M.G., Vervoort, J., Golovlev, E.L., van Berkel, W.J.H., Golovleva, L.A. and Rietjens, I.M.C.M. 2000. Identification of fluoropyrogallols as new intermediates in biotransformation of monofluorophenols in *Rhodococcus opacus* 1cp. *Appl Environ Microbiol* **66**, 2148-2153.
95. Fleming, I. 1976. *Frontier orbitals and organic chemical reactions*. John Wiley & Sons, London, 249 p.
96. Flo, T.H., Smith, K.D., Sato, S., Rodriguez, D.J., Holmes, M.A., Strong, R.K., Akira, S. and Aderem, A. 2004. Lipocalin 2 mediates an innate immune response to bacterial infection by sequestering iron. *Nature* **432**, 917-921.
97. Fraaije, M.W., Veeger, C. and van Berkel, W.J.H. 1995. Substrate specificity of flavin-dependent vanillyl-alcohol oxidase from *Penicillium simplicissimum*. Evidence for the production of 4-hydroxycinnamyl alcohols from 4-allylphenols. *Eur J Biochem* **234**, 271-277.
98. Fraaije, M.W. and van Berkel, W.J.H. 1997. Catalytic mechanism of the oxidative demethylation of 4-(methoxymethyl)phenol by vanillyl-alcohol oxidase. Evidence for formation of a *p*-quinone methide intermediate. *J Biol Chem* **272**, 18111-18116.
99. Fraaije, M.W., van Berkel, W.J.H., Benen, J.A., Visser, J. and Mattevi, A. 1998. A novel oxidoreductase family sharing a conserved FAD-binding domain. *Trends Biochem Sci* **23**, 206-207.
100. Fraaije, M.W., van den Heuvel, R.H.H., van Berkel, W.J.H. and Mattevi, A. 1999. Covalent flavinylation is essential for efficient redox catalysis in vanillyl-alcohol oxidase. *J Biol Chem* **274**, 35514-35520.
101. Fraaije, M.W. and Mattevi, A. 2000. Flavoenzymes: diverse catalysts with recurrent features. *Trends Biochem Sci* **25**, 126-132.
102. Fraaije, M.W., van den Heuvel, R.H.H., van Berkel, W.J.H. and Mattevi, A. 2000. Structural analysis of flavinylation in vanillyl-alcohol oxidase. *J Biol Chem* **275**, 38654-38658.
103. Fraaije, M.W., Kamerbeek, N.M., van Berkel, W.J.H. and Janssen, D.B. 2002. Identification of a Baeyer-Villiger monooxygenase sequence motif. *FEBS Lett* **518**, 43-47.
104. Fraaije, M.W., Wu, J., Heuts, D.P., van Hellemond, E.W., Spelberg, J.H. and Janssen, D.B. 2005. Discovery of a thermostable Baeyer-Villiger monooxygenase by genome mining. *Appl Microbiol Biotechnol* **66**, 393-400.

105. Friess, S.L. and Soloway, A.H. 1951. Reactions of peracids. V. The reaction of substituted acetophenones with perbenzoic acid. *J Am Chem Soc* **73**, 3968-3972.
106. Fukuda, O., Sakaguchi, S. and Ishii, Y. 2001. A new strategy for catalytic Baeyer-Villiger oxidation of KA-oil with molecular oxygen using N-hydroxyphthalimide. *Tetrahedron Lett* **42**, 3479-3481.
107. Fukui, K., Yonezawa, T., Nagata, C. and Shingu, H. 1954. Molecular orbital theory of orientation in aromatic, heteroaromatic, and other conjugated molecules. *J Chem Phys* **22**, 1433-1442.
108. Galán, B., Diaz, E., Prieto, M.A. and Garcia, J.L. 2000. Functional analysis of the small component of the 4-hydroxyphenylacetate 3-monooxygenase of *Escherichia coli* W: a prototype of a new Flavin:NAD(P)H reductase subfamily. *J Bacteriol* **182**, 627-636.
109. Gatti, D.L., Palfey, B.A., Lah, M.S., Entsch, B., Massey, V., Ballou, D.P. and Ludwig, M.L. 1994. The mobile flavin of 4-OH benzoate hydroxylase. *Science* **266**, 110-114.
110. Goa, J. 1953. A micro biuret method for protein determination. Determination of total protein in cerebrospinal fluid. *Scan J Clin Lab Invest* **5**, 218-222.
111. Göbel, M., Kranz, O.H., Kaschabek, S.R., Schmidt, E., Pieper, D.H. and Reineke, W. 2004. Microorganisms degrading chlorobenzene via a *meta*-cleavage pathway harbor highly similar chlorocatechol 2,3-dioxygenase-encoding gene clusters. *Arch Microbiol* **182**, 147-156.
112. Golovleva, L.A., Zaborina, O., Pertsova, R., Baskunov, B., Schurukhin, Y. and Kuzmin, S. 1991. Degradation of polychlorinated phenols by *Streptomyces rochei* 303. *Biodegradation* **2**, 201-208.
113. Griffin, M. and Trudgill, P.W. 1972. The metabolism of cyclopentanol by *Pseudomonas* N.C.I.B. 9872. *Biochem J* **129**, 595-603.
114. Guillén, F., Martínez, Á.T. and Martínez, M.J. 1992. Substrate specificity and properties of the aryl-alcohol oxidase from the ligninolytic fungus *Pleurotus eryngii*. *Eur J Biochem* **209**, 603-611.
115. Gunter, S.E. 1953. The enzymic oxidation of *p*-hydroxymandelic acid *p*-hydroxybenzoic acid. *J Bacteriol* **66**, 341-346.
116. Hage, A., Schoemaker, H.E. and Field, J.A. 1999. Reduction of aryl acids by white-rot fungi for the biocatalytic production of aryl aldehydes and alcohols. *Appl Microbiol Biotechnol* **52**, 834-838.
117. Hall, T.A. 1999. BioEdit: a user-friendly biological sequence alignment editor and analysis program for Windows 95/98/NT. *Nucl Acids Symp Ser* **41**, 95-98.
118. Hamood, A.N., Colmer, J.A., Ochsner, U.A. and Vasil, M.L. 1996. Isolation and characterization of a *Pseudomonas aeruginosa* gene, *ptxR*, which positively regulates exotoxin A production. *Mol Microbiol* **21**, 97-110.
119. Han, S., Eltis, L.D., Timmis, K.N., Muchmore, S.W. and Bolin, J.T. 1995. Crystal structure of the biphenyl-cleaving extradiol dioxygenase from a PCB-degrading pseudomonad. *Science* **270**, 976-980.
120. Hanne, L.F., Kirk, L.L., Appel, S.M., Narayan, A.D. and Bains, K.K. 1993. Degradation and induction specificity in *Actinomycetes* that degrade *p*-nitrophenol. *Appl Environ Microbiol* **59**, 3505-3508.
121. Harayama, S., Polissi, A. and Reikik, M. 1991. Divergent evolution of chloroplast-type ferredoxins. *FEBS Lett* **285**, 85-88.
122. Harayama, S., Kok, M. and Neidle, E.L. 1992. Functional and evolutionary relationships among diverse oxygenases. *Annu Rev Microbiol* **46**, 565-601.
123. Harpel, M.R. and Lipscomb, J.D. 1990. Gentisate 1,2-dioxygenase from *Pseudomonas*. Purification, characterization, and comparison of the enzymes from *Pseudomonas testosteroni* and *Pseudomonas acidovorans*. *J Biol Chem* **265**, 6301-6311.
124. Harpel, M.R. and Lipscomb, J.D. 1990. Gentisate 1,2-dioxygenase from *Pseudomonas*. Substrate coordination to active site Fe²⁺ and mechanism of turnover. *J Biol Chem* **265**, 22187-22196.
125. Hartog, J. and Wouters, W. 1988. Flesinoxan hydrochloride. *Drugs Future* **13**, 31-33.
126. Harwood, C.S. and Parales, R.E. 1996. The beta-ketoadipate pathway and the biology of self-identity. *Annu Rev Microbiol* **50**, 553-590.
127. Havel, J. and Reineke, W. 1993. Microbial degradation of chlorinated acetophenones. *Appl Environ Microb* **59**, 2706-2712.
128. Hayatsu, M., Hirano, M. and Tokuda, S. 2000. Involvement of two plasmids in fenitrothion degradation by *Burkholderia* sp. strain NF100. *Appl Environ Microbiol* **66**, 1737-1740.
129. He, Z. and Spain, J.C. 2000. One-step production of picolinic acids from 2-aminophenols catalyzed by 2-aminophenol 1,6-dioxygenase. *J Ind Microbiol Biotechnol* **25**, 25-28.
130. Hecht, H.J., Kalisz, H.M., Hendle, J., Schmid, R.D. and Schomburg, D. 1993. Crystal structure of glucose oxidase from *Aspergillus niger* refined at 2.3 Å resolution. *J Mol Biol* **229**, 153-172.

131. Held, M., Suske, W., Schmid, A., Engesser, K.-H., Kohler, H.-P.E., Witholt, B. and Wubbolts, M.G. 1998. Preparative scale production of 3-substituted catechols using a novel monooxygenase from *Pseudomonas azelaica* HBP 1. *J Mol Catal B: Enzym* **5**, 87-93.
132. Held, M., Schmid, A., Kohler, H.P., Suske, W., Witholt, B. and Wubbolts, M.G. 1999. An integrated process for the production of toxic catechols from toxic phenols based on a designer biocatalyst. *Biotechnol Bioeng* **62**, 641-648.
133. Higson, F.K. and Focht, D.D. 1990. Bacterial degradation of ring-chlorinated acetophenones. *Appl Environ Microbiol* **56**, 3678-3685.
134. Hilker, I., Alphand, V., Wohlgenuth, R. and Furstoss, R. 2004. Microbial transformations, 56. Preparative scale asymmetric Baeyer-Villiger oxidation using a highly productive "two-in-one" resin-based *in situ* SFPR concept. *Adv Synth Catal* **346**, 203-214.
135. Hopper, D.J., Jones, H.G., Elmorsi, E.A. and Rhodes-Roberts, M.E. 1985. The catabolism of 4-hydroxyacetophenone by an *Alcaligenes* sp. *J Gen Microbiol* **131**, 1807-1814.
136. Howell, L.G., Spector, T. and Massey, V. 1972. Purification and properties of *p*-hydroxybenzoate hydroxylase from *Pseudomonas fluorescens*. *J Biol Chem* **247**, 4340-4350.
137. Hudlicky, M. 1990. *Oxidations in organic chemistry*. ACS Monograph 186. American Chemical Society, Washington, DC, 164 p.
138. Hugo, N., Armengaud, J., Gaillard, J., Timmis, K.N. and Jouanneau, Y. 1998. A novel [2Fe-2S] ferredoxin from *Pseudomonas putida* mt2 promotes the reductive reactivation of catechol 2,3-dioxygenase. *J Biol Chem* **273**, 9622-9629.
139. Hugo, N., Meyer, C., Armengaud, J., Gaillard, J., Timmis, K.N. and Jouanneau, Y. 2000. Characterization of three XylT-like [2Fe-2S] ferredoxins associated with catabolism of cresols or naphthalene: evidence for their involvement in catechol dioxygenase reactivation. *J Bacteriol* **182**, 5580-5585.
140. Husain, M. and Massey, V. 1979. Kinetic studies on the reaction of *p*-hydroxybenzoate hydroxylase. Agreement of steady state and rapid reaction data. *J Biol Chem* **254**, 6657-6666.
141. Husain, M., Entsch, B., Ballou, D.P., Massey, V. and Chapman, P.J. 1980. Fluoride elimination from substrates in hydroxylation reactions catalyzed by *p*-hydroxybenzoate hydroxylase. *J Biol Chem* **255**, 4189-4197.
142. Hutchinson, J. and Sandford, G. 1997. Elemental fluorine in organic chemistry. *Top Curr Chem* **193**, 1-43.
143. Innis, M.A. and Gelfand, D.H. 1990. Optimization of PCRs. In: *PCR protocols: A guide to methods and amplification* (Eds. M.A. Innis, D.H. Gelfand, J.J. Snisky and T.J. White). Academic Press, San Diego, pp. 3-12.
144. Ismaiel, A.M., De Los Angeles, J., Teitler, M., Ingher, S. and Glennon, R.A. 1993. Antagonism of 1-(2,5-dimethoxy-4-methylphenyl)-2-aminopropane stimulus with a newly identified 5-HT₂-versus 5-HT_{1C}-selective antagonist. *J Med Chem* **36**, 2519-2525.
145. Itagaki, E. 1986. Studies on steroid monooxygenase from *Cylindrocarpon radlicola* ATCC 11011. Purification and characterization. *J Biochem* **99**, 815-824.
146. Itoh, N., Matsuda, M., Mabuchi, M., Dairi, T. and Wang, J. 2002. Chiral alcohol production by NADH-dependent phenylacetaldehyde reductase coupled with *in situ* regeneration of NADH. *Eur J Biochem* **269**, 2394-2402.
147. Jadan, A.P., van Berkel, W.J.H., Golovleva, L.A. and Golovlev, E.L. 2001. Purification and properties of *p*-hydroxybenzoate hydroxylases from *Rhodococcus* strains. *Biochemistry (Mosc)* **66**, 898-903.
148. Jadan, A.P., Moonen, M.J.H., Boeren, S.A., Golovleva, L.A., Rietjens, I.M.C.M. and van Berkel, W.J.H. 2004. Biocatalytic potential of *p*-hydroxybenzoate hydroxylase from *Rhodococcus rhodnii* 135 and *Rhodococcus opacus* 557. *Adv Synth Catal* **346**, 367-375.
149. Jain, R.K., Dreisbach, J.H. and Spain, J.C. 1994. Biodegradation of *p*-nitrophenol via 1,2,4-benzenetriol by an *Arthrobacter* sp. *Appl Environ Microbiol* **60**, 3030-3032.
150. Johnson, G.R., Jain, R.K. and Spain, J.C. 2000. Properties of the trihydroxytoluene oxygenase from *Burkholderia cepacia* R34: an extradiol dioxygenase from the 2,4-dinitrotoluene pathway. *Arch Microbiol* **173**, 86-90.
151. Johnson, G.R., Jain, R.K. and Spain, J.C. 2002. Origins of the 2,4-dinitrotoluene pathway. *J Bacteriol* **184**, 4219-4232.
152. Jones, K.H., Smith, R.T. and Trudgill, P.W. 1993. Diketocamphane enantiomer-specific 'Baeyer-Villiger' monooxygenases from camphor-grown *Pseudomonas putida* ATCC 17453. *J Gen Microbiol* **139**, 797-805.

153. Jones, K.H., Trudgill, P.W. and Hopper, D.J. 1993. Metabolism of *p*-cresol by the fungus *Aspergillus fumigatus*. *Appl Environ Microbiol* **59**, 1125-1130.
154. Jones, K.H., Trudgill, P.W. and Hopper, D.J. 1994. 4-Ethylphenol metabolism by *Aspergillus fumigatus*. *Appl Environ Microbiol* **60**, 1978-1983.
155. Kadiyala, V. and Spain, J.C. 1998. A two-component monooxygenase catalyzes both the hydroxylation of *p*-nitrophenol and the oxidative release of nitrite from 4-nitrocatechol in *Bacillus sphaericus* JS905. *Appl Environ Microbiol* **64**, 2479-2484.
156. Kälin, M., Neujahr, H.Y., Weissmahr, R.N., Sejlitz, T., Johl, R., Fiechter, A. and Reiser, J. 1992. Phenol hydroxylase from *Trichosporon cutaneum*: gene cloning, sequence analysis, and functional expression in *Escherichia coli*. *J Bacteriol* **174**, 7112-7120.
157. Kamerbeek, N.M., Moonen, M.J.H., van der Ven, J.G.M., van Berkel, W.J.H., Fraaije, M.W. and Janssen, D.B. 2001. 4-Hydroxyacetophenone monooxygenase from *Pseudomonas fluorescens* ACB. A novel flavoprotein catalyzing Baeyer-Villiger oxidation of aromatic compounds. *Eur J Biochem* **268**, 2547-2557.
158. Kamerbeek, N.M., Janssen, D.B., van Berkel, W.J.H. and Fraaije, M.W. 2003. Baeyer-Villiger monooxygenases, an emerging family of flavin-dependent biocatalysts. *Adv Synth Catal* **345**, 667-678.
159. Kamerbeek, N.M., Olsthoorn, A.J., Fraaije, M.W. and Janssen, D.B. 2003. Substrate specificity and enantioselectivity of 4-hydroxyacetophenone monooxygenase. *Appl Environ Microbiol* **69**, 419-426.
160. Kamerbeek, N.M., Fraaije, M.W. and Janssen, D.B. 2004. Identifying determinants of NADPH specificity in Baeyer-Villiger monooxygenases. *European Journal of Biochemistry* **271**, 2107-2116.
161. Kaschabek, S.R. and Reineke, W. 1992. Maleylacetate reductase of *Pseudomonas* sp. strain B13: dechlorination of chloromaleylacetates, metabolites in the degradation of chloroaromatic compounds. *Arch Microbiol* **158**, 412-417.
162. Kaschabek, S.R. and Reineke, W. 1995. Maleylacetate reductase of *Pseudomonas* sp. strain B13: specificity of substrate conversion and halide elimination. *J Bacteriol* **177**, 320-325.
163. Keller, S., Wage, T., Hohaus, K., Hölzer, M., Eichhorn, E. and van Pée, K.-H. 2000. Purification and partial characterization of tryptophan 7-halogenase (PrnA) from *Pseudomonas fluorescens*. *Angew Chem, Int Ed* **39**, 2300-2302.
164. Kennedy, S.I.T. and Fewson, C.A. 1968. Enzymes of the mandelate pathway in *Bacterium* NCIB 8250. *Biochem J* **107**, 497-506.
165. Kirchner, U., Müller, R. and van Berkel, W.J.H. 1999. Novel two-component phenol hydroxylase from a thermophilic *Bacillus* strain. In: *13th International Congress on Flavins and Flavoproteins*, (Eds. S. Ghisla, P. Kroneck, P. Macheroux and H. Sund). Agency for Scientific Publication, Berlin, pp. 387-390.
166. Kita, A., Kita, S., Fujisawa, I., Inaka, K., Ishida, T., Horiike, K., Nozaki, M. and Miki, K. 1999. An archetypical extradiol-cleaving catecholic dioxygenase: the crystal structure of catechol 2,3-dioxygenase (metapyrocatechase) from *Pseudomonas putida* mt-2. *Structure Fold Des* **7**, 25-34.
167. Kitagawa, W., Kimura, N. and Kamagata, Y. 2004. A novel *p*-nitrophenol degradation gene cluster from a gram-positive bacterium, *Rhodococcus opacus* SAO101. *J Bacteriol* **186**, 4894-4902.
168. Koerts, J., Velraeds, M.M., Soffers, A.E., Vervoort, J. and Rietjens, I.M. 1997. Influence of substituents in fluorobenzene derivatives on the cytochrome P450-catalyzed hydroxylation at the adjacent ortho aromatic carbon center. *Chem Res Toxicol* **10**, 279-288.
169. Kohler, H.P., Schmid, A. and van der Maarel, M. 1993. Metabolism of 2,2'-dihydroxybiphenyl by *Pseudomonas* sp. strain HBP1: production and consumption of 2,2',3-trihydroxybiphenyl. *J Bacteriol* **175**, 1621-1628.
170. Komiyama, M. and Hirai, H. 1984. Selective synthesis using cyclodextrins as catalyst. 2. The *para*-oriented carboxylation of phenols. *J Am Chem Soc* **106**, 174-178.
171. Konkil, J.T., Fan, J., Jayachandran, B. and Kirk, K.L. 2002. Syntheses of 6-fluoro-*meta*-tyrosine and of its metabolites. *J Fluorine Chem* **115**, 27-32.
172. Kröckel, L. and Focht, D.D. 1987. Construction of chlorobenzene-utilizing recombinants by progenitive manifestation of a rare event. *Appl Environ Microbiol* **53**, 2470-2475.
173. Kroutil, W., Mang, H., Edegger, K. and Faber, K. 2004. Biocatalytic oxidation of primary and secondary alcohols. *Adv Synth Catal* **346**, 125-142.

174. Krow, G.R. 1993. The Baeyer-Villiger oxidation of ketones and aldehydes. In: *Organic Reactions* 43, (Ed. L.A. Paquette). John Wiley & Sons, New York, pp. 251-798.
175. Kukor, J. and Olsen, R. 1992. Complete nucleotide sequence of *tbuD*, the gene encoding phenol/cresol hydroxylase from *Pseudomonas pickettii* PKO1, and functional analysis of the encoded enzyme. *J Bacteriol* **174**, 6518-6526.
176. Lah, M.S., Palfey, B.A., Schreuder, H.A. and Ludwig, M.L. 1994. Crystal structures of mutant *Pseudomonas aeruginosa* *p*-hydroxybenzoate hydroxylases: the Tyr201Phe, Tyr385Phe, and Asn300Asp variants. *Biochemistry* **33**, 1555-1564.
177. Laskowski, R.A., MacArthur, M.W., Moss, D.S. and Thornton, J.M. 1993. PROCHECK: a program to check the stereochemical quality of protein structures. *J Appl Crystallogr* **26**, 283-291.
178. Latus, M., Seitz, H., Eberspacher, J. and Lingens, F. 1995. Purification and characterization of hydroxyquinol 1,2-dioxygenase from *Azotobacter* sp. strain GP1. *Appl Environ Microbiol* **61**, 2453-2460.
179. Lau, S.S., Monks, T.J., Everitt, J.I., Kleymenova, E. and Walker, C.L. 2001. Carcinogenicity of a nephrotoxic metabolite of the "nongenotoxic" carcinogen hydroquinone. *Chem Res Toxicol* **14**, 25-33.
180. Lauritsen, F.R. and Lunding, A. 1998. A study of the bioconversion potential of the fungus *Bjerkandera adusta* with respect to a production of chlorinated aromatic compounds. *Enzyme Microb Technol* **22**, 459-465.
181. Lendenmann, U. and Spain, J.C. 1996. 2-aminophenol 1,6-dioxygenase: a novel aromatic ring cleavage enzyme purified from *Pseudomonas pseudoalcaligenes* JS45. *J Bacteriol* **178**, 6227-6232.
182. Liese, A., Seelbach, K. and Wandrey, C. 2000. *Industrial biotransformations*. Wiley-VCH, Weinheim, 423 p.
183. Lipscomb, J.D. and Orville, A.M. 1992. Mechanistic aspects of dihydroxybenzoate dioxygenases. In: *Degradation of environmental pollutants by microorganisms and their metalloenzymes* 28, (Eds. H. Sigel and A. Sigel). Dekker, New York, pp. 243-298.
184. Liu, W.-H., Li, R.-M., Kung, K.-H. and Cheng, T.-L. 2003. Bioconversion of benzoic acid to *cis,cis* muconic acid by *Corynebacterium pseudodiphtheriticum*. *Food Sci Agri Chem* **5**, 7-12.
185. Lobos, J.H., Leib, T.K. and Su, T.M. 1992. Biodegradation of bisphenol A and other bisphenols by a gram-negative aerobic bacterium. *Appl Environ Microbiol* **58**, 1823-1831.
186. Lomovskaya, O. and Lewis, K. 1992. *emr*, an *Escherichia coli* locus for multidrug resistance. *Proc Natl Acad Sci U S A* **89**, 8938-8942.
187. Louie, T.M., Webster, C.M. and Xun, L. 2002. Genetic and biochemical characterization of a 2,4,6-trichlorophenol degradation pathway in *Ralstonia eutropha* JMP134. *J Bacteriol* **184**, 3492-3500.
188. Ludwig, T., Ermert, J. and Coenen, H.H. 2002. 4-[¹⁸F]Fluoroarylalkylethers via an improved synthesis of n.c.a. 4-[¹⁸F]fluorophenol. *Nucl Med Biol* **29**, 255-262.
189. Luzhkov, V.B. and Venanzi, C.A. 1995. Computer modeling of phenyl acetate hydrolysis in water and in reaction with β -cyclodextrin: Molecular orbital calculations with the semiempirical AM1 method and the Langevin dipole solvent model. *J Phys Chem* **99**, 2312-2323.
190. Maeda-Yorita, K. and Massey, V. 1993. On the reaction mechanism of phenol hydroxylase. New information obtained by correlation of fluorescence and absorbance stopped flow studies. *J Biol Chem* **268**, 4134-4144.
191. Malito, E., Alfieri, A., Fraaije, M.W. and Mattevi, A. 2004. Crystal structure of a Baeyer-Villiger monooxygenase. *Proc Natl Acad Sci U S A* **101**, 13157-13162.
192. Mann, J. 1987. Modern methods for the introduction of fluorine into organic molecules: an approach to compounds with altered chemical and biological activities. *Chem Soc Rev* **16**, 381-436.
193. Massey, V. 1994. Activation of molecular oxygen by flavins and flavoproteins. *J Biol Chem* **269**, 22459-22462.
194. Mattevi, A., Vanoni, M.A., Todone, F., Rizzi, M., Teplyakov, A., Coda, A., Bolognesi, M. and Curti, B. 1996. Crystal structure of D-amino acid oxidase: a case of active site mirror-image convergent evolution with flavocytochrome b2. *Proc Natl Acad Sci U S A* **93**, 7496-7501.
195. Mattevi, A., Fraaije, M.W., Mozzarelli, A., Olivi, L., Coda, A. and van Berkel, W.J.H. 1997. Crystal structures and inhibitor binding in the octameric flavoenzyme vanillyl-alcohol oxidase: the shape of the active-site cavity controls substrate specificity. *Structure* **5**, 907-920.
196. Mattevi, A. 1998. The PHBH fold: not only flavoenzymes. *Biophys Chem* **70**, 217-222.

197. Matthews, C., Rossiter, J.T. and Ribbons, D.W. 1991. Production of pyridine xynthons by biotransformations of benzene precursors and their cyclization with nitrogen nucleophiles. *Biocatal Biotransform* **12**, 241-254.
198. Mazzini, C., Lebreton, J. and Furstoss, R. 1996. Flavin-catalyzed Baeyer-Villiger reaction of ketones: Oxidation of cyclobutanones to γ -lactones using hydrogen peroxide. *J Org Chem* **61**, 8-9.
199. Meyer, A., Schmid, A., Held, M., Westphal, A.H., Rothlisberger, M., Kohler, H.P., van Berkel, W.J.H. and Witholt, B. 2002. Changing the substrate reactivity of 2-hydroxybiphenyl 3-monooxygenase from *Pseudomonas azelaica* HBP1 by directed evolution. *J Biol Chem* **277**, 5575-5582.
200. Meyer, A., Wursten, M., Schmid, A., Kohler, H.P. and Witholt, B. 2002. Hydroxylation of indole by laboratory-evolved 2-hydroxybiphenyl 3-monooxygenase. *J Biol Chem* **277**, 34161-34167.
201. Middelhoven, W.J., Coenen, A., Kraakman, B. and Sollewijn Gelpke, M.D. 1992. Degradation of some phenols and hydroxybenzoates by the imperfect ascomycetous yeasts *Candida parapsilosis* and *Arxula adenivorans*: evidence for an operative gentisate pathway. *Antonie Van Leeuwenhoek* **62**, 181-187.
202. Mihovilovic, M.D., Müller, B. and Stanetty, P. 2002. Monooxygenase-mediated Baeyer-Villiger oxidations. *Eur J Org Chem* **2002**, 3711-3730.
203. Mihovilovic, M.D., Kapitan, P., Rydz, J., Rudroff, F., Ogink, F.H. and Fraaije, M.W. 2005. Biooxidation of ketones with a cyclobutanone structural motif by recombinant whole-cells expressing 4-hydroxyacetophenone monooxygenase. *J Mol Catal B: Enzym* **32**, 135-140.
204. Miller, M.A. and Lipscomb, J.D. 1996. Homoprotocatechuate 2,3-dioxygenase from *Brevibacterium fuscum*. A dioxygenase with catalase activity. *J Biol Chem* **271**, 5524-5535.
205. Minor, W., Steczko, J., Bolin, J.T., Otwinowski, Z. and Axelrod, B. 1993. Crystallographic determination of the active site iron and its ligands in soybean lipoxygenase L-1. *Biochemistry* **32**, 6320-6323.
206. Miyamoto, M., Matsumoto, J., Iwaya, T. and Itagaki, E. 1995. Bacterial steroid monooxygenase catalyzing the Baeyer-Villiger oxidation of C-21-ketosteroids from *Rhodococcus rhodochrous*: The isolation and characterization. *Biochim Biophys Acta* **1251**, 115-124.
207. Miyauchi, K., Adachi, Y., Nagata, Y. and Takagi, M. 1999. Cloning and sequencing of a novel meta-cleavage dioxygenase gene whose product is involved in degradation of γ -hexachlorocyclohexane in *Sphingomonas paucimobilis*. *J Bacteriol* **181**, 6712-6719.
208. Moonen, M.J.H., Rietjens, I.M.C.M. and van Berkel, W.J.H. 1999. Purification and some properties of acetophenone monooxygenase. In: *13th International Congress on Flavins and Flavoproteins*, (Eds. S. Ghisla, P. Kroneck, P. Macheroux and H. Sund). Agency for Scientific Publication, Berlin, pp. 375-378.
209. Moonen, M.J.H., Rietjens, I.M.C.M. and van Berkel, W.J.H. 2001. ¹⁹F NMR study on the biological Baeyer-Villiger oxidation of acetophenones. *J Ind Microbiol Biotechnol* **26**, 35-42.
210. Moonen, M.J.H., Westphal, A.H., Rietjens, I.M.C.M. and van Berkel, W.J.H. 2005. Enzymatic Baeyer-Villiger oxidation of benzaldehydes. *Adv Synth Catal*, in press.
211. Morandi, P., Valzasina, B., Colombo, C., Curti, B. and Vanoni, M.A. 2000. Glutamate synthase: Identification of the NADPH-binding site by site-directed mutagenesis. *Biochemistry* **39**, 727-735.
212. Morii, S., Sawamoto, S., Yamauchi, Y., Miyamoto, M., Iwami, M. and Itagaki, E. 1999. Steroid monooxygenase of *Rhodococcus rhodochrous*: Sequencing of the genomic DNA, and hyperexpression, purification, and characterization of the recombinant enzyme. *J Biochem* **126**, 624-631.
213. Mosqueda, G. and Ramos, J.-L. 2000. A set of genes encoding a second toluene efflux system in *Pseudomonas putida* DOT-T1E is linked to the *tod* genes for toluene metabolism. *J Bacteriol* **182**, 937-943.
214. Müller, F., Voordouw, G., van Berkel, W.J.H., Steennis, P.J., Visser, S. and van Rooijen, P.J. 1979. A study of *p*-hydroxybenzoate hydroxylase from *Pseudomonas fluorescens*. Improved purification, relative molecular mass, and amino acid composition. *Eur J Biochem* **101**, 235-244.
215. Müller, F. 1987. Flavin radicals; chemistry and biochemistry. In: *Free Radical Biology & Medicine* **3**. Pergamon Journals, USA, pp. 215-230.
216. Murahashi, S., Ono, S. and Imada, Y. 2002. Asymmetric Baeyer-Villiger reaction with hydrogen peroxide catalyzed by a novel planar-chiral bisflavin. *Angew Chem, Int Ed* **41**, 2366-2368.
217. Murakami, S., Okuno, T., Matsumura, E., Takenaka, S., Shinke, R. and Aoki, K. 1999. Cloning of a gene encoding hydroxyquinol 1,2-dioxygenase that catalyzes both intradiol and extradiol ring cleavage of catechol. *Biosci Biotechnol Biochem* **63**, 859-865.

218. Muraki, T., Taki, M., Hasegawa, Y., Iwaki, H. and Lau, P.C. 2003. Prokaryotic homologs of the eukaryotic 3-hydroxyanthranilate 3,4-dioxygenase and 2-amino-3-carboxymuconate-6-semialdehyde decarboxylase in the 2-nitrobenzoate degradation pathway of *Pseudomonas fluorescens* strain KU-7. *Appl Environ Microbiol* **69**, 1564-1572.
219. Nakagawa, H. and Takeda, Y. 1962. Phenol hydroxylase. *Biochim Biophys Acta* **62**, 423-426.
220. Nakai, C., Nakazawa, T. and Nozaki, M. 1988. Purification and properties of catechol 1,2-dioxygenase (pyrocatechase) from *Pseudomonas putida* mt-2 in comparison with that from *Pseudomonas arvilla* C-1. *Arch Biochem Biophys* **267**, 701-713.
221. Nakamura, S., Ogura, Y., Yano, K., Higashi, N. and Arima, K. 1970. Kinetic studies on the reaction mechanism of *p*-hydroxybenzoate hydroxylase. *Biochemistry* **9**, 3235-3242.
222. Nordlund, I., Powlowski, J. and Shingler, V. 1990. Complete nucleotide sequence and polypeptide analysis of multicomponent phenol hydroxylase from *Pseudomonas* sp. strain CF600. *J Bacteriol* **172**, 6826-6833.
223. Nordlund, I. and Shingler, V. 1990. Nucleotide sequences of the *meta*-cleavage pathway enzymes 2-hydroxymuconic semialdehyde dehydrogenase and 2-hydroxymuconic semialdehyde hydrolase from *Pseudomonas* CF600. *Biochim Biophys Acta* **1049**, 227-230.
224. Norris, D.B. and Trudgill, P.W. 1971. The metabolism of cyclohexanol by *Nocardia globerula* CL1. *Biochem J* **121**, 363-370.
225. Ogata, Y. and Sawaki, Y. 1969. Kinetics of the Baeyer-Villiger reaction of benzaldehydes with perbenzoic acid in aquoorganic solvents. *J Org Chem* **34**, 3985-3991.
226. O'Hagan, D. and B. Harper, D. 1999. Fluorine-containing natural products. *J Fluorine Chem* **100**, 127-133.
227. O'Hagan, D., Schaffrath, C., Cobb, S.L., Hamilton, J.T.G. and Murphy, C.D. 2002. Biosynthesis of an organofluorine molecule. *Nature* **416**, 279.
228. Ohlendorf, D.H., Orville, A.M. and Lipscomb, J.D. 1994. Structure of protocatechuate 3,4-dioxygenase from *Pseudomonas aeruginosa* at 2.15 Å resolution. *J Mol Biol* **244**, 586-608.
229. Ohtsubo, Y., Miyauchi, K., Kanda, K., Hatta, T., Kiyohara, H., Senda, T., Nagata, Y., Mitsui, Y. and Takagi, M. 1999. PcpA, which is involved in the degradation of pentachlorophenol in *Sphingomonas chlorophenolica* ATCC39723, is a novel type of ring-cleavage dioxygenase. *FEBS Lett* **459**, 395-398.
230. Ono, K., Nozaki, M. and Hayaishi, O. 1970. Purification and some properties of protocatechuate 4,5-dioxygenase. *Biochim Biophys Acta* **220**, 224-238.
231. Otto, K., Hofstetter, K., Witholt, B. and Schmid, A. 2002. Purification and characterization of SMO: A novel NADH dependent two-component flavoprotein. In: *14th International Symposium on Flavins and Flavoproteins*, (Eds. R. Perham, S.K. Chapman and N.S. Scrutton). Agency for Scientific Publication, Berlin, pp. 1027-1033.
232. Ougham, H.J., Taylor, D.G. and Trudgill, P.W. 1983. Camphor revisited: Involvement of a unique monooxygenase in metabolism of 2-oxo- Δ^3 -4,5,5-trimethylcyclopentenylacetic acid by *Pseudomonas putida*. *J Bacteriol* **153**, 140-152.
233. Page, R.D.M. 1996. TREEVIEW: An application to display phylogenetic trees on personal computers. *Comput Appl Biosci* **12**, 357-358.
234. Palfey, B.A., Moran, G.R., Entsch, B., Ballou, D.P. and Massey, V. 1999. Substrate recognition by "password" in *p*-hydroxybenzoate hydroxylase. *Biochemistry* **38**, 1153-1158.
235. Palfey, B.A., Basu, R., Frederick, K.K., Entsch, B. and Ballou, D.P. 2002. Role of protein flexibility in the catalytic cycle of *p*-hydroxybenzoate hydroxylase elucidated by the Pro293Ser mutant. *Biochemistry* **41**, 8438-8446.
236. Peelen, S., Rietjens, I.M.C.M., Boersma, M.G. and Vervoort, J. 1995. Conversion of phenol derivatives to hydroxylated products by phenol hydroxylase from *Trichosporon cutaneum*. A comparison of regioselectivity and rate of conversion with calculated molecular orbital substrate characteristics. *Eur J Biochem* **227**, 284-291.
237. Polissi, A. and Harayama, S. 1993. *In vivo* reactivation of catechol 2,3-dioxygenase mediated by a chloroplast-type ferredoxin: a bacterial strategy to expand the substrate specificity of aromatic degradative pathways. *EMBO J* **12**, 3339-3347.
238. Powlowski, J., Ballou, D.P. and Massey, V. 1990. Studies of the oxidative half-reaction of anthranilate hydroxylase (deaminating) with native and modified substrates. *J Biol Chem* **265**, 4969-4975.
239. Prakash, D., Chauhan, A. and Jain, R.K. 1996. Plasmid-encoded degradation of *p*-nitrophenol by *Pseudomonas cepacia*. *Biochem Biophys Res Commun* **224**, 375-381.

240. Que, L.J. and Ho, R.Y.N. 1996. Dioxygen activation by enzymes with mononuclear non-heme iron active sites. *Chemical reviews* **96**, 2607-2624.
241. Reetz, M.T., Brunner, B., Schneider, T., Schulz, F., Clouthier, C.M. and Kayser, M.M. 2004. Directed evolution as a method to create enantioselective cyclohexanone monooxygenases for catalysis in Baeyer-Villiger reactions. *Angew Chem, Int Ed* **43**, 4075-4078.
242. Reetz, M.T., Daligault, F., Brunner, B., Hinrichs, H. and Deege, A. 2004. Directed evolution of cyclohexanone monooxygenases: enantioselective biocatalysts for the oxidation of prochiral thioethers. *Angew Chem, Int Ed* **43**, 4078-4081.
243. Renz, M. and Meunier, B. 1999. 100 years of Baeyer-Villiger oxidations. *Eur J Org Chem* **4**, 737-750.
244. Ridder, L., Mulholland, A.J., Vervoort, J. and Rietjens, I.M.C.M. 1998. Correlation of calculated activation energies with experimental rate constants for an enzyme catalyzed aromatic hydroxylation. *J Am Chem Soc* **120**, 7641-7642.
245. Rieble, S., Joshi, D.K. and Gold, M.H. 1994. Purification and characterization of a 1,2,4-trihydroxybenzene 1,2-dioxygenase from the basidiomycete *Phanerochaete chrysosporium*. *J Bacteriol* **176**, 4838-4844.
246. Rietjens, I.M.C.M., Cnubben, N.H.P., de Jager, P.A., Boersma, M.G. and Vervoort, J. 1993. Application of NMR in biotransformation studies. In: *Toxicology: molecules to morals* (Ed. M.I. Weitzer). Redwood Press, Melksham, United Kingdom, pp. 94-109.
247. Roach, P.L., Clifton, I.J., Fülöp, V., Harlos, K., Barton, G.J., Hajdu, J., Andersson, I., Schofield, C.J. and Baldwin, J.E. 1995. Crystal structure of isopenicillin N synthase is the first from a new structural family of enzymes. *Nature* **375**, 700-704.
248. Roberts, S.M. and Wan, P.W.H. 1998. Enzyme-catalysed Baeyer-Villiger oxidations. *J Mol Catal B: Enzym* **4**, 111-136.
249. Robinson, R.P., Laird, E.R., Donahue, K.M., Lopresti-Morrow, L.L., Mitchell, P.G., Reese, M.R., Reeves, L.M., Rouch, A.I., Stam, E.J. and Yocum, S.A. 2001. Design and synthesis of 2-oxoimidazolidine-4-carboxylic acid hydroxyamides as potent matrix metalloproteinase-13 inhibitors. *Bioorg Med Chem Lett* **11**, 1211-1213.
250. Ronen, Z. and Abeliovich, A. 2000. Anaerobic-aerobic process for microbial degradation of tetrabromobisphenol A. *Appl Environ Microbiol* **66**, 2372-2377.
251. Rosenfeld, J., Capdevielle, J., Guillemot, J.C. and Ferrara, P. 1992. In-gel digestion of proteins for internal sequence analysis after one- or two-dimensional gel electrophoresis. *Anal Biochem* **203**, 173-179.
252. Ryerson, C.C., Ballou, D.P. and Walsh, C. 1982. Mechanistic studies on cyclohexanone oxygenase. *Biochemistry* **21**, 2644-2655.
253. Sali, A. and Blundell, T.L. 1993. Comparative protein modelling by satisfaction of spatial restraints. *J Mol Biol* **234**, 779-815.
254. Sambrook, J., Fritsch, E.F. and Maniatis, T. 1989. *Molecular cloning: A laboratory manual*. Cold Spring Harbor Laboratory Press, New York.
255. Sandford, G. 2000. Organofluorine chemistry. *Philos Transact Ser A Math Phys Eng Sci* **358**, 455-471.
256. Sato, N., Urugami, Y., Nishizaki, T., Takahashi, Y., Sasaki, G., Sugimoto, K., Nonaka, T., Masai, E., Fukuda, M. and Senda, T. 2002. Crystal structures of the reaction intermediate and its homologue of an extradiol-cleaving catecholic dioxygenase. *J Mol Biol* **321**, 621-636.
257. Schmid, A., Hofstetter, K., Feiten, H.-J., Hollmann, F. and Witholt, B. 2001. Integrated biocatalytic synthesis on gram scale: The highly enantioselective preparation of chiral oxiranes with styrene monooxygenase. *Adv Synth Catal* **343**, 732-737.
258. Schmid, A., Vereyken, I., Held, M. and Witholt, B. 2001. Preparative regio- and chemoselective functionalization of hydrocarbons catalyzed by cell free preparations of 2-hydroxybiphenyl 3-monooxygenase. *J Mol Catal B: Enzym* **11**, 455-462.
259. Schmidt, A., Bahr, U. and Karas, M. 2001. Influence of pressure in the first pumping stage on analyte desolvation and fragmentation in nano-ESI MS. *Anal Chem* **73**, 6040-6046.
260. Schmidt, S. and Kirby, G.W. 2001. Dioxygenative cleavage of C-methylated hydroquinones and 2,6-dichlorohydroquinone by *Pseudomonas* sp. HH35. *Biochim Biophys Acta* **1568**, 83-89.
261. Schopfer, L.M., Wessiak, A. and Massey, V. 1991. Interpretation of the spectra observed during oxidation of *p*-hydroxybenzoate hydroxylase reconstituted with modified flavins. *J Biol Chem* **266**, 13080-13085.

262. Schreuder, H.A., Prick, P.A., Wierenga, R.K., Vriend, G., Wilson, K.S., Hol, W.G.J. and Drenth, J. 1989. Crystal structure of the *p*-hydroxybenzoate hydroxylase-substrate complex refined at 1.9 Å resolution. Analysis of the enzyme-substrate and enzyme-product complexes. *J Mol Biol* **208**, 679-696.
263. Schreuder, H.A., Mattevi, A., Obmolova, G., Kalk, K.H., Hol, W.G.J., van der Bolt, F.J.T. and van Berkel, W.J.H. 1994. Crystal structures of wild-type *p*-hydroxybenzoate hydroxylase complexed with 4-aminobenzoate, 2,4-dihydroxybenzoate, and 2-hydroxy-4-aminobenzoate and of the Tyr222Ala mutant complexed with 2-hydroxy-4-aminobenzoate. Evidence for a proton channel and a new binding mode of the flavin ring. *Biochemistry* **33**, 10161-10170.
264. Schwab, J.M. 1981. Stereochemistry of an enzymic Baeyer-Villiger reaction. Application of deuterium NMR. *J Am Chem Soc* **103**, 1876-1878.
265. Schwab, J.M., Li, W. and Thomas, L.P. 1983. Cyclohexanone oxygenase: stereochemistry, enantioselectivity, and regioselectivity of an enzyme-catalyzed Baeyer-Villiger reaction. *J Am Chem Soc* **105**, 4800-4804.
266. Seibold, B., Matthes, M., Eppink, M.H.M., Lingens, F., van Berkel, W.J.H. and Müller, R. 1996. 4-Hydroxybenzoate hydroxylase from *Pseudomonas* sp. CBS3. Purification, characterization, gene cloning, sequence analysis and assignment of structural features determining the coenzyme specificity. *Eur J Biochem* **239**, 469-478.
267. Sheng, D., Ballou, D. and Massey, V. 1999. The intermediates involved in the catalytic reaction of cyclohexanone monooxygenase. In: *13th International Congress on Flavins and Flavoproteins*, (Eds. S. Ghisla, P. Kroneck, P. Macheroux and H. Sund). Agency for Scientific Publication, Berlin, pp. 367-370.
268. Sheng, D., Ballou, D.P. and Massey, V. 2001. Mechanistic studies of cyclohexanone monooxygenase: chemical properties of intermediates involved in catalysis. *Biochemistry* **40**, 11156-11167.
269. Shevchenko, A., Wilm, M., Vorm, O. and Mann, M. 1996. Mass spectrometric sequencing of proteins from silver-stained polyacrylamide gels. *Anal Chem* **68**, 850-858.
270. Shoun, H., Beppu, T. and Arima, K. 1979. On the stable enzyme-substrate complex of *p*-hydroxybenzoate hydroxylase. Evidences for the proton uptake from the substrate. *J Biol Chem* **254**, 899-904.
271. Simpson, H.D., Alphand, V. and Furstoss, R. 2001. Microbiological transformations. 49. Asymmetric biocatalysed Baeyer-Villiger oxidation: improvement using a recombinant *Escherichia coli* whole cell biocatalyst in the presence of an adsorbent resin. *J Mol Catal B: Enzym* **16**, 101-108.
272. Sippl, M.J. 1993. Recognition of errors in three-dimensional structures of proteins. *Proteins* **17**, 355-362.
273. Smith, C.P. and Chater, K.F. 1998. Structure and regulation of controlling sequences for the *Streptomyces coelicolor* glycerol operon. *J Mol Biol* **204**, 569-580.
274. Spain, J.C. and Gibson, D.T. 1991. Pathway for biodegradation of *p*-nitrophenol in a *Moraxella* sp. *Appl Environ Microbiol* **57**, 812-819.
275. Spain, J.C., Nishino, S.F., Witholt, B., Tan, L.-S. and Duetz, W.A. 2003. Production of 6-phenylacetylene picolinic acid from diphenylacetylene by a toluene-degrading *Acinetobacter* strain. *Appl Environ Microbiol* **69**, 4037-4042.
276. Spector, T. and Massey, V. 1972. Studies on the effector specificity of *p*-hydroxybenzoate hydroxylase from *Pseudomonas fluorescens*. *J Biol Chem* **247**, 4679-4687.
277. Spence, E.L., Kawamukai, M., Sanvoisin, J., Braven, H. and Bugg, T.D. 1996. Catechol dioxygenases from *Escherichia coli* (MhpB) and *Alcaligenes eutrophus* (MpcI): sequence analysis and biochemical properties of a third family of extradiol dioxygenases. *J Bacteriol* **178**, 5249-5256.
278. Staskawicz, B., Dahlbeck, D., Keen, N. and Napoli, C. 1987. Molecular characterization of cloned avirulence genes from race 0 and race 1 of *Pseudomonas syringae* pv. *glycinea*. *J Bacteriol* **169**, 5789-5794.
279. Stehr, M., Diekmann, H., Smau, L., Seth, O., Ghisla, S., Singh, M. and Macheroux, P. 1998. A hydrophobic sequence motif common to N-hydroxylating enzymes. *Trends Biochem Sci* **23**, 56-57.
280. Steiner, R.A., Kalk, K.H. and Dijkstra, B.W. 2002. Anaerobic enzyme-substrate structures provide insight into the reaction mechanism of the copper-dependent quercetin 2,3-dioxygenase. *Proc Natl Acad Sci U S A* **99**, 16625-16630.

281. Stewart, J.D. 1998. Cyclohexanone monooxygenase: A useful reagent for asymmetric Baeyer-Villiger reactions. *Curr Org Chem* **2**, 195-216.
282. Stewart, J.D., Reed, K.W., Martinez, C.A., Zhu, J., Chen, G. and Kayser, M.M. 1998. Recombinant baker's yeast as a whole-cell catalyst for asymmetric Baeyer-Villiger oxidations. *J Am Chem Soc* **120**, 3541-3548.
283. Strukul, G. 1998. Transition metal catalysis in the Baeyer-Villiger oxidation of ketones. *Angew Chem, Int Ed* **37**, 1198-1209.
284. Studier, F.W. and Moffatt, B.A. 1986. Use of bacteriophage T7 RNA polymerase to direct selective high-level expression of cloned genes. *J Mol Biol* **189**, 113-130.
285. Sugimoto, K., Senda, T., Aoshima, H., Masai, E., Fukuda, M. and Mitsui, Y. 1999. Crystal structure of an aromatic ring opening dioxygenase LigAB, a protocatechuate 4,5-dioxygenase, under aerobic conditions. *Structure Fold Des* **7**, 953-965.
286. Suh, J.K., Poulsen, L.L., Ziegler, D.M. and Robertus, J.D. 1999. Lysine 219 participates in NADPH specificity in a flavin-containing monooxygenase from *Saccharomyces cerevisiae*. *Arch Biochem Biophys* **372**, 360-366.
287. Suske, W.A., Held, M., Schmid, A., Fleischmann, T., Wubbolts, M.G. and Kohler, H.P. 1997. Purification and characterization of 2-hydroxybiphenyl 3-monooxygenase, a novel NADH-dependent, FAD-containing aromatic hydroxylase from *Pseudomonas azelaica* HBP1. *J Biol Chem* **272**, 24257-24265.
288. Suske, W.A., van Berkel, W.J.H. and Kohler, H.P. 1999. Catalytic mechanism of 2-hydroxybiphenyl 3-monooxygenase, a flavoprotein from *Pseudomonas azelaica* HBP1. *J Biol Chem* **274**, 33355-33365.
289. Sze, I.S. and Dagley, S. 1984. Properties of salicylate hydroxylase and hydroxyquinol 1,2-dioxygenase purified from *Trichosporon cutaneum*. *J Bacteriol* **159**, 353-359.
290. Tahallah, N., Pinkse, M., Maier, C.S. and Heck, A.J. 2001. The effect of the source pressure on the abundance of ions of noncovalent protein assemblies in an electrospray ionization orthogonal time-of-flight instrument. *Rapid Commun Mass Spectrom* **15**, 596-601.
291. Takenaka, S., Murakami, S., Shinke, R., Hatakeyama, K., Yukawa, H. and Aoki, K. 1997. Novel genes encoding 2-aminophenol 1,6-dioxygenase from *Pseudomonas* species AP-3 growing on 2-aminophenol and catalytic properties of the purified enzyme. *J Biol Chem* **272**, 14727-14732.
292. Takeo, M., Fujii, T., Takenaka, K. and Maeda, Y. 1998. Cloning and sequencing of a gene cluster for the *meta*-cleavage pathway of aniline degradation in *Acinetobacter* sp. strain YAA. *J Ferment Bioeng* **85**, 514-517.
293. Tanaka, A., Terasawa, T., Hagihara, H., Ishibe, N., Sawada, M., Sakuma, Y., Hashimoto, M., Takasugi, H. and Tanaka, H. 1998. Inhibitors of acyl-CoA:cholesterol O-acyltransferase. 3. Discovery of a novel series of N-alkyl-N-[(fluorophenoxy)benzyl]-N'-arylureas with weak toxicological effects on adrenal glands. *J Med Chem* **41**, 4408-4420.
294. Tanner, A. and Hopper, D.J. 2000. Conversion of 4-hydroxyacetophenone into 4-phenyl acetate by a flavin adenine dinucleotide-containing Baeyer-Villiger-type monooxygenase. *J Bacteriol* **182**, 6565-6569.
295. Taylor, D.G. and Trudgill, P.W. 1986. Camphor revisited: Studies of 2,5-diketocamphane 1,2-monooxygenase from *Pseudomonas putida* ATCC 17453. *J Bacteriol* **165**, 489-497.
296. Taylor, M.G. and Massey, V. 1990. Decay of the 4a-hydroxy-FAD intermediate of phenol hydroxylase. *J Biol Chem* **265**, 13687-13694.
297. ten Brink, G.J., Vis, J.M., Arends, I.W. and Sheldon, R.A. 2001. Selenium-catalyzed oxidations with aqueous hydrogen peroxide. 2. Baeyer-Villiger reactions in homogeneous solution. *J Org Chem* **66**, 2429-2433.
298. ten Brink, G.J., Arends, I.W. and Sheldon, R.A. 2004. The Baeyer-Villiger reaction: new developments toward greener procedures. *Chemical reviews* **104**, 4105-4124.
299. Thompson, J.D., Higgins, D.G. and Gibson, T.J. 1994. CLUSTAL W: improving the sensitivity of progressive multiple sequence alignment through sequence weighting, position-specific gap penalties and weight matrix choice. *Nucleic Acids Res* **22**, 4673-4680.
300. Titus, G.P., Mueller, H.A., Burgner, J., Rodriguez De Cordoba, S., Penalva, M.A. and Timm, D.E. 2000. Crystal structure of human homogentisate dioxygenase. *Nat Struct Biol* **7**, 542-546.
301. Tomasek, P.H. and Crawford, R.L. 1986. Initial reactions of xanthone biodegradation by an *Arthrobacter* sp. *J Bacteriol* **167**, 818-827.

302. Tropel, D., Meyer, C., Armengaud, J. and Jouanneau, Y. 2002. Ferredoxin-mediated reactivation of the chlorocatechol 2,3-dioxygenase from *Pseudomonas putida* GJ31. *Arch Microbiol* **177**, 345-351.
303. Turfitt, G.E. 1948. The microbiological degradation of steroids, Part IV. *Biochem J* **42**, 376-383.
304. Uotila, J.S., Kitunen, V.H., Coote, T., Saastamoinen, T., Salkinoja-Salonen, M. and Apajalahti, J.H. 1995. Metabolism of halohydroquinones in *Rhodococcus chlorophenolicus* PCP-1. *Biodegradation* **6**, 119-126.
305. Utkin, I.B., Yakimov, M.M., Matveeva, L.N., Kozlyak, E.I., Rogozhin, I.S., Solomon, Z.G. and Bezborodov, A.M. 1991. Degradation of styrene and ethylbenzene by *Pseudomonas* species Y2. *FEMS Microbiol Lett* **77**, 237-242.
306. Vaalburg, W., Coenen, H.H., Crouzel, C., Elsinga, P.H., Langstrom, B., Lemaire, C. and Meyer, G.J. 1992. Amino acids for the measurement of protein synthesis in vivo by PET. *Int J Rad Appl Instrum [B]* **19**, 227-237.
307. Vallon, O. 2000. New sequence motifs in flavoproteins: Evidence for common ancestry and tools to predict structure. *Proteins* **38**, 95-114.
308. van Berkel, W., Westphal, A., Eschrich, K., Eppink, M. and de Kok, A. 1992. Substitution of Arg214 at the substrate-binding site of *p*-hydroxybenzoate hydroxylase from *Pseudomonas fluorescens*. *Eur J Biochem* **210**, 411-419.
309. van Berkel, W.J.H. and Müller, F. 1989. The temperature and pH dependence of some properties of *p*-hydroxybenzoate hydroxylase from *Pseudomonas fluorescens*. *Eur J Biochem* **179**, 307-314.
310. van Berkel, W.J.H. and Müller, F. 1991. Flavin-dependent monooxygenases with special reference to 4-hydroxybenzoate hydroxylase. In: *Chemistry and biochemistry of flavoenzymes 2*, (Ed. F. Müller). CRC Press, Boca Raton, Florida, pp. 1-29.
311. van Berkel, W.J.H. and van den Tweel, W.J.J. 1991. Purification and characterisation of 3-hydroxyphenylacetate 6-hydroxylase: a novel FAD-dependent monooxygenase from a *Flavobacterium* species. *Eur J Biochem* **201**, 585-592.
312. van Berkel, W.J.H., Westphal, A.H., Eschrich, K., Eppink, M.H.M. and de Kok, A. 1992. Substitution of Arg214 at the substrate-binding site of *p*-hydroxybenzoate hydroxylase from *Pseudomonas fluorescens*. *Eur J Biochem* **210**, 411-419.
313. van Berkel, W.J.H., Eppink, M.H.M., Middelhoven, W.J., Vervoort, J. and Rietjens, I.M.C.M. 1994. Catabolism of 4-hydroxybenzoate in *Candida parapsilosis* proceeds through initial oxidative decarboxylation by a FAD-dependent 4-hydroxybenzoate 1-hydroxylase. *FEMS Microbiol Lett* **121**, 207-215.
314. van Berkel, W.J.H., Eppink, M.H.M. and Schreuder, H.A. 1994. Crystal structure of *p*-hydroxybenzoate hydroxylase reconstituted with the modified FAD present in alcohol oxidase from methylotrophic yeasts: evidence for an arabinoflavin. *Protein Sci* **3**, 2245-2253.
315. van Berkel, W.J.H., Eppink, M.H.M. and Schreuder, H.A. 1999. Coenzyme recognition by flavoprotein aromatic hydroxylases. In: *13th International Congress on Flavins and Flavoproteins*, (Eds. S. Ghisla, P. Kroneck, P. Macheroux and H. Sund). Agency for Scientific Publication, Berlin, pp. 343-349.
316. van den Heuvel, R.H.H., Fraaije, M.W., Lasane, C. and van Berkel, W.J.H. 1998. Regio- and stereospecific conversion of 4-alkylphenols by the covalent flavoprotein vanillyl-alcohol oxidase. *J Bacteriol* **180**, 5646-5651.
317. van den Heuvel, R.H.H., Fraaije, M.W., Ferrer, M., Mattevi, A. and van Berkel, W.J.H. 2000. Inversion of stereospecificity of vanillyl-alcohol oxidase. *Proc Natl Acad Sci U S A* **97**, 9455-9460.
318. van den Heuvel, R.H.H., Fraaije, M.W., Mattevi, A. and van Berkel, W.J.H. 2000. Asp-170 is crucial for the redox properties of vanillyl-alcohol oxidase. *J Biol Chem* **275**, 14799-14808.
319. van den Heuvel, R.H.H., Fraaije, M.W. and van Berkel, W.J.H. 2000. Direction of the reactivity of vanillyl-alcohol oxidase with 4-alkylphenols. *FEBS Lett* **481**, 109-112.
320. van den Heuvel, R.H.H., Laane, C. and van Berkel, W.J.H. 2001. Exploring the biocatalytic potential of vanillyl-alcohol oxidase by site-directed mutagenesis. *Adv Synth Catal* **343**, 515-520.
321. van den Heuvel, R.H.H., Partridge, J., Laane, C., Halling, P.J. and van Berkel, W.J.H. 2001. Tuning of the product spectrum of vanillyl-alcohol oxidase by medium engineering. *FEBS Lett* **503**, 213-216.
322. van der Bolt, F.J.T., van den Heuvel, R.H.H., Vervoort, J. and van Berkel, W.J.H. 1997. ¹⁹F NMR study on the regiospecificity of hydroxylation of tetrafluoro-4-hydroxybenzoate by wild-type and Y385F *p*-hydroxybenzoate hydroxylase: evidence for a consecutive oxygenolytic dehalogenation mechanism. *Biochemistry* **36**, 14192-14201.

323. van der Werf, M.J. 2000. Purification and characterization of a Baeyer-Villiger monooxygenase from *Rhodococcus erythropolis* DCL14 involved in three different monocyclic monoterpene degradation pathways. *Biochem J* **347**, 693-701.
324. Vervoort, J., de Jager, P.A., Steenbergen, J. and Rietjens, I.M.C.M. 1990. Development of a ¹⁹F-n.m.r. method for studies on the *in vivo* and *in vitro* metabolism of 2-fluoroaniline. *Xenobiotica* **20**, 657-670.
325. Vervoort, J., Rietjens, I.M.C.M., van Berkel, W.J.H. and Veeger, C. 1992. Frontier orbital study on the 4-hydroxybenzoate-3-hydroxylase-dependent activity with benzoate derivatives. *Eur J Biochem* **206**, 479-484.
326. Vetting, M.W., D'Argenio, D.A., Ornston, L.N. and Ohlendorf, D.H. 2000. Structure of *Acinetobacter* strain ADP1 protocatechuate 3,4-dioxygenase at 2.2 Å resolution: implications for the mechanism of an intradiol dioxygenase. *Biochemistry* **39**, 7943-7955.
327. Vetting, M.W. and Ohlendorf, D.H. 2000. The 1.8 Å crystal structure of catechol 1,2-dioxygenase reveals a novel hydrophobic helical zipper as a subunit linker. *Structure Fold Des* **8**, 429-440.
328. Vetting, M.W., Wackett, L.P., Que, L., Jr., Lipscomb, J.D. and Ohlendorf, D.H. 2004. Crystallographic comparison of manganese- and iron-dependent homoprotocatechuate 2,3-dioxygenases. *J Bacteriol* **186**, 1945-1958.
329. Vollmer, M.D., Stadler-Fritzsche, K. and Schlömann, M. 1993. Conversion of 2-chloromaleylacetate in *Alcaligenes eutrophus* JMP134. *Arch Microbiol* **159**, 182-188.
330. Vrieling, A., Lloyd, L.F. and Blow, D.M. 1991. Crystal structure of cholesterol oxidase from *Brevibacterium sterolicum* refined at 1.8 Å resolution. *J Mol Biol* **219**, 533-554.
331. Walsh, C.T. and Chen, Y.-C.J. 1988. Enzymatische Baeyer-Villiger-Oxidationen durch flavinabhängige Monooxygenasen. *Angew Chem* **100**, 342-352.
332. Walton, A.Z. and Stewart, J.D. 2002. An efficient enzymatic Baeyer-Villiger oxidation by engineered *Escherichia coli* cells under non-growing conditions. *Biotechnol Prog* **18**, 262-268.
333. Wang, J., Ortiz-Maldonado, M., Entsch, B., Massey, V., Ballou, D. and Gatti, D.L. 2002. Protein and ligand dynamics in 4-hydroxybenzoate hydroxylase. *Proc Natl Acad Sci U S A* **99**, 608-613.
334. Weber, H., Braunegg, G., de Raadt, A., Feichtenhofer, S., Griengl, H., Lübke, K., Klingler, M.F., Kreiner, M. and Lehmann, A. 1998. Microbial hydroxylation of benzoxazoles containing fluorine atoms in the aromatic ring – tracing of the products by ¹⁹F NMR. *J Mol Catal B: Enzym* **5**, 191-198.
335. Weber, K. and Osborn, M. 1969. The reliability of molecular weight determinations by dodecyl sulfate-polyacrylamide gel electrophoresis. *J Biol Chem* **244**, 4406-4412.
336. Wessiak, A., Schopfer, L.M. and Massey, V. 1984. pH Dependence of the reoxidation of *p*-hydroxybenzoate hydroxylase 2,4-dihydroxybenzoate complex. *J Biol Chem* **259**, 12547-12556.
337. Westphal, A.H. and de Kok, A. 1988. Lipoamide dehydrogenase from *Azotobacter vinelandii*. Molecular cloning, organization and sequence analysis of the gene. *Eur J Biochem* **172**, 299-305.
338. Westphal, A.H., Kirchner, U., Müller, R., van den Heuvel, R.H.H. and van Berkel, W.J.H. 2002. The flavin reductase component of phenol hydroxylase from *Bacillus thermoglucosidasius* A7. In: *14th International Symposium on Flavins and Flavoproteins*, (Eds. R. Perham, S.K. Chapman and N.S. Scrutton). Agency for Scientific Publication, Berlin, pp. 1047-1052.
339. Whiting, A.K., Boldt, Y.R., Hendrich, M.P., Wackett, L.P. and Que, L., Jr. 1996. Manganese(II)-dependent extradiol-cleaving catechol dioxygenase from *Arthrobacter globiformis* CM-2. *Biochemistry* **35**, 160-170.
340. Wierenga, R.K., de Jong, R.J., Kalk, K.H., Hol, W.G.J. and Drenth, J. 1979. Crystal structure of *p*-hydroxybenzoate hydroxylase. *J Mol Biol* **131**, 55-73.
341. Wierenga, R.K., Drenth, J. and Schulz, G.E. 1983. Comparison of the three-dimensional protein and nucleotide structure of the FAD-binding domain of *p*-hydroxybenzoate hydroxylase with the FAD- as well as NADPH-binding domains of glutathione reductase. *J Mol Biol* **167**, 725-739.
342. Wierenga, R.K., Terpstra, P. and Hol, W.G.J. 1986. Prediction of the occurrence of the ADP-binding βαβ-fold in proteins, using an amino acid sequence fingerprint. *J Mol Biol* **187**, 101-107.
343. Willetts, A. 1997. Structural studies and synthetic applications of Baeyer-Villiger monooxygenases. *Trends Biotechnol* **15**, 55-62.
344. Wolgel, S.A., Dege, J.E., Perkins-Olson, P.E., Jaurez-Garcia, C.H., Crawford, R.L., Munck, E. and Lipscomb, J.D. 1993. Purification and characterization of protocatechuate 2,3-dioxygenase from *Bacillus macerans*: a new extradiol catecholic dioxygenase. *J Bacteriol* **175**, 4414-4426.
345. Xu, D., Ballou, D.P. and Massey, V. 2001. Studies of the mechanism of phenol hydroxylase: mutants Tyr289Phe, Asp54Asn, and Arg281Met. *Biochemistry* **40**, 12369-12378.

346. Xu, L., Resing, K., Lawson, S.L., Babbitt, P.C. and Copley, S.D. 1999. Evidence that *pcpA* encodes 2,6-dichlorohydroquinone dioxygenase, the ring cleavage enzyme required for pentachlorophenol degradation in *Sphingomonas chlorophenolica* strain ATCC 39723. *Biochemistry* **38**, 7659-7669.
347. Xu, X.H., Yao, G.M., Li, Y.M., Lu, J.H., Lin, C.J., Wang, X. and Kong, C.H. 2003. 5-Fluorouracil derivatives from the sponge *Phakellia fusca*. *J Nat Prod* **66**, 285-288.
348. Xu, Y., Chen, M., Zhang, W. and Lin, M. 2003. Genetic organization of genes encoding phenol hydroxylase, benzoate 1,2-dioxygenase alpha subunit and its regulatory proteins in *Acinetobacter calcoaceticus* PHEA-2. *Curr Microbiol* **46**, 235-240.
349. Xun, L., Bohuslavsek, J. and Cai, M. 1999. Characterization of 2,6-dichloro-*p*-hydroquinone 1,2-dioxygenase (PcpA) of *Sphingomonas chlorophenolica* ATCC 39723. *Biochem Biophys Res Commun* **266**, 322-325.
350. Xun, L.Y. and Sandvik, E.R. 2000. Characterization of 4-hydroxyphenylacetate 3-hydroxylase (HpaB) of *Escherichia coli* as a reduced flavin adenine dinucleotide-utilizing monooxygenase. *Appl Environ Microbiol* **66**, 481-486.
351. Zocher, F., Krebsfänger, N., Yoo, O.J. and Bornscheuer, U.T. 1998. Enantioselectivity of a recombinant esterase from *Pseudomonas fluorescens*. *J Mol Catal B: Enzym* **5**, 199-202.
352. Zylstra, G.J., Bang, S.-W., Newman, L.M. and Perry, L.L. 2000. Microbial degradation of mononitrophenols and mononitrobenzoates. In: *Biodegradation of nitroaromatic compounds and explosives* (Eds. J.C. Spain, J.B. Hughes and H.-J. Knackmuss). CRC Press, Boca Raton, pp. 145-160.

Summary

This thesis deals with the oxidative enzymes involved in the degradation of 4-hydroxyacetophenone in the bacterium *Pseudomonas fluorescens* ACB. Acetophenones are aromatic compounds appearing in the environment as degradation products of industrial compounds as for instance the flame-retardant tetrabromobisphenol A. There is not much known about the properties of the oxidative enzymes involved in the degradation of acetophenones. For *P. fluorescens* ACB it was reported that 4-hydroxyacetophenone is converted via a Baeyer-Villiger type of reaction to hydroquinone. However, the enzyme(s) involved in this reaction and the further degradation of hydroquinone remained elusive.

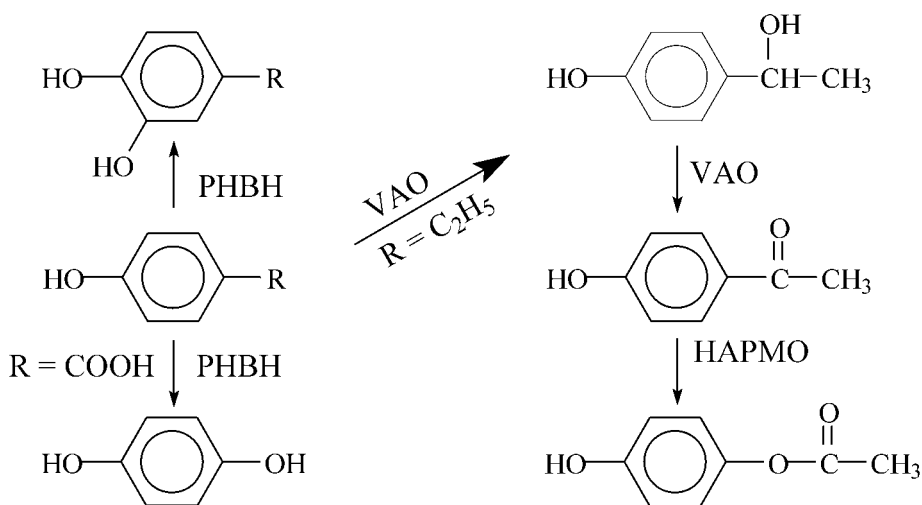
The PhD-project described in this thesis was part of the NWO-program “Procesvernieuwing voor een Schoner Milieu” (“Improvement of Processes for a Cleaner Environment”). The first aim of the research was to develop a biocatalyst for the Baeyer-Villiger oxidation of aromatic compounds. The Baeyer-Villiger reaction converts ketones to esters or lactones and offers many interesting possibilities for the production of valuable fine chemicals and pharmaceuticals. A biological Baeyer-Villiger catalyst is often regio- and/or enantioselective and uses molecular oxygen as clean oxidant. The use of such biocatalyst might present an alternative for chemical Baeyer-Villiger reactions, which make use of environmentally unfriendly and often explosive peroxides. The second aim was to explore the degradation pathway of 4-hydroxyacetophenone in *P. fluorescens* ACB with special focus on the degradation of hydroquinone.

Flavin containing oxygenases and oxidases

The Baeyer-Villiger monooxygenase described in this thesis is capable of converting 4-hydroxyacetophenones into the corresponding phenyl acetate. This enzyme contains a FAD (flavin adenine dinucleotide) cofactor as redox-active prosthetic group. FAD originates from vitamin B2 (riboflavin) and colors the enzyme yellow. Flavin serves also as a cofactor in other oxidative enzymes acting on phenolic compounds. **Chapter 2** gives an overview of the structure and function of these proteins (flavoproteins). Oxidative flavoproteins can be distinguished in three classes:

- Aromatic hydroxylases. Many enzymes of this class are known and they function often (regio)selective. The model enzyme of this class is *p*-hydroxybenzoate hydroxylase (PHBH).
- Baeyer-Villiger monooxygenases. Until now only one enzyme acting on phenols is known in this class: 4-hydroxyacetophenones monooxygenase (HAPMO), described in this thesis. HAPMO has a broad substrate specificity.
- Oxidases. Only a few oxidases act on phenols. They have a broad substrate specificity. Model enzyme of this class is vanillyl-alcohol oxidase (VAO). VAO shows besides oxidation, oxidative deamination, oxidative demethylation and dehydrogenation, also enantioselective hydroxylation.

The following scheme depicts the oxidative reactions of PHBH, HAPMO and VAO:



Flavoenzyme catalyzed oxidative reactions of phenolic compounds

4-Hydroxyacetophenone monooxygenase (HAPMO)

Chapter 3 of this thesis describes the characterization of 4-hydroxyacetophenone monooxygenase (HAPMO) from *P. fluorescens* ACB. As indicated above, HAPMO is a flavoprotein that catalyzes the Baeyer-Villiger oxidation of acetophenones to the corresponding phenyl acetates. NADPH is needed as co-enzyme.

Chapter 3 first describes the cultivation of *P. fluorescens* ACB in a 200 liter batch fermentor. In this cultivation process, 4-hydroxyacetophenone is used as sole carbon source to induce the production of HAPMO and accompanying enzymes. After harvesting of the bacteria and removal of the cell walls, HAPMO was purified from the cell extract. HAPMO appeared to be a homodimer of 140 kDa, harboring in each subunit a tightly bound FAD. The esterase (4-hydroxyphenyl acetate hydrolase) responsible for the conversion of 4-hydroxyphenyl acetate to hydroquinone was partially purified.

After determination of the N-terminal protein sequences of HAPMO and 4-hydroxyphenyl acetate hydrolase, primers are designed to screen a library of genomic DNA of *P. fluorescens* ACB. Following this strategy, gene sequences and thereby amino acid sequences of HAPMO and 4-hydroxyphenyl acetate hydrolase were determined. Subsequently the HAPMO gene was cloned and expressed in *E. coli*. HAPMO is composed of 640 amino acids and has a mass of 71,844 Da per monomer. The amino acid sequence of this enzyme appeared to be related to other Baeyer-Villiger monooxygenases, including cyclohexanone monooxygenase and steroid monooxygenase. However HAPMO was found to contain a unique additional N-terminal domain of about 135 amino acids. The precise function of this domain is still unclear.

HAPMO catalyzes the conversion of a wide range of acetophenones. 4-Aminoacetophenone is the best substrate. HAPMO is also highly active with 4-hydroxypropiophenone and 4-hydroxybenzaldehyde. The substrate specificity and biocatalytic features of HAPMO are further described in **Chapter 4** and **5**.

Biological Baeyer-Villiger oxidation of fluorinated acetophenones

Chapter 4 of this thesis describes the conversion of fluorinated acetophenones by whole cells of *P. fluorescens* ACB and by purified HAPMO. Product analysis was performed by ^{19}F NMR. This technique has the advantage that no purification of products is required, because the natural abundance of the ^{19}F isotope is 100% and biological samples contain no fluorinated endogenous compounds. In view of the production of valuable acylcatechols, special attention is given in this chapter to the Baeyer-Villiger oxidation of 4-fluoro-2-hydroxyacetophenone. Acylcatechols can be used as building blocks for the chemical and especially the pharmaceutical industry. It turned out that the use of purified HAPMO is essential for the production of 4-fluoro-2-hydroxyphenyl acetate (4-fluoroacylcatechol). This is because *P. fluorescens* ACB contains an esterase (4-hydroxyphenyl acetate hydrolase) that rapidly converts phenyl acetates to the corresponding phenols (see also Chapter 3). 4-Fluoro-2-hydroxyphenyl acetate appeared to be a rather unstable compound. At pH 8.0, the pH optimum of HAPMO, this ester is spontaneously hydrolyzed to 4-fluorocatechol. The stability of 4-fluoro-2-hydroxyphenyl acetate could be improved by performing the HAPMO-mediated conversion of 4-fluoro-2-hydroxyacetophenone at pH 6. Although the enzyme is less active at this pH, the ester could be obtained in high yield.

Enzymatic Baeyer-Villiger oxidation of benzaldehydes

Fluorophenols are interesting building blocks for the production of medicines, like enzyme inhibitors and receptor-antagonists. ^{18}F labeled phenols for instance are valuable starting compounds for the production of radiochemicals that can be used to follow amino acid metabolism and the protein synthesis *in vivo*. Phenols can be produced by the Baeyer-Villiger oxidation of benzaldehydes. This is especially true for benzaldehydes having electron-donating substituents. However, the chemical oxidation of fluorobenzaldehydes mainly results in the production of fluorobenzoic acids.

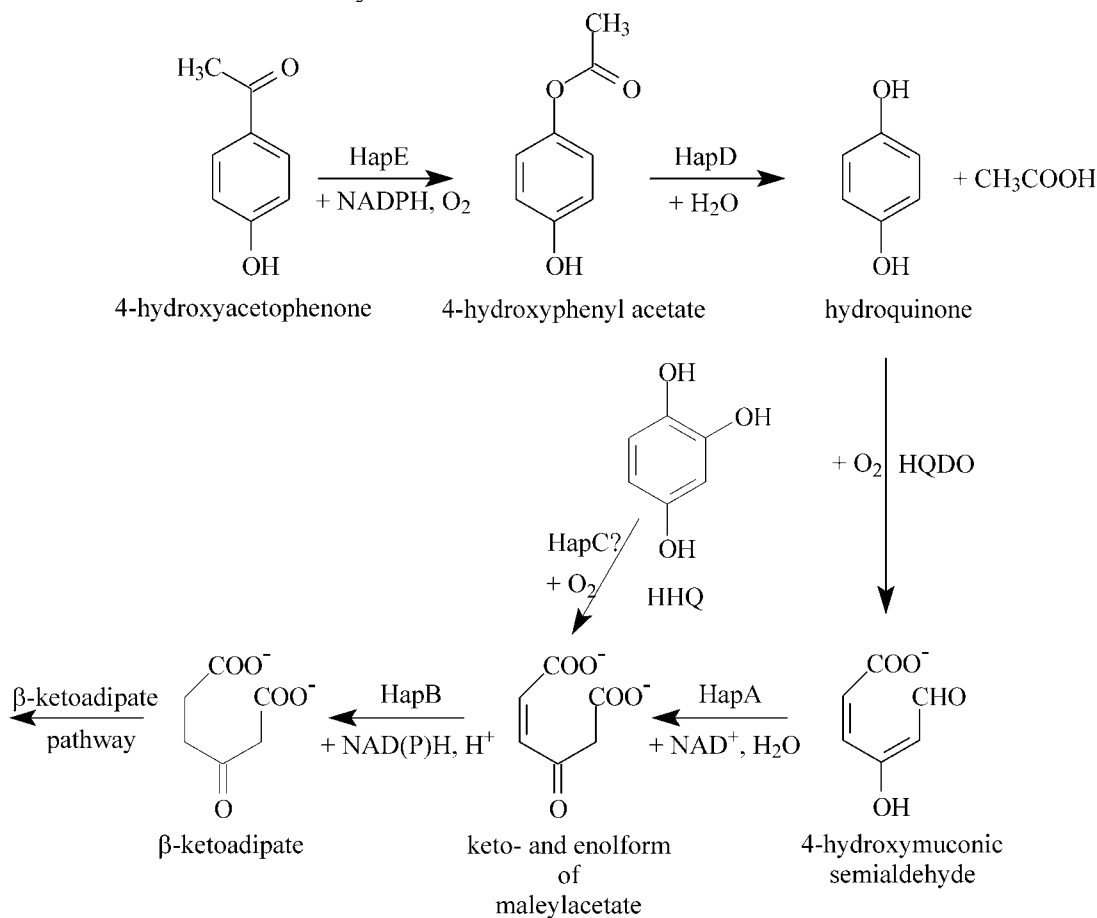
In **Chapter 5**, the enzymatic oxidation of (fluoro)benzaldehydes was addressed. For this we used HAPMO as a clean and selective Baeyer-Villiger biocatalyst. HAPMO is active with a wide range of benzaldehydes. The enzymatic reactions with 4-amino- and 4-hydroxybenzaldehyde were inhibited at high substrate concentrations. Fluorinated benzaldehydes were more slowly converted but are not prone to substrate inhibition. Interestingly, HAPMO converts fluorobenzaldehydes almost exclusively to fluorophenols. This preference for the production of fluorophenols instead of fluorobenzoic acids deviates from the chemical reaction and suggests that the active site of HAPMO directs the selectivity of the reaction by facilitating the migration of the aromatic ring in the initially formed oxygenated product intermediate.

Degradation pathway of 4-hydroxyacetophenone in *Pseudomonas fluorescens* ACB

Chapter 6 describes the degradation of 4-hydroxyacetophenone to β -keto adipate by *P. fluorescens* ACB (see scheme below). As described above, the first enzyme of this pathway is catalyzed by HAPMO (HapE). The formed 4-hydroxyphenyl acetate is then hydrolyzed by an esterase (HapD) to hydroquinone (1,4-dihydroxybenzene). This compound can theoretically be converted in two different ways. The first possibility is via hydroxylation to 1,2,4-trihydroxybenzene (HHQ) followed by ring fission by a

Summary

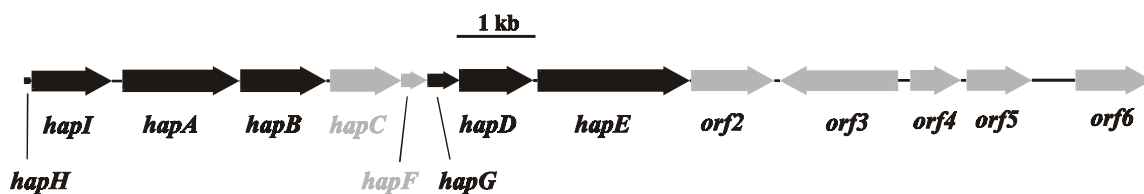
1,2,4-trihydroxybenzene dioxygenase (HHQ 1,2-dioxygenase) producing maleylacetate. However, whole cells of *P. fluorescens* ACB convert 4-fluoroacetophenone to 4-fluorophenol as end product (**Chapter 4**). This suggests that *P. fluorescens* ACB does not possess phenol hydroxylase activity and thereby can not catalyze the conversion of hydroquinone to 1,2,4-trihydroxybenzene. The second possibility is direct ring fission of hydroquinone to 4-hydroxymuconic semialdehyde by a hydroquinone dioxygenase. LC-MS data in **Chapter 6** clearly show that the latter pathway is operative in *P. fluorescens* ACB. Furthermore, ^{19}F NMR studies revealed that 2,3-difluoro-4-hydroxymuconic semialdehyde, produced from 2,3-difluorohydroquinone, is converted to difluorinated maleylacetate.



The degradation pathway of 4-hydroxyacetophenone in *Pseudomonas fluorescens* ACB

Gene cluster of 4-hydroxyacetophenone (HAP) degradation

Chapter 6 also describes also the gene cluster (*hapABCFGDE*) that encodes the enzymes involved in this degradation pathway. Beyond the genes encoding HAPMO (*hapE*) and 4-hydroxyphenyl acetate hydrolase (*hapD*) (see **Chapter 3**), genes coding for 4-hydroxymuconic semialdehyde dehydrogenase (*hapA*) and maleylacetate reductase (*hapB*) could be identified:



The *hap*(*HIABCFGDE*) gene cluster of *P. fluorescens* ACB involved in the degradation of 4-hydroxyacetophenone

Upstream of *hapA* an open reading frame (*hapI* = *orf1*) was found with unknown function. Downstream of *hapE* some open reading frames (*orf2-orf6*) were found that are not involved in the degradation pathway of 4-hydroxyacetophenone. In between *hapB* and *hapD* three genes are present (*hapCFG*) with indistinct function. Especially *hapC* drew our attention, because the enzyme encoded by this gene could be responsible for ring fission of hydroquinone. However, sequence analysis and modeling of the HapC protein indicated that this is very unlikely. The HapC protein (theoretical mass 32,159 Da) appeared to have the structural characteristics of iron(III)-dependent intradiol dioxygenases. These enzymes consist of two identical subunits that contain two strictly conserved tyrosines and histidines for iron ligation per subunit. HapC resembles HHQ 1,2-dioxygenases and is therefore probably not active with hydroquinone.

Sequences of hydroquinone dioxygenases are only known for LinE and PcpA, which use respectively 2,6-dichloro- and 2-chlorohydroquinone as physiological substrate. These enzymes are also capable of converting hydroquinone to 4-hydroxymuconic semialdehyde, but have a completely different amino acid sequence as HapC. LinE and PcpA contain per subunit two conserved histidines and a carboxylate group in the active site and belong to the family of iron(II)-dependent extradiol dioxygenases. This supports that HapC is not responsible for the ring fission of hydroquinone and thus is not involved in the degradation pathway of 4-hydroxyacetophenone. Therefore, it was decided to isolate the enzyme, responsible for the ring fission of hydroquinone, directly from *P. fluorescens* ACB. This ‘reverse genetics’ strategy should clarify the ‘missing link’ in the degradation of 4-hydroxyacetophenone.

Hydroquinone dioxygenase (HQDO)

Purification of HQDO was strongly hampered by the instability of the enzyme. Addition of possible protecting compounds like protease inhibitors, anti-oxidants and ‘iron pills’ showed no improvement (**Chapter 7**). A breakthrough in HQDO research occurred when it was found that the enzyme could be stabilized by the addition of the inhibitor 4-hydroxybenzoate. This aromatic compound binds in the HQDO active site, but is not converted to a ring splitted product. This stabilization by 4-hydroxybenzoate led to the isolation of an almost pure enzyme and a strong improvement of the enzyme yield. Characterization of the substrate specificity showed that HQDO converts a wide range of hydroquinones including chloro-, bromo-, fluoro-, methyl- and methoxyhydroquinone. The conversion is regioselective. The enzyme has a preference for ring opening of difluorohydroquinone in between a hydroxylated (C-OH) and a hydrogenated (C-H) carbon atom. On the other hand, monofluorohydroquinone shows ring fission between C-OH and C-F. Besides 4-hydroxybenzoate, many other phenolic compounds inhibit the enzyme activity of HQDO, among them hydroxyhydroquinone

(HHQ) and tetrafluorohydroquinone. Inhibition studies with specific ‘metal detectors’ showed that the enzyme activity is dependent on iron(II) ions.

Native HQDO consists of two subunits and is a $\alpha_2\beta_2$ heterotetramer with a mass of 112.4 kDa on the basis of ESI-MS measurements. The subunits have a mass of respectively 17.7 and 38.3 kDa for the α - and the β -subunit. The amino acid sequence was obtained by N-terminal sequence and MALDI-ToF-ToF analysis. The active site and the iron(II) binding site are in the β -subunit as shown by ESI-MS analysis.

On the basis of the amino acid sequences of tryptic peptides, it was established that the β -subunit of HQDO is encoded by the *hapI* gene of the *hap* gene cluster. Furthermore, genetic information of other organisms indicated that upstream *hapI*, a gene is present that encodes the α -subunit of HQDO (*hapH*).

HQDO (HapHI) constitutes a new type of enzyme in the iron(II)-dependent dioxygenase family. Until now only 5 gene clusters are known that possess one or two of the *hapHI* genes. Furthermore HQDO is not closely related to the above described chlorohydroquinone dioxygenases.

The biochemical characterization of HQDO and the identification of the *hapHI* genes unambiguously show that HapC is not involved in the degradation of 4-hydroxyacetophenone. HapC presumably is necessary in another degradation pathway for the ring fission of HHQ. In several other microorganisms, a gene comparable with *hapG* codes for a ferredoxin necessary for the reactivation of iron(II)-dependent catechol dioxygenases. As HQDO easily loses its metal cofactor, this suggests a possible role for the protein encoded by *hapG*.

Conclusions

- *Pseudomonas fluorescens* ACB is capable of degrading 4-hydroxyacetophenone to β -keto adipate by means of 5 enzymes. Two of these enzymes use molecular oxygen for catalysis: 4-hydroxyacetophenone monooxygenase (HAPMO) and hydroquinone dioxygenase (HQDO).
- HAPMO is an NADPH-dependent FAD-containing enzyme, consisting of two identical subunits of 72 kDa. HAPMO is a type I Baeyer-Villiger monooxygenase with a unique N-terminal domain with unknown function. HAPMO has a broad substrate specificity. Besides aromatic ketones, benzaldehydes are good substrates. Produced aromatic esters are spontaneously hydrolyzed to the corresponding phenols at high pH.
- HQDO is a novel iron(II) dependent dioxygenase converting hydroquinone to 4-hydroxymuconic semialdehyde. HQDO is a $\alpha_2\beta_2$ heterotetramer of 112.4 kDa, with the active site presumably located in the β -subunit. Binding of the competitive inhibitor 4-hydroxybenzoate protects HQDO against thermal inactivation. HQDO has a broad substrate specificity. Besides from hydroquinone, HQDO catalyzes the oxidative ring fission of chloro-, bromo-, fluoro-, methyl-, and methoxyhydroquinone. Ring fission is regioselective. HQDO is not active with 1,2,4-trihydroxybenzene (HHQ) and catechol. HQDO from *P. fluorescens* ACB is the first HQDO with a known sequence.
- Genes encoding the enzymes involved in the 4-hydroxyacetophenone metabolism in *P. fluorescens* ACB are positioned in the *hap* gene cluster. These enzymes are: HAPMO (HapE), 4-hydroxyphenyl acetate hydrolase (HapD), HQDO (HapHI), 4-hydroxymuconic semialdehyde dehydrogenase (HapA), and maleylacetate

Summary

reductase (HapB). The *hapC* gene, which is embedded in the *hap* gene cluster, is not involved in the degradation of 4-hydroxyacetophenone, but codes for an enzyme, that is related to the family of iron(III)-dependent intradiol dioxygenases on the base of the protein sequence. The *hapC* gene codes presumably for a HHQ 1,2-dioxygenase. This gene probably persisted as a remnant during evolution or is involved in another degradation pathway.

SAMENVATTING

De natuur heeft diverse oplossingen bedacht om chemische stoffen af te breken. In de bodem bv. zijn bacteriën, schimmels en gisten verantwoordelijk voor de afbraak van plantenmateriaal. Deze micro-organismen zijn ook in staat om allerlei milieuvriendelijke, door de mens, geproduceerde chemicaliën zoals pesticiden en herbiciden af te breken tot minder toxische verbindingen. Zij maken daarbij gebruik van enzymen. Enzymen zijn eiwitten met een actief centrum die omzettingen van stof A naar stof B versnellen (= katalyseren). Vele enzymen uit aërobe micro-organismen maken bij de afbraak van chemische stoffen gebruik van zuurstof uit de lucht. Hierbij kan er één zuurstofatoom van moleculaire zuurstof in het substraat ingebouwd worden door een mono-oxygenase of kunnen er twee zuurstofatomen ingebouwd worden door een dioxygenase. Vele dioxygenases zijn op deze manier in staat om de benzeenring van aromatische verbindingen open te breken.

Acetofenonen zijn aromatische verbindingen die in het milieu voorkomen als afbraakproducten van industriële chemicaliën zoals bijvoorbeeld de vlamvertrager tetrabromobisfenol A. In dit proefschrift worden de enzymen beschreven die betrokken zijn bij de afbraak van 4-hydroxyacetofenon door de bacterie *Pseudomonas fluorescens* ACB. Een nieuw type mono-oxygenase en een nieuw type dioxygenase katalyseren respectievelijk de eerste en derde stap in de afbraak van 4-hydroxyacetofenon. 4-Hydroxyacetofenon wordt zo uit de natuur verwijderd en wordt uiteindelijk omgezet tot CO₂ en H₂O. Beide oxidatieve enzymen katalyseren ook de omzetting van een reeks andere verbindingen (substraatanalogen). Onderzoek naar de biochemische, structurele en biokatalytische eigenschappen van deze enzymen kan er daarom toe bijdragen dat er op een milieuvriendelijke wijze nieuwe chemicaliën gemaakt kunnen worden, die een opstap vormen voor de productie van belangrijke verbindingen voor bijvoorbeeld de farmaceutische industrie.

Het OIO-project beschreven in dit proefschrift was onderdeel van het NWO-programma Procesvernieuwing voor een Schoner Milieu. Het eerste doel van het onderzoek was een biokatalysator ontwikkelen voor de Baeyer-Villiger oxidatie van aromatische verbindingen. De Baeyer-Villiger reactie kan m.b.v een peroxide een keton omzetten naar een ester of lacton en biedt vele interessante mogelijkheden voor de productie van waardevolle fijnchemicaliën en farmaceutische verbindingen. Een biologische Baeyer-Villiger katalysator werkt vaak regio- en/of enantioselectief en gebruikt moleculaire zuurstof als schone oxidant, zodat er in tegenstelling tot de chemische reactie geen gebruik hoeft te worden gemaakt van milieuvriendelijke en vaak explosieve peroxides. Het tweede doel was de afbraakroute van 4-hydroxyacetophenone in *P. fluorescens* ACB op te helderen met speciale aandacht voor de afbraak van hydrochinon.

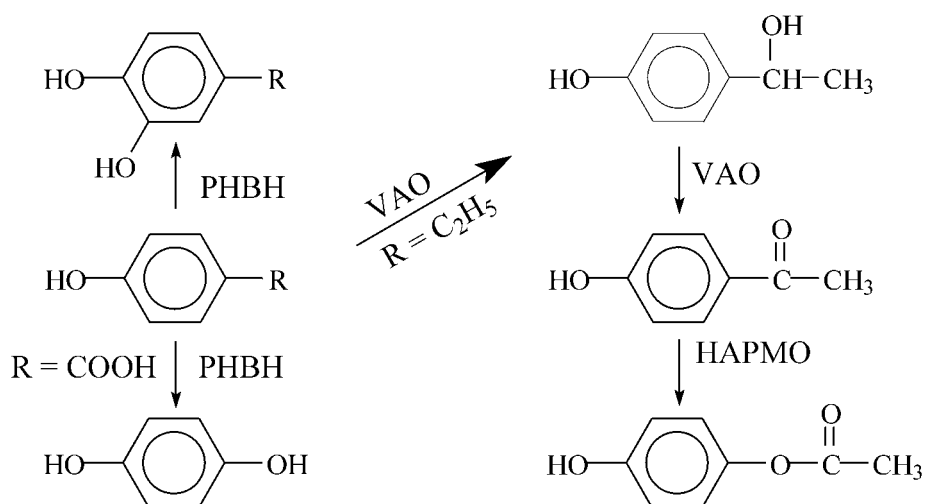
Flavine bevattende oxygenases en oxidases

De in dit proefschrift beschreven Baeyer-Villiger mono-oxygenase, verantwoordelijk voor de omzetting van 4-hydroxyacetofenon in *P. fluorescens* ACB, bevat een FAD (flavine adenine dinucleotide) cofactor. Deze prosthetische groep komt voort uit vitamine B2 (riboflavine) en geeft het enzym een gele kleur. Flavine wordt als cofactor ook aangetroffen in vele andere oxidatieve enzymen die actief zijn met

fenolische verbindingen. In **hoofdstuk 2** wordt een overzicht gegeven van de functie van deze eiwitten (flavoproteïnen). Hierbij kunnen drie klassen worden onderscheiden:

- Aromatische hydroxylases. Van deze klasse zijn vele enzymen bekend en ze werken vaak zeer (regio)selectief. Het modelenzym van deze klasse is *p*-hydroxybenzoesaat hydroxylase (PHBH).
- Baeyer-Villiger mono-oxygenases. Het enige tot nu toe bekende enzym van deze klasse dat actief is met fenolen betreft het in dit proefschrift beschreven 4-hydroxyacetofenon mono-oxygenase (HAPMO). HAPMO heeft een brede substraatspecificiteit.
- Oxidases. Weinig oxidases zijn actief met fenolen. Ze hebben een brede substraatspecificiteit. Modelenzym van deze klasse is vanillyl-alcohol oxidase (VAO). VAO vertoont naast oxidase, oxidatieve deaminering, oxidatieve demethylering en dehydrogenering ook enantioselectieve hydroxylering.

In het onderstaande schema zijn de oxiderende reacties van PHBH, HAPMO en VAO weergegeven:



Flavoenzym gekatalyseerde oxidatieve reacties met fenolische verbindingen

4-Hydroxyacetofenon mono-oxygenase (HAPMO)

Hoofdstuk 3 van dit proefschrift beschrijft de karakterisering van 4-hydroxyacetofenon mono-oxygenase (HAPMO) uit *P. fluorescens* ACB en de klonering van het HAPMO (*hapE*) gen. Zoals hierboven aangegeven is HAPMO een flavoproteïne die de Baeyer-Villiger oxidatie van acetofenonen katalyseert. Bij deze reactie wordt één zuurstofatoom ingebouwd, afkomstig van moleculaire zuurstof, tussen de benzeenring en de carbonylgroep van het substraat. Verder is voor deze reactie NADPH nodig als co-enzym. Het fysiologisch substraat 4-hydroxyacetofenon wordt door HAPMO geoxideerd tot 4-hydroxyfenyl acetaat.

Allereerst wordt in **hoofdstuk 3** de groei van *P. fluorescens* ACB in een 200 liter batch fermentor beschreven. Omdat bij deze bacteriekweek 4-hydroxyacetofenon wordt gebruikt als enige koolstofbron, wordt de productie van HAPMO en bijbehorende enzymen sterk geïnduceerd. Na het oogsten van de bacteriën en het verwijderen van hun celwand, zijn HAPMO en een hydrolase (verantwoordelijk voor de verdere omzetting van 4-hydroxyfenyl acetaat) gezuiverd uit het celvrije extract. HAPMO blijkt een

homodimeer te zijn van 140 kDa waarbij iedere subunit één stevig gebonden FAD molecuul bevat. Het esterase (4-hydroxyfenyl acetaat hydrolase) verantwoordelijk voor de omzetting van 4-hydroxyfenyl acetaat naar hydrochinon is gedeeltelijk gezuiverd.

Na bepaling van de N-terminale eiwitsequenties van HAPMO en het 4-hydroxyfenyl acetaat hydrolase zijn er primers (stukjes DNA) ontworpen om een bibliotheek te screenen van het *P. fluorescens* ACB genomisch DNA. Via deze strategie zijn de gensequenties en daaruit voortvloeiende aminozuurvolgordes van HAPMO en het esterase bepaald. Vervolgens is het HAPMO gen gekloneerd en in *E. coli* tot expressie gebracht. HAPMO is opgebouwd uit 640 aminozuren en heeft een massa van 71.844 Da per monomeer. De aminozuurvolgorde van dit enzym is verwant met andere Baeyer-Villiger mono-oxygenases zoals cyclohexanon mono-oxygenase en steroïde mono-oxygenase. HAPMO bevat echter een uniek extra N-terminaal domein van ongeveer 135 aminozuren. De precieze functie van dit domein is vooralsnog onduidelijk.

HAPMO katalyseert de omzetting van een breed scala acetofenonen. Van deze verbindingen blijkt 4-aminoacetofenon het beste substraat te zijn. Daarnaast is HAPMO erg actief met 4-hydroxypropiofenon en 4-hydroxybenzaldehyde. De substraatspecificiteit van HAPMO wordt verder beschreven in **hoofdstuk 4** en **5**.

Biologische Baeyer-Villiger oxidatie van gefluorideerde acetofenonen

Hoofdstuk 4 van dit proefschrift beschrijft de omzetting van gefluorideerde acetofenonen door hele cellen van *P. fluorescens* ACB en door gezuiverd HAPMO. Voor de productanalyse is hierbij gebruik gemaakt van ^{19}F NMR. Deze techniek heeft het grote voordeel dat de gevormde producten niet gezuiverd hoeven te worden omdat de natuurlijk aanwezigheid van het ^{19}F isotoop 100% is en omdat biologische monsters geen gefluorideerde endogene verbindingen bevatten. In dit hoofdstuk is de aandacht speciaal gericht op de omzetting van 4-fluoro-2-hydroxyacetofenon, omdat de Baeyer-Villiger oxidatie van 2-hydroxyacetofenonen leidt tot waardevolle acylcatecholen. Acylcatecholen kunnen als bouwstenen dienen voor de chemische en met name de farmaceutische industrie. Het gebruik van gezuiverd HAPMO bleek essentieel voor de vorming van 4-fluoro-2-hydroxyfenyl acetaat, omdat in de bacteriecel deze verbinding onmiddellijk wordt gehydrolyseerd door het aanwezige esterase (4-hydroxyfenyl acetaat hydrolase) (zie ook Hoofdstuk 3). Verder bleek het enzymatisch gevormde 4-fluoro-2-hydroxyfenyl acetaat niet stabiel te zijn. Rond het pH optimum van HAPMO (pH 8) hydrolyseert deze ester spontaan tot 4-fluorocatechol. De stabiliteit van het 4-fluoro-2-hydroxyfenyl acetaat kon sterk verbeterd worden door de enzymatische reactie uit te voeren bij pH 6. Weliswaar is het enzym dan katalytisch minder actief, maar de ester kan dan met hoge opbrengst verkregen worden.

Enzymatische Baeyer-Villiger oxidatie van benzaldehydes

De Baeyer-Villiger oxidatie van (gefluorideerde) benzaldehydes is beschreven in **hoofdstuk 5**. De chemische Baeyer-Villiger oxidatie van benzaldehydes leidt tot de vorming van een mengsel van benzoëzuur en fenol. Uitgaande van gefluorideerde benzaldehydes kunnen zo fluorfenolen geproduceerd worden, die als bouwsteen dienen voor de productie van geneesmiddelen. Hierbij valt te denken aan enzymremmers en receptor-antagonisten. Verder zijn ^{18}F gelabelde fenolen met name geschikt voor de

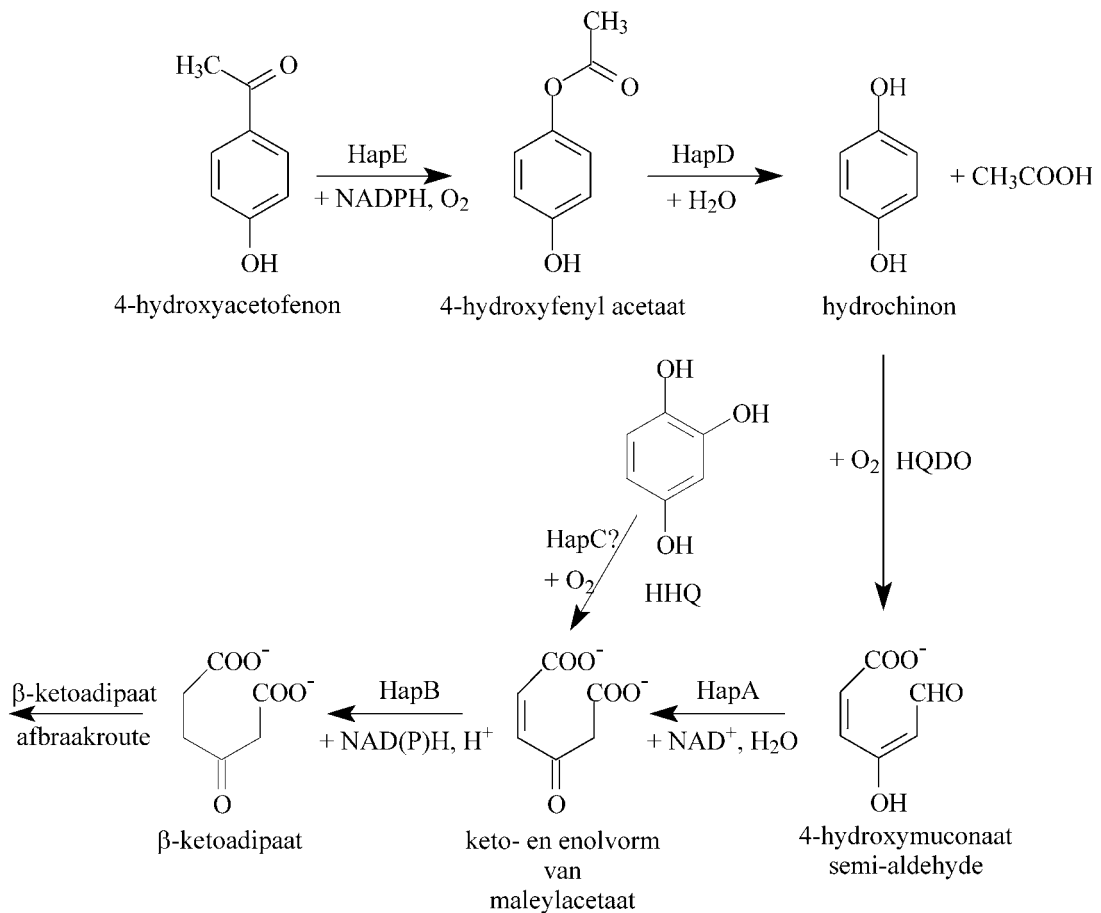
productie van biochemicalïen die gebruikt worden voor het volgen van het aminozuur metabolisme en de eiwit synthese *in vivo*.

Omdat de chemische Baeyer-Villiger oxidatie van (fluor)benzaldehydes niet erg milieuvriendelijk en ook weinig selectief is, is onderzocht of HAPMO als biokatalysator gebruikt kan worden voor de schone productie van (fluor)fenolen uit (fluor)benzaldehydes. Benzaldehydes blijken goede substraten voor HAPMO te zijn. 4-Amino- en 4-hydroxybenzaldehyde worden het snelst omgezet maar vertonen remming bij hoge substraatconcentraties. Gefluorideerde benzaldehydes worden langzamer omgezet maar hebben het voordeel dat ze geen substraatremming vertonen. Nog belangrijker is echter dat HAPMO de benzaldehydes bijna exclusief omzet via de fluorfenyl acetaat esters naar de fluorfenolen en niet naar de fluorbenzoëzuren. Deze voorkeur voor de productie van fluorfenolen wijkt af van de chemische reactie. Waarschijnlijk kan het actieve centrum van HAPMO tijdens de reactie de migratie van de aromatische ring vergemakkelijken.

Afbraakroute van 4-hydroxyacetofenon door *Pseudomonas fluorescens* ACB

In **hoofdstuk 6** wordt beschreven hoe 4-hydroxyacetofenon in *P. fluorescens* ACB wordt afgebroken tot β -ketoacidaat (zie onderstaand schema). Het eerste enzym in deze route is het hierboven beschreven HAPMO (HapE). De 4-hydroxyfenyl acetaat ester die zo ontstaat wordt vervolgens door een esterase (HapD) gehydrolyseerd tot hydrochinon (1,4-dihydroxybenzeen). Dit hydrochinon kan theoretisch op twee manieren verder worden omgezet. De eerste manier is via hydroxylering tot 1,2,4-trihydroxybenzeen (HHQ) en dan ringsplitsing met een 1,2,4-trihydroxybenzeen dioxygenase (HHQ 1,2-dioxygenase) tot maleylacetaat. Echter, hele cellen van *P. fluorescens* ACB zetten 4-fluoroacetofenon om tot 4-fluorofenol als eindproduct (**hoofdstuk 4**). Dit wijst er op dat *P. fluorescens* ACB geen fenol hydroxylase activiteit bezit en zo de omzetting van hydrochinon naar 1,2,4-trihydroxybenzeen niet kan katalyseren. Een andere mogelijkheid is de directe ringsplitsing van hydrochinon tot 4-hydroxymuconaat semi-aldehyde m.b.v. een hydrochinon dioxygenase. In **hoofdstuk 6** wordt via LC-MS aangetoond dat deze weg inderdaad door *P. fluorescens* ACB bewandeld wordt. Uit ^{19}F NMR studies blijkt dat het door hydrochinon dioxygenase (HQDO) gevormde 4-hydroxymuconaat semi-aldehyde via maleylacetaat verder wordt omgezet tot β -ketoacidaat.

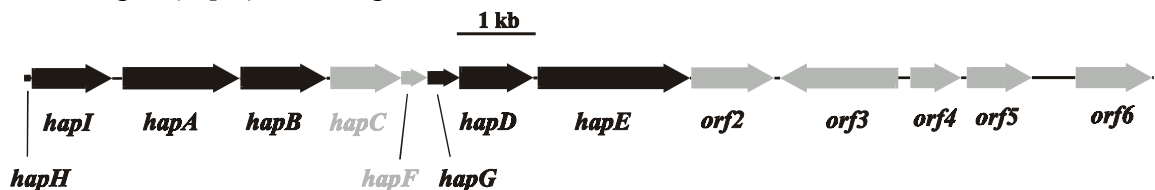
Samenvatting



De afbraakroute van 4-hydroxyacetofenon door *Pseudomonas fluorescens* ACB

Gen cluster van de 4-hydroxyacetofenon (HAP) afbraak

In **hoofdstuk 6** wordt naast de afbraakroute van 4-hydroxyacetofenon ook de gen cluster (*hapABCFGDE*) beschreven, die codeert voor de enzymen die betrokken zijn bij deze afbraakroute. Behalve de genen die coderen voor HAPMO (*hapE*) en 4-hydroxyfenyl acetaat hydrolase (*hapD*) (zie **hoofdstuk 3**) konden het 4-hydroxymuconaat semi-aldehyde dehydrogenase gen (*hapA*) en het maleylacetaat reductase gen (*hapB*) worden geïdentificeerd:



De *hap(HIABCFGDE)* gen cluster uit *P. fluorescens* ACB betrokken bij de afbraak van 4-hydroxyacetofenon

Vóór *hapA* werd een open reading frame (*hapI = orf1*) aangetroffen met onbekende functie. Na *hapE* komen enkele open reading frames die niet betrokken zijn bij de afbraakroute van 4-hydroxyacetofenon (*orf2 t/m orf6*). Tussen *hapB* en *hapD* bevinden

zich 3 genen (*hapCFG*) waarvan de functie onduidelijk is. Vooral *hapC* trok onze aandacht, omdat het enzym gecodeerd door dit gen mogelijk verantwoordelijk zou kunnen zijn voor de ringsplitsing van hydrochinon. Sequentie analyse en modeling van de eiwitstructuur wezen er echter op, dat dit waarschijnlijk niet het geval is. Het HapC eiwit (theoretische massa 32.159 Da) bleek de typische structuurkenmerken te hebben van ijzer(III) afhankelijke intradiol dioxygenases. Deze intradiol dioxygenases zijn opgebouwd uit twee identieke subunits die ieder twee strikt geconserveerde tyrosines en histidines bezitten voor ijzer binding. HapC lijkt het meest op een HHQ 1,2-dioxygenase en is daarom waarschijnlijk niet actief met hydrochinon.

Van de hydrochinon dioxygenases zijn alleen sequenties bekend van LinE en PcpA, die respectievelijk 2,6-dichloor- en 2-chloorhydrochinon gebruiken als fysiologisch substraat. Deze enzymen zijn ook in staat om hydrochinon om te zetten tot 4-hydroxyuconaat semi-aldehyde, maar hebben een heel andere aminozuurvolgorde dan HapC. LinE en PcpA bezitten per subunit twee geconserveerde histidines en een carboxylaat groep in hun actieve centrum en behoren tot de ijzer(II)-afhankelijke extradiol dioxygenases. Dit ondersteunt het feit dat HapC niet verantwoordelijk is voor de ringsplitsing van hydrochinon en dus niet betrokken is bij de afbraakroute van 4-hydroxyacetofenon. Daarom werd besloten om het enzym verantwoordelijk voor de ringsplitsing van hydrochinon (HQDO) rechtstreeks uit *P. fluorescens* ACB te isoleren. Deze ‘omgekeerde genetische’ strategie zou moeten leiden tot opheldering van de ontbrekende schakel in de afbraak van 4-hydroxyacetofenon.

Hydrochinon dioxygenase (HQDO)

Er kwamen in eerste instantie vele problemen naar voren, bij pogingen om HQDO zuiver in handen te krijgen, omdat het enzym zeer labiel bleek te zijn. Toevoegingen van mogelijk beschermende stoffen zoals protease remmers, antioxidanten en ‘staalpillen’ bracht daarin geen verbetering (**hoofdstuk 7**).

Een doorbraak in het HQDO onderzoek werd verkregen, nadat duidelijk werd dat het enzym gestabiliseerd kon worden door toevoeging van de remmer 4-hydroxybenzoaat. Deze aromaat bindt in het actieve centrum van HQDO op de substraat bindingsplaats, maar wordt niet omgezet tot een product met een geopende ring. Stabilisering door 4-hydroxybenzoaat leidde tot een bijna zuiver enzym en tot een enorme verbetering in enzym opbrengst. Karakterisering van de substraatspecificiteit liet zien dat HQDO nog een hele reeks andere hydrochinonen kan omzetten, zoals chloor-, broom-, fluor-, methyl- en methoxyhydrochinon. De omzetting is regioselectief. In het geval van difluorhydrochinonen heeft het enzym een voorkeur voor opening van de ring tussen een gehydroxyleerd (C-OH) en een gehydrogeneerd (C-H) koolstofatoom. Monofluorhydrochinon wordt echter gesplitst tussen C-OH en C-F. Naast 4-hydroxybenzoaat remmen vele andere fenolische verbindingen de enzymactiviteit van HQDO, waaronder hydroxyhydrochinon (HHQ). Remmingstudies met specifieke ‘metaaldetectoren’ wezen erop, dat het enzym voor zijn activiteit afhankelijk is van ijzer(II) ionen.

Het gezuiverde HQDO is opgebouwd uit twee subunits en vormt een $\alpha_2\beta_2$ heterotetrameer met een massa van 112,4 kDa op basis van ESI-MS metingen. De subunits hebben een massa van 17,7 en 38,3 kDa voor respectievelijk de α - en β -subunit. M.b.v. N-terminale sequentie en MALDI-ToF-ToF analyse werd informatie verkregen over de aminozuurvolgorde van beide subunits. Het actieve centrum met de ijzer(II) bindingsplaats bevindt zich in de β -subunit als bepaald m.b.v. ESI-MS analyse.

Op basis van de N-terminale eiwit sequentie en MALDI-ToF-MS van tryptische peptiden kon worden aangetoond dat de β -subunit van HQDO wordt gecodeerd door het *orf1* gen van de *hap* cluster. Bovendien kon m.b.v. genetische informatie van andere organismen worden vastgesteld dat onmiddellijk voor *hapI* zich het gen bevindt, dat codeert voor de α -subunit van HQDO (*hapH*).

HQDO (HapHI) is een nieuw type enzym binnen de familie van de ijzer(II)-afhankelijke dioxygenases. Er zijn tot nu toe slechts 5 gen clusters bekend die een of twee van de *hapHI* genen bezitten. Verder vertoont HQDO weinig verwantschap met de hierboven beschreven chloorhydrochinon dioxygenases.

Met de biochemische karakterisering van HQDO en de identificatie van de *hapHI* genen is onomstotelijk aangetoond, dat HapC niet betrokken is bij de afbraak van 4-hydroxyacetofenon. HapC is vermoedelijk nodig in een andere afbraakroute voor de ringsplitsing van HHQ.

In verschillende andere micro-organismen die verwant zijn aan *P. fluorescens* ACB codeert het *hapG* voor een ferredoxine dat nodig is voor de reactivering van ijzer(II)-afhankelijke catechol dioxygenases. Omdat HQDO een zeer labiel eiwit is, dat afhankelijk is van ijzer(II) ionen, suggereert dit een mogelijke rol voor *hapG*.

Conclusies

- *Pseudomonas fluorescens* ACB is in staat om 4-hydroxyacetofenon m.b.v. 5 enzymen om te zetten tot β -keto adipaat. Twee van deze enzymen gebruiken daarvoor zuurstof: 4-hydroxyacetofenon mono-oxygenase (HAPMO) en hydrochinon dioxygenase (HQDO).
- HAPMO is een NADPH-afhankelijk FAD bevattend enzym, bestaande uit twee identieke subunits van ieder 72 kDa. HAPMO is een type I Baeyer-Villiger mono-oxygenase met een uniek N-terminaal domein met onbekende functie. HAPMO heeft een brede substraatspecificiteit. Naast aromatische ketonen zijn benzaldehydes goede HAPMO substraten. Gevormde aromatische esters worden bij hoge pH spontaan gehydrolyseerd tot de corresponderende fenolen.
- HQDO is een nieuw type ringsplitsend dioxygenase dat hydrochinon omzet in 4-hydroxymuconaat semi-aldehyde. HQDO is een $\alpha_2\beta_2$ heterotetrameer van 112,4 kDa, met de actieve bindingsplaats vermoedelijk alleen in de β -subunit. IJzer(II) ionen worden alleen in de β -subunit gebonden en zijn betrokken bij de katalyse. Binding van de competitieve remmer 4-hydroxybenzoaat stabiliseert het HQDO waardoor het mogelijk is het enzym te zuiveren en biochemisch te karakteriseren. HQDO heeft een brede substraatspecificiteit. Naast hydrochinon katalyseert het enzym ook de oxidatieve ringsplitsing van chloor-, broom-, fluor-, methyl- en methoxyhydrochinon. De ringsplitsing verloopt regioselectief. HQDO is niet actief met 1,2,4-trihydroxybenzeen (HHQ) en met catechol. HQDO uit *P. fluorescens* ACB is de eerste HQDO waarvan de sequentie bepaald is.
- De genen coderende voor de enzymen betrokken bij het 4-hydroxyacetofenon metabolisme in *P. fluorescens* ACB, bevinden zich in de *hap* gen cluster. Deze enzymen zijn: HAPMO (HapE), 4-hydroxyfenyl acetaat hydrolase (HapD), HQDO (HapHI), 4-hydroxymuconaat semi-aldehyde dehydrogenase (HapA) en het maleylacetaat reductase (HapB). Het *hapC* gen, dat midden in de *hap* cluster is gelokaliseerd, is niet betrokken bij de afbraak van 4-hydroxyacetofenon, maar codeert voor een enzym dat qua sequentie nauw verwant is aan de familie van

Samenvatting

ijzer(III)-afhankelijke intradiol dioxygenases. Het *hapC* gen codeert waarschijnlijk voor een HHQ 1,2-dioxygenase. Mogelijk is dit gen tijdens de evolutie als ‘verontreiniging’ in de cluster achtergebleven of is het betrokken bij een andere afbraakroute.

Nawoord

Mijn promotietijd was een leuke en zeer leerzame periode in mijn leven. Daarom wil ik in de eerste plaats Willem van Berkel bedanken voor zijn geduld en opbouwende kritiek en niet in de laatste plaats voor zijn begrip voor mijn RSI. Ook de vrijheid die je me gaf om met het hydroquinone dioxygenase verder te gaan i.p.v. met het HAPMO heb ik zeer op prijs gesteld. Ik ben oprecht blij dat jij mijn begeleider was in deze periode.

Daarnaast wil ik Ivonne Rietjens bedanken voor het feit dat zij mijn promotor was en ook actief betrokken was met name bij de hoofdstukken 4 en 5. Hierbij kon ^{19}F NMR als handig meetinstrument gebruikt worden, waarmee je me overigens al tijdens mijn afstudeervak kennis had laten maken. Als professor Biochemie, was Sacco de Vries ook een extra push om het af te maken. Bedankt dat je mijn promotor wilde zijn.

De samenwerking met mijn collega oio Nanne Kamerbeek, zijn begeleider Marco Fraaije en hun professor Dick Janssen van de RUG in Groningen resulteerde natuurlijk tot hoofdstuk 3 en 6, maar daarnaast was het heel plezierig om vanuit verschillende kanten aan een enzym te werken.

I want to thank Silvia Synowsky and Robert van den Heuvel from Utrecht University for the MS en MALDI-ToF-ToF experiments in chapter 7. These measurements gave me insight in the heterotetrameric character of HQDO and solved part of the sequence of the α -subunit of HQDO.

Verder wil ik ook mensen van organische chemie bedanken. Maurice Franssen voor je altijd aanwezige interesse en voor het mee nadenken van een mechanisme voor HQDO. Bep van Veldhuizen en later Barend van Lagen voor hun hulp bij de NMR-metingen, vooral als het fieldsignaal weer eens aan de andere kant van de wereld lag. Daarnaast was Adrie de Jager(†) van Biofysica er ook altijd voor NMR problemen. Fred van den End wil ik graag bedanken voor de hulp met de 200 liter fermentor.

Verder wil ik al mijn lab 5-genoten en -gasten bedanken: Michel, Robert, Agnieschka, Ulrike, Miriam, Patricia. Natuurlijk ook dank aan alle (ex-)aio's, oio's en post-docs voor de gezellige aio-weekenden, de lunches en alle gesprekken over werk en andere zaken: Eyke, Peter-Leon, Robert, Sofia, Ruchira, Maarten, Yves, Yee, Hans, Nicole, Vief, Monique, Jose, Rummyana, Mark Hink, Mark Kwaaitaal, Kees-Jan, Marloes, Annechien, Marco, Harrold, Henno, Jean-Louis, Lars, Petra en Gideon. Een speciaal bedankje aan Yves, omdat hij het al die jaren met mij op de kamer heeft volgehouden. Daarnaast een bedankje aan mijn afstudeerstudent Ludwin van Aart. Of course also thanks to Alex Vinogradov for study on the unfolding and limited proteolysis of HAPMO as published in the Flavin book 2002. Laura wil ik graag bedanken voor alle regelzaakjes maar zeker ook voor het feit dat je altijd een luisterend oor had voor mij. Heel belangrijk waren ook de drie analisten Adrie, Willy en Sjef voor mij. Adrie jij ging me helpen omdat ik niet meer alles kon vanwege mijn RSI. Daarnaast heb je vele computerprobleempjes voor mij opgelost. Willy, jij nam het stokje van Adrie over en het lukte jou om HQDO met een redelijke opbrengst te zuiveren en zonder jou had hoofdstuk 7 niet bestaan. Sjef bedankt voor de hulp met de HPLC, LC-MS metingen en met de MALDI-ToF-uitwerkingen. Bedankt ook alle overige collega's voor jullie aanwezigheid.

Natuurlijk wil ik ook mijn ouders bedanken voor hun altijd aanwezige steun en belangstelling. Daarnaast wil ik ook Sylvia, Rog er en Maud bedanken in het bijzonder

Nawoord

voor de weekendjes met Maikel. Sylvia en Ruchira wil ik bedanken voor het feit dat zij mijn paranimfen wilden zijn. Vielen Dank Maria und Peter(†) Mies für das Vertrauen in mir und für den vorrausschauende Blick von Peter. Heel belangrijk zijn ook mijn twee mannen, Maikel en Adrie, die er altijd voor mij waren en die me weer genoeg energie gaven om het boekje af te maken.

Curriculum vitae

Maria Johanna Hendrika Moonen was born in Horst, The Netherlands, on March 20th 1971. She completed High School (Atheneum) at Blariacumcollege in Venlo-Blerick in 1989. In September of the same year, she started her study in Molecular Sciences at Wageningen Agricultural University. In June of 1990 she switched to Food Technology at the same university. In May 1992 she gave birth to her son Maikel. For her Master's degree she did a five months research project in the Laboratory of Biochemistry at Wageningen Agricultural University under supervision of Ans Soffers and dr. Ivonne Rietjens on the subject of MO-QSAR for detoxification of fluoronitrobenzenes by glutathione S-transferases. Another five months research project was performed at the Laboratory of Toxicology under supervision of PhD student Gerlienke Schuur and Dr. Bram Brouwer on the the *in vitro* inhibition of the sulfation of thyroid hormone by hydroxylated PCBs, PCDDs and PCDFs. In January 1997 she graduated. From February 1997 till February 1998 she did administrative work at the SNS bank Gelderland in Wageningen.

In April 1998 she started her PhD research titled "Development of biocatalysts for Baeyer-Villiger monooxygenase catalyzed reactions: kinetic and mechanistic characterization of the enzyme and improvement of the biocatalyst". This project was subsidized by the Dutch Organization of Scientific Research (NWO) and was part of the program "Procesvernieuwing voor een Schoner Milieu". The research was carried out at the Laboratorium of Biochemistry at Wageningen University under supervision of dr. W.J.H. van Berkel. In the same project Nanne Kamerbeek did his PhD research at the University of Groningen (under supervision of dr. Marco Fraaije and Prof. dr. Dick Janssen).

List of publications

Soffers, A.E., Ploemen, J.H., **Moonen, M.J.H.**, Wobbes, T., van Ommen, B., Vervoort, J., van Bladeren, P.J. and Rietjens, I.M.C.M. 1996. Regioselectivity and quantitative structure-activity relationships for the conjugation of a series of fluoronitrobenzenes by purified glutathione S-transferase enzymes from rat and man. *Chem Res Toxicol* **9**, 638-646.

Schuur, A.G., Legger, F.F., van Meeteren, M.E., **Moonen, M.J.H.**, van Leeuwen-Bol, I., Bergman, A., Visser, T.J. and Brouwer, A. 1998. In vitro inhibition of thyroid hormone sulfation by hydroxylated metabolites of halogenated aromatic hydrocarbons. *Chem Res Toxicol* **11**, 1075-1081.

Moonen, M.J.H., Rietjens, I.M.C.M. and van Berkel, W.J.H. 1999. Purification and some properties of acetophenone monooxygenase. In: *13th International Congress on Flavins and Flavoproteins* (Eds. S. Ghisla, P. Kroneck, P. Macheroux and H. Sund). Agency for Scientific Publication, Berlin, pp. 375-378.

Kamerbeek, N.M., **Moonen, M.J.H.**, Van der Ven, J.G.M., Van Berkel, W.J.H., Fraaije, M.W. and Janssen, D.B. 2001. 4-Hydroxyacetophenone monooxygenase from *Pseudomonas fluorescens* ACB. A novel flavoprotein catalyzing Baeyer-Villiger oxidation of aromatic compounds. *Eur J Biochem* **268**, 2547-2557.

Moonen, M.J.H., Rietjens, I.M.C.M. and van Berkel, W.J.H. 2001. ¹⁹F NMR study on the biological Baeyer-Villiger oxidation of acetophenones. *J Ind Microbiol Biotechnol* **26**, 35-42.

Moonen, M.J.H., Fraaije, M.W., Rietjens, I.M.C.M., Laane, C. and Van Berkel, W.J.H. 2002. Flavoenzyme-catalyzed oxygenations and oxidations of phenolic compounds. *Adv Synth Catal* **344**, 1023-1035.

Moonen, M.J.H., van Berkel, W.J.H., Vinogradov, A., Kamerbeek, N.M. and Fraaije, M.W. 2002. Unfolding and limited proteolysis of 4-hydroxyacetophenone monooxygenase from *Pseudomonas fluorescens* ACB. In: *14th International Symposium on Flavins and Flavoproteins* (Eds. S. Chapman, R. Perham and N. Scrutton). Agency for Scientific Publication, Berlin, pp. 1011-1014.

Jadan, A.P., **Moonen, M.J.H.**, Boeren, S., Golovleva, L.A., Rietjens, I.M.C.M. and van Berkel, W.J.H. 2004. Biocatalytic potential of *p*-hydroxybenzoate hydroxylase from *Rhodococcus rhodnii* 135 and *Rhodococcus opacus* 557. *Adv Synth Catal* **346**, 367-375.

Moonen, M.J.H., Westphal, A.H., Rietjens, I.M.C.M. and van Berkel, W.J.H. 2005. Enzymatic Baeyer-Villiger oxidation of benzaldehydes. *Adv Synth Catal*, in press.

Training and Supervision M&T and VLAG

Period	Activity	Place	Time	Credit points
April, 1998	Preparation of research proposal	Wageningen	4 weeks	4.0
May, 1998	M&T Progress report meeting	Ede	1 day	0.2
November, 1998	M&T course. Biodegradation by micro-organisms of chemicals in the environment: new frontiers and techniques in research	Wageningen University	1 week	1.0
December, 1998	NWO Protein Research meeting	Lunteren	2 days	0.4
March, 1999	NWO Biomolecular Chemistry meeting	Lunteren	2 days	0.4
April, 1999	Study group day of NVB	Wageningen	1 day	0.2
June, 1999	M&T Progress report meeting	Ede	1 day	0.2
August-September, 1999	Flavins and Flavoproteins: 13 th International symposium	Konstanz, Germany	7 days	1.4
November, 1999	NMR in environmental biotechnology	Wageningen NMR center	1 day	0.2
December, 1999	NWO Protein Research meeting	Lunteren	2 days	0.4
October, 1999 - March, 2000	English for PhD students	Wageningen Language Center	13 days	2.6
March, 2000	NWO Biomolecular Chemistry meeting	Lunteren	2 days	0.4
April, 2000	ISEB 4: 4 th International symposium on environmental biotechnology	Noordwijkerhout	3 days	0.6
December, 2000	NWO Protein Research meeting	Lunteren	2 days	0.4
March, 2001	NWO Biomolecular Chemistry meeting	Lunteren	2 days	0.4
April, 2001	Bioinformatics	Wageningen University	2 weeks	2.0
October, 2001	VLAG course: Protein engineering	Wageningen University	3 days	0.6
December, 2001	NWO Protein Research meeting	Lunteren	2 days	0.4
March, 2002	NWO Biomolecular Chemistry meeting	Lunteren	2 days	0.4
July, 2002	Flavins and Flavoproteins: 14 th International symposium	Cambridge, United Kingdom	5 days	1.0
December, 2002	NWO Protein Research meeting	Lunteren	2 days	0.4
March, 2003	NWO Biomolecular Chemistry meeting	Lunteren	2 days	0.4
October, 2003	DSM Scientific Meeting: Biocatalysis & Biotransformations	Vaals	2 days	0.4
December, 2003	NWO Protein Research meeting	Lunteren	2 days	0.4
March, 2004	NWO Biomolecular Chemistry meeting	Lunteren	2 days	0.4
Total period	Literature study programmes	Wageningen	3 weeks	3.0

Moonen, Maria J.H.

Novel oxygenases acting on phenolic compounds

Title in Dutch: Nieuwe oxygenases actief met phenolische verbindingen

Thesis Wageningen University, The Netherlands

With references — with summary in Dutch

ISBN:

Cover: Free interpretation of a fermentor for cultivating *Pseudomonas fluorescens* ACB



The research described in this thesis was performed in the Laboratory of Biochemistry of Wageningen University, the Netherlands. The research was financially supported by NWO, The Hague, The Netherlands in the program “Procesvernieuwing voor een Schoner Milieu”

Copyright© 2005 by M.J.H. Moonen

All rights reserved

Printed by Ponsen & Looijen, Wageningen